Harjit Singh · Janet A. Neutze *Editors*

Radiology Fundamentals

Introduction to Imaging & Technology

Fourth Edition

Springer

Radiology Fundamentals

Harjit Singh • Janet A Neutze
Editors

Jonathan R Enterline • Joseph S Fotos
Associate Editors

Jonathan J Douds • Megan Jenkins Kalambo
• Marsha J Bluto
Contributing Editors

Radiology Fundamentals

Introduction to Imaging & Technology

Fourth Edition

Springer

Editors
Harjit Singh, MD, FSIR
Professor of Radiology, Surgery,
and Medicine
Director of Education, Penn State Heart
and Vascular Institute
Fellowship Director, Cardiovascular
and Interventional Radiology
Pennsylvania State College of Medicine
Penn State Hershey Medical Center
Hershey, PA, USA
hsingh@hmc.psu.edu

Janet A Neutze, MD
Associate Professor of Radiology
Associate Division Chief, Ultrasound
Co-director, Radiology Medical Student
Education Program
Pennsylvania State College of Medicine
Penn State Hershey Medical Center
Hershey, PA, USA
jneutze@hmc.psu.edu

Associate Editors
Jonathan R Enterline, MD
Resident, Department of Radiology
Pennsylvania State College of Medicine
Penn State Hershey Medical Center
Hershey, PA, USA

Joseph S Fotos, MD
Resident, Department of Radiology
Pennsylvania State College of Medicine
Penn State Hershey Medical Center
Hershey, PA, USA

Contributing Editors
Jonathan J Douds, BS
Medical Student
Pennsylvania State College of Medicine
Penn State Hershey Medical Center
Hershey, PA, USA

Megan Jenkins Kalambo, MD
Resident, Department of Radiology
University of Texas Health Science Center
at Houston, Houston, TX, USA

Marsha J Bluto, MD
Practicing Physician
Physical Medicine and Rehabilitation
Mill Valley, CA, USA

ISBN 978-1-4614-0943-4 e-ISBN 978-1-4614-0944-1
DOI 10.1007/978-1-4614-0944-1
Springer New York Dordrecht Heidelberg London

Library of Congress Control Number: 2011938463

© Springer Science+Business Media, LLC 2012
All rights reserved. This work may not be translated or copied in whole or in part without the written permission of the publisher (Springer Science+Business Media, LLC, 233 Spring Street, New York, NY 10013, USA), except for brief excerpts in connection with reviews or scholarly analysis. Use in connection with any form of information storage and retrieval, electronic adaptation, computer software, or by similar or dissimilar methodology now known or hereafter developed is forbidden.
The use in this publication of trade names, trademarks, service marks, and similar terms, even if they are not identified as such, is not to be taken as an expression of opinion as to whether or not they are subject to proprietary rights.
While the advice and information in this book are believed to be true and accurate at the date of going to press, neither the authors nor the editors nor the publisher can accept any legal responsibility for any errors or omissions that may be made. The publisher makes no warranty, express or implied, with respect to the material contained herein.

Printed on acid-free paper

Springer is part of Springer Science+Business Media (www.springer.com)

To everyone who worked so hard on this book over the years, thank you. I couldn't have done it without you. To my wife, Bina and my children, thank you for the support and encouragement.
To Dad, thanks for watching over me.

HS

For all of those who helped – thanks.
For all of those who waited – thanks;
I'm coming home now.

JAN

To all those that ever wrote a book, I can now empathize. To my family and wonderful wife, Lindsey, for their endless love, encouragement, and prayers.

JE

To my lovely wife, Melissa, thank you for your love, encouragement and boundless support. To all of those who have worked so hard on this project over the years, thank you. Your contributions will be appreciated for years to come.

JF

PREFACE TO THE FOURTH EDITION

The fourth edition of the Radiology Syllabus is directed towards medical students, non-radiology housestaff, physician assistants, nurse practitioners, radiologist assistants and other allied health professionals as a curriculum guide to supplement their radiology education. This book serves only as an introduction to the dynamic field of radiology. In fact, the most difficult decision in compiling this fourth edition did not involve what to include, but rather determining what to leave out. The goal of this text is to provide the reader with examples and brief discussions of basic radiographic principles that should serve as the foundation for further learning. We hope that it will foster and further stimulate the process at the heart of medical education: self-directed learning.

Each edition continues to expand upon the first edition of the photocopied pages and films, written and organized by the original authors, Dr. William Hendrick and Dr. Carlton “Tad” Phelps. As mentors, Dr. Hendrick and Dr. Phelps of Albany Medical Center wanted a curriculum guide to reinforce the teaching concepts of their radiology elective. Dr. Harjit Singh, editor and author of much of the text of the first print edition, formalized the material in 1988. Our third edition, updated by faculty and students at Penn State Hershey was a first effort at organizing and digitizing the information for publication. Dr. Marsha Bluto led that conversion of both text and images. Drs. Megan Jenkins and Jonathan Enterline assisted in the multiple rewrites and desktop publishing.

Our fourth edition is an effort to expand and reinforce the original authors’ work by 14 new contributors. Dr. Joseph Fotos and Jonathan Douds (MD 2012) are new additions to the writing, illustrating, and editing side.

Radiology continues to explode in breath and depth. Health practitioners are using radiology studies not just to confirm a clinical suspicion but to make a diagnosis. We are performing 20 times more CT scans than we did in 1980! From both cost and safety standpoints, clinicians and radiologist need to know what they are doing. We hope this book, used in conjunction with lectures, electives, and discussions, is a start.

Hershey, PA, USA

Harjit Singh
Janet A Neutze

CONTENTS

1 Patient Radiation Safety and Risk 1
2 Introduction to Radiology Concepts 7
3 Conventional Radiology 11
4 Ultrasound 17
5 Computed Tomography 23
6 MRI 29
7 Nuclear Medicine 31
8 Cardiovascular and Interventional Radiology 35
9 Heart and Mediastinum 39
10 Lateral Chest 45
11 Pulmonary Mass Lesions 51
12 Air Space Disease 59
13 Interstitial Disease 63
14 Atelectasis 69
15 Pulmonary Vasculature 75
16 Pulmonary Edema 83
17 Pneumothorax 89
18 Miscellaneous Chest Conditions 95
19 Tubes and Lines 105
20 Breast Imaging 111

21 **Women's Ultrasound** 125
22 **Women's Health Interventions** 131
23 **Abdominal Calcifications** 137
24 **Abnormal Air Collections in the Abdomen** 143
25 **Barium Studies of the Upper GI Tract** 147
26 **Barium Enema and CT Colonography** 157
27 **Bowel Obstruction** 167
28 **Inflammatory Bowel Disease** 175
29 **Defecography** 181
30 **Intra-abdominal Lymphadenopathy** 189
31 **The Gallbladder** 193
32 **Abdominal and Pelvic Pain Evaluation** 201
33 **Imaging the Trauma Patient** 211
34 **Concerning Lesions** 219
35 **Incidental Lesions** 229
36 **Radionucleotide Evaluation of GI Bleeding** 237
37 **Radionucleotide Bone Imaging** 241
38 **Lung Ventilation and Perfusion Imaging** 247
39 **Radionucleotide Cardiac Imaging** 251
40 **F-18 FDG Positron Emission Tomography** 255
41 **Diagnostic Arteriography** 263
42 **Pulmonary Arteriography and IVC Filter Placement** 267
43 **Percutaneous Nephrostomy Placement** 273
44 **TIPS** 277
45 **Central Venous Access** 283
46 **Fractures: Part I** 287
47 **Fractures: Part 2** 299
48 **Arthritides** 315
49 **Bone Tumor Characteristics** 321
50 **CNS Anatomy** 327

51 The Cervical Spine 329

52 Head Trauma 333

53 Stroke 339

54 Headache and Back Pain 345

55 Radiology Coming Soon 349

Index 355

CONTRIBUTORS

Amit K Agarwal, MD
Assistant Professor of Radiology
Penn State Hershey Medical Center
Hershey, Pennsylvania
Chapter 50: CNS Anatomy
Chapter 51: The Cervical Spine
Chapter 52: Head Trauma

Karen L Brown, MS, CHP, DABR
Associate Health Physicist
Division of Health Physics
Instructor-Radiology
Penn State Hershey Medical Center
Hershey, Pennsylvania
Chapter1: Patient Radiation Safety and Risk

Karen M Brown, MD, MS
Fellow, Musculoskeletal Radiology
University of California, San Francisco
Chapter 46: Fractures, Part 1
Chapter 47: Fractures, Part 2
Chapter 48: Arthritides

Allene Salcedo Burdette, MD
Assistant Professor of Radiology, Surgery and Medicine
Penn State Heart and Vascular Institute
Hershey, Pennsylvania
Chapter 55: Radiology Coming Soon

Rekha A Cherian, MD
Assistant Professor of Radiology
Penn State Hershey Medical Center
Hershey, Pennsylvania
Chapter 9: Heart and Mediastinum
Chapter 10: Lateral Chest
Chapter 11: Pulmonary Mass Lesions
Chapter 12: Air Space Disease
Chapter 13: Interstitial Disease

Jonathan R Enterline, MD
Resident, Department of Radiology
Penn State Hershey Medical Center
Hershey, Pennsylvania
Chapter 34: Concerning Lesions
Chapter 35: Incidental Lesions
Chapter 46: Fractures, Part 1
Chapter 47: Fractures, Part 2
Chapter 48: Arthritides
Chapter 49: Bone Tumor Characteristics

Joseph S Fotos, MD
Resident, Department of Radiology
Penn State Hershey Medical Center
Hershey, Pennsylvania
Chapter 3: Conventional Radiology
Chapter 4: Ultrasound
Chapter 9: Heart and Mediastinum
Chapter 13: Interstitial Disease
Chapter 53: Stroke

Hassan M Hal, MD, PhD
Assistant Professor of Radiology
Penn State Hershey Medical Center
Hershey, Pennsylvania
Chapter 25: Barium Studies of the Upper GI Tract
Chapter 26: Barium Enema & CT Colonography
Chapter 29: Defecography

Carlos Jamis-Dow, MD
Associate Professor of Radiology
Penn State Hershey Medical Center
Hershey, Pennsylvania

Chapter 14: Atelectasis
Chapter 15: Pulmonary Vasculature
Chapter 16: Pulmonary Edema
Chapter 17: Pneumothorax
Chapter 18: Miscellaneous Chest Conditions
Chapter 19: Tubes and Lines

Claudia J Kasales, MD
Professor of Radiology
Division Chief, Ultrasound Penn State Hershey Medical Center
Hershey, Pennsylvania
Chapter 4: Ultrasound
Chapter 5: Computed Tomography
Chapter 32: Abdominal and Pelvic Pain Evaluation
Chapter 33: Imaging of the Trauma Patient
Chapter 35: Incidental Lesions

Steven King, CHP, CMHP
Director, Division of Health Physics
Senior Instructor – Radiology
Penn State Hershey Medical Center
Hershey, Pennsylvania
Chapter 1: Patient Radiation Safety and Risk

Frank C Lynch, MD, FSIR
Professor of Radiology, Surgery and Medicine
Penn State Heart and Vascular Institute
Medical Director, Nursing Vascular Access Team
Penn State Hershey Medical Center
Hershey, Pennsylvania
Chapter 42: Pulmonary Arteriography & IVC Filter Placement
Chapter 45: Central Venous Access

Michael M Moore, MD
Assistant Professor of Radiology and Pediatrics
Penn State Hershey Medical Center
Hershey, Pennsylvania
Chapter 55: Radiology Coming Soon

Janet A Neutze, MD
Associate Professor of Radiology
Associate Division Chief, Ultrasound
Co-Director, Radiology Medical Education Program

Penn State Hershey Medical Center
Hershey, Pennsylvania
Chapter 21: Women's Ultrasound
Chapter 54: Headache and Back Pain

Tao Ouyang, MD
Assistant Professor of Radiology
Penn State Hershey Medical Center
Hershey, Pennsylvania
Chapter 53: Stroke
Chapter 54: Headache and Back Pain

Christine M Peterson, MD
Assistant Professor of Radiology
Director of Abdominal Computed Tomography
Co-director, Radiology Medical Education Program
Penn State Hershey Medical Center
Hershey, Pennsylvania
Chapter 30: Intra-abdominal Lymphadenopathy

Susann E Schetter, DO
Division Chief, Breast Imaging
Associate Professor of Radiology
Penn State Hershey Medical Center
Hershey, Pennsylvania
Chapter 20: Breast Imaging

Leslie B Scorza, MD
Associate Professor of Radiology, Surgery and Medicine
Penn State Heart and Vascular Institute
Medical Director Nursing Vascular Access Team
Penn State Hershey Medical Center
Hershey, Pennsylvania
Chapter 8: Cardiovascular and Interventional Radiology
Chapter 41: Diagnostic Arteriography

Harjit Singh, MD, FSIR
Professor of Radiology, Surgery, and Medicine
Director of Education, Penn State Heart and Vascular Institute
Fellowship Director, Cardiovascular and Interventional Radiology
Penn State Hershey Medical Center
Hershey, Pennsylvania
Chapter 2: Introduction to Radiology Concepts
Chapter 3: Conventional Radiology

Chapter 6: MRI
Chapter 23: Abdominal Calcifications
Chapter 24: Abnormal Air Collections in the Abdomen
Chapter 27: Bowel Obstruction
Chapter 28: Inflammatory Bowel Disease
Chapter 31: The Gallbladder
Chapter 37: Radionuclide Bone Imaging
Chapter 38: Lung Ventilation and Perfusion
Chapter 39: Radionuclide Cardiac Imaging
Chapter 40: F-18 FDG Positron Emission Tomography
Chapter 42: Pulmonary Arteriography and IVC Filter Placement
Chapter 43: Percutaneous Nephrostomy Placement

Eric A Walker, MD
Associate Professor of Radiology
Penn State Hershey Medical Center
Hershey, Pennsylvania
Chapter 46: Fractures, Part 1
Chapter 47: Fractures, Part 2
Chapter 48: Arthritides

Peter N Waybill, MD, FSIR
Professor of Radiology, Medicine and Surgery
Chief, Cardiovascular and Interventional Radiology
Penn State Heart and Vascular Institute
Penn State Hershey Medical Center
Hershey, Pennsylvania
Chapter 44: TIPS

Scott Winner, MD
Assistant Professor of Radiology and Humanities
Penn State Hershey Medical Center
Hershey, Pennsylvania
Chapter 7: Nuclear Medicine
Chapter 36: Radionuclide Evaluation of GI Bleeding
Chapter 40: F-18 FDG Positron Emission Tomography

1

PATIENT RADIATION SAFETY AND RISK

Objectives:
1. Understand the difference between nonionizing and ionizing radiation.
2. Understand the difference between stochastic and nonstochastic effects.
3. Be able to discuss the concept of ALARA.

Everyone is concerned about patient radiation dose. From 1993 through 2008, radiation dose attributed to medical radiation rose 82% from 0.54 to 3 mSv per capita. The largest component of the medical patient radiation dose was CT scanning (49%). This is despite the fact that CT scanning makes up only 17% of the total medical procedures that contributes to a patient radiation dose (NCRP Report 160).

Radiation dose for all diagnostic exams should be minimized to the lowest amount of radiation needed to produce a diagnostic quality exam. (Tables 1.1–1.3).

What Is Radiation?

Radiation is emitted from unstable atoms. Unstable atoms are said to be "radioactive" because they release energy (radiation). The radiation emitted may be electromagnetic energy (X-rays and gamma rays) or particles such as alpha or beta particles. Radiation can also be produced by high-voltage devices such as X-ray machines. X-rays are a form of electromagnetic energy with a wavelength that places it into an ionizing radiation category. In a diagnostic exam, these photons can penetrate the body and are recorded on digital or film medium to produce an image of various densities that show details inside the body.

H Singh and JA Neutze (eds.), *Radiology Fundamentals: Introduction to Imaging & Technology*, DOI 10.1007/978-1-4614-0944-1_1,
© Springer Science+Business Media, LLC 2012

Table 1-1 Typical effective radiation dose from diagnostic X-ray: Single exposure

Exam (Mettler et al. 2008)	Effective dose mSv (mrem)
Chest	0.1 (10)
Cervical spine	0.2 (20)
Thoracic spine	1.0 (100)
Lumbar spine	1.5 (150)
Pelvis	0.7 (70)
Abdomen or hip	0.6 (60)
Mammogram (2 view)	0.36 (36)
Dental bitewing	0.005 (0.5)
Dental (panoramic)	0.01 (1)
DEXA (whole body)	0.001 (0.1)
Skull	0.1 (10)
Hand or foot	0.005 (0.5)

Table 1-2 The table shows the dose a patient could receive if undergoing an entire procedure that may be diagnostic or interventional. For example, a lumbar spine series usually consists of five X-ray exams (Mettler et al. 2008)

Examinations and procedures	Effective dose mSv (mrem)
Intravenous pyelogram	3.0 (300)
Upper GI	6.0 (600)
Barium enema	7.0 (700)
Abdomen kidney, ureter, bladder (KUB)	0.7 (70)
CT head	2.0 (200)
CT chest	7.0 (700)
CT abdomen/pelvis	10.0 (1,000)
Whole-body CT screening	10.0 (1,000)
CT biopsy	1.0 (100)
Calcium scoring	2.0 (200)
Coronary angiography	20.0 (2,000)
Cardiac diagnostic and intervention	30.0 (3,000)
Pacemaker placement	1.0 (100)
Peripheral vascular angioplasties	5.0 (500)
Noncardiac embolization	55.0 (5,500)
Vertebroplasty	16.0 (1,600)

Table 1-3 Typical effective radiation dose from nuclear medicine examinations (Mettler et al. 2008)

Nuclear medicine scan radiopharmaceutical (common trade name)	Effective dose mSv (mrem)
Brain (PET) 18F FDG	14.1 (1,410)
Brain (perfusion) 99mTc HMPAO	6.9 (690)
Hepatobiliary (liver flow) 99mTc Sulfur Colloid	2.1 (210)
Bone 99mTc MDP	6.3 (630)
Lung perfusion/ventilation 99mTc MAA and 133Xe	2.5 (250)
Kidney (filtration rate) 99mTc DTPA	1.8 (180)
Kidney (tubular function) 99mTc MAG3	2.2 (220)
Tumor/infection 67Ga	2.5 (250)
Heart (stress-rest) 99mTc sestamibi (Cardiolite)	9.4 (940)
Heart (stress-rest) 201Tl chloride	41.0 (4,100)
Heart (stress-rest) 99mTc tetrofosmin (Myoview)	11.0 (1,100)
Various PET studies 18F FDG	14.0 (1,400)

Light, radio, and microwaves are nonionizing types of electromagnetic radiation. Radio waves are used to generate MRI images. X-rays and gamma rays are *ionizing* forms of electromagnetic radiation and can produce charged particles (ions) in matter. When ionizations occur in tissue they can lead to cellular damage. Most damage is repaired by natural processes. In some cases, the damage cannot be repaired or is not repaired correctly which can lead to biological effects.

There are two categories of biological effects related to radiation exposure:

Nonstochastic (also called deterministic)
Stochastic (also called probabilistic)

- *Nonstochastic* effects can occur when the amount of radiation energy imparted to tissue (dose) exceeds a threshold value. Below the threshold, no effect is observed. Above the threshold, the effect is certain.

  Examples:

  - Skin injury
  - Cataracts

- *Stochastic effects* can manifest at any dose, meaning there is no threshold below which the effect cannot occur. In reality, the probability of a stochastic effect increases as radiation dose imparted to the tissue increases.

  Examples:

  - Cancer
  - Leukemia

Where Do We Use Radiation in a Hospital?

- X-ray equipment
- Radiography
  - Fluoroscopy
  - Mammography
  - Cardiac catheterization
  - Computed tomography
  - Radiation therapy (linear accelerator)
- Radioactive material
  - Nuclear medicine
  - Radiation therapy (Tables 1.1–1.3)

What Are the Risks?

There is no threshold for stochastic effects so any imaging procedure or therapy that involves the use of radiation involves some risk. When performed properly, the risk is usually very small and is far outweighed by the medical benefit of having the procedure. Regardless, the concept of ALARA (keeping the radiation dose *A*s *L*ow *A*s *R*easonably *A*chievable should always be employed to minimize the risk).

A small percentage of imaging and therapy studies performed in the hospital can potentially exceed threshold values for nonstochastic effects.

Radiation therapy and interventional fluoroscopy procedures may result in radiation doses that exceed the threshold dose for skin injuries, and less frequently for cataract induction. The procedures performed in these areas are often life-saving and every effort to minimize the magnitude of these effects is taken.

Resources

As you continue your career in medicine, you will specialize. Part of medicine in virtually all areas of specialization involves ordering X-rays or nuclear procedures for your patients.

In the news media, great attention has been paid to the increase in medical radiation dose to members of the public. Currently, there are discussions and debates

over the appropriateness of ordering certain exams without need. This will become a financial restraint as well as a public health question.
Some resources to look into:

- ACR Appropriateness Criteria
  http://www.acr.org/secondarymainmenucategories/quality_safety/app_criteria.aspx
- Image Wisely Campaign (Adult)
  http://www.rsna.org/Media/rsna/upload/Wisely_525.pdf
- Image Gently Campaign (pediatrics)
  http://www.pedrad.org/associations/5364/ig/
- Health Physics Society
  http://hps.org/physicians/blog/
  http://hps.org/publicinformation/asktheexperts.cfm

References

Mettler FA Jr, Huda W, Yoshizumi TT, Mahesh M. Effective doses in radiology and diagnostic nuclear medicine: A catalog. Radiology 248(1):254–263; 2008. Available at: http://radiology.rsna.org/content/248/1/254.long. Accessed 8 May 2011.

National Council on Radiation Protection and Measurements. Ionizing radiation exposure of the population of the United States. Washington, DC: National Council on Radiation Protection and Measurements; NCRP Report No. 160; 2009. Summary of the report available at: http://www.ncrponline.org/Press_Rel/Rept_160_Press_Release.pdf. Accessed 8 May 2011.

2

INTRODUCTION TO RADIOLOGY CONCEPTS

Objectives:

1. Identify the four naturally occurring densities visible on a conventional radiograph in order from highest to lowest density.
2. Define and give two examples of the silhouette sign on a frontal chest radiograph.

Radiographic Densities

Let us disregard the anatomy seen on the radiograph for now and concentrate on basic radiographic principles. In Fig. 2.1, you can see examples of the four basic densities, bone, soft tissue, fat, and air, which are visible on a conventional radiograph.

Main Radiographic Densities

1. *Bone* – This is the most dense of the four basic densities and appears white or "radiodense" as radiologists prefer to say.
2. *Soft tissue* – All fluids and soft tissues have the same density on a conventional radiograph. This density is slightly less than bone but slightly greater than fat. One advantage of CT scanning is that various soft tissues and fluids can be discriminated as different radiographic densities to a much greater degree than conventional radiographs.
3. *Fat* – This density may seem the least obvious to you. Fat can be seen interposed between various soft tissue and fluid densities. Abdominal fat allows us to see the edges of various soft tissue structures since the fat is slightly less dense than the organs themselves.

H Singh and JA Neutze (eds.), *Radiology Fundamentals: Introduction to Imaging & Technology*, DOI 10.1007/978-1-4614-0944-1_2,

© Springer Science+Business Media, LLC 2012

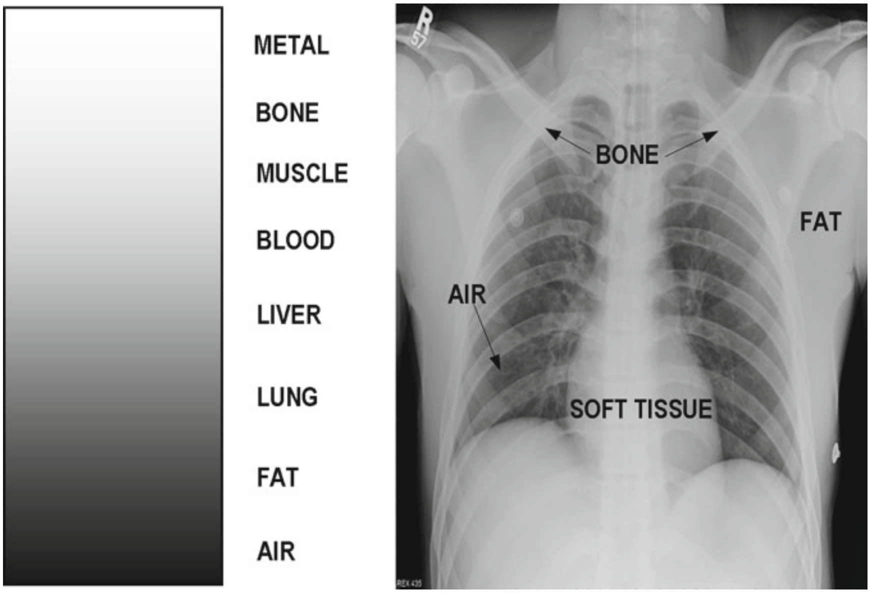

FIGURE 2.1 - RADIOGRAPHIC DENSITIES
Note how the four basic densities are visible on a chest radiograph

4. *Air* – The lungs, the tracheal lumen, and the air surrounding the patient are examples of air densities. Air densities are generally quite dark, almost black, on the radiograph. Thus, the lungs are not radiodense but are instead said to be "radiolucent." Why does the air in the lungs appear less black (more radiodense) than the air around the patient? This is because the air density in the lungs is added to the densities of the superimposed chest wall structures.

There is an additional density on some radiographs which may be more dense than bone: metal density. This is not included in the above classification because it is not a naturally occurring density. Examples of metallic density on the radiograph include orthopedic hardware, the wire sutures in the sternum in the patients who have undergone cardiac surgery, and the wire leads seen in a pacemaker.

Radiographic densities are normally additive in an arithmetic way. This means that a soft tissue density which is twice as thick as an adjacent soft tissue structure will be twice as white. Conversely, a structure which is half as dense as an adjacent structure but twice as thick will demonstrate an identical radiographic density.

The Silhouette Sign

What is the effect of juxtaposition of structures of varying density upon each other? When two structures of different densities are adjacent (i.e., abutting each other), the interface between them will be clearly delineated on the radiograph. For example, the soft tissue density of the heart is clearly delineated from the air density of the lung along the cardiac border (see Fig. 2.2). However, when two structures of the same density are adjacent or overlapping, their margins cannot be distinguished. For example, when pneumonia fills the alveoli of the right lung with fluid the lung becomes fluid density and the normal interface between the right heart border (soft tissue density) and the lung (air) may become invisible; the right heart border can no longer be seen.

This is called the silhouette sign and is one of the most useful principles in radiology.

Other examples of the silhouette sign include the following:

1. The heart cannot be distinguished separately from the blood within the cardiac chambers because both are soft tissue/fluid density.
2. The dome of the liver and the inferior aspect of the right hemidiaphragm cannot be distinguished radiographically since both are soft tissue density. You would

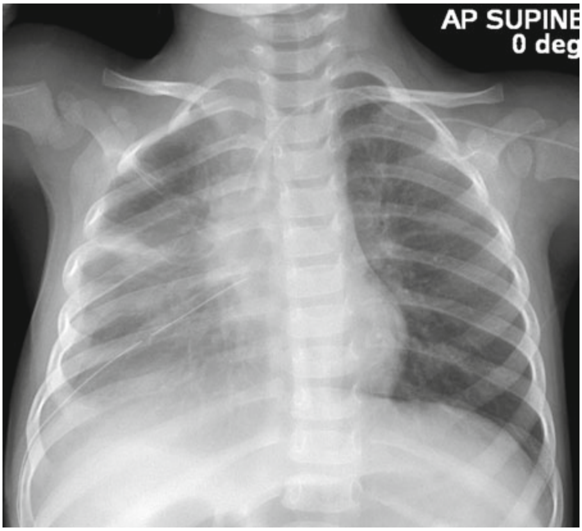

FIGURE 2.2 - THE SILHOUETTE SIGN
A right middle lobe pneumonia illustrates silhouetting of the right heart border by the area of consolidation. Compare to the crisp left heart border

only see the dome of the liver and the right hemidiaphragm separately when free intraperitoneal air is present. This is because the air density is interposed between the two soft tissue densities.

The silhouette sign will be used repeatedly in all sections of this textbook and in interpreting radiographs clinically. It is very important that you have a clear understanding of this principle.

3

CONVENTIONAL RADIOLOGY

Objectives:

1. State the convention for describing standard radiographic projections.
2. Explain why cardiac size differs on AP vs. PA radiographs.
3. Define the "lordotic projection" view and two indications for its use.
4. Discuss how the following variables and techniques may alter the appearance of a conventional chest radiograph: underexposure, rotation, inspiration, and expiration.

The main purpose of this chapter is to demonstrate the effect of various technical factors on the appearance of conventional radiographs.

The Radiograph Projection

The radiographic projection is named according to the direction in which the X-ray beam passes through the body of the patient when the radiograph is taken (Fig. 3.1).

In other words, if the X-ray detector was placed behind the patient and the X-ray tube was placed in front of the patient, the X-rays would pass from the front of the patient through the back of the patient onto the X-ray detector in an anteroposterior (AP) radiograph. In a posterior–anterior (PA) radiograph the detector is located along the anterior aspect of the patient's body with the X-ray tube posterior to the patient. In this situation, the X-ray beam passes through the patient from posterior to anterior.

Note the difference in the size of the heart shadow between the AP and PA radiograph in Fig. 3.1. Because X-rays diverge from a point source, objects which are

---

H Singh and JA Neutze (eds.), *Radiology Fundamentals: Introduction to Imaging & Technology*, DOI 10.1007/978-1-4614-0944-1_3,
© Springer Science+Business Media, LLC 2012

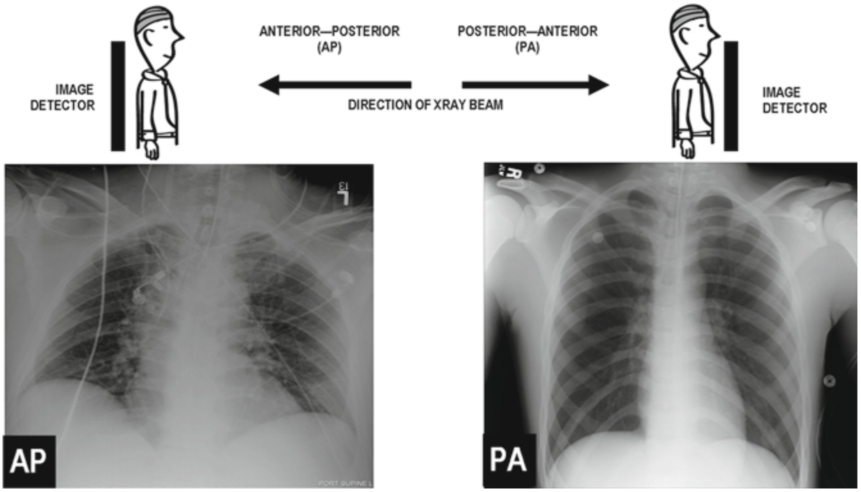

FIGURE 3.1 - THE AP AND PA VIEWS
How does this affect the appearance of various anatomical structures in the chest?

situated farther from the detector will cast a larger shadow. Since the heart is an anterior structure, it will be magnified more on the AP radiograph because the anterior structures are farther from the radiographic detector. Demonstrate this principle for yourself by shining a flashlight on your hand so that it casts a shadow on the wall. The farther your hand is from the wall (which in this case acts like the X-ray detector) the more magnified and fuzzy the shadow becomes.

Next, look at Fig. 3.2. This is the “Lordotic Projection.” With this projection, the X-ray source is angled toward the head and the clavicles project superior to the lung apex on the radiograph. This view is used to detect possible apical abnormalities such as tuberculosis or a lung tumor in the apex, called a Pancoast tumor. CT scans are now more commonly used because of increased sensitivity and specificity relative to the apical lordotic chest X-ray.

Look at Fig. 3.3. The heads of the clavicles and the spinous processes have been marked on the diagram. Since the clavicular heads are anterior structures and the spinous processes are quite posterior, they will move in opposite directions on the radiographs relative to a central axis of rotation. Using this principle of rotations, acquiring two radiographs, one in straight PA and one in slight rotation may help to determine the position of an abnormality in the lung.

Finally, note Fig. 3.4. The two radiographs were obtained within minutes of each other. Although this is an extreme example, it is important to realize that radiographs exposed at less than full inspiration produce artifactual crowding of the pulmonary vasculature, which can simulate pulmonary edema.

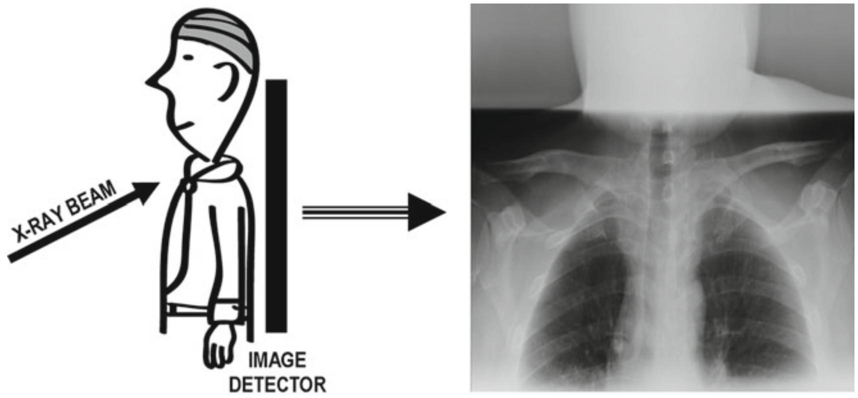
X-RAY BEAM
IMAGE
DETECTOR

FIGURE 3.2 - THE LORDOTIC PROJECTION
The lordotic view is especially useful for visualizing the lung apices. The clavicles are projected cephalad, allowing a clear view of the lung apices

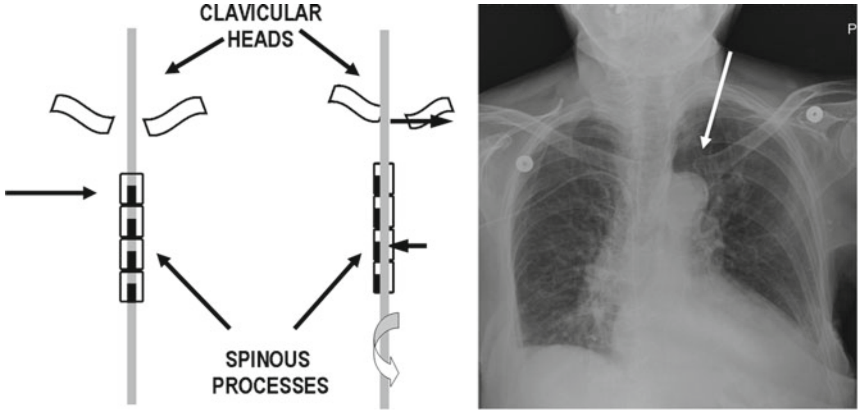
CLAVICULAR
HEADS
SPINOUS
PROCESSES
P

FIGURE 3.3 - ROTATION OF THE CHEST
In this illustration, note how the clavicle heads and spinous processes of the vertebral bodies appear in the AP position and with rotation of the chest to the left. On the chest X-ray, the *arrow* points to the left clavicular head, indicating that the patient is rotated to the left

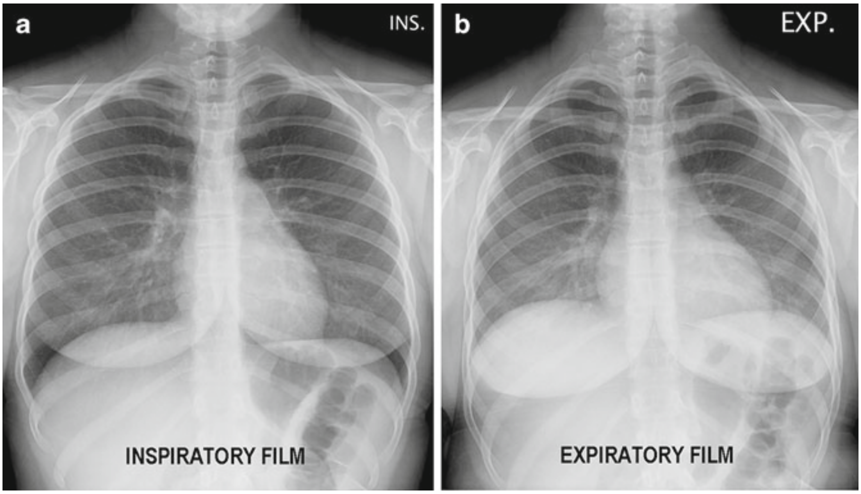

FIGURE 3.4 - INSPIRATORY AND EXPIRATORY FILMS
The radiographs here are those of inspiration and expiration. Note the difference in the size of the lungs and their apparent difference in densities

In some situations, expiratory radiographs are intentionally obtained. The most common situation is when looking for a small pneumothorax. In this situation, the pneumothorax will become slightly larger relative to the lung as air is expired.

Next examine Fig. 3.5. Can you find examples of the four basic densities? Can you find examples of summation of radiographic densities due to superimposition of structures? Superimposed kidneys and stool-filled colon will be more dense than each structure by itself. Examples of the silhouette sign? Kidneys adjacent to liver or spleen will silhouette and obscure each other' margins.

And last, but certainly not least, Fig. 3.6 is an image from a normal air contrast barium enema. This demonstrates how certain substances such as barium can be used to make certain anatomic structures more visible on the radiograph (in this case, barium and air in the large bowel).

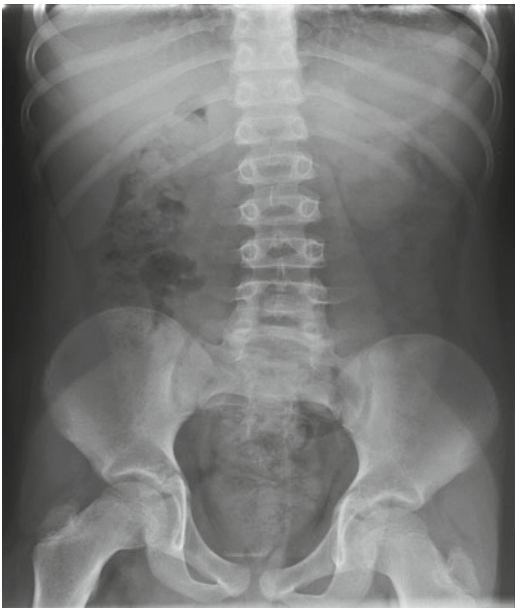

FIGURE 3.5 - NORMAL KUB

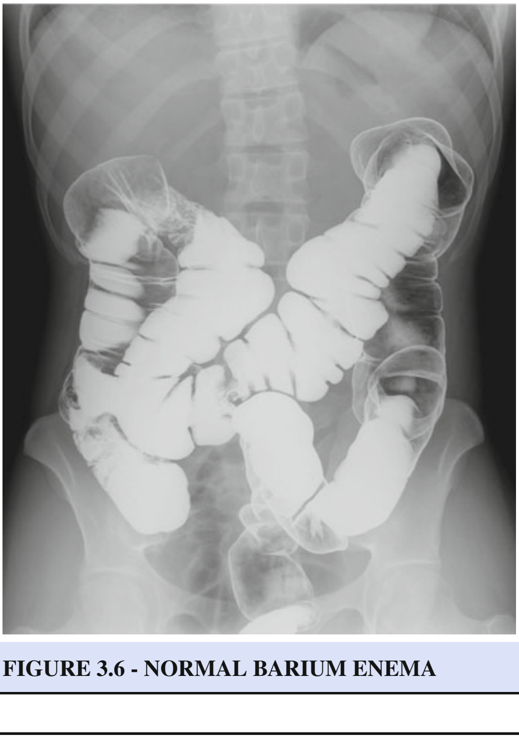

FIGURE 3.6 - NORMAL BARIUM ENEMA

4

ULTRASOUND

Objectives:

1. State the function of the transducer used in ultrasonography.
2. Define the term "sonolucent."
3. Give examples of structures that transmit sound well and that transmit sound poorly.

Ultrasound

Ultrasound uses no ionizing radiation and it can image directly in any body plane. In practice, an ultrasonographer (either a technologist or a radiologist) places gel on the patient's skin and moves a transducer across the surface of the patient's body. The gel forms an acoustic seal between the transducer and the skin for better transmission of sound, which results in better images.

The transducer can both send out and receive high frequency sound waves which transmit through, or reflect off, structures in the body. The returning sound waves are categorized by their intensity (referred to as echogenicity) and duration of time that it takes for them to return. It is the time that it takes for the echo to return from its encounter with an acoustic interface, i.e., a structure within the body which reflects sound, that allows its location within the image to be assigned (Fig. 4.1).

The intensity of the returning echo (echogenicity) of tissues varies greatly. Some tissues, like abdominal fat, are higher in echogenicity than other soft tissues. On the ultrasound image, such structures will appear "whiter," and are described as being "increased" in echotexture or "hyperechoic." Tissues/interfaces that return echoes of lower intensity are displayed as "darker" on ultrasound images and are described as "decreased" in echotexture or "hypoechoic." By evaluating the echotexture of tissues, we can distinguish one organ from another and look for pathologic processes.

H Singh and JA Neutze (eds.), *Radiology Fundamentals: Introduction to Imaging & Technology*, DOI 10.1007/978-1-4614-0944-1_4,
© Springer Science+Business Media, LLC 2012

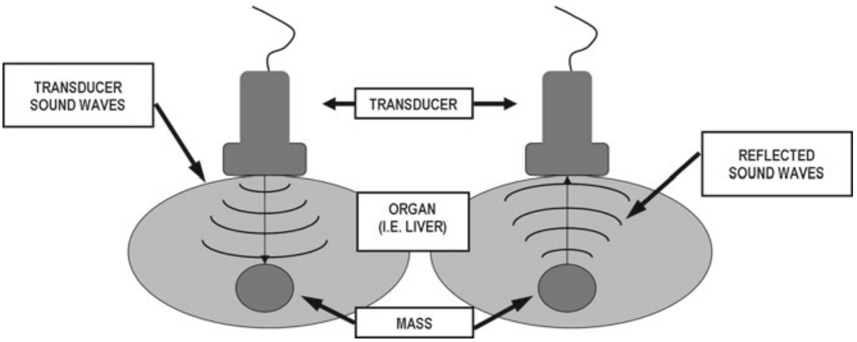

FIGURE 4.1 - ULTRASOUND
The ultrasound transducer acts similar to the sonar on a submarine. The transducer sends a short burst of high frequency sound into the tissue. Some part of the sound is reflected back by the tissues and the reflected signal is "read" by the transducer and an image is created

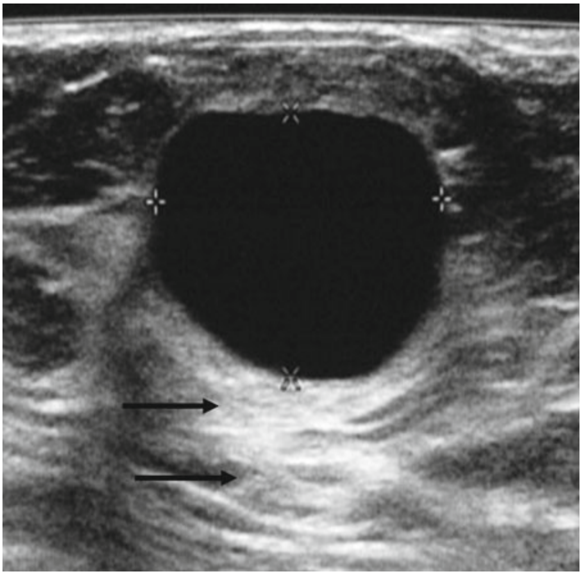

FIGURE 4.2 - SIMPLE BREAST CYST
"Anechoic" cyst, having no internal echoes. Note the increased echogenicity (arrows) beneath the cyst, referred to as "acoustic enhancement"

Fluid-filled structures (such as the gallbladder or urinary bladder) have few or no internal acoustic interfaces and hence appear "clear black" or sonolucent on ultrasound. Look at the simple cyst found when scanning the breast of a patient in Fig. 4.2. Note that the cyst depicted in this image is "anechoic," having no internal echoes.

$$X \propto \left(\frac{1}{D}\right)^2$$

FIGURE 4.3 - INVERSE SQUARE LAW
This is the inverse square law, as it applies to radiography, where X is the exposure at a given distance, D, from a radiation source. If, for example, the distance is doubled, the exposure would be one-fourth of its original strength

Sound waves traveling through the fluid-filled cyst lose less energy (since they encounter fewer acoustic interfaces). For this reason, they can reflect back to the transducer with more intensity when they reach the far wall of the cyst. This phenomenon is referred to as "acoustic enhancement" (arrows).

Some structures that are very dense, such as calcified structures or bone, will prevent sound waves from passing beyond them. As a result, there is no imaging information that can be obtained deep to those structures. A dark band-like "shadow" is produced beyond the echodense structure. This dark shadow can be quite prominent, helping identify even very small calcifications, such as kidney stones.

Orientation as to the direction of the "plane of section" in an ultrasound scan is aided by the indicator in the alpha-numeric label on each image. Some sections are slightly oblique (not in any of the three traditional planes of anatomic section). It is the ultrasonographer who has the advantage of knowing in which plane the view was obtained.

Scans are normally viewed in "real-time." This means that structures can be seen to move in the image (for example, cardiac valves) and structures can pass into and out of the field of view. The images that the ultrasonographer records are only selected "frozen" images from an extensive examination. In some situations, it may be advantageous to record the examination in real time, known as a video or cine clip.

Ultrasound weakens or attenuates rapidly by the inverse square law with distance from the transducer; (Fig. 4.3) therefore, structures closer to the transducer are better visualized. Many transducers have been adapted to get them close to the imaged structures. Transducers are included on endoscopes, allowing assessment of the duodenum, common bile duct, and pancreas. An endovaginal transducer provides very detailed imaging of the uterus and ovaries. Endorectal transducers allow high-resolution imaging of the prostate and rectum.

Color and Power Doppler Imaging in Ultrasound

When an ultrasound beam encounters a moving structure, a change in the pitch or frequency of the returning echo, compared to the echo sent out by the transducer, occurs. This is called the Doppler shift and it is encountered in "real life" when you hear a siren from a car as it drives past you: the siren changes pitch or frequency. By using information generated by this Doppler shift, images can be generated, giving information about the speed and direction of the moving structure. This is most commonly used in evaluating blood vessels and blood flow. In conventional color Doppler, the displayed color identifies the direction of flow as well as the speed of flow. Power Doppler, which measures the concentration of moving structures, is more sensitive to low flow states, but does not allow an evaluation of direction or speed.

Calculating the velocity of moving red blood cells numerically can allow an estimation of the diameter of the vessel in which the cells are flowing. This is the basis of arterial spectral (duplex) assessment in the carotids and extremities. A spectral Doppler study will display gray-scale images, color images, and wave-form images of the vessel being evaluated. As the vessel lumen narrows, generally the velocity of red cells moving through it increases. By using multiple calculations along the path of the vessel, multiple velocity measurements and ratios of velocities can be calculated, allowing one to diagnose, quantify, and monitor focal areas of vascular narrowing.

Color/power Doppler and spectral imaging is used to assess for possible clot in veins, evaluate areas of arterial narrowing/stenosis, e.g., carotid stenosis, and to determine if masses and organs have increased blood flow to them. You might see increased blood flow in a malignant tumor or reduced blood flow in a torsed testicle or ovary. Doppler imaging is also used to diagnose vascular malformations and assess for the presence of varicose veins.

Indications for Ultrasound Use

Ultrasound usually works best in thinner individuals, since the transducer is closer to the imaged structures in those patients. For larger patients, ultrasound can be limited. Ultrasound is particularly useful in evaluation of the upper abdomen, female pelvis organs, and superficial structures like the thyroid, breast, and scrotum. Ultrasound can also be used to guide the placement of needles into structures during biopsy or fine needle aspiration. It allows one to see the needle moving in real time as it enters the target, whereas in CT-guided biopsies, the images are obtained after the needle has been advanced into the organ/mass.

Since ultrasound does not use ionizing radiation, it is one of the safest imaging modalities for women of reproductive age and young children. It is ideal for prenatal imaging.

Ultrasound is least useful in the chest since air in the lung is a relatively poor transmitter of sound. For this reason, ultrasound also does not work well in patients with large amounts of bowel gas. It is also of limited use in the head since the dense bony skull is a poor transmitter of sound, primarily reflecting it. However, ultrasound can be used to examine the brains of infants since access to the intracranial structures can be achieved through the open fontanels.

5

COMPUTED TOMOGRAPHY

Objectives:

1. State how the densities on a CT scan are assigned.
2. Define the terms “pixel” and “voxel.”
3. Compare and contrast the spatial and density resolution achieved with a CT scan with that of conventional radiographs.
4. State how to determine if contrast material is used when viewing a CT.

CT Imaging Orientation

Computed tomography (CT) uses ionizing radiation to create a cross-sectional image. This allows visualization of a greater variety of tissue structures beyond the four basic densities (air, bone, soft tissue, and fat) that are seen on a conventional radiograph. Unlike conventional X-rays, which utilize one projection to form an image, CT uses multiple small projections across the body and combines the information to form the image. It is this combining of the images that allows greater soft tissue detail to be displayed.

Each individual picture of a CT study is referred to as a section or an axial “slice.” This is because the picture must be interpreted as if the patient has been completely sectioned in an axial plane, like a loaf of bread, with the viewer looking at the section from the feet toward the head (Fig. 5.1).

Pixels and Voxels

If you look closely at the CT scan, you will realize that the picture is actually made up of thousands of little squares called “pixels” (picture elements). Each pixel represents tissue that is about 1 mm or less on each of the two sides, and is assigned

H Singh and JA Neutze (eds.), *Radiology Fundamentals: Introduction to Imaging & Technology*, DOI 10.1007/978-1-4614-0944-1_5,
© Springer Science+Business Media, LLC 2012

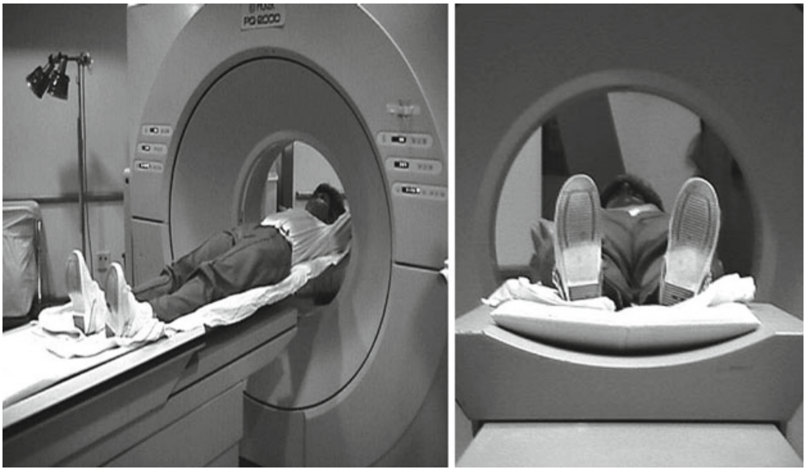

FIGURE 5.1 - COMPUTED TOMOGRAPHY (CT)
The patient is placed in the CT gantry and images are obtained in axial sections called "slices." When reviewing the images, the radiologist interprets each image as if (s)he were at the patient's feet, looking toward the patient's head

a gray-scale value from 0 (black) to 255 (white). The gray-scale value reflects how much of the X-ray beam that small piece of tissue (represented by the pixel) attenuated or "blocked" as it was passing through the patient. Darker shades (closer to black) represent structures that attenuate very little of the beam (like gas) while whiter shades represent structures that strongly attenuate the beam (like bone or calcification) (Fig. 5.2).

The thickness of the slice of a CT study is typically 1 mm or less, thus creating a three-dimensional volume element or "voxel" which is shaped like a cube. The word voxel is short for "volume pixel," the smallest distinguishable box-shaped part of a three-dimensional image. Pixel intensity represents an average from tissue within the "voxel." Although the spatial resolution of the CT scan is less than that of a conventional radiograph, the density resolution is much greater. Earlier models of CT scanners used the "step and shoot" method to acquire images. While lying on a motorized table the patient was slowly moved into the scanning gantry and a single slice was obtained while the patient was asked to hold his or her breath. These scanners, though remarkable for their generation, sometimes caused small pathology to be "missed" as patients would not hold their breath in the same fashion each time. These studies had long acquisition times.

Current generation scanners move the patient continuously through the scanning gantry during a single breath-hold. The patient is advanced while the X-ray tubes

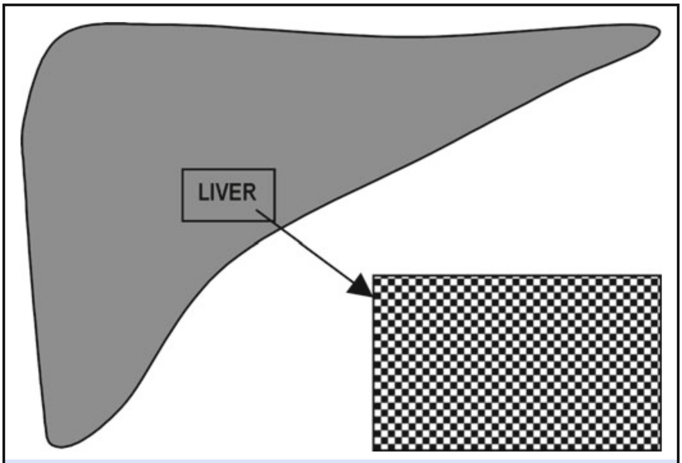

FIGURE 5.2 - CT PIXELS CONCEPT
As you look at the CT slice, it is important to keep in mind that each image is really made up of thousands of pixels (picture elements), each of which represents tissue which is about 1 mm^2

continuously rotate, acquiring a data set that is much like a spiral in configuration (thus the name “spiral CT”). Current scans are performed much more rapidly than with the old “step and shoot” method. The data can then be reformatted into coronal, sagittal, and oblique planes. Current scanners have the capability of obtaining voxels of data so small that the reformatted images in other planes offer nearly identical resolution.

CT Values or Hounsfield Units

The amount of the X-ray beam that a particular voxel of tissue attenuates can be represented by a number called the Hounsfield Unit (HU), named after Sir Godfrey N. Hounsfield, an electrical engineer who won the Nobel Prize in 1979 for his pioneering work in the development of CT. By looking at the Hounsfield Unit value of a structure, you can get an idea of what types of tissue may be present (bone, calcification, water, blood, etc.). Also, by looking at changes in the Hounsfield Unit value of tissue on images obtained before intravenous contrast compared to after intravenous contrast, you can determine how vascular a structure is. Listed in Table 5.1 below is a basic guide to HU values prior to contrast.

Table 5-1 Typical HU for different tissues

Substance	Hounsfield units (HU)
Air	−1,000
Fat	−100
Water	0
Muscle/soft tissue	+40
Contrast	+130
Bone	+1,000

Contrast Studies

Intravenous contrast as well as oral and sometimes rectal contrast agents may be used in CT scans. The small “+C” label in the alpha-numeric image of each section indicates that intravenous contrast was used. Also, if the aorta, kidneys or ureter are radiopaque or white, it is a good indication that IV contrast was used. If the stomach, small or large bowel is radiopaque, oral contrast has been given.

Optimizing the Visualization of Specific Structures

Since CT scans are created from digital data, the gray-scale display can be manipulated in such a way as to display the same information in various formats. These different formats are called window settings and amount to changing the total number of gray scales displayed and the value at which the gray scale is centered. Such changes determine which type of tissue is best displayed even in the same body “slice.” Commonly used window settings include soft tissue (mediastinal and abdomen), bone and lung (pulmonary). In Fig. 5.3, you see the same image displayed using different windows. In the mediastinal window, soft tissue structures are discernable from each other. In the pulmonary window, the lung parenchyma is well seen but the soft tissue structures all look the same. Additional electronic manipulation with filters and subtraction will provide more information and perhaps answer the clinical question that the raw images can only infer.

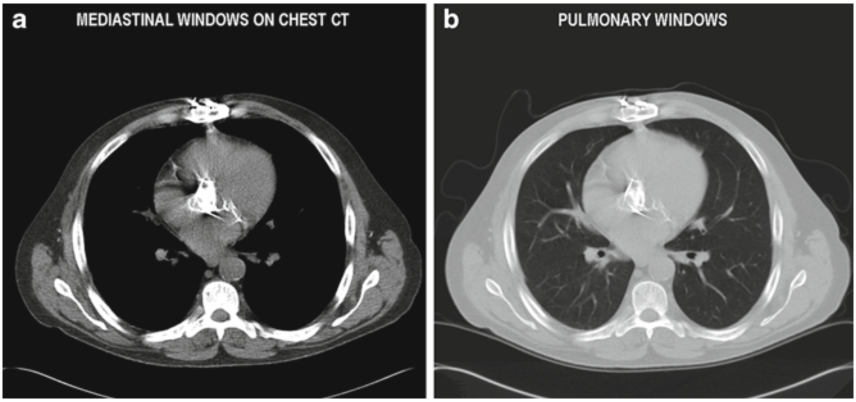
a
MEDIASTINAL WINDOWS ON CHEST CT
b
PULMONARY WINDOWS

FIGURE 5.3 - CT SCAN OF THE CHEST
Note how the mediastinal windows (**a**) allow for optimal visualization of the mediastinal structures and the pulmonary windows (**b**) for lung parenchyma

6

MRI

Objectives:

1. Identify and characterize the tissue appearance of normal and common abnormal findings on CT and MRI.
2. State one advantage and three disadvantages that MRI has over CT.

Magnetic resonance imaging (MRI) has its greatest application in the fields of neuroradiology and musculoskeletal radiology.

To form a magnetic resonance image, the patient is placed in a strong uniform magnetic field. The magnetic field aligns hydrogen nuclei within the patient in the direction of the field. The nuclei are "disturbed" from this orientation by application of an external radiofrequency (RF) pulse. After the RF pulse is stopped, the hydrogen nuclei return to their alignment within the externally imposed magnetic field, giving off RF signals as they lose energy (Fig. 6.1).

The frequency of the RF signal emitted from the hydrogen nucleus as it returns to its orientation within the field is determined by the strength of that field. Therefore, the location of the RF signal given off by each hydrogen nucleus can be calculated. Each RF signal is analyzed by the computer for its intensity and other criteria. The signals are then assigned gray-scale values (white to black) on the detector by the computer. Since this process of creating an image based on tissue characteristics is completely different from the absorption of X-rays by different tissues, MRI images can show different types of pathologies, hence its utility. For example, MRI can discriminate soft tissue differences better than CT scans and is often used to define soft tissue abnormalities like herniated discs, ligament tears, and soft tissue tumors in the spine.

There are two basic sequences in MRI that are important to understand and recognize. These sequences are known as the T1-weighted and T2-weighted sequences. The "weighting" represents the exploitation of specific properties of hydrogen atoms that are exposed to a magnetic field. T1-weighted images classically

H Singh and JA Neutze (eds.), *Radiology Fundamentals: Introduction to Imaging & Technology*, DOI 10.1007/978-1-4614-0944-1_6,
© Springer Science+Business Media, LLC 2012

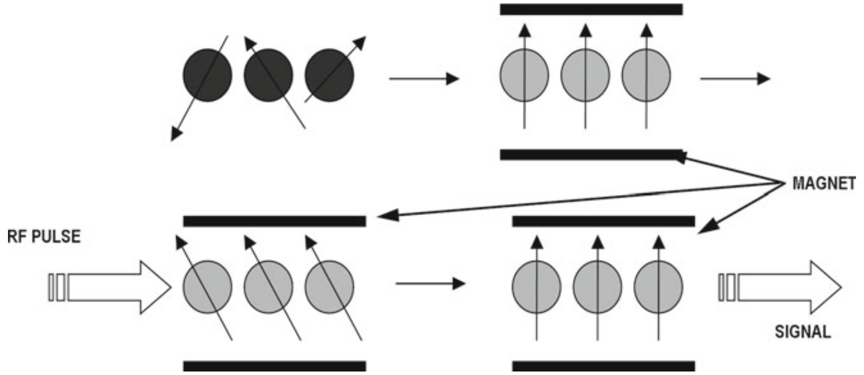

FIGURE 6.1 - MAGNETIC RESONANCE IMAGING – HYDROGEN NUCLEI
In their natural state, hydrogen atoms are spinning with their axes of rotation randomly oriented. When placed in a magnetic field, they align in a uniform direction. An RF pulse is applied, knocking the H-atoms out of their magnetic field orientation. Once the RF pulse is stopped, the atoms return to their previous alignment, giving off a signal which is then used to form the image

demonstrate water as hypointense (dark) and fat as hyperintense (bright), with different soft tissues expressed as a gradient in between. In T2-weighted images water is represented as hyperintense and fat as hypointense (again with soft tissues in the middle). Many of the more complicated sequences (Gradient Echo, FLAIR, etc.) are based on these basic sequences.

Advantages and Disadvantages of MRI

With the advent of multislice CT scanners, CT scans can be acquired or reformatted in many planes. Therefore, a prior advantage that MRI had, exclusive multiplane capacity, is nearly gone. However, MRI's clear advantage is that it uses no ionizing radiation. Disadvantages of MRI are that it is generally more costly than CT, less available, and takes longer to perform. Another disadvantage is the inability to scan patients who have ferromagnetic material such as shrapnel. These metallic fragments can actually move with the magnetic field and cause the patient significant discomfort or damage. Although MRI-compatible pacemakers are in development, generally speaking pacemakers are contraindicated because of their ferromagnetic properties; the MRI can heat the leads and inappropriately trigger the pacemaker. But some metal, based on location, type, or duration in place may not be a contraindication to an MRI. Check with your patient's radiologist if you are not sure if your patient is an MRI candidate.

7

NUCLEAR MEDICINE

Objectives:

1. To understand the definition of the term radiopharmaceutical.
2. To understand how the component parts of a radiopharmaceutical contribute to a diagnostic nuclear medicine image.

Introduction to Nuclear Medicine

The first step in any nuclear medicine diagnostic imaging study involves the administration of a radiopharmaceutical to a patient. A radiopharmaceutical is a chemical combination of a radionuclide and a pharmaceutical (Fig. 7.1). A radionuclide is an unstable isotope of an element which emits radiation to achieve stability. When this radiation is in the form of gamma rays, it can be detected by a nuclear medicine gamma camera (Fig. 7.2). A pharmaceutical is a compound which localizes in normal or diseased tissue. A nuclear medicine image depends on the physiologic distribution of the pharmaceutical which is administered.

For instance, a bone scan is performed by injecting a patient with the radiopharmaceutical technetium 99m methylene diphosphonate (Tc-99m MDP). The pharmaceutical, methylene diphosphonate, is concentrated in the mineral phase of bone by osteoblasts. The radionuclide, Tc-99m, emits a 140-keV gamma photon which is easily detected by a gamma camera. Thus, a bone scan is an image of the distribution of functioning osteoblasts) (Fig. 7.3).

There are many different radiopharmaceuticals used in nuclear medicine. All of them are either swallowed by the patient, injected, or inhaled. The radiation clears from the patient's body by a combination of physiologic clearance of the pharmaceutical and physical decay of the radionuclide. The dose of radiation to the patient in a diagnostic study is generally very low, and does not harm the patient.

H Singh and JA Neutze (eds.), *Radiology Fundamentals: Introduction to Imaging & Technology*, DOI 10.1007/978-1-4614-0944-1_7,
© Springer Science+Business Media, LLC 2012

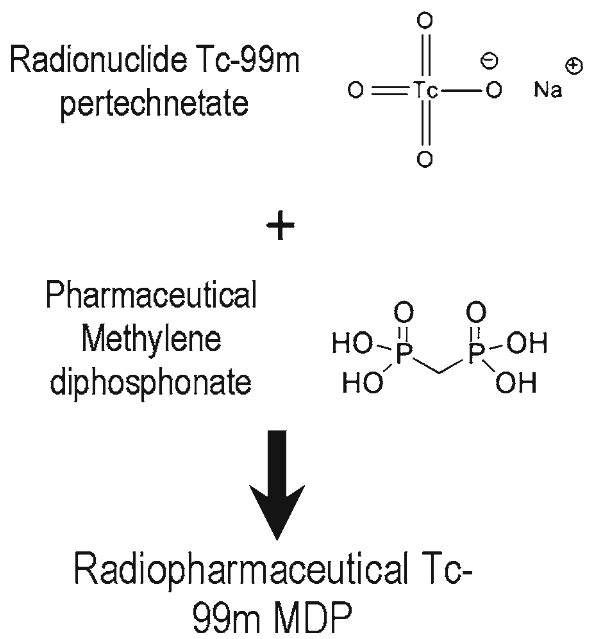
Radionuclide Tc-99m pertechnetate
O
O
Tc
O
O
Na
+
Pharmaceutical Methylene diphosphonate
O
O
HO
P
P
OH
HO
OH
Radiopharmaceutical Tc-99m MDP

FIGURE 7.1 - RADIOPHARMACEUTICAL
Figure showing example of how technetium 99m-methylene diphosphonate is created

However, each radiopharmaceutical has strict dose limits to prevent overexposing the patient, family, and community members to unnecessary radiation.

Upcoming chapters review common nuclear medicine studies of the heart, lungs, bone, and gastrointestinal tract. In addition, there is a chapter on oncologic imaging with PET/CT with radiopharmaceutical fluorine-18 fluorodeoxyglucose (F-18 FDG) (Fig. 7.3).

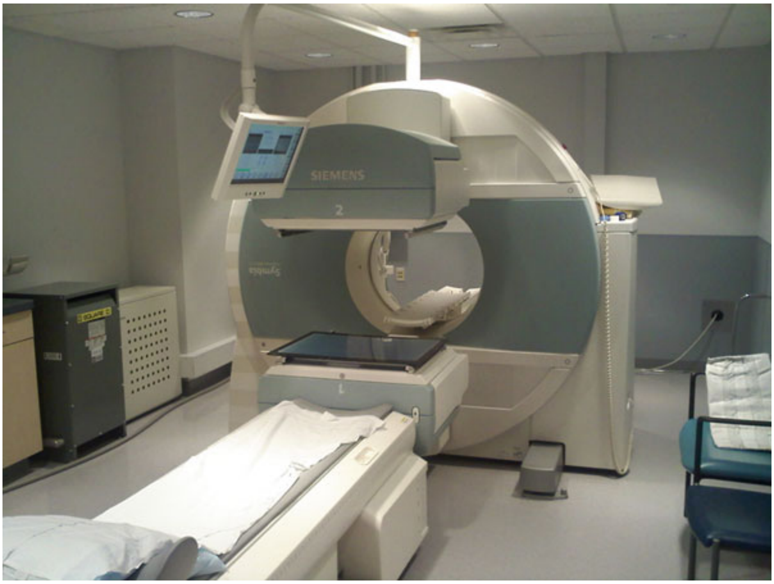

SIEMENS
2
Symbia

FIGURE 7.2 - EXAMPLE OF A GAMMA RAY DETECTOR AND CAMERA
The Gamma camera detectors can rotate around the patient for ease of multiplanar imaging

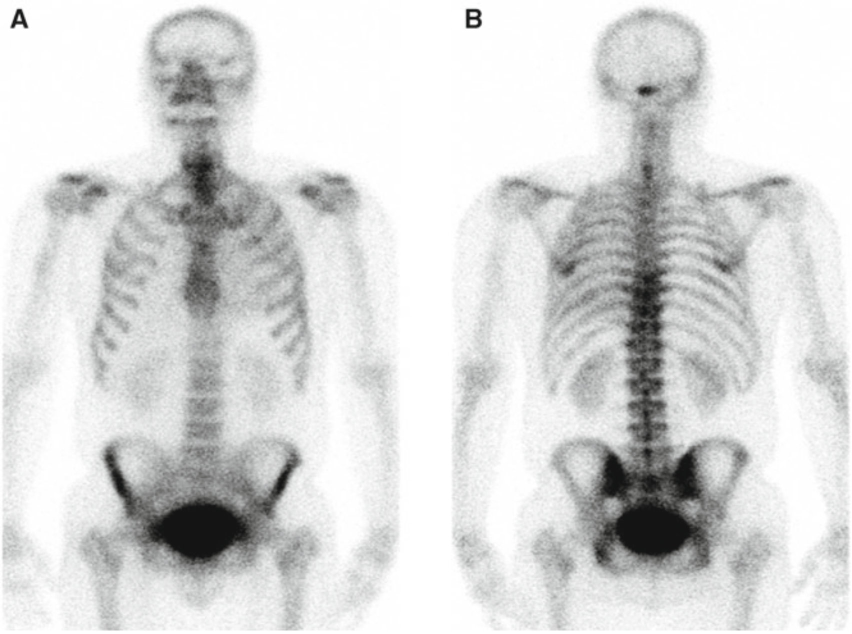

FIGURE 7.3 - TECHNETIUM BONE SCAN A-ANTERIOR, B-POSTERIOR
Normal anterior and posterior body images of a 50-year-old patient diagnosed with lung cancer. There is no abnormal radiotracer uptake noted to suggest metastatic disease. There is normal distribution of radiopharmaceutical in the bones and normal physiologic excretion of Tc-99m MDP by the kidneys into the urinary bladder

8

CARDIOVASCULAR AND INTERVENTIONAL RADIOLOGY

Objectives:

1. What is digital subtraction angiography (DSA)?
2. What types of procedures are performed in cardiovascular and interventional radiology (CVIR)?

In cardiovascular and interventional radiology (CVIR), a combination of needles, wires, catheters, balloons, and stents are used to accomplish many things through small access points in the skin.

Digital Subtraction Angiography

Arteriograms are used to diagnose the changes in the vasculature associated with atherosclerosis, vasculitis, and injury, either iatrogenic or traumatic. The femoral artery is a commonly used entry point and is accessed at the level of the femoral head where its position is relatively superficial; therefore, hemostasis can be achieved with ease as the artery can be compressed against the femoral head once the procedure is completed. Different catheters are used to access the branch arteries requiring imaging. Once the catheter is in the appropriate vessel, iodinated contrast is injected at a controlled rate and volume via an injector.

Imaging can be acquired on film radiographs (which are processed similarly to routine radiographs) or more commonly with digital subtraction angiography (DSA). In DSA, images are processed with the help of a computer. The initial image has no contrast and is called the mask. The X-ray images are then obtained in rapid sequence while contrast is injected. The computer then digitally "subtracts" the

H Singh and JA Neutze (eds.), *Radiology Fundamentals: Introduction to Imaging & Technology*, DOI 10.1007/978-1-4614-0944-1_8,
© Springer Science+Business Media, LLC 2012

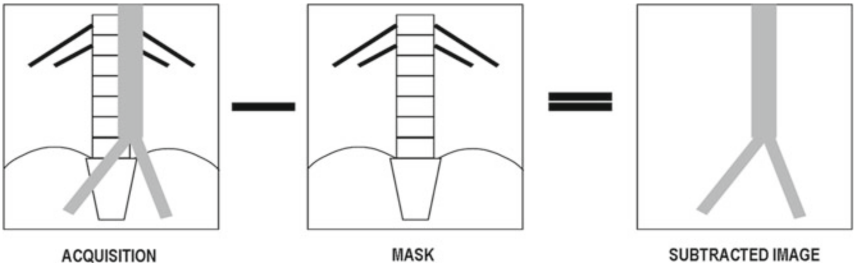

FIGURE 8.1 - DIGITAL SUBTRACTION ACQUISITION (DSA) CONTRAST IS INJECTED IN THE PATIENT'S AORTA AND IMAGES ARE ACQUIRED
Just before the contrast is injected, the computer acquired a mask, as seen in the center. As the contrast images are acquired, the computer subtracts the mask from the images leaving the only portion which has changed between the two, the intra-arterial contrast

mask from the subsequent images leaving only the contrast, thereby yielding fine detail imaging of the vasculature (Fig. 8.1).

If an area of stenosis or narrowing is identified, it can be treated using percutaneous transluminal angioplasty (PTA), with or without the use of a metallic stent. If blood flow cessation is required in an area of bleeding (e.g., after trauma) or as preoperative embolization, a catheter can be advanced to the vessel requiring embolization and different materials can be delivered into the artery to stop flow. Embolization materials include metallic coils, Gelfoam®, polyvinyl alcohol particles (PVA, fixed-size particulate material), alcohol, chemotherapeutic material, autologous clot, biocompatible glue, and other agents.

Central Venous Access

Central venous access can be accomplished in many different ways. There are catheters used for short-term to intermediate-term access such as the peripherally inserted central catheter (PICC) and nontunneled central lines. Long-term access catheters include tunneled infusion catheters and subcutaneous chest or arm ports. Dialysis access catheters such as tunneled hemodialysis catheters are also placed in the CVIR department. Access can be obtained with either vascular ultrasound, contrast venography, carbon dioxide venography, or by using anatomic landmarks. With the use of real-time imaging (fluoroscopy), placement of the line can be quick, accurate, and safe. Difficult access pathways can be potentially treated with angioplasty (balloon dilation) if necessary as well.

Other CVIR Activities

Gastroenteric access can also be performed entirely percutaneously. The placement of gastric tubes (G-tubes) or gastrojejunostomy tubes (G–J tubes) is accomplished with fluoroscopic guidance in a multiplanar fashion (many X-ray angles). The use of fluoroscopy allows the quick, accurate, and safe placement of gastroenteric tubes.

Pulmonary angiography and placement of inferior cava filters can both be performed through the same access point, whether the common femoral vein or the internal jugular vein. Careful evaluation of the inferior cava prior to filter placement should be performed to ensure proper positioning.

Genitourinary procedures are commonly performed in the CVIR department. The types of procedures include percutaneous nephrostomy placement (PCN), percutaneous nephro-lithotomy (PCNL), placement and exchange of nephroureteral stents (NUS) and ureteral ballooning.

Women's health interventions represent a subset of procedures focusing on gynecologic issues. The subset of procedures includes uterine fibroid embolization, ovarian vein embolization for pelvic congestion syndrome and fallopian tube recanalization.

Biliary procedures are commonly performed on patients who are clinically ill as a result of biliary obstruction. Percutaneous drainage with placement of an internal/external drainage catheter can be a precursor to surgical resection of a biliary or pancreatic mass. The biliary system is frequently decompressed on a long-term basis, so biliary tube maintenance is also conducted by Interventional Radiology. If the patient is not an operative candidate, an interventional radiologist can place metallic stents (similar to those used in the arterial system) into the biliary system. This palliates symptoms and improves quality of life without the need for external drains.

Other CVIR procedures and activities include but are not limited to the following:

1. Abscess drainage (using CT, ultrasound, and/or fluoroscopy)
2. Intraoperative cases (e.g., thoracic and abdominal aortic stent grafts)
3. Noninvasive cardiac and vascular imaging (e.g., cardiac MRI, coronary CT angiography, and duplex ultrasound)
4. Percutaneous oncologic interventions (e.g., transarterial chemoembolization, radiofrequency ablation, and cryoablation)
5. Percutaneous biopsies (using CT, ultrasound, and/or fluoroscopy)
6. Minimally invasive venous procedures (e.g., endovenous laser or radiofrequency ablation, sclerotherapy, and phlebectomy)

The scope of Interventional Radiology is quite extensive and diverse. The interventional procedures expand the diagnostic and therapeutic armamentarium of the radiology department.

9

HEART AND MEDIASTINUM

Objectives:

1. List the structures that normally form the left and right mediastinal borders on a PA chest radiograph.
2. State the criteria for cardiac size assessment on a PA chest radiograph, and technical factors which may affect this assessment.
3. Identify the radiographic divisions of the mediastinum and the differential diagnosis of masses arising from each division.

Cardiac Contours

When evaluating the cardiac/pericardial outline and mediastinal contours, it is easiest to follow the right and left borders that these structures make with the aerated lung. Although the mediastinum is optimally visualized by various cross-sectional imaging techniques, the initial stage of evaluation is often through plain radiographs.

The first convex segment along the left mediastinal border is the aortic knob formed by the aortic arch. The segment inferior to the aortic knob represents the main pulmonary artery. The large convex border inferiorly is formed by the left ventricle, with a small contribution from the left atrium. On the right, the shadow of the superior vena cava is visualized superiorly. The right lateral border of the right atrium forms the convexity seen inferiorly. These contours vary from individual to individual and certainly can change dramatically in abnormal situations. Any review of the cardiomediastinal silhouette should begin with an evaluation of these contours (Fig. 9.1).

H Singh and JA Neutze (eds.), *Radiology Fundamentals: Introduction to Imaging & Technology*, DOI 10.1007/978-1-4614-0944-1_9,
© Springer Science+Business Media, LLC 2012

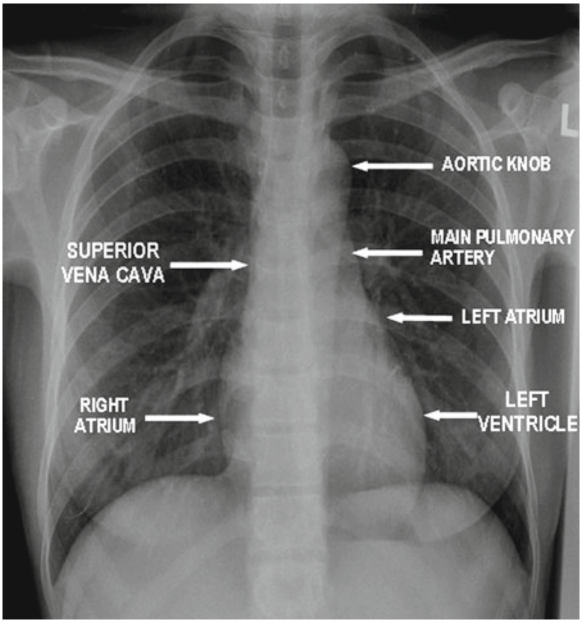

FIGURE 9.1 - CARDIAC CONTOURS

Cardiac Measurement on the Plain Radiograph

The largest structure occupying the mediastinum is, of course, the heart. Recall from an earlier chapter that the cardiac size may vary depending on the projection of the radiograph (PA vs. AP). On an upright PA radiograph, the heart is said to be normal if its transverse diameter is no greater than 50–55% of the transverse diameter of the internal bony thorax. This will not hold true on AP radiographs, since the heart will be artificially magnified. It may also not hold true in cases where the radiograph has not been exposed at total lung capacity. Figure 9.2 demonstrates both a normal and an enlarged heart and shows examples of the points of measurement for both the heart and thoracic dimensions.

The Mediastinum

It is important to know the distribution of lymph nodes in the chest, as their enlargement can change the appearance of the mediastinum on a chest radiograph. Figure 9.3 identifies where common lymph nodes are located. Figure 9.4 shows a lateral view

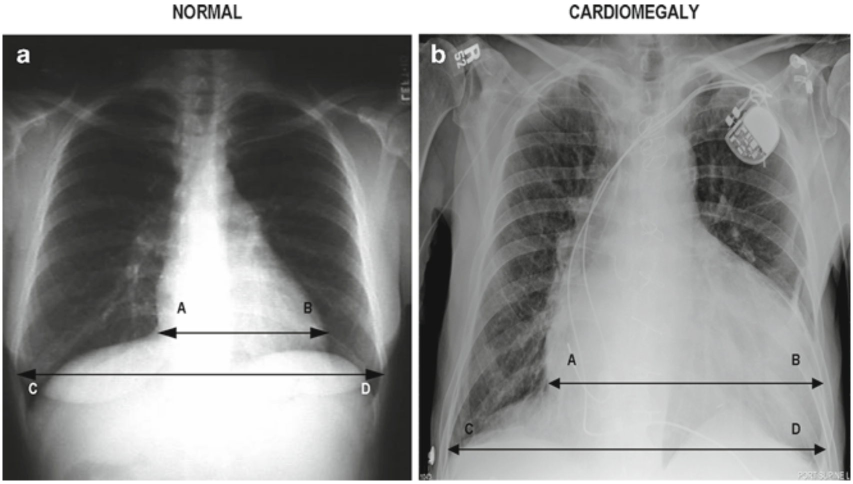

FIGURE 9.2 - MEASURING THE CARDIAC SILHOUETTE
(**a**) When evaluating the size of the heart, A–B should be 50–55% the measurement of C–D (the transverse thoracic diameter). (**b**) Shows marked enlargement of the cardiac silhouette with mild pulmonary vascular congestion. Note how the ratio of A–B to C–D is greater than 50%

of the chest demonstrating the divisions of the mediastinum: anterior, middle, and posterior. These are used in creating a differential diagnosis for mediastinal masses (Figs. 9.3 and 9.4).

Be sure to note that the radiographic divisions of the mediastinum differ from the anatomic definitions of the mediastinum. Anatomically the mediastinum is divided into a superior and inferior component with the inferior component subdivided into anterior, middle, and posterior compartments. Radiographically, we rely on the anterior, middle, and posterior designations from the top to the bottom of the thorax.

The anterior mediastinum is defined posteriorly by a line drawn along the anterior margin of the heart and ascending aorta. Normally, fat, thymic tissue and lymph nodes are present in this region. The posterior border of the middle mediastinum extends to the posterior border of the trachea and along the posterior surface of the heart. Middle mediastinal structures include the central airways, heart and great vessels and lymph nodes. The posterior mediastinum lies posterior to this and contains the esophagus, descending aorta, and paravertebral tissues. The differential diagnosis for mediastinal masses (Fig. 9.5) is not as important as having a systematic method for reviewing conventional radiographs to decide whether what you are seeing is normal or abnormal. CT is almost universally employed as a next imaging step when a questionable mediastinal mass is appreciated on the plain radiograph. In some cases, MRI is used for evaluation of mediastinal abnormalities as well.

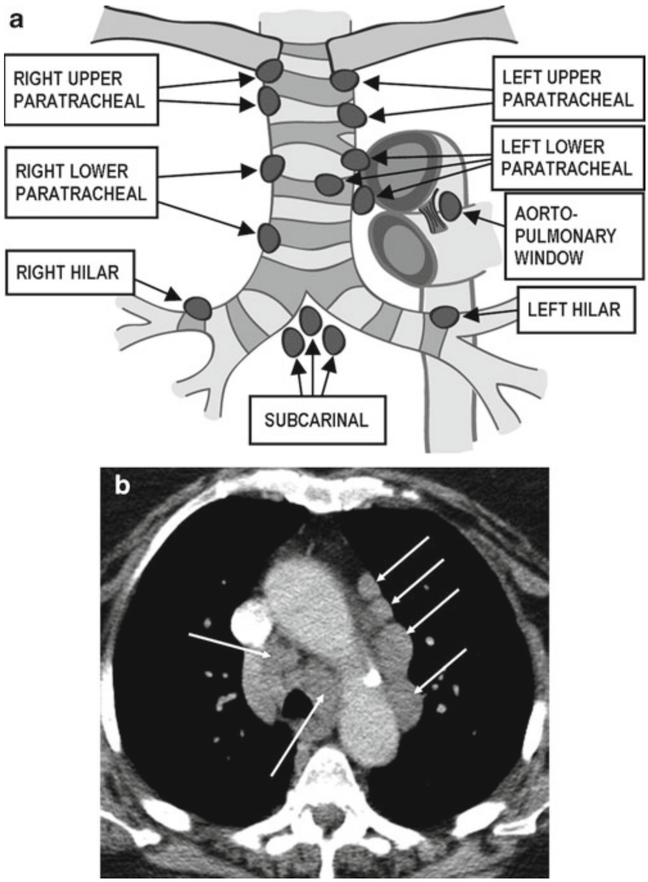
a
RIGHT UPPER PARATRACHEAL
RIGHT LOWER PARATRACHEAL
RIGHT HILAR
LEFT UPPER PARATRACHEAL
LEFT LOWER PARATRACHEAL
AORTO-PULMONARY WINDOW
LEFT HILAR
SUBCARINAL
b

FIGURE 9.3 - LYMPH NODES OF THE MEDIASTINUM
(**a**) It is important to know the location of the lymph nodes in the chest. Enlargement on these nodes can change the appearance of the mediastinum on a chest X-ray and so familiarity with their location is important. (**b**) An example of mediastinal lymphadenopathy on an axial CT slice

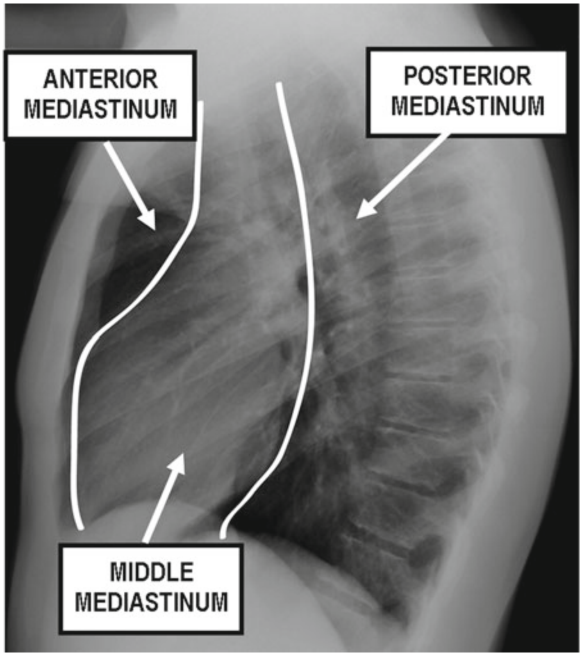

FIGURE 9.4 - THE MEDIASTINAL DIVISIONS
The subdivisions are the anterior, middle, and posterior mediastinum. These are important to know since they are critical to the differential diagnosis

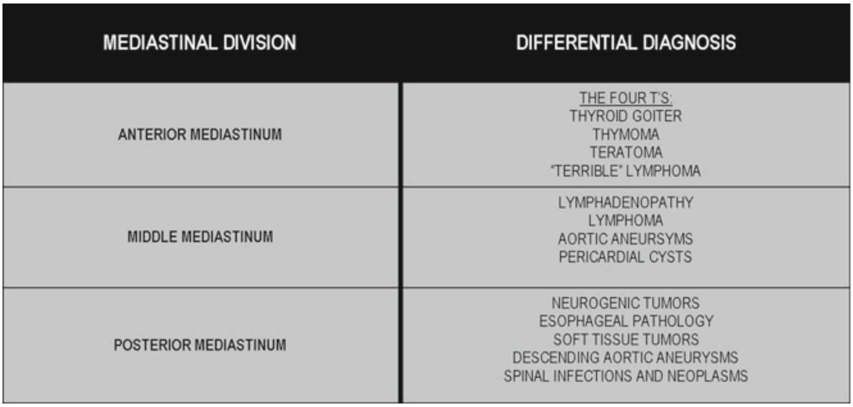

MEDIASTINAL DIVISION	DIFFERENTIAL DIAGNOSIS
ANTERIOR MEDIASTINUM	THE FOUR T'S: THYROID GOITER THYMOMA TERATOMA "TERRIBLE" LYMPHOMA
MIDDLE MEDIASTINUM	LYMPHADENOPATHY LYMPHOMA AORTIC ANEURSYMS PERICARDIAL CYSTS
POSTERIOR MEDIASTINUM	NEUROGENIC TUMORS ESOPHAGEAL PATHOLOGY SOFT TISSUE TUMORS DESCENDING AORTIC ANEURYSMS SPINAL INFECTIONS AND NEOPLASMS

FIGURE 9.5 - MEDIASTINAL MASSES
A differential diagnosis of mediastinal masses may be made by the primary site of origin of the mass

10

LATERAL CHEST

Objectives:

1. Use a systematic method for review of the left lateral chest radiograph.
2. List four methods by which the left and right hemidiaphragms can be distinguished on the lateral view.
3. State why the thoracic structures in a left lateral chest radiograph appear smaller than their counterparts on the right.

Begin by reviewing the systematic approach to the left lateral chest radiograph in Fig. 10.1.

One should view the retrosternal airspace, pulmonary arteries at the hilum, tracheal air column, retrotracheal triangle, large rectangular area extending inferiorly from the retrotracheal triangle to the diaphragms (with a gradual gradation of density from lighter to darker as one moves inferiorly), the costophrenic angles, their respective hemidiaphragms as one moves anteriorly, and finally the lung projected over the surface of the cardiac pericardial silhouette and hilar anatomical structures.

If you proceed in this manner on each radiograph, you will develop a consistent method for detecting abnormalities. This takes practice.

Chest Projection

Figure 10.2 is a schematic of a skin lesion arising from the soft tissues of the back which is projected over the right lung on the frontal view. The lateral view can be useful in ascertaining whether a structure lies within or outside the patient. Without a lateral view, the position of any abnormality projected over the lungs cannot be determined with certainty, in most cases.

H Singh and JA Neutze (eds.), *Radiology Fundamentals: Introduction to Imaging & Technology*, DOI 10.1007/978-1-4614-0944-1_10,
© Springer Science+Business Media, LLC 2012

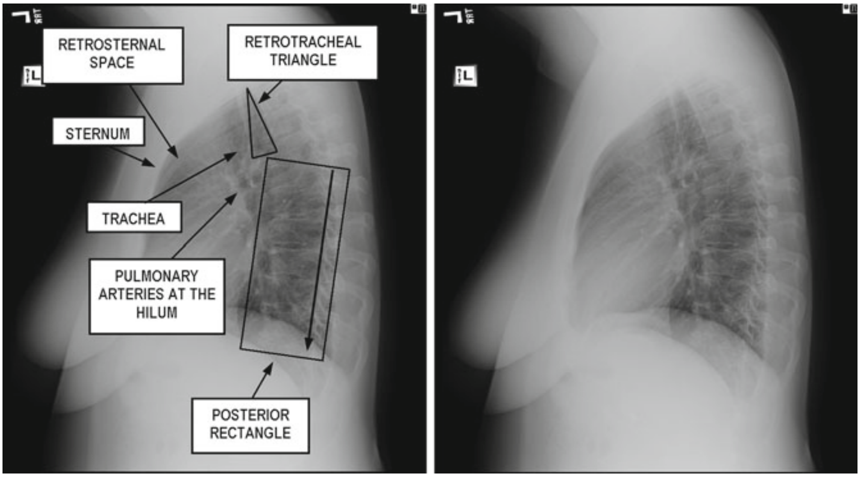
RETROSTERNAL SPACE
RETROTRACHEAL TRIANGLE
L
STERNUM
TRACHEA
PULMONARY ARTERIES AT THE HILUM
POSTERIOR RECTANGLE
L

FIGURE 10.1 - THE LATERAL CHEST
The different spaces noted in the lateral chest should be approached in a methodical fashion

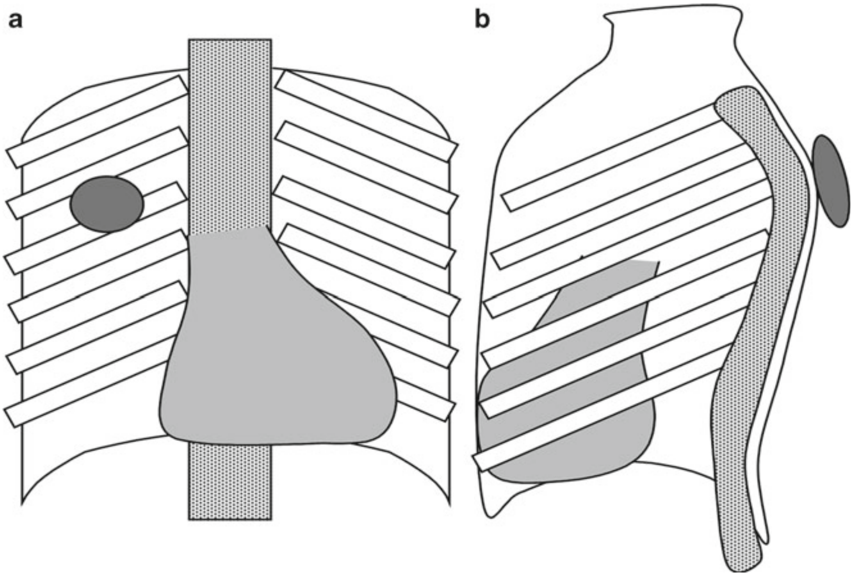

FIGURE 10.2 - THE LATERAL CHEST PROJECTION
Note that the lesion projected over the chest on the PA projection (**a**), assumed to be an intrathoracic mass, is actually in the soft tissues of the back, seen on the lateral (**b**)

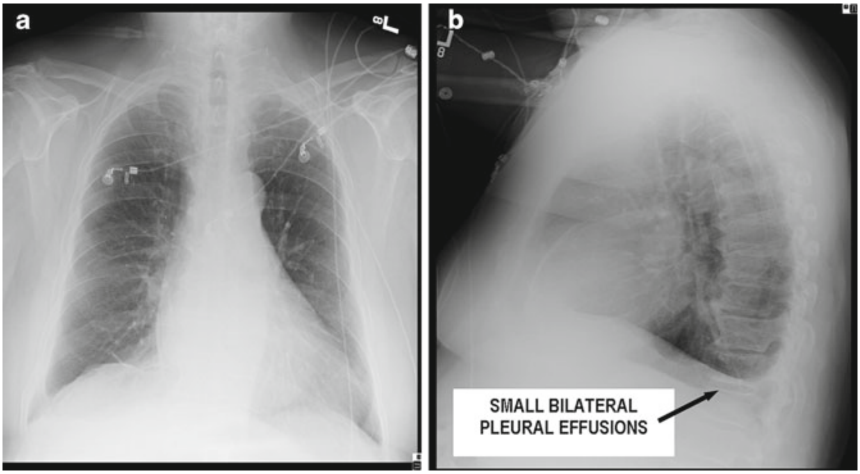

FIGURE 10.3 - BILATERAL PLEURAL EFFUSIONS FRONTAL (A) AND LATERAL (B) VIEWS OF A PATIENT WITH SUSPECTED BILATERAL PLEURAL EFFUSIONS Note that although bilateral pleural effusions are clearly evident on the lateral projection, (b) the costophrenic angles are clear and sharp on the frontal view (a)

Figure 10.3 demonstrates frontal and lateral views of a patient with suspected bilateral pleural effusions. The bilateral pleural effusions are clearly evident on the lateral projection as curved menisci. However, the costophrenic angles are clear and sharp on the frontal view. This is a good example of how small pleural fluid accumulations that may be of clinical significance can be overlooked if one relies only on the frontal (AP or PA) projections. In a similar manner, patients with small areas of consolidation or nodules in the lower lobes may not be correctly diagnosed if one does not carefully review the lateral projection, as the lower lungs are obscured by the hemidiaphragms on the frontal view.

Hemidiaphragms

There are four basic methods for determining which hemidiaphragm and which costophrenic angle is the left vs. the right on the lateral view. See Fig. 10.4 for correlation.

1. Since the anterior portion of the left hemidiaphragm comes into contact with the inferior aspect of the heart, it is obscured (do you remember the silhouette sign?). For this reason, the left hemidiaphragm cannot usually be traced as far anteriorly as the right hemidiaphragm.

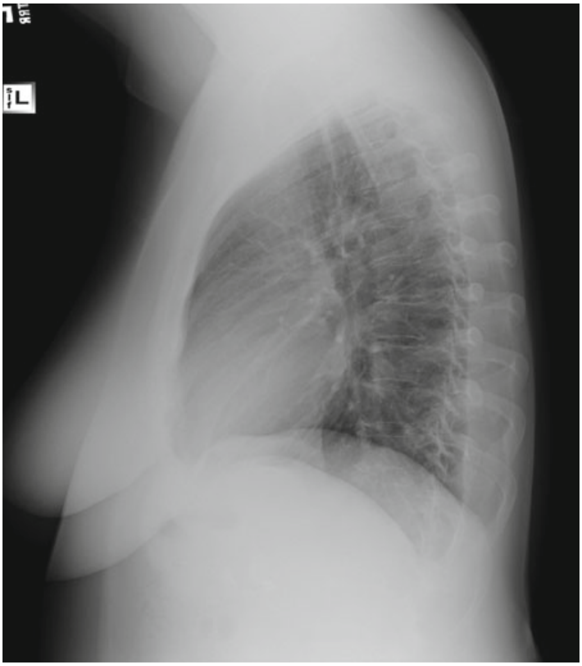

FIGURE 10.4 - HEMIDIAPHRAGMS
Lateral chest with well-visualized hemidiaphragms

2. Lateral chest X-rays in most X-ray departments are performed as left laterals. This means the patient's left side is placed against the X-ray radiograph, and the beam traverses the patient from right to left. This is noted by an "L" marker somewhere on the radiograph. As you recall, objects which are further from the radiograph are magnified more. If one looks at the posterior portion of the left lateral chest radiograph, two sets of ribs, a large set and a corresponding small set, can be seen. One can reason that the larger set of ribs must be located further from the radiograph, in other words, on the right side.
3. Since the left hemidiaphragm lies directly above the stomach, the left hemidiaphragm can be seen to have the stomach beneath it on the lateral view, if the left hemidiaphragm is slightly higher than the right in this region.
4. By correlating the height of the hemidiaphragm on the frontal projection with the highest point of the hemidiaphragm on the lateral projection, one may be able to distinguish left from right on the lateral view.

By following the hemidiaphragm posteriorly and noting at which set of ribs it terminates, one can determine whether the hemidiaphragm is on the left or right side. Note that this also allows one to distinguish the left and right costophrenic angles on the lateral view. Think about these relationships since they represent a recapitulation of two important principles presented earlier – the silhouette sign and the principle of magnification.

Identifying Hilar Enlargement

Figure 10.5 illustrates a problem encountered when viewing frontal chest radiographs: determining whether increased soft tissue prominence in the hilar region is the result of enlargement of the pulmonary arteries or secondary to an abnormal mass such as hilar lymphadenopathy. Note that on this PA view, the pulmonary artery segment is not enlarged. In most cases, computed tomography of the chest would be used to confirm the plain radiograph density. Less commonly, MRI is used for this purpose, since flowing blood in a large vessel such as the left pulmonary artery gives no signal on MRI, whereas any soft tissue lesion should produce a detectable signal.

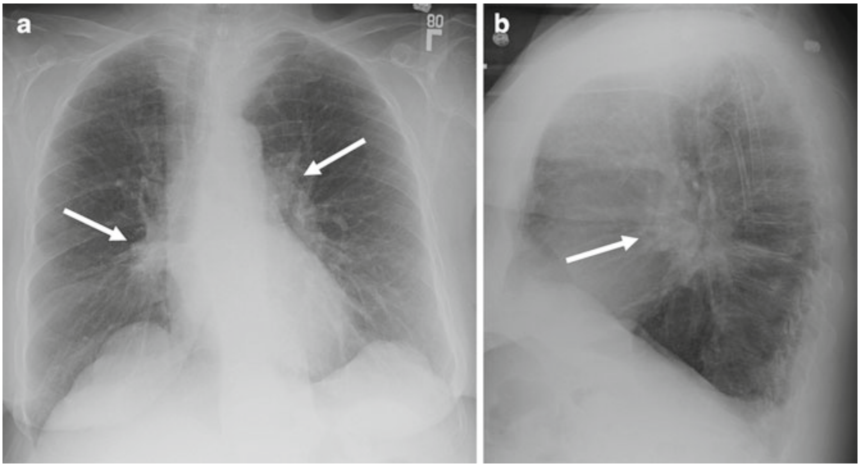

FIGURE 10.5 - HILAR ADENOPATHY
PA (**a**) and lateral (**b**) chest radiographs show a patient with hilar adenopathy (*arrows*)

11

PULMONARY MASS LESIONS

Objectives:

1. When evaluating a possible mass on a chest radiograph, remember to use the following terms in your consideration of the lesion and its description: size, location, margin characteristics, involvement of contiguous structures, calcification or cavitation, solitary versus multiple, time course of growth/old radiograph comparison, and related findings.
2. List four differential diagnoses for a solitary pulmonary nodule.
3. Discuss the significance of calcification within a pulmonary mass lesion.
4. Define “round pneumonia” and “pseudotumor.”

Masses within the lung are commonly suspected and/or appreciated on the conventional chest radiograph. There are many criteria which you should evaluate on arriving at a list of potential differential diagnoses for a mass lesion. However, before you consider the differential diagnosis of a mass lesion you should:

1. Make sure the “mass” is in the lung and not a superimposed structure related to the chest wall as would be the case in a patient with a skin lesion or other external density.
2. CHECK OLD STUDIES! – The “cancer” you have just diagnosed may be a benign nodule which has been present for many years. If old studies are not available at your institution, you should ask the patient if old studies are available.

H Singh and JA Neutze (eds.), *Radiology Fundamentals: Introduction to Imaging & Technology*, DOI 10.1007/978-1-4614-0944-1_11,
© Springer Science+Business Media, LLC 2012

Criteria to Consider in the Evaluation of a Mass Lesion

1. *Size*: Although this is an obvious criteria for evaluation, bigger lesions are not always malignant and smaller lesions are not always benign.
2. *Location*: Assess the location of the mass with respect to the pulmonary lobes and pulmonary segments (if possible). Computerized tomography may help in this regard, as the location of a lesion with respect to a fissure can be quite confusing on a conventional radiograph due to undulations of the fissures. However, the further a lesion can be localized the better, since this may help the bronchoscopist or surgeon.
3. *Margin characteristics*: Assess whether the margins of the lesion are smooth or irregular. Obviously, the more irregular the margins of the mass, the more suspicious we are that we are dealing with a malignant process. However, many benign inflammatory lesions have quite irregular margins. Also, metastatic lesions may be very smoothly demarcated. Hence, although the contours of a lesion should be evaluated, they are not absolute indicators of a benign versus malignant lesion.
4. *Involvement of contiguous structures*: This may be a very important indicator of the etiology of the lesion. A mass which is close to the chest wall and destroys a rib has a high probability of being a malignant process (although, again, this is not an absolute phenomenon as some infectious pulmonary lesions such as actinomycosis may destroy adjacent ribs).
5. *Presence or absence of cavitation or calcification*: Cavitation may be seen in malignant and benign processes. Calcification, although once thought to indicate that a lesion was benign, is now known to be seen in both malignant and benign processes and, hence, is another nonspecific indicator of the etiology of the lesion.
6. *Solitary or multiple lesions*: Obviously, multiple pulmonary nodules have a different connotation and differential diagnosis than a solitary lesion in many cases. For this reason, when one pulmonary nodule is appreciated, a careful search for other nodules should be made. Computerized tomography, because of its sensitivity for detection of nodules, is often very useful in this regard.

The aforementioned characteristics, along with the time course of a lesion as evidenced by old studies, as well as any other related findings (e.g., adenopathy or an accompanying pleural effusion) are what the differential diagnosis will be based on. The clinical history is of paramount importance in evaluating a pulmonary nodule.

Pulmonary Nodules and Masses

The following series of radiographs depict various causes of pulmonary nodules or masses. Try to describe each in terms of the criteria provided and arrive at a brief differential diagnosis.

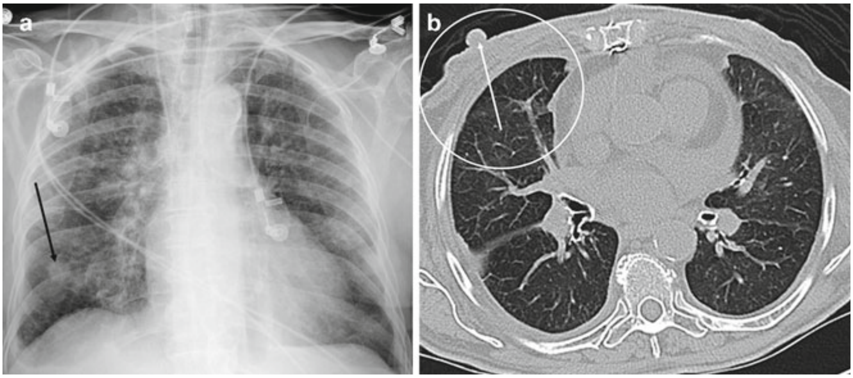

FIGURE 11.1 - NIPPLE SHADOWS
Image (**a**) depicts what appears to be a pulmonary mass lesion on a frontal chest X-ray (*black arrow*). However its classic position and smooth margination suggests a nipple shadow. This is confirmed on the corresponding CT slice, image (**b**) (*arrow* inside of *circle*)

As always, the point is not to memorize the numerous possible diagnoses for each abnormality. Hopefully, that will come with time and experience. You should however be fastidious in employing these criteria and remembering the pitfalls for all cases of pulmonary mass lesions.

Figure 11.1a demonstrates a symmetrically placed, approximately 1-cm, soft tissue nodular opacity projected over the lower right chest. While this may be confused with pulmonary mass lesions, its smooth margination (it is unusually well outlined because it is surrounded by air) and classical position suggests that it represents a nipple shadow. When a questionable nodule is suspected to be a nipple shadow, a repeat study with small metallic markers taped to the nipples may confirm a nipple shadow and preclude further work-up. Figure 11.1b demonstrates the nipple on a CT scan.

Coin Lesion

Figure 11.2 demonstrates a solitary pulmonary nodule in the left lower lung behind the heart. This is the so-called coin lesion, although, of course it is a three-dimensional sphere. This lesion turned out to be a granuloma, but there are no distinguishing characteristics on the radiograph which would allow you to make this diagnosis. CT might demonstrate benign characteristics. A biopsy was necessary to make a benign diagnosis, in this case.

In one study of solitary pulmonary nodules with no evidence of cavitation or calcification on plain radiographs, half were granulomas due to old tuberculosis and fungal disease of other unidentified sources; one-fourth were primary carcinomas of

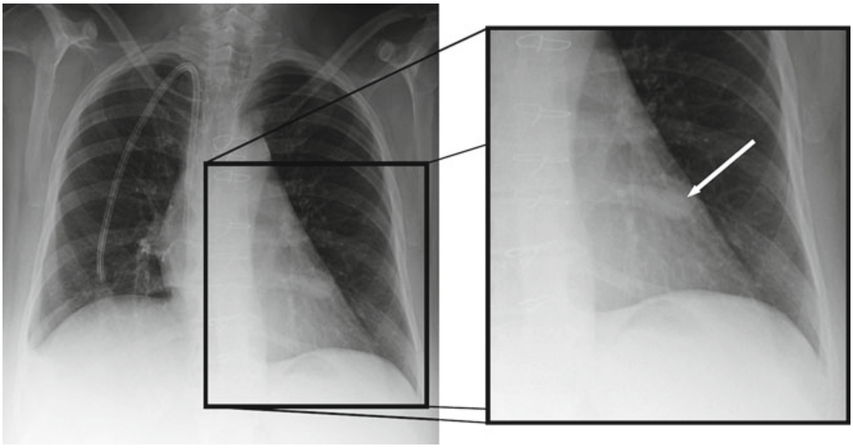

FIGURE 11.2 - COIN LESION
Always remember that this lesion is actually a three-dimensional sphere

the lung. Other less common causes of solitary pulmonary nodules include hamartoma, solitary metastatic tumors, carcinoid tumors, round pneumonia, arterial venous malformations, and cysts.

Hamartoma

Figure 11.3 demonstrates a large smoothly marginated solitary lesion without evidence of cavitation in the left paracardiac region.

Mottled densities may be seen within the mass representing “popcorn” like calcifications. Although calcification within a lesion does not guarantee that it is of benign etiology, this pattern of calcification is nearly always associated with a particular benign neoplasm of the lung, a hamartoma. Of course, comparison with old studies also showed the mass to be unchanged in size. In this case, detection of this pattern of calcification made surgical removal for diagnosis unnecessary.

Cavitary Lesion

Figure 11.4 was obtained from a 60-year-old man with a history of heavy smoking who now presents with weight loss and hemoptysis. The current abnormality contains obvious cavitation. It is also contiguous to the left lateral chest wall, but we take careful note of the fact that it does not erode or destroy the ribs and does not

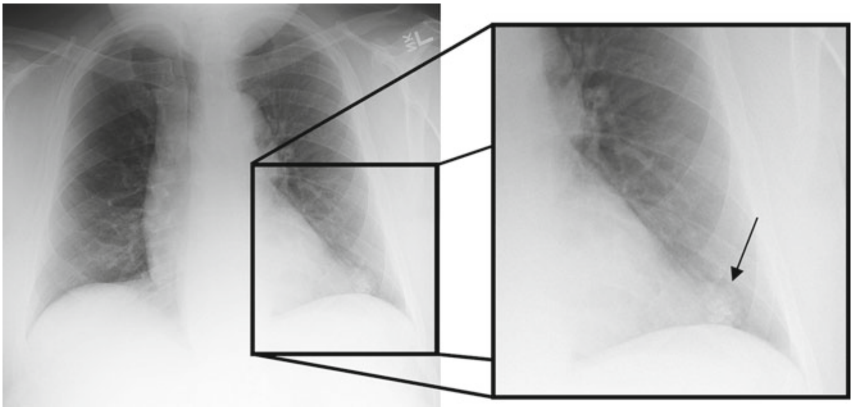

FIGURE 11.3 - HAMARTOMA
Hamartoma in the left lower lobe. Note the speckled appearance of the lesion suggesting calcification, typical of this lesion

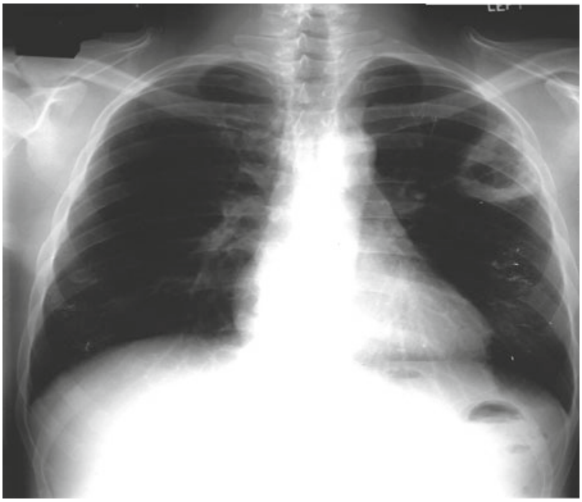

FIGURE 11.4 - CAVITARY LESION
Note the area of decreased density in the left upper lobe within the area of parenchymal disease

produce a pleural effusion on this view. The hilum on the left side has a relatively normal appearance without definite evidence of lymphadenopathy. Again, as in so many disease processes of the chest, CT scans would usually be more sensitive than the conventional radiograph in evaluating this patient for hilar and mediastinal lymphadenopathy.

The differential diagnosis of this cavitary lesion includes a primary lung neoplasm. Cavitation is most common in the squamous cell type of primary lung carcinoma. A lung abscess could give a similar appearance if the patient's symptoms related more to an inflammatory process than this patient's obviously malignant symptomatology. Cavitation may be artifactually simulated by a number of conditions, and before cavitation is accepted as a finding, it must be clearly present. Often debris or soft tissue density will be seen within a cavity. This can represent clotted blood, a superimposed fungal infection (aspergillus fungus ball) or necrotic debris from the inner wall of the neoplasm. This lesion turned out to be a squamous cell carcinoma.

Pulmonary Nodules

Figure 11.5 demonstrates multiple pulmonary nodules in both lungs which are highly suspicious for metastases. It is their multiplicity which strongly suggests their etiology, and for this reason any time one nodule is found, others must be looked for carefully.

Because metastases to the lungs are essentially an embolic process, metastases are more common in the lower lobes because of the normally increased blood flow to this region. Also, metastases are often initially detected in the subpleural,

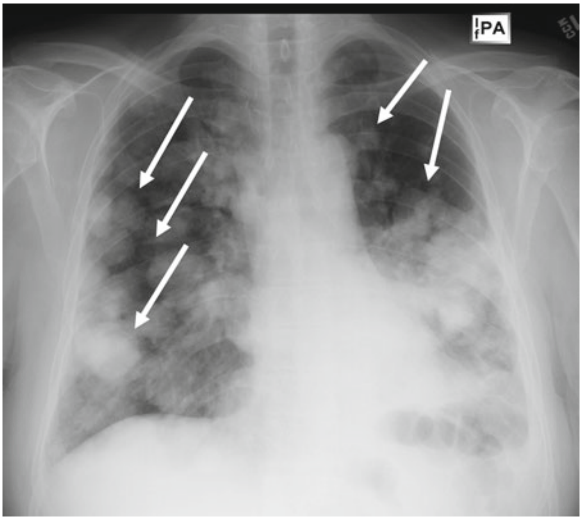

FIGURE 11.5 - PULMONARY NODULES
Frontal chest radiograph demonstrating numerous pulmonary nodules throughout both lung fields (*arrows*)

peripheral portion of the lung, since this is where the smaller blood vessels are, which are more prone to embolization. For this reason, computerized tomography (CT) is the most sensitive test for detecting early metastatic disease. The problem with CT scans is that multiple processes may masquerade as metastases on the CT scan. Hence, CT is very sensitive but not highly specific.

Round Pneumonia

Figure 11.6 is a frontal chest radiograph of a patient with a small amount of blood tinged sputum and a fever of 101°. Obviously, the presence of the fairly well-marginated mass lesion in the right mid lung is of concern for possible malignancy. However, because this patient's symptoms were primarily those of someone with pneumonia, a trial of antibiotics for 2 weeks was performed. A follow-up radiograph at that time showed some improvement. This is an example of "round pneumonia." Although more commonly seen in children, round pneumonia can also occur in adults, as in this case. Inflammatory exudate spreads from alveolar unit to alveolar unit through the pores of Kohn, opacifying the lung in an ever expanding manner from a central focus. In certain cases, the pattern of expansion and flow of exudate can be very well defined and simulate a mass lesion.

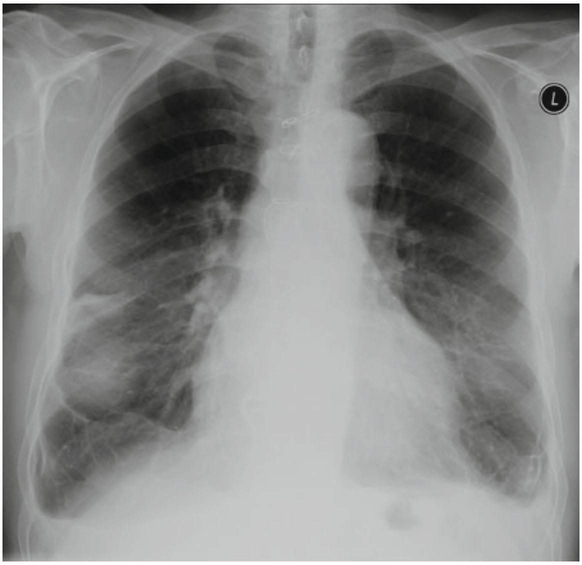

FIGURE 11.6 - ROUND PNEUMONIA
Round pneumonia in the right lower lung

This case demonstrates the importance of paying attention to the clinical presentation of the patient in addition to the radiographic findings when evaluating a potential pulmonary mass.

Pseudotumor

Figure 11.7 demonstrates a well-defined density projected over the right mid lung. The lateral view demonstrates that this density has a lentiform (or lens-like) configuration and lies within the right major fissure.

This density represents the so-called pseudotumor, which can be caused by fluid loculated within a fissure. Clues to the diagnosis include location in the area of the fissure, ovoid shape with long axis in the plane of the fissure, and association with a pleural effusion either on the same radiograph or on prior studies.

In summary, the differential diagnosis of solitary or multiple pulmonary nodules is long. Much time and expense can be saved through careful observation and analysis of the plain radiographs and comparisons with old radiographs as well as correlation with the patient's clinical presentation.

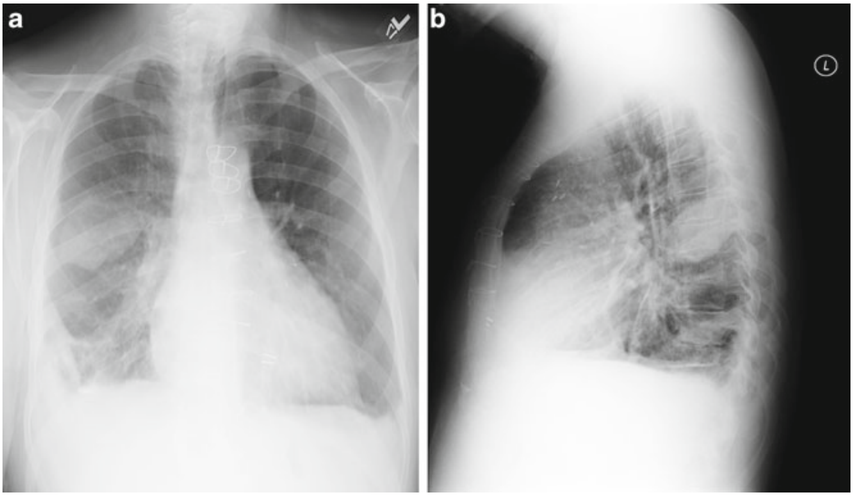

FIGURE 11.7 - PSEUDOTUMOR
Frontal (**a**) and lateral (**b**) chest radiographs demonstrating a pseudotumor in the right mid-lung along the major fissure

12

AIR SPACE DISEASE

Objectives:

1. Define "pulmonary acinus."
2. List the radiographic findings characteristic of air space disease.
3. List the major differential diagnostic categories for acute air space disease.
4. List two causes of chronic air space disease.

The purpose of this unit is to demonstrate the appearance of air space disease in the lungs.

The pulmonary acinus is the basic structural unit of the lung involved in gas exchange. It consists of a terminal bronchiole and the alveolar ducts, sacs, and alveoli distal to it. Recall that a terminal bronchiole is the most peripheral airway that is purely conductive in function with no gas exchange capability.

The acinus is visible when opacified on the plain chest radiograph as a slightly irregular nodular shadow approximately 8 mm in size (Fig. 12.1a). Disease within the air space manifest on the radiograph as soft tissue density. Disease may involve numerous acini or spread from one acinar unit to another via the pores of Kohn and canals of Lambert (Fig. 12.1b). The opacified acini become confluent, producing a fluffy, homogeneous radiographic pattern characteristic of air space disease as noted on Fig. 12.2.

Since disease which primarily affects the air space tends to spare the larger conductive airways, these airways become visible as tubular, branching, air-filled structures surrounded by the fluid-filled acini. These air-filled structures are normally surrounded by air-filled lung and are hence not distinguished normally on the chest radiograph. These air-filled bronchi surrounded by opacified air space are called air bronchograms. Air bronchograms are the radiographic hallmark of air space disease. Figure 12.3 is an excellent example of air bronchograms in a patient with pneumonia. The distribution of air space disease may be useful in determining its etiology.

H Singh and JA Neutze (eds.), *Radiology Fundamentals: Introduction to Imaging & Technology*, DOI 10.1007/978-1-4614-0944-1_12,
© Springer Science+Business Media, LLC 2012

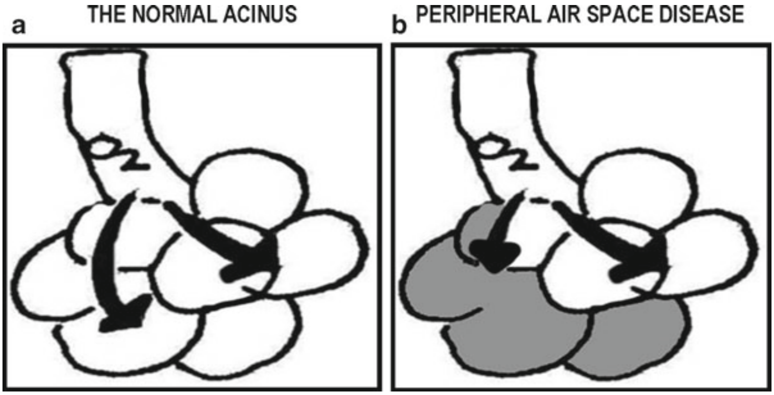
a
THE NORMAL ACINUS
b
PERIPHERAL AIR SPACE DISEASE
O2
O2

FIGURE 12.1 - LUNG ACINUS
The normal acinus (**a**) is approximately 8 mm in diameter. In the picture on the *right*, volume is unaffected and the airways remain patent (**b**)

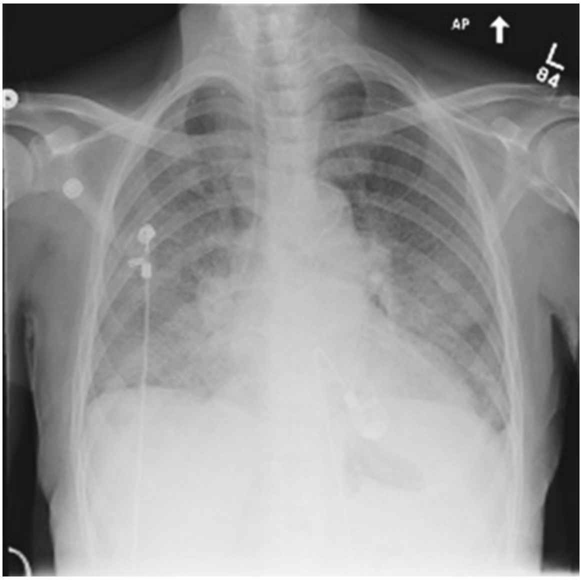

FIGURE 12.2 AIR SPACE CONSOLIDATION
Frontal chest radiograph demonstrating diffuse air space disease

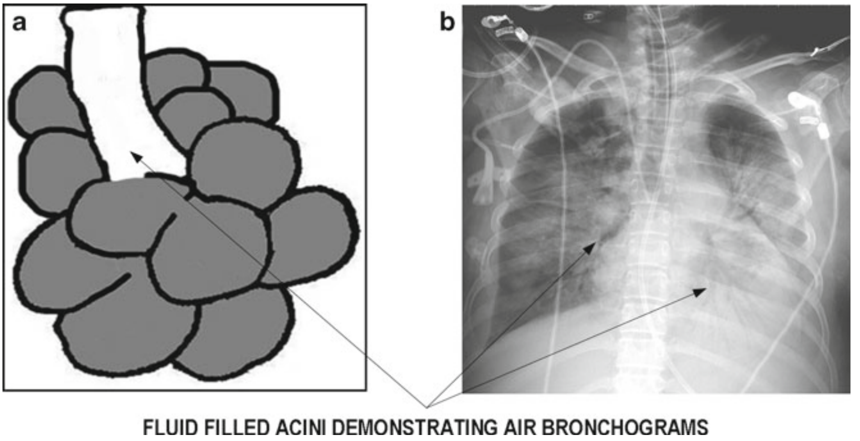

FIGURE 12.3 - AIR BRONCHOGRAMS
Schematic (**a**) and radiograph (**b**) of an air bronchogram. Note that the bronchi are usually not seen in a normal chest X-ray. With the acini surrounding the bronchus filled with fluid, the bronchus is outlined (*arrows*)

Figure 12.4 demonstrates a right lower lung pneumonia on the frontal radiograph. The right dome of diaphragm and right heart border are preserved. A lateral view is necessary to localize this to the right middle or lower lobes.

Consider the differential for acute airspace disease:

1. Pulmonary Edema: transudate fills the alveoli.
2. Infection: pneumonic exudate fills the alveoli.
3. Hemorrhage: blood fills the alveoli.

Within each of these major categories, however, multiple pathologies may be included.

1. Pulmonary edema – cardiogenic (CHF) or noncardiogenic (ARDS).
2. Infection – numerous organisms may cause pneumonia.
3. Hemorrhage – may be produced by many causes including pulmonary contusion, pulmonary infarcts, Goodpasture's syndrome and diseases which produce vasculitis such as collagen vascular diseases.

This list is certainly not inclusive of all possibilities. Clinical information must be coordinated with old studies to narrow the diagnostic possibilities. In other words, fever would suggest pneumonia, while hemoptysis would suggest pulmonary hemorrhage. The distribution of the abnormality may also help. Cardiogenic edema tends to be diffuse, predominantly perihilar and bilateral and also associated with other findings (enlarged heart, pleural effusions). Pneumonia is classically more focal.

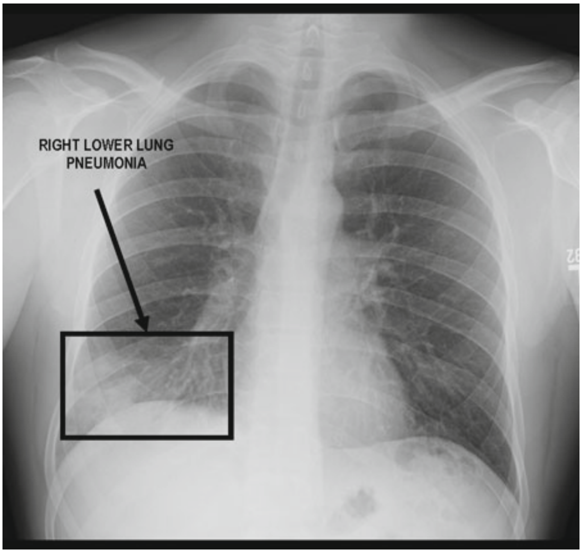

FIGURE 12.4 - PNEUMONIA Patchy airspace disease in the right lower lung consistent with pneumonia

Pathologic processes involving the air space (alveoli) can be further subdivided into acute and chronic in nature. The time course of appearance and regression of airspace disease is useful. Edema can come and go quickly (onset may be within minutes, regression can occur within hours). Pneumonia and hemorrhage move more slowly, especially in regression. The slowest moving processes which present with airspace patterns are neoplasms such as bronchoalveolar carcinoma or pulmonary lymphoma which may present as chronic airspace disease.

13

INTERSTITIAL DISEASE

Objectives:

1. Define "pulmonary interstitium."
2. List the anatomic subdivisions of the pulmonary interstitium.
3. Define each of the radiologic findings associated with interstitial disease: Kerley lines, peribronchial cuffing, subpleural thickening, reticular, or reticulonodular pattern.
4. Understand the statement "Memorizing all the causes of interstitial disease is an exercise in futility!"

Introduction

The alveoli, conductive airways, and blood vessels of the lung are surrounded by the pulmonary interstitium. The interstitial space can be subdivided into three components as noted in the accompanying drawings. Recall that the acinus is the basic structural unit of the lung, supplied by a terminal bronchiole. A secondary pulmonary lobule contains 3–12 acini (Fig. 13.1). The interstitium is a continuum of dense elastic tissue and collagen throughout the lung that merges into the elastic component of the alveolar walls. It is not normally visible on the plain radiograph and becomes visible only when disease increases its volume and/or radiographic density.

The anatomic subdivisions of the interstitial space are useful since involvement of various subdivisions give rise to the specific radiographic findings associated with interstitial disease. These radiographic findings are as follows: Kerley lines, peribronchial cuffing, reticular or reticulonodular opacities, and subpleural thickening. One should strongly resist the tendency to define specific findings of interstitial disease prior to applying the proper terminology. Failure to do so will lead to the application of the wrong group of differential diagnoses to an abnormal chest radiograph.

H Singh and JA Neutze (eds.), *Radiology Fundamentals: Introduction to Imaging & Technology*, DOI 10.1007/978-1-4614-0944-1_13,
© Springer Science+Business Media, LLC 2012

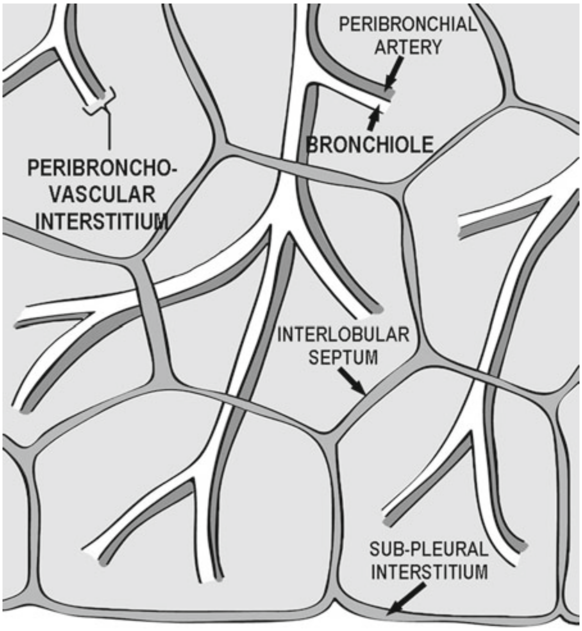

FIGURE 13.1 - SECONDARY PULMONARY LOBULES
It is helpful to identify the subdivisions of the interstitial space

Kerley Lines

In viewing a gross lung specimen with the naked eye, it is easy to see that the lung is subdivided into numerous secondary pulmonary lobules by connective tissue septa. It is the engorgement of these septa which produce Kerley lines, identified by and named for Dr. Peter Kerley, an Irish radiologist. In addition to lymphatics, the septa also contain pulmonary venules. The short, 1–2 cm horizontal lines in the inferolateral aspect of the lungs are called Kerley B lines (Fig. 13.2). The less commonly seen 2–6 cm septa visualized radiating from the hila to the upper lobes cast shadows known as Kerley A lines when thickened. Kerley also described C lines which have no distinct anatomic correlate and are due to superimposition of A and B lines into a web-like pattern.

Peribronchial Cuffing

Bronchi, when seen on end, cast thin-walled ring shadows on the normal chest radiograph. These are usually appreciated adjacent to the nodular shadow cast by a branch of the pulmonary artery on end. Remember that the bronchus and pulmonary artery travel together and bifurcate to the terminal bronchial-pulmonary arterial

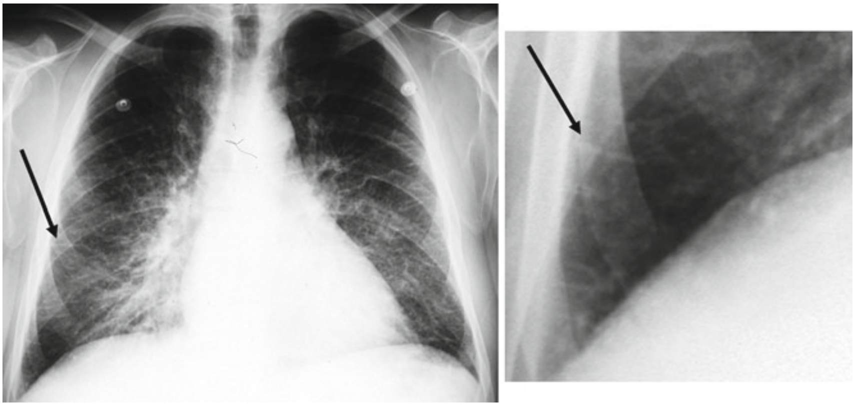

FIGURE 13.2 - KERLEY B LINES

level. When the perivascular component of the interstitial space becomes engorged, the normally “paper thin” bronchial wall takes on a thickened appearance (Fig. 13.3).

Causes of peribronchial thickening are varied and include CHF and infection. Diseases which thicken the bronchial wall on an inflammatory basis such as chronic bronchitis or cystic fibrosis may also lead to a “thickened bronchial wall.”

Reticular and Reticulonodular Patterns

Not infrequently, there are diffuse increased linear and/or fine nodular opacities in the lungs (Fig. 13.4). In this situation, the descriptive terms reticular or, if there is a nodular component, reticulonodular may be employed to describe the findings. While most interstitial diseases have an air space component, identifying an abnormality as predominantly interstitial helps in the differential diagnoses. Common causes include CHF and atypical infections.

Subpleural Thickening

When accumulation of fluid or thickening of the subpleural interstitial space occurs, increased radiographic density which outlines the fissures is produced. This occurs frequently in early pulmonary edema and is commonly wrongly attributed to “fluid within the fissure.” Any process affecting the subpleural interstitial space will give this appearance of thickened fissures. Hence, thickening of the visceral pleural

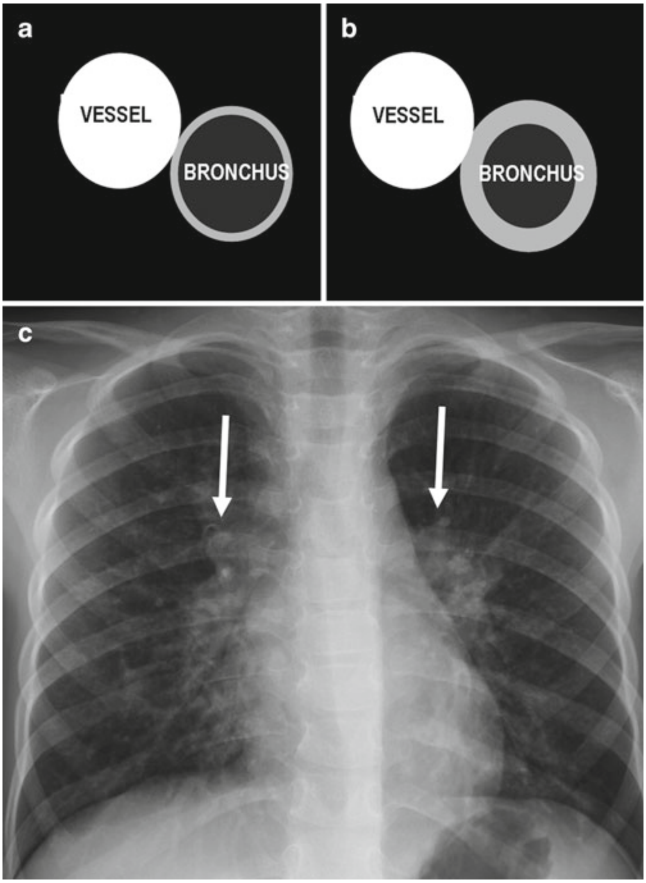

FIGURE 13.3 - PERIBRONCHIAL CUFFING
(**a**) Normal bronchovascular bundle. (**b**) peribronchial cuffing. (**c**) AP radiography showing examples of peribronchial cuffing

shadow can be seen in patients with early interstitial pneumonia or evolving interstitial disease from any cause.

The Differential Diagnosis for Interstitial Disease Is Exhaustive

There are literally hundreds of causes of interstitial disease. These range from early CHF, to atypical infections and idiopathic interstitial pneumonia, to the distinctly interstitial form of metastatic disease seen in carcinoma of the lung, breast, and stomach called lymphangitis carcinomatosis. Memorization is fruitless. The importance is to be able to recognize the radiographic findings of interstitial disease when you see them.

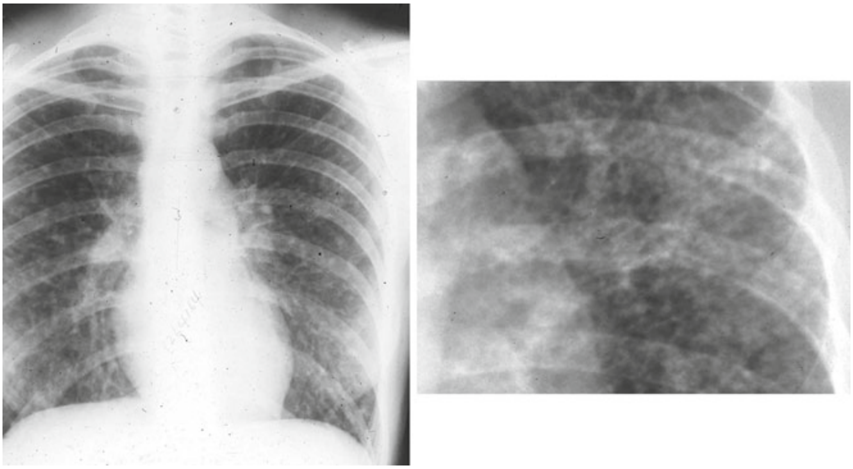

FIGURE 13.4 - RETICULONODULAR DISEASE
PA radiograph and close-up of same patient showing reticulonodular lung disease

14

ATELECTASIS

Objectives:
1. Define “atelectasis.”
2. Define and give examples of: postobstructive atelectasis, cicatrization atelectasis, adhesive atelectasis, and passive atelectasis.
3. Explain why loss of lung volume does not always lead to increased radiographic density.

Introduction

You will find few chest radiographic reports that do not include the term atelectasis. Atelectasis means incomplete lung expansion. This term is frequently tossed about and little thought is given to its significance. It is important to think about the underlying pathophysiology any time the term atelectasis is employed in describing a chest radiograph finding. Pneumonia and atelectasis are always considered in the differential diagnosis of air space opacities. It can be difficult to differentiate between the two processes without examining the patient for signs of pneumonia (fevers, elevated WBC, lung auscultation findings, etc.).

There are four basic mechanisms which lead to atelectasis or loss of lung volume. These can occur individually or in combination and are listed below:

1. Postobstructive atelectasis
2. Cicatrization atelectasis
3. Adhesive atelectasis
4. Passive atelectasis

H Singh and JA Neutze (eds.), *Radiology Fundamentals: Introduction to Imaging & Technology*, DOI 10.1007/978-1-4614-0944-1_14,
© Springer Science+Business Media, LLC 2012

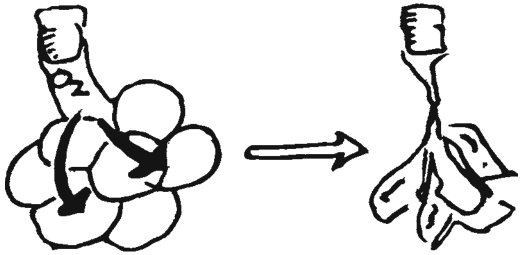

FIGURE 14.1 - POSTOBSTRUCTIVE ATELECTASIS
An airway obstruction results in collapse (incomplete expansion) of the airway and airspaces distal to the obstruction

Postobstructive Atelectasis

When a bronchus is obstructed, air within the alveoli and the bronchi distal to the obstruction is reabsorbed leading to volume loss as depicted in Fig. 14.1. Endobronchial tumor, extrinsic compression of a bronchus by a mass, a foreign body in the bronchus or a mucous plug can lead to postobstructive atelectasis.

In situations in which the inspired gas contains an elevated proportion of oxygen in comparison to room air, postobstructive atelectasis is more likely to occur. This is because alveoli will rapidly reabsorb gas that is rich in oxygen. Hence, postobstructive atelectasis, especially on the basis of mucous plugging, is a commonly observed phenomena on portable radiographs obtained in the operating room or in the intensive care units where patients often breathe gas mixtures with a greater percentage of oxygen than found in room air.

Cicatrization Atelectasis

Cicatrix is a medical word for scar or replacement of normal tissue by fibrous tissue. This form of atelectasis occurs secondary to healing of inflammation from infection, radiation therapy, etc. It is characterized by marked perialveolar fibrosis with resultant loss of airspace as noted in Fig. 14.2.

Adhesive Atelectasis

When type II pneumocytes lining the alveolus decrease their surfactant production, the alveolus can no longer remain inflated and adhesive atelectasis occurs. Collapse results, according to the law of LaPlace. LaPlace's law states that the pressure (P)

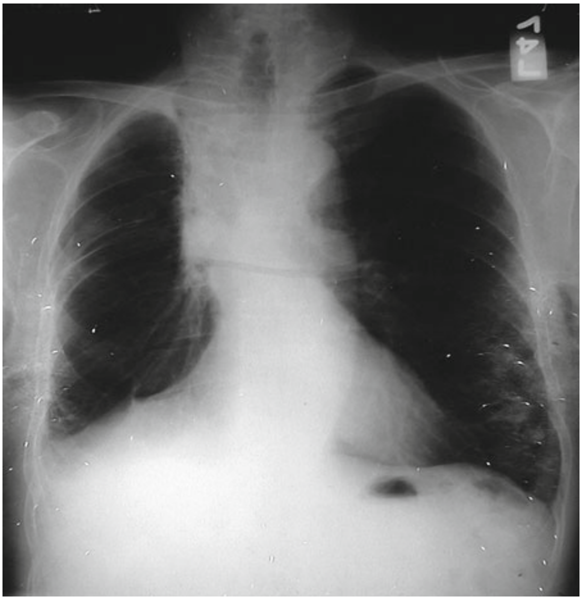

FIGURE 14.2 - CICATRIZATION
Replacement of normal tissue by fibrous tissue in the right middle lobe

required to keep an alveolus open is directly proportional to the wall tension (T) and inversely proportional to its radius (r). Hence, for any given tension, the smaller the radius, the larger the pressure required to keep that alveolus open. Surfactant decreases the surface tension, helping reduce the pressure required to keep small alveoli open (or maintain smaller alveoli open at a lower pressure) (Fig. 14.3).

The prototype of adhesive atelectasis is the respiratory distress syndrome of prematurity, which occurs in infants whose type II pneumocytes have not matured enough to produce surfactant. Adhesive atelectasis may also be seen commonly following cardiac surgery. The cooling of the heart performed to decrease the heart's metabolic requirements while on bypass also decreases the metabolic rate of type II pneumocytes in the adjacent lung. The most common location for this is in the left lower lobe as most cooling is provided in the region of the left ventricle.

Passive Atelectasis

The lung is highly elastic and normally exists at a volume "greater than it desires to be." The chest wall is also elastic and exists at a volume slightly "less than it would like to be." The equilibrium between the lung and chest wall establishes these relative

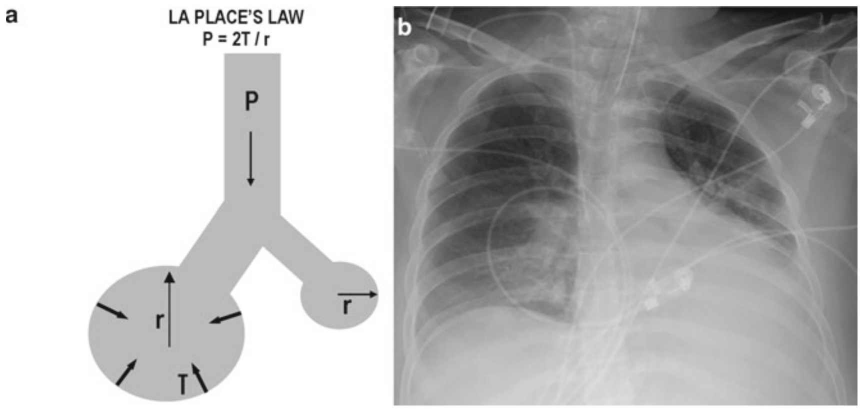

FIGURE 14.3 - ADHESIVE ATELECTASIS
(**a**) Figure illustrating LaPlace's Law. (**b**) AP CXR showing LLL adhesive atelectasis

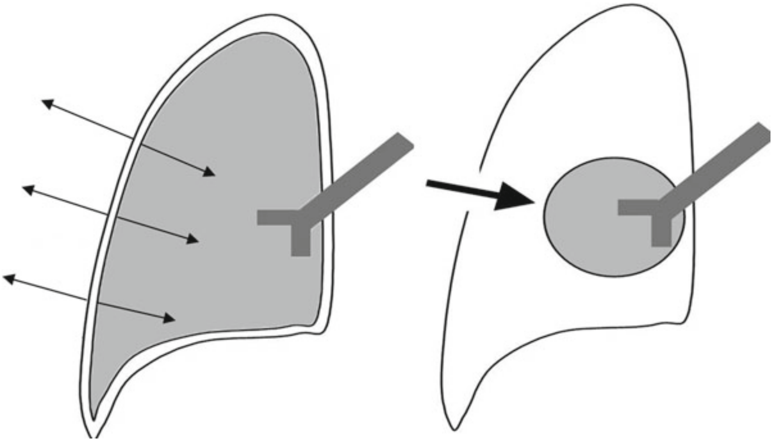

FIGURE 14.4 - NORMAL AND ABNORMAL FORCES ON THE LUNG
The normal elastic forces between the chest wall and the lung oppose each other, resulting in a certain equilibrium as noted in the picture on the *left*. With a pneumothorax, as seen on the *right*, when the chest wall is compromised, air enters the thorax, allowing the lung to collapse

volumes as you may recall from physiology. When something is introduced to change the equilibrium, the lung and chest wall also change volume in a predictable manner.

Anytime the lung loses volume due to a manifestation of its propensity for elastic recoil, this is termed passive atelectasis. The most obvious example of this is a pneumothorax but similar changes occur when fluid is introduced into the pleural space as in a pleural effusion (Fig. 14.4).

Radiographic Opacity

Finally, it is important to remember that loss of volume does not imply increased radiographic opacity. Normal lung is so transparent to X-rays that it does not increase in opacity until it has lost 90–95% of its volume. Hence the small areas of atelectasis seen on chest radiographs represent small foci of lung parenchyma which have lost nearly all of their air.

15

PULMONARY VASCULATURE

Objectives:

1. Give three examples of technical factors that may make pulmonary vessels look more prominent.
2. Describe the physiology in pulmonary perfusion between the cephalad and more caudad portions of the lung in an upright patient.
3. Be able to distinguish pulmonary veins from pulmonary arteries in a PA chest X-ray and provide two criteria for differentiation.
4. Give two criteria for distinguishing a vessel on end from a pulmonary nodule.
5. List the components of the hilar shadow on a conventional chest radiograph.
6. State which hilum is usually higher on the upright chest radiograph.
7. List three physiological states in which the pulmonary vasculature is abnormal on the chest radiograph and give specific radiographic criteria for distinguishing them from one other.

Pulmonary Vessel Distribution in the Lung

We have already seen how inspiration and expiration can affect the appearance of the pulmonary vessels. Other technical factors such as under-penetration and supine positioning can also make the vessels look artifactually prominent.

In Fig. 15.1, note the difference in the number and size of blood vessels within the lung as one moves from the lung apex to the lung base. The vessels are larger and more numerous in the lung base because the force of gravity augments the hydrostatic force generated by the right ventricle. In the apices, the hydrostatic force generated by the right ventricle is diminished by gravity. In effect, the right ventricle is pumping "uphill" to the apices of the lung. Of course, when the patient changes position, this relationship is also changed.

H Singh and JA Neutze (eds.), *Radiology Fundamentals: Introduction to Imaging & Technology*, DOI 10.1007/978-1-4614-0944-1_15,
© Springer Science+Business Media, LLC 2012

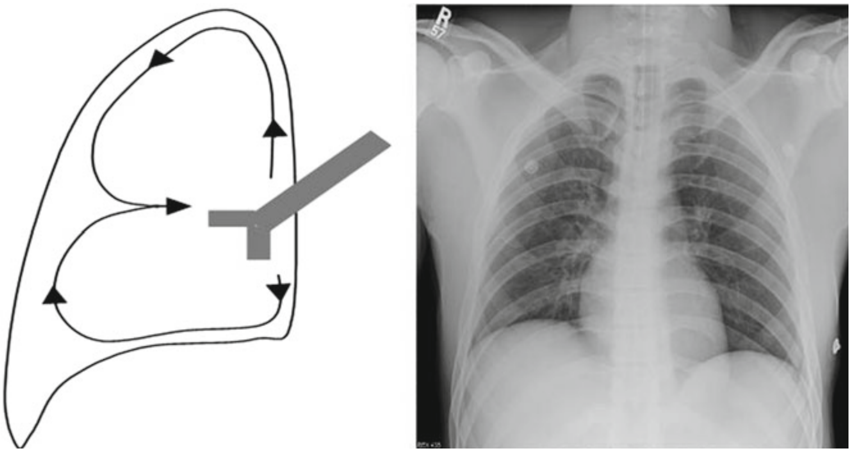

FIGURE 15.1 - PULMONARY VASCULAR FLOW
Pulmonary arteries tend to run in a vertical fashion, while pulmonary veins are more horizontal. Note the difference in number and size of blood vessels within the lung from apex to base

In general, the greatest perfusion will be to the portion of the lung which is most dependent. Certain pathologic situations can change this normal perfusion gradient as we will see later in this section.

Identifying Pulmonary Vessels

To identify pulmonary vasculature, look for the round, well-defined nodular shadows most easily noted centrally, close to the hilum. These are vessels on end (an artery or vein running in a plane perpendicular to the detector). Vessels can be confused with pulmonary nodules in some patients. However, they can often be distinguished from a true nodule by two criteria:

1. Since bronchi and pulmonary arteries travel together, look for a bronchus that is on end adjacent to the suspected vessel on end. A bronchus is air filled and thus will have a black center while the vessel will be uniform in opacity (Fig. 15.2).
2. A true nodule is spherical and should appear round on both PA and lateral views. A vessel on end will only have a round (“on end”) appearance on one view, having the tubular appearance of a vessel on the other projection.

Another way to identify vessels is by noting the hila. The hila are composed mainly of the shadow of the pulmonary arteries although there is a slight contribution from the bronchial structures. The left hilum is normally higher than the right in approximately 97% of patients. This is because the left pulmonary artery must

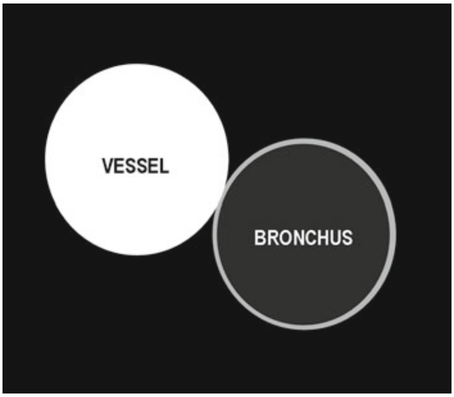

FIGURE 15.2 - VESSEL AND BRONCHUS
Note that the pulmonary artery and accompanying bronchus should be of relatively equal size and that the bronchial wall should be thin and sharp

pass over the left main bronchus in its proximal course while the right pulmonary artery travels adjacent but not over the right main bronchus. In 3% of patients the hila are of equal height. *The right hilum is never higher than the left in a normal patient*.

Pulmonary Artery Hypertension

Figure 15.3 shows the radiographic appearance of pulmonary arterial hypertension. Note the enlargement of the main and central pulmonary arteries. Note the rapid tapering of the pulmonary arteries peripherally causing the lungs to have a relatively oligemic (hypovascular) appearance.

Pulmonary arterial hypertension may occur as an idiopathic condition in young females or be related to a number of other causes, including acute or chronic pulmonary embolism, severe pulmonary lung disease either as a primary process (interstitial fibrosis, COPD, diseases associated with vasculitis) or on the basis of restriction related to the chest wall (severe kyphoscoliosis, morbid obesity, chronic fibrothorax, neurologic disorders which may impair the respiratory muscles, or chronic upper airway obstruction). Pulmonary arterial hypertension may also be produced as a result of chronic left to right intracardiac shunts (such as atrial septal defects or ventricular septal defects) or extracardiac shunts which can produce changes in the pulmonary vasculature resulting in elevated pulmonary arterial pressure. Finally, pulmonary arterial hypertension may be produced from long standing pulmonary venous or precapillary hypertension such as may be seen in chronic left ventricular failure.

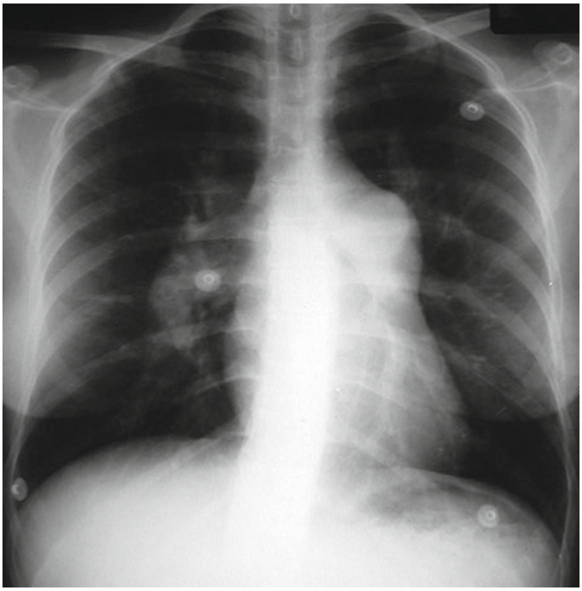

FIGURE 15.3 - PULMONARY ARTERIAL HYPERTENSION

Note the enlarged central pulmonary arteries with “pruning” of the vessels more peripherally

Shunt Vascularity

Figure 15.4 may at first appear identical to the radiograph on the previous patient. The enlargement of the hila and main pulmonary artery segments are similar. However, note that the pulmonary vasculature is much more prominent in the periphery of the lung than on the previous study.

This patient has a large atrial septal defect producing a left to right intracardiac shunt, thereby increasing pulmonary blood flow. Other left to right shunts (ventricular septal defect, patent ductus arteriosus) could give a similar appearance although both would be considerably less likely in an adult. The distinction between pulmonary arterial hypertension and the pattern caused by a left to right shunt may be confusing in patients with chronic shunts who have developed pulmonary arterial hypertension (Eisenmenger Syndrome).

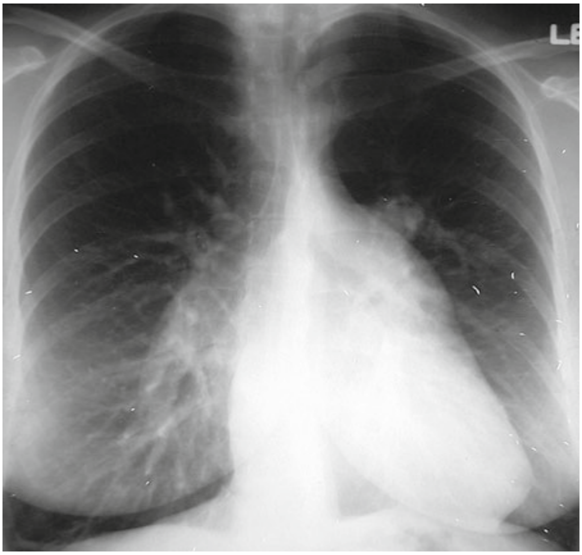

FIGURE 15.4 - SHUNT VASCULARITY
Note the prominence of the central hilar vessels as well as the more peripheral vessels, a pattern consistent with shunt vascularity

Pulmonary Venous Hypertension

Figure 15.5 is from a patient with pulmonary venous hypertension. Although the central pulmonary vasculature is prominent, it is not nearly as prominent as in pulmonary arterial hypertension or as in patients with left to right shunts. There is a convexity along the left cardiac border which is similar to that seen in the previous two examples; however, it is located slightly more inferior with respect to the aortic knob. This represents a dilated left atrial appendage. The left atrium is not normally a border-forming structure on the frontal radiograph; however, with dilation due to increased left atrial pressure, it may become visible. There is prominence of the upper lobe vasculature relative to the lower lobes (cephalization) representing redistribution of blood flow to the upper lobes. There may also be Kerley lines and peribronchial cuffing as well as thickening of the fissures on the lateral view. All of the latter findings should sound familiar to you as radiographic components of interstitial disease. The interstitial findings relate to the inability of blood in the pulmonary venous side of the pulmonary circulation to return from the lungs to the heart. The increased pressure on the venous side of the circuit may lead to transudation of fluid into the interstitium producing these findings.

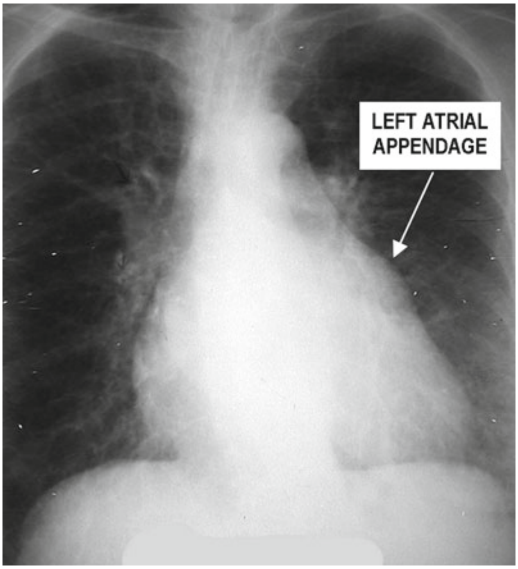

FIGURE 15.5 - PULMONARY VENOUS HYPERTENSION Frontal radiograph demonstrating pulmonary venous hypertension, note the left atrial appendage (*arrow*)

Any obstructive lesion on the left side of the heart (where blood coming from the lungs is headed) can produce this appearance. Hence, processes which cause left ventricular failure, mitral stenosis, or obstruction to flow of blood into or out of the left atrium such as left atrial myxoma could produce the findings of pulmonary venous hypertension.

On a statistical basis, findings of pulmonary venous hypertension are much more common than the other two categories described since left ventricular failure is such a common clinical problem. The chest radiograph is useful in distinguishing the less common, but by no means rare, causes of increased pulmonary vascularity (Fig. 15.6).

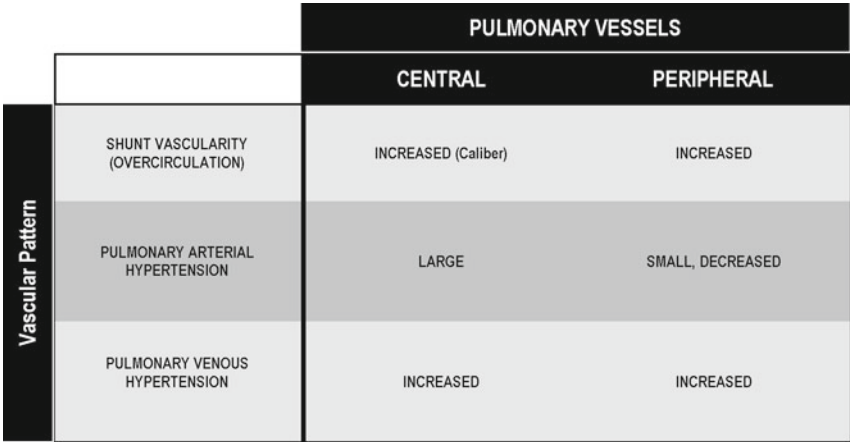

		PULMONARY VESSELS	
		CENTRAL	PERIPHERAL
Vascular Pattern	SHUNT VASCULARITY (OVERCIRCULATION)	INCREASED (Caliber)	INCREASED
	PULMONARY ARTERIAL HYPERTENSION	LARGE	SMALL, DECREASED
	PULMONARY VENOUS HYPERTENSION	INCREASED	INCREASED

FIGURE 15.6 - RADIOGRAPHIC DIFFERENCES BETWEEN SHUNT VASCULARITY Pulmonary arterial hypertension and pulmonary venous hypertension. By examining the caliber of the central and peripheral pulmonary vessels one can determine the vascular pattern

16

PULMONARY EDEMA

Objectives:

1. State the chest radiograph findings of left ventricular failure.
2. Identify one pulmonary disease that may alter the radiographic distribution of pulmonary edema.

Pulmonary edema secondary to left ventricular failure is one of the more common problems encountered in clinical medicine. The term congestive heart failure (CHF) is often applied both clinically and radiographically. Technically, CHF is a clinical diagnosis with a constellation of findings some of which are radiographic. Nevertheless, the terms cardiogenic pulmonary edema, left ventricular failure and CHF are often used synonymously in informal discussion.

The chest radiograph is an excellent tool for the early diagnosis of pulmonary edema and for assessing the effectiveness of treatment. This is because the chest radiograph is very reflective of minute to minute changes in cardiopulmonary function and circulating blood volume. A detailed description of the physiologic aspects of chest radiographic interpretation is beyond the scope of this discussion (Fig. 16.1). We will emphasize the changes in radiographic appearance on the chest X-ray only.

Changes of Cephalization

Figure 16.2 shows a normal and abnormal appearance of the pulmonary vasculature. As discussed in Chap. 14, the upper lobe vessels are normally smaller than those in the lower lobes due to the effect of gravity on the pulmonary circulation. The first abnormality detected in patients with early stages of left ventricular failure is redistribution of pulmonary blood flow to the upper lung zones, so called cephalization. With cephalization, the upper lobe vessels become engorged and

H Singh and JA Neutze (eds.), *Radiology Fundamentals: Introduction to Imaging & Technology*, DOI 10.1007/978-1-4614-0944-1_16,
© Springer Science+Business Media, LLC 2012

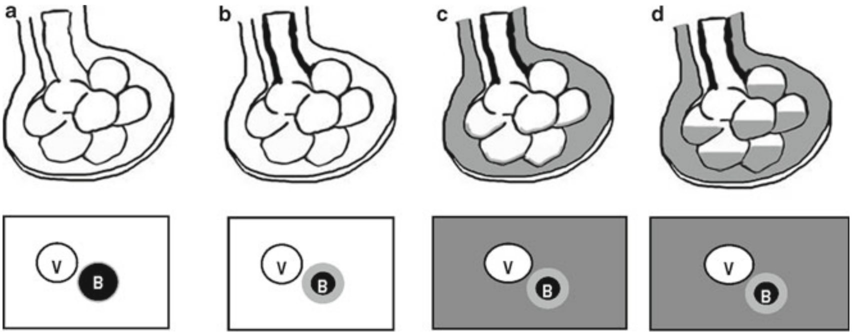

FIGURE 16.1 - PULMONARY EDEMA
(**a**) The normal alveolus and vessel/bronchus relationship is noted. (**b**) Shows peribronchial cuffing. (**c**) As the edema worsens, fluid starts to spill into the alveoli. (**d**) Shows the alveoli filled with fluid, markedly interfering with gas exchange

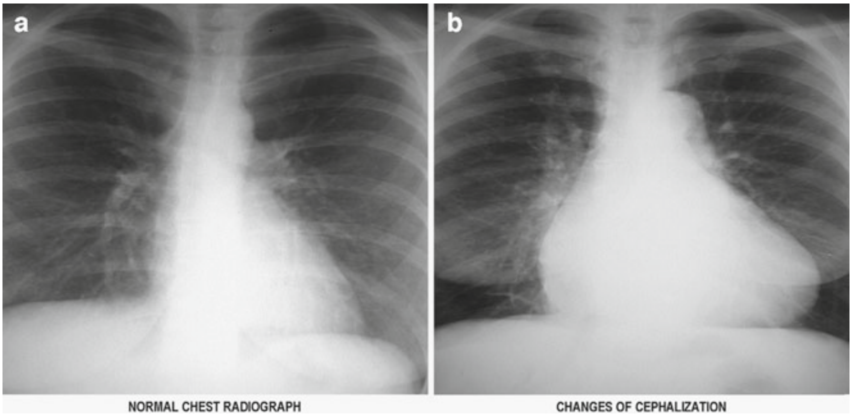

FIGURE 16.2 - REDISTRIBUTION OF VASCULAR FLOW (CEPHALIZATION)
Comparison of a normal chest radiograph (**a**) and one with cephalization (**b**). Note the distribution of the pulmonary vasculature in the normal radiograph. Look carefully at the right suprahilar region and compare the vessels in this region to the vessels in the right lower lung. Now look at the radiograph showing cephalization. Note the prominence of the suprahilar vessels compared to those of the right lower lobe in the case of cephalization

larger than the lower lobe vessels. Cephalization may be a subtle finding for those not used to scrutinizing the pulmonary vasculature closely. Remember that in the supine patient, the normal cranio-caudal gradation of perfusion due to gravity will no longer be present. Hence, cephalization will always be present on supine radiographs and therefore is lost as a useful diagnostic sign. This is another reason for obtaining an upright radiograph of the chest whenever possible.

Interstitial Edema

The next observable abnormality is the accumulation of fluid within the lung interstitium. This is the earliest stage at which there is radiographically detectable "extravascular lung water." Because this fluid is confined to the interstitium it does not seriously compromise gas exchange. The findings (peribronchial cuffing, Kerley A and B lines and subpleural interstitial thickening) are identical to other forms of interstitial disease.

The transition from cephalization to interstitial edema to airspace edema may be quite rapid in many circumstances and all of the described phases may not be discreetly observed (Fig. 16.3). These changes have been shown to correlate quite well with pulmonary capillary wedge pressures as measured with the Swan-Ganz catheter.

Figure 16.4 shows the most severe form of pulmonary edema. This is airspace or alveolar edema. Edema fluid spills into the alveoli, forming a barrier to gas exchange causing clinically evident respiratory impairment. The radiographic findings will be those of airspace disease with air bronchogram and confluent acinar shadows producing a fluffy white appearance.

Figure 16.5 shows a patient with pulmonary edema predominantly in the upper lobes. This patient also has underlying chronic obstructive pulmonary disease (COPD). In COPD, the pulmonary capillary beds may be destroyed in certain regions of the lung (in this case in the lower lobes) relegating pulmonary edema to an atypical distribution. One must always keep in mind that the appearance of pulmonary edema may be modified by the presence of severe COPD.

Pulmonary edema may be distinguishable from other forms of airspace disease radiographically by virtue of the fact that it is often bilateral and symmetric (as opposed to pneumonia or pulmonary hemorrhage which are more commonly asymmetrically distributed within the lungs). Pulmonary edema may have a fairly rapid

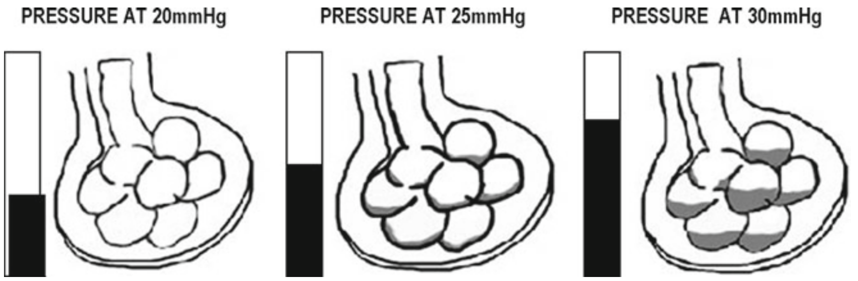

FIGURE 16.3 - PULMONARY EDEMA AND CAPILLARY WEDGE PRESSURE
Cephalization occurs when the pulmonary capillary wedge pressure is about 15–20 mm of mercury (mm Hg). Between 20 and 25 mm Hg one will observe predominantly interstitial edema. Alveolar edema occurs at capillary wedge pressures greater than 25 mm Hg

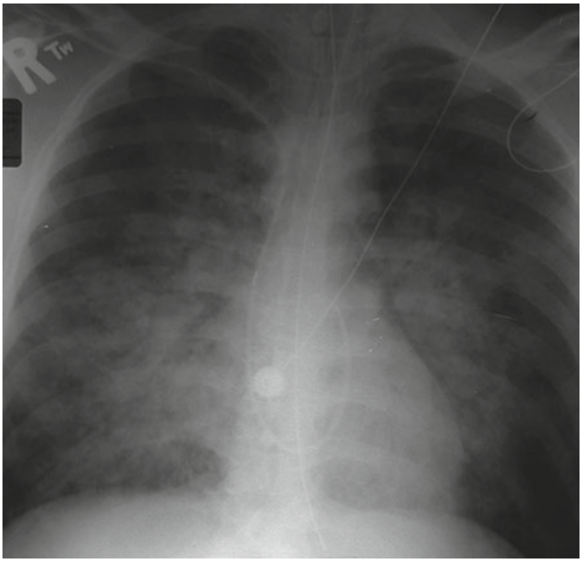

FIGURE 16.4 - AIRSPACE/ALVEOLAR EDEMA
Airspace with air bronchogram and confluent acinar opacities producing a fluffy white appearance

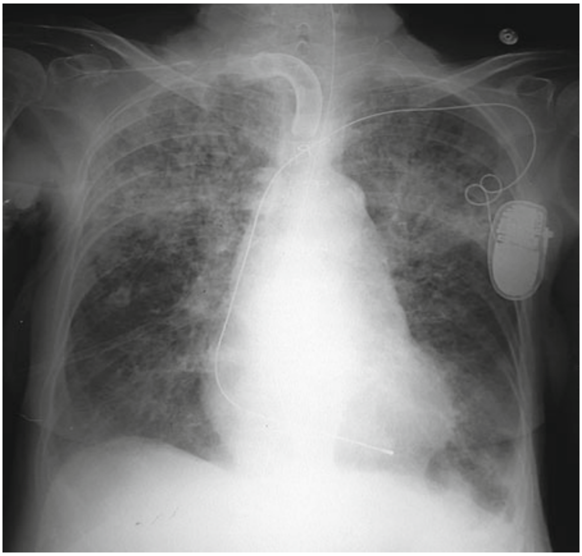

FIGURE. 16.5 PULMONARY EDEMA
Upper lobe predominant pulmonary edema in a patient with underlying COPD

onset and resolution (in comparison to pneumonia which usually develops and resolves more slowly). Of course, the diagnosis is best made by correlating the radiograph with an accurate history and physical examination as well as appropriate laboratory data.

Finally, noncardiogenic pulmonary edema, seen as a part of the adult respiratory distress syndrome (ARDS) is commonly seen in intensive care unit patients as the result of various etiologies such as sepsis and head trauma. Although the radiographic appearance of ARDS is similar to that of cardiogenic edema, the two are not totally identical, reflecting their very different physiological derangements. ARDS does not have the cardiomegaly or pleural effusions as usually seen in CHF.

17

PNEUMOTHORAX

Objectives:
1. Define “pneumothorax.”
2. State how you would distinguish a pneumothorax from a skin fold overlying the chest.
3. Discuss the findings you would expect to see in a tension pneumothorax.
4. Discuss the most common location for a pneumothorax in an upright patient, supine patient, and patient in the decubitus position.

A diagnosis that seems to cause much confusion in the clinical situation is that of a pneumothorax, which is the presence of air in the pleural space. Air is not normally present in this space. The visceral and parietal pleura are exclusively in contact with each other except for a very thin layer of intervening fluid which is not normally visible radiographically (Fig. 17.1). The expected appearance of a pneumothorax can be anticipated by using the basic principles which have already been introduced.

Radiographic Appearance of a Pneumothorax

Since a pneumothorax is composed of air, one would expect it to be less dense (darker) radiographically than the lung, which has a small soft tissue component in addition to its air space component. Since air rises, the pneumothorax will occupy the least-dependent (highest) position anatomically possible within the chest. This, of course, will vary depending on the patient’s position. For example, in the upright patient, the highest point will be in the apex of the thorax. In a lateral decubitus position the lateral aspect of the higher hemithorax will be least dependent. However, if the pleural space is not normal (for example, if the visceral and parietal pleura are

H Singh and JA Neutze (eds.), *Radiology Fundamentals: Introduction to Imaging & Technology*, DOI 10.1007/978-1-4614-0944-1_17,
© Springer Science+Business Media, LLC 2012

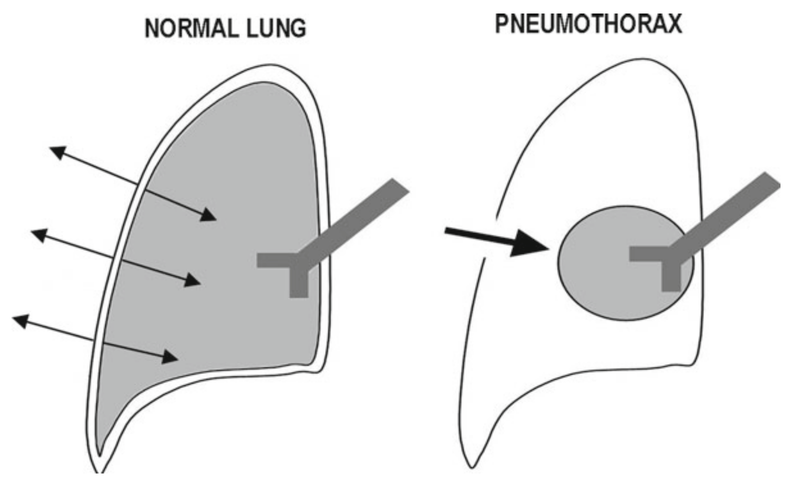

FIGURE 17.1 - NORMAL AND ABNORMAL FORCES ON THE LUNG
The normal elastic forces between the chest wall and the lung oppose each other, resulting in a certain equilibrium as noted in the picture on the *left*. With a pneumothorax (as depicted on the *right*) the chest wall is compromised, allowing air to enter the thorax and the lung to collapse

fused due to an old infection or trauma) then air may not be able to flow normally to the highest point in the chest. The term "loculated" is often applied to pleural air (or pleural effusion) which is constrained in such a manner. The compliance of the underlying lung may also affect the distribution of pleural air. In patients with rigid lungs (due to fibrosis, ARDS, pulmonary edema, etc.) the distribution of air in the surrounding pleural space may be altered.

Since the pleura have a small but detectable radiographic opacity, it will have the appearance of a thin white line at the edge of a pneumothorax in most cases. The pleura may become more easily visualized if it becomes thickened, in which case the white line will be more visible. The pleura will only be visualized in tangent as its density *en face* (head on) will not be great enough to produce a detectable shadow on the radiograph (Fig. 17.2).

Indirect signs of a pneumothorax include sharp mediastinal or diaphragmatic borders and increased lucency, reflecting the location of the pneumothorax. Current digital X-ray technology allows for image manipulation that aids in detection of pneumothoraces.

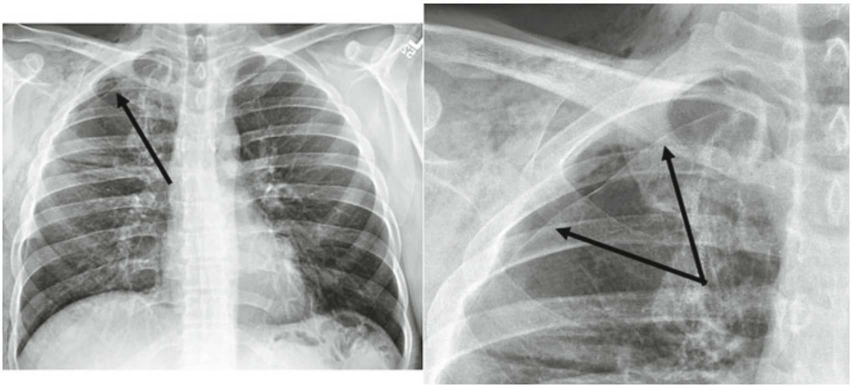

FIGURE 17.2 - PNEUMOTHORAX
Note how the edge of the right lung is delineated by a sharply demarcated *thin white line* (*arrows*), the visceral pleura, beyond which no pulmonary markings are identified (best seen on close up image on *right*)

Tension Pneumothorax

In certain cases, air may be trapped in the pleural space on inspiration but not released on expiration, producing a collection of air capable of exerting positive pressure on surrounding structures.

Figure 17.3 shows such a collection which is termed a "tension pneumothorax." This clinical situation is potentially life threatening since the increased intrathoracic pressure may shift the mediastinum enough to impair function of the contralateral lung as well as to impair venous return to the heart. Signs indicating a tension pneumothorax include mediastinal shift away from the side with the pneumothorax and depression of the ipsilateral hemidiaphragm. Chest tubes (thoracostomy tubes) are inserted to evacuate pneumothoraces.

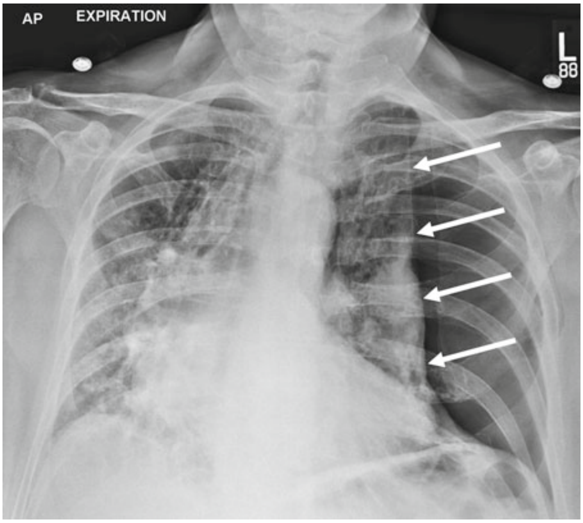

FIGURE 17.3 - TENSION PNEUMOTHORAX
Increased lucency of the right hemithorax with slight leftward mediastinal shift, widening of the right intercostal spaces and inferior displacement of the right hemidiaphragm, consistent with a right tension pneumothorax

Deep Sulcus Sign

Figure 17.4 shows a radiograph obtained portably in a supine patient. One will notice a collection of air in the right costophrenic sulcus. When the patient is supine, this is often the least-dependent position of the chest.

This finding constitutes what is called a “deep costophrenic sulcus sign.” The deep costophrenic sulcus sign may be seen in supine patients who have a pneumothorax. The “deep sulcus sign” reflects the pneumothorax that is anterior and lateral. In this case, if one looks closely, the pleural line can be observed.

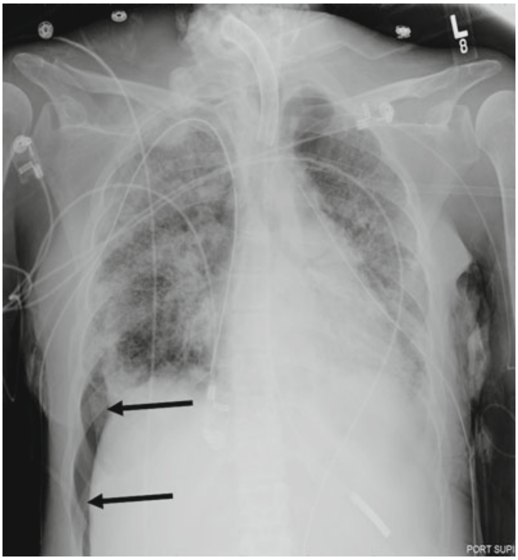
L
8
PORT SUPI

FIGURE 17.4 - DEEP SULCUS SIGN
Note the collection of air (*arrows*) in the right costophrenic sulcus

18

MISCELLANEOUS CHEST CONDITIONS

Objectives:
1. Describe the radiologic appearance and etiology of calcific pericarditis.
2. Describe three distinct radiological appearances of intrathoracic tuberculosis.
3. Describe the appearance of two AIDS defining pulmonary illnesses.
4. Describe the chest radiograph findings in pulmonary embolus.
5. State the relationship between asbestos exposure and bronchogenic carcinoma of the lung.
6. List the differential diagnosis of an opacified hemithorax.

The following radiographs show examples of entities with diagnostic radiographic presentations. By seeing the “classic” examples of these entities, you will hopefully gain enough familiarity to make the diagnosis should you encounter them clinically.

Calcific Pericarditis

Figure 18.1 shows frontal and lateral views of a patient with the diagnosis of calcific pericarditis. Note the rim of calcium surrounding the cardiac pericardial silhouette on both the frontal and lateral views. In severe cases, this may cause decreased diastolic filling of the cardiac chambers and require surgical removal of the pericardium.

Currently, the most common etiology for calcific pericarditis is viral infection, often Coxsackie B virus. In the older population, granulomatous pericarditis secondary to tuberculosis is the most common cause of calcific pericarditis.

H Singh and JA Neutze (eds.), *Radiology Fundamentals: Introduction to Imaging & Technology*, DOI 10.1007/978-1-4614-0944-1_18,
© Springer Science+Business Media, LLC 2012

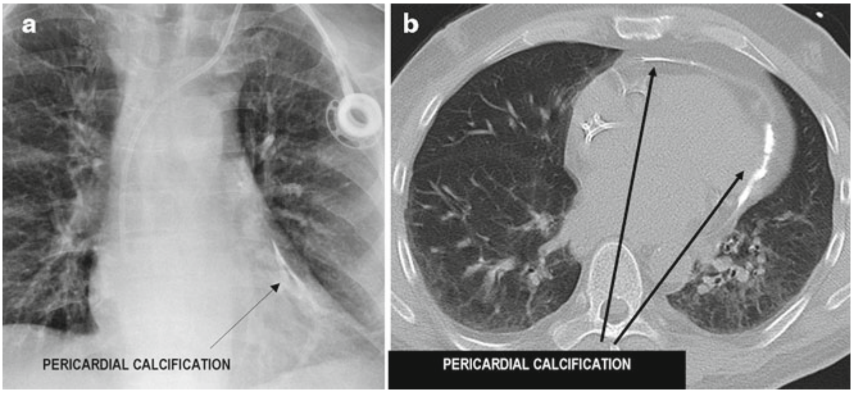

FIGURE 18.1 - CALCIFIC PERICARDITIS
(**a**) A cropped chest radiograph shows a rim of calcium along the left heart border (*arrows*). (**b**) An axial CT slice from the same patient again demonstrates the rim of calcium along the left heart border but also shows a rim of calcium along the anterior heart border that was not seen on plain radiograph. In severe cases this may cause decreased diastolic filling of the cardiac chambers and require surgical removal of the pericardium

Any cause of pericardial irritation (uremia, radiation) can eventually lead to calcific pericarditis. Approximately 50% of these cases of calcific pericarditis will have radiographically visible calcification.

Tuberculosis

Figure 18.2a shows a thick-walled cavitary lesion in the right upper lobe with surrounding areas of inhomogeneous parenchymal consolidation. In addition, there is parenchymal air space disease in the left mid lung. This is the appearance of cavitary tuberculosis with endobronchial spread. The air within the cavitary lesion comes from erosion of the initial focus of disease into the tracheal bronchial tree of the right upper lobe. The necrotic caseous material within the consolidation is aspirated into the more dependent lingula, in this case, causing spread of disease. The differential diagnosis for a cavitary upper lobe lesion should always include tuberculosis, especially if the lesion involves primarily the apical or posterior segments.

Figure 18.2b also shows innumerable punctate nodular opacities distributed throughout both lungs. This is the appearance of a hematogenously disseminated infection to the lungs, in this case, miliary tuberculosis. This is an advanced case of this disease, and cavitation does not occur in this process. Healing, with proper therapy, will be complete with no radiographically visible residual abnormality within the lung.

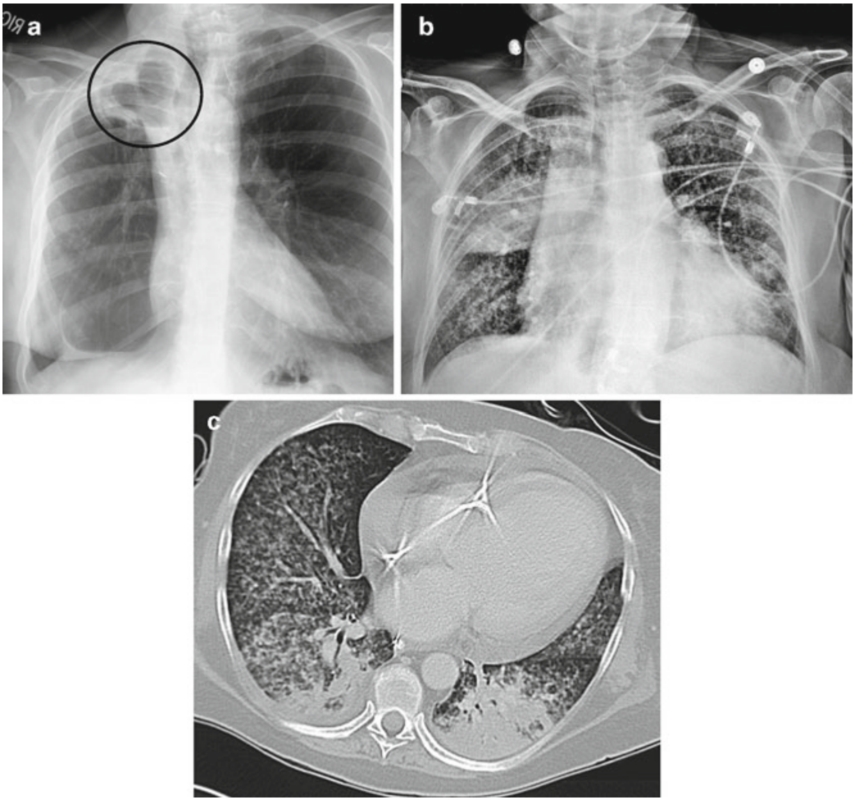

FIGURE 18.2 - CAVITARY TUBERCULOSIS
(**a**) Demonstrates a cavitary lesion in the right upper lobe with surrounding areas of heterogeneous parenchymal consolidation from a patient with known TB. Miliary tuberculosis: (**b, c**) are from the same patient with known miliary TB. The plain chest radiograph shows innumerable punctate nodular opacities distributed throughout both lungs and a focal area of consolidation in the right mid lung. The axial CT image again shows innumerable punctate nodular opacities in both lungs and areas of consolidation. Though this appearance is nonspecific as it can be seen with miliary tumor metastasis, it is characteristic of hematogenously disseminated miliary tuberculosis

Mediastinal Lymphadenopathy

Figure 18.3 shows widening of the superior mediastinum in both the right and left paratracheal regions extending down to the superior aspect of both hila and subcarinal region. This is the appearance of mediastinal lymphadenopathy. One cause of mediastinal lymphadenopathy is infection with mycobacterium avium-intracellulare (MAI).

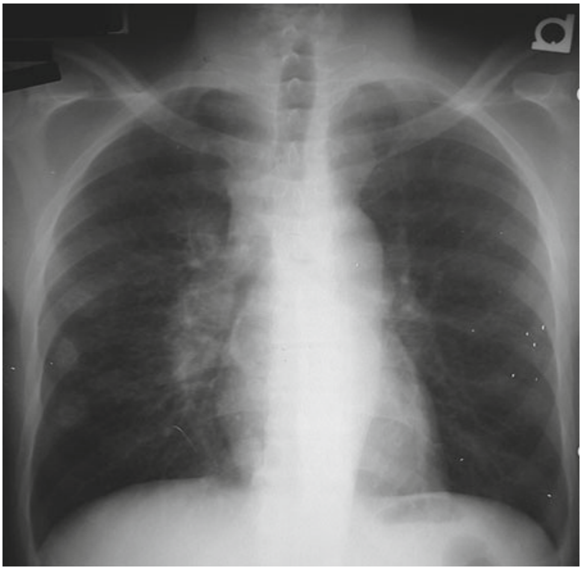

FIGURE 18.3 - LYMPHADENOPATHY
Widening of the superior mediastinum in both the right and left paratracheal regions extending down to both hila and subcarinal region, in a case of mycobacterium avium-intracellulare (MAI) infection

MAI infections may present with a minimum of pulmonary findings and only mediastinal and hilar lymphadenopathy, as noted in this case. Fungal disease such as histoplasmosis may give a similar presentation. Of course, lymphoma and other malignant causes of lymphadenopathy and other nonmalignant causes, such as sarcoidosis, would be in the differential diagnosis. Patients who are HIV positive have a considerably elevated risk for the development of all forms of mycobacterium infections.

Kaposi's Sarcoma

In an HIV positive individual, a chest X-ray with many large nodules can have an extensive differential diagnosis. The differential should include all forms of metastatic neoplasm as well as an unusual presentation of opportunistic infection such as fungal disease. It should also include Kaposi's sarcoma, a usually rare malignancy which is seen frequently in HIV positive individuals. The radiographic manifestations of Kaposi's sarcoma in the chest are many. Multiple nodules are commonly seen. A slightly nodular, pneumonia-like appearance extending from the hila into the mid and lower lungs is another presentation commonly seen in Kaposi's sarcoma.

Pneumocystis Carinii Pneumonia

Figure 18.4 shows diffuse reticular disease distributed homogeneously throughout both lungs and associated with minimal volume loss in a young HIV positive patient. Note that the patient is intubated, indicating that respiratory failure is present. This is a common presentation of pneumocystis carinii pneumonia (PCP), a disease caused by the yeast-like fungus Pneumocystis jirovecii (an organism initially classified erroneously as a protozoan), seen almost exclusively in the HIV positive population. Severe bullous disease as residua of PCP infection may predispose the patient to super-infection, as well as pneumothorax. Pneumatoceles of smaller size and less extensive distribution may also be seen as residua of PCP infection.

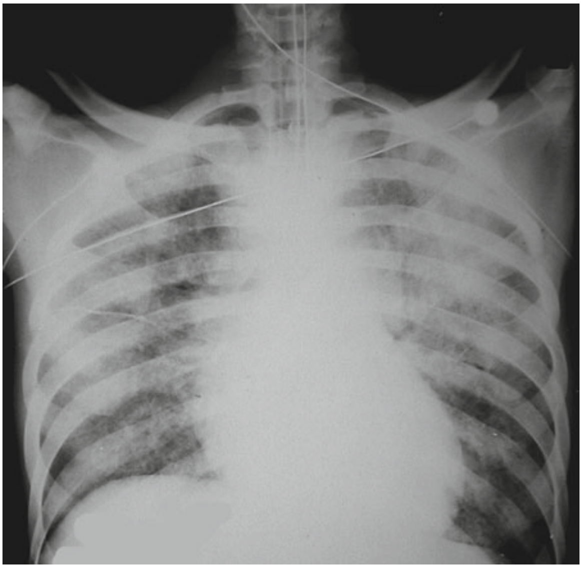

FIGURE 18.4 - PCP PNEUMONIA
Diffuse bilateral interstitial reticular opacities with minimal volume loss in a young HIV positive patient

Pulmonary Embolus

Pulmonary embolus is seen as a complication of many surgical procedures and has an increased incidence in hospitalized patients in general. The most common radiographic presentation of pulmonary embolus is a normal chest radiograph (seen in approximately 50–75% of individuals). Approximately 5% of patients with pulmonary emboli will have a generalized decreased perfusion of the lung (relative oligemia) which can be detected if one looks closely at the radiograph. This is referred to as the Westermark sign as seen in Fig. 18.5. Note also the prominence of the right hilar pulmonary artery due to increased pressure proximal to the obstruction caused by the large embolus found in this patient (Fleischner sign).

The diagnosis of pulmonary embolus is usually made after a nuclear medicine study, ventilation perfusion (VQ) scan, or chest CT (Fig. 18.6).

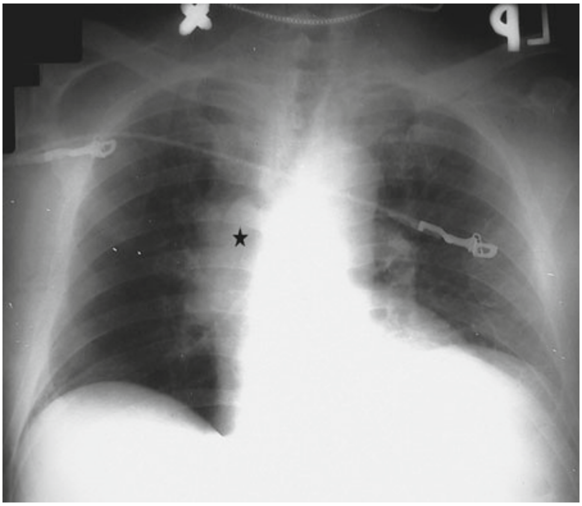

FIGURE 18.5 - WESTERMARK SIGN
Note the lucency of the right lung, signifying Westermark's sign. In addition, the enlarged right pulmonary artery (*filled star*), due to increased pressure proximal to the obstruction, is caused by a large embolus found in the patient (Fleischner sign)

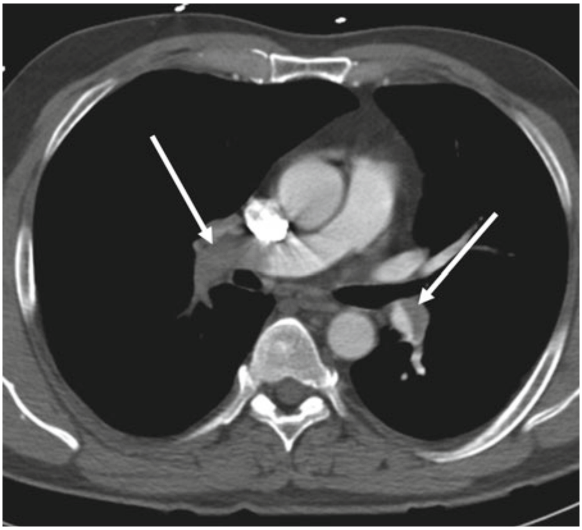

FIGURE 18.6 - PULMONARY EMBOLI
Axial CT image showing large filling defects (*white arrows*) in both the right main and a left interlobar pulmonary artery representing two distinct pulmonary emboli

Asbestos

Figure 18.7 is a radiograph from a patient with numerous calcified and noncalcified bilateral pleural plaques. These are secondary to asbestos exposure. There is a long latent period between time of asbestos exposure and the development of the plaques, on the order of 10 to 15 years in most cases. The plaques are associated with the parietal pleura, unique to asbestos plaques. Calcified pleural thickening may also be seen in patients with an old empyema or an old hemothorax. These characteristically primarily involve the *visceral* pleura and are often unilateral. Radiographically, you cannot tell between visceral and parietal pleural calcification so clinical history is important (Fig. 18.8).

Bronchogenic carcinoma is the most commonly associated malignancy in patients with a history of asbestos exposure. Mesothelioma, although more uniquely associated with asbestos exposure, is much less common. Patients with a history of asbestos exposure also have increased incidence of esophageal, gastric, and other gastrointestinal carcinomas because asbestos fibers are swallowed as well as inhaled. A patient with a history of asbestos exposure as well as significant smoking history has a very substantially increased risk of developing bronchogenic carcinoma.

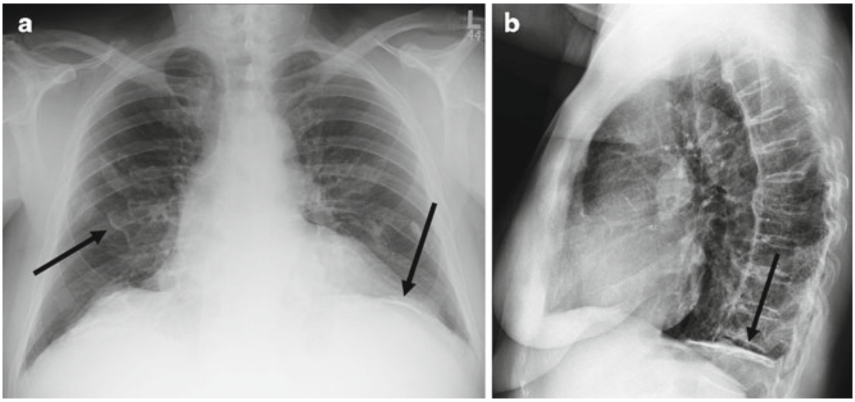

FIGURE 18.7 - (A, B) PLEURAL PLAQUES
PA and lateral X-ray of different patients showing calcified pleural plaques (*arrows*) secondary to asbestos exposure

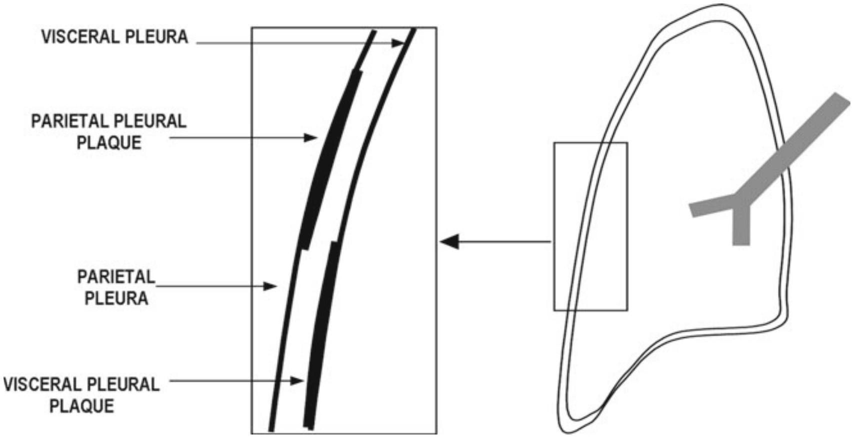
VISCERAL PLEURA
PARIETAL PLEURAL PLAQUE
PARIETAL PLEURA
VISCERAL PLEURAL PLAQUE

FIGURE 18.8 - PLEURAL PLAQUES
After a latent period of 10–15 years, asbestos exposure can result in parietal pleural plaques, a unique location related to the asbestos exposure. Patients with a history of empyema or hemothorax will have visceral pleural plaques

Opacified Hemithorax

Figure 18.9 shows a case of homogeneously increased opacity in the left hemithorax. Note that the mediastinum is shifted toward the left side so that the heart is not clearly distinguished, obscured by the surrounding increased opacity. This patient has undergone a left pneumonectomy, the post pneumonectomy space being filled with fluid. Note that there is still a small apical collection of air and therefore an air fluid level. Eventually the whole hemithorax will fill with fluid. The right lung has undergone compensatory hyperinflation.

Other differential diagnoses in patients with a unilateral opacified hemithorax include a large pleural effusion, pneumonectomy, and total atelectasis of the lung. In a patient with a large pleural effusion, it would be expected that the mediastinum would be at least in the midline or, most likely, shifted to the opposite side of the opacified hemithorax due to the mass effect of fluid in the chest. Patients with complete atelectasis of the lung or pneumonectomy will have mediastinal shift to the same side as the opacified hemithorax. A quick history and physical examination should allow one to distinguish between atelectasis and pneumonectomy. A large scar on the chest wall may be present with the latter.

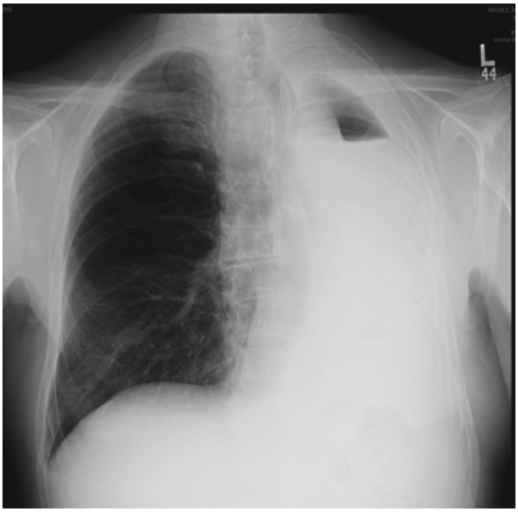

FIGURE 18.9 - OPACIFIED HEMITHORAX
Homogenously increased opacity in the left hemithorax. Note that the mediastinum is shifted toward the left and the heart is not clearly distinguished from the surrounding increased density

19

TUBES AND LINES

Objective:

1. State the ideal positions for the endotracheal tube, central venous catheter, and nasogastric tube.

The main point of the following radiographs is to show normal and abnormal positions of various commonly seen tubes and catheters.

The Endotracheal Tube

Figure 19.1 shows proper positioning of an endotracheal (ET) tube terminating approximately 3 cm above the carina. The ideal position for an endotracheal tube is 3–4 cm above the carina. Portable radiographs, like this one, are commonly obtained to check endotracheal tube position.

The reason for positioning the ET tube 3–4 cm above the carina is that the tube moves within the trachea with changes in head position because the tube is fixed at its insertion point in the nose or the mouth. With flexion of the neck, the position of the tube moves inferiorly about 2 cm. With extension, the tube moves superiorly approximately 2 cm. Ideal positioning assures that the endotracheal tube tip or balloon cuff will not enter one of the main bronchi inferiorly or the larynx superiorly with changes in the patient's head position. The ET tube tip should be no higher than 7–8 cm above the carina and no lower than 2–3 cm above the carina.

Figure 19.2 shows an endotracheal tube with its tip positioned in the proximal right main bronchus. Atelectasis (collapse) of the left lung is seen. Atelectasis

H Singh and JA Neutze (eds.), *Radiology Fundamentals: Introduction to Imaging & Technology*, DOI 10.1007/978-1-4614-0944-1_19,
© Springer Science+Business Media, LLC 2012

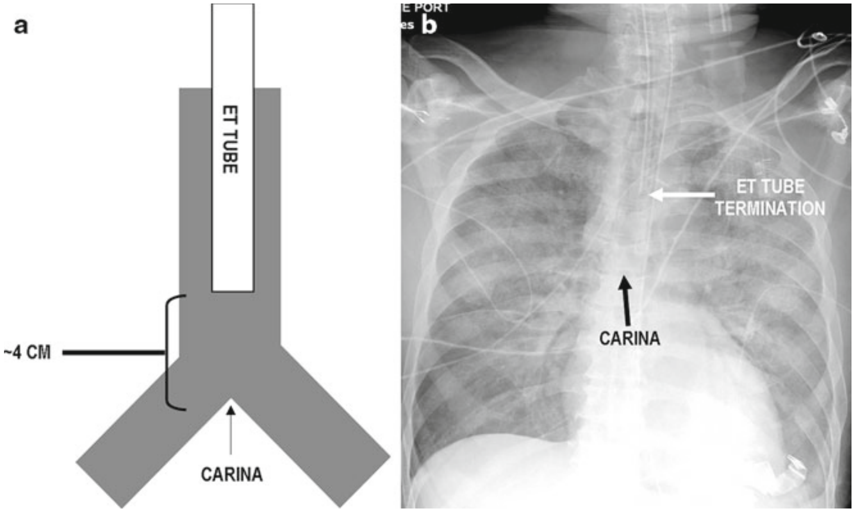

FIGURE 19.1 - (A, B) PROPER ENDOTRACHEAL TUBE POSITIONING
The endotracheal tube tip should ideally be placed roughly 4 cm above the carina. The vertical radiopaque line represents a marker placed within the wall of the tube to make it visible on radiographs

occurs because the left lung is not ventilated. This is a common complication related to misplacement of the ET tube but it readily resolves when the ET tube is appropriately repositioned.

Central Venous Catheters

Figure 19.3 shows the pathways of central venous catheters. Catheters can be inserted via the subclavian vein or the internal jugular vein. They then traverse the brachiocephalic vein to get to the superior vena cava. If the line is a temporary venous access such as a peripherally introduced central catheter (PICC) or a permanent central venous access line such as an infusion catheter, the catheter tip will be at the cavoatrial junction (#1). If the line is an exchange or dialysis catheter, either temporary or permanent, the tip will be at the mid-right atrium (#2). If the line is a Swan–Ganz catheter, the tip will be in either the main pulmonary artery or a central pulmonary artery branch (#3).

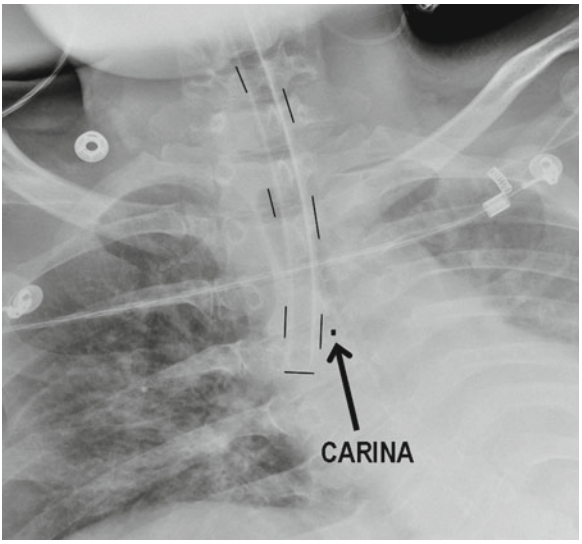

FIGURE 19.2 - RIGHT MAIN BRONCHUS INTUBATION
Endotracheal tube tip is in the right main bronchus. Diffusely increased opacity throughout the left lung is probably secondary to atelectasis, a common complication of improper endotracheal tube placement

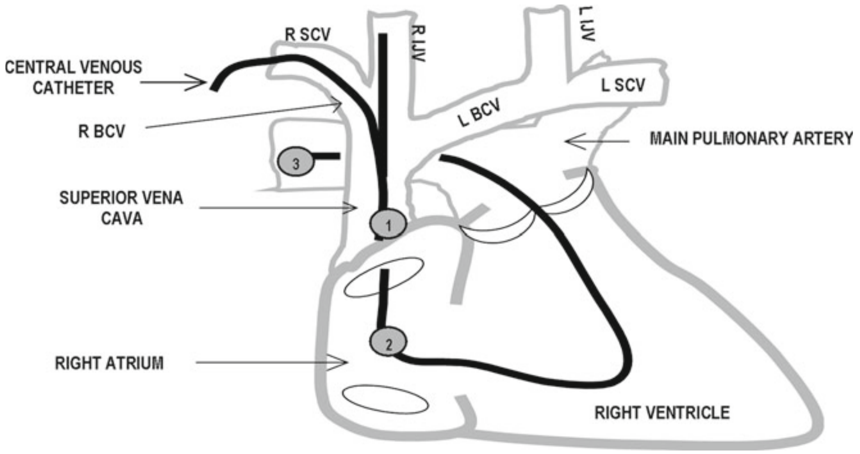
CENTRAL VENOUS CATHETER
R SCV
R IJV
L IJV
L SCV
L BCV
R BCV
MAIN PULMONARY ARTERY
3
SUPERIOR VENA CAVA
1
2
RIGHT ATRIUM
RIGHT VENTRICLE

FIGURE 19.3 - COMMON PATHWAYS OF CENTRAL VENOUS CATHETERS
Nomenclature: *SCV* subclavian vein, *IJV* internal jugular vein, *BCV* brachiocephalic vein. The numbers denote the ideal tip placement for the following catheter types: (1) PICC, (2) dialysis catheter, and (3) Swan–Ganz catheter

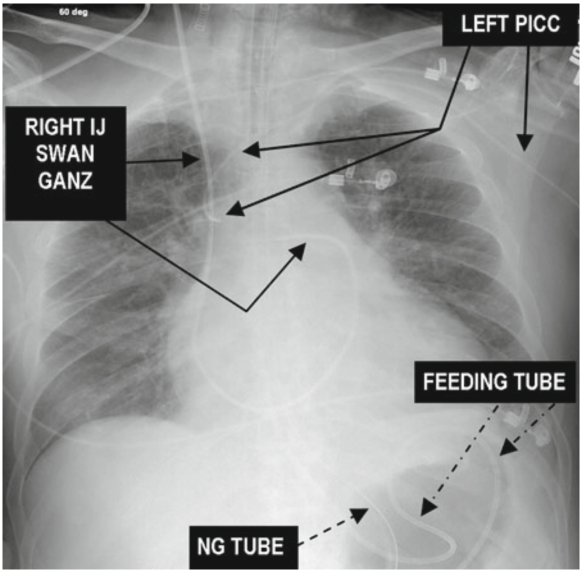

FIGURE 19.4 - CENTRAL CATHETERS
Note the Swan as it curves through the heart. The PICC terminates in the SVC. Also note the NG tube and feeding tube coiled in the stomach

Figure 19.4 shows two central catheters. The first is a PICC inserted via the left basilic vein and terminating near the confluence of the brachiocephalic veins where they converge to form the superior vena cava. The second is a Swan–Ganz catheter entering from a right internal jugular vein approach with the tip in the right pulmonary artery.

An increasingly uncommon complication of insertion of arterial or venous catheters in the subclavian region is pneumothorax since these vessels lie close to the apex of the lung. When venous access is attempted, the pleural space may be entered. For this reason, an upright radiograph should be obtained after line placement in these patients, as pneumothoraces will be more visible on an upright study.

Figure 19.5 shows an appropriately positioned PICC, with the tip in the superior vena cava. These catheters are of very weak radiopacity so that proper radiographic technique must be employed to visualize them. It is routine to obtain post line placement radiographs so that problems can be detected early.

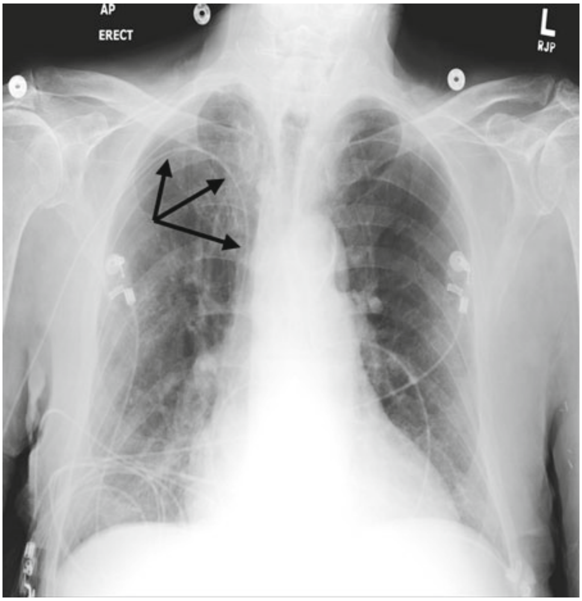

FIGURE 19.5 - PICC PLACEMENT
Right peripherally inserted central catheter (PICC) with tip appropriately positioned in the superior vena cava

The Nasogastric Tube

Figure 19.6 shows a normally positioned nasogastric tube. The tube tip should terminate in the stomach, which lies in the left upper quadrant of the abdomen. The radiopaque marker on the tube shows a single gap in the distal portion, approximately 8–10 cm from the tip, denoting the location of the side hole. The side hole should also be within the stomach.

REMEMBER: *You MUST ALWAYS know that a line or tube is correctly placed before using it*!

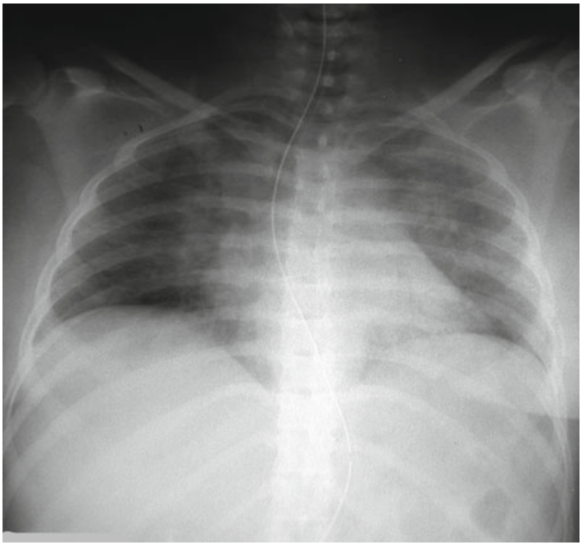

FIGURE 19.6 - NASOGASTRIC TUBE
Nasogastric tube tip is below the diaphragm, excluded from the field of view, in satisfactory position. Refer to Fig. 18.4 to see NG tube coiled in stomach

20

BREAST IMAGING

Objectives:
1. Describe the two views used in a standard mammography examination.
2. State other imaging modalities used for evaluating the breast.
3. Understand that radiation doses vary due to technology and breast size.
4. State the overall sensitivity of mammography and what conditions may alter the sensitivity of the examination for detecting cancer.
5. State the main radiographic criteria for detection of breast carcinoma.
6. Understand the BI-RADS classification.

Breast carcinoma is the most common neoplasm in women, with approximately 200,000 new cases each year. The early detection of breast cancer with mammography has contributed to a decrease in mortality of up to 40%. There have also been improvements in the therapy for breast cancer with agents that target cancers based on their individual biology.

The success of screening mammography is best accomplished with compliance with annual examinations. This increases the sensitivity of detecting subtle changes and is especially true in denser breast tissue. It is important to note the difference between screening and diagnostic mammography. Screening mammography is the annual mammogram that images the breast tissue in the craniocaudal (CC) and mediolateral oblique view (MLO) views, which are described below. Diagnostic mammograms are used to better characterize a suspicious finding after it is found on a screening mammogram or in a patient with a problem such as palpable lump. Diagnostic mammograms involve extra views, spot views of the lesion in question, and magnification views.

The introduction of digital mammography has proven to be beneficial in women with dense breast tissue, premenopausal and younger women, and those at high risk for breast cancer. The early results describe a benefit of up to 30% improvement in the detection of occult malignancies in this population.

H Singh and JA Neutze (eds.), *Radiology Fundamentals: Introduction to Imaging & Technology*, DOI 10.1007/978-1-4614-0944-1_20,
© Springer Science+Business Media, LLC 2012

The purpose of the following section is to acquaint you with some basic aspects of breast imaging and the early detection of breast cancer.

Standard Mammography Views: CC and MLO

Figure 20.1 demonstrates the two standard views obtained during a routine mammogram.

The craniocaudad view (CC) is obtained by placing the X-ray tube overhead and the film cassette or digital detector beneath the breast so that the beam traverses the breast in a craniocaudad direction as the name implies.

A MLO is obtained by placing the film cassette or digital detector in the axilla and allowing the X-ray beam to traverse the breast from the medial breast to the lateral breast and axilla. The breast is compressed during mammography for the purpose of decreasing the amount of tissue the X-ray beam must traverse. This decreases patient radiation dosage. Compression also functions to stabilize the breast and reduce motion artifact as well as to spread out superimposed structures. Compression of the breast maximizes the mammogram image quality. This compression may be uncomfortable for some patients, but it is brief in duration and results in a mammogram which has higher diagnostic quality.

Figure 20.2 shows an example of a typical mammogram consisting of CC and MLO views. The darker, more lucent areas represent fat while the whiter, less transparent areas are composed of fibroglandular tissue. Fibroglandular tissue is comprised of the glandular tissue of the breast, as well as the underlying fibrous elements which add support to the overall structure.

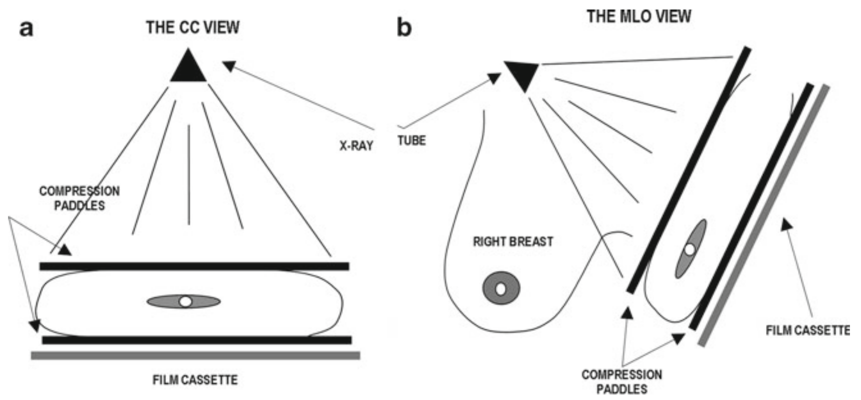

FIGURE 20.1 - THE CC AND MLO BREAST VIEWS
In the CC view (**a**), the breast is compressed between two radiolucent paddles to spread the tissue out, reducing tissue overlap and also decreasing dose. In the MLO View (**b**), the breast is compressed in an oblique fashion, with the tail of breast tissue which extends toward the axilla, included on the film

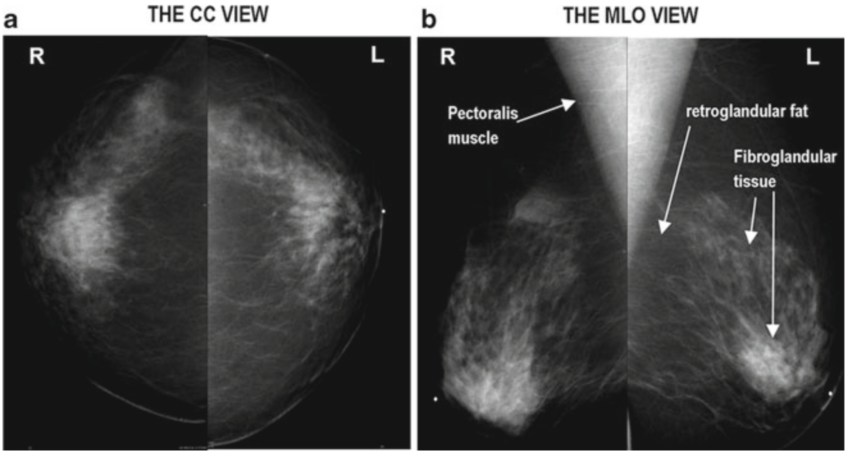

FIGURE 20.2 - THE CC AND MLO BREAST VIEWS
These are the mammographic images produced by the technique in Figure 20.1. Note the added visualization of the pectoralis muscle on the MLO view

The fibroglandular tissue is generally distributed in what may be termed a cone with the nipple at the apex and the base closer to the chest wall. Between the posterior aspect of the cone of fibroglandular tissue and the underlying pectoral muscle is the retroglandular fat. Well-positioned MLO mammogram views should contain the fibroglandular tissue in its entirety, the retroglandular fat and a good portion of the pectoralis muscle.

Dense Fibroglandular Breast Tissue

Figure 20.3 demonstrates a breast with a predominance of dense fibroglandular tissue. For comparison, Fig. 20.4 demonstrates breasts that are predominantly fatty tissue which are more commonly found in older women.

Sensitivity for detecting a small carcinoma is diminished in dense breasts. This must be kept in mind when reading a mammographic report. Often, radiologists will include a statement in their reports to the effect that the sensitivity of the study is diminished due to the overall density of the breast. Digital mammography is 30% more sensitive in the detection of abnormalities in patients with dense breasts (Pisano et al. 2005).

Dense breast parenchyma may be anticipated in younger and premenopausal women, lowering the sensitivity of identifying smaller cancers. The young breast is

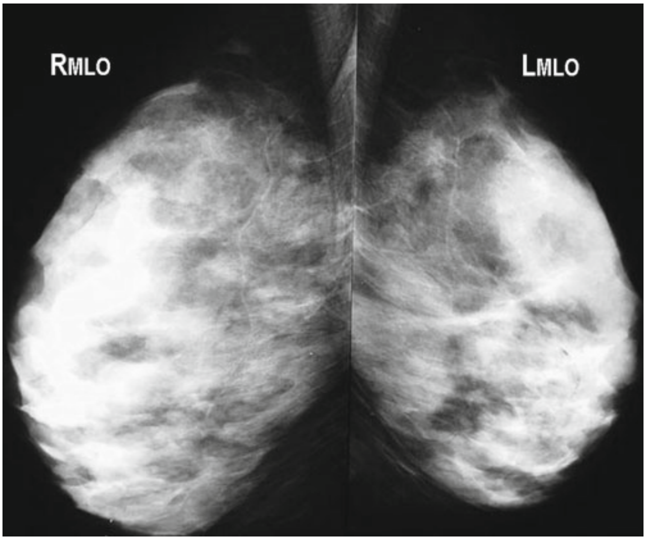

FIGURE 20.3 - DENSE BREAST TISSUE

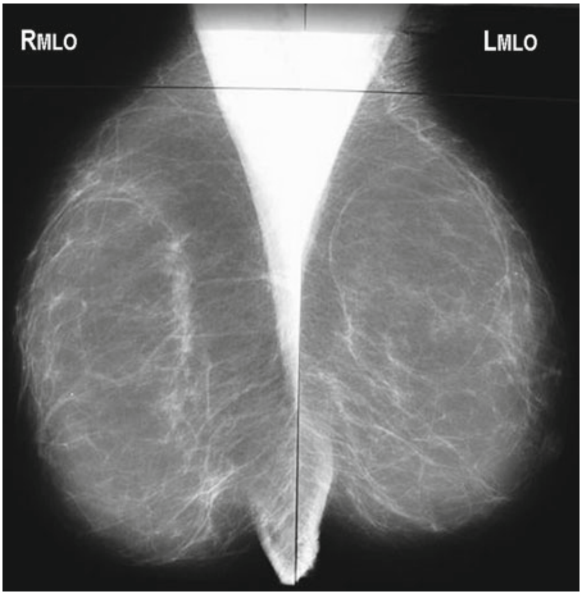

FIGURE 20.4 FATTY BREAST TISSUE
An example of fatty breast tissue for comparison to the dense breast tissue in Fig. 20.3

also more sensitive to the potential carcinogenic effects of radiation and for that reason screening of women of average risk begins at age 40.

It is important that high-risk younger women be screened. Women with first-degree relatives with breast cancer or with known genetic mutations should be screened annually, at an age 10-years younger than the age of the first-degree relative's cancer. Women who have had chest radiation for Hodgkins lymphoma are also considered high risk and should begin screening 8 years following the therapy, but not before age 25. Women under 40 years who have had biopsies showing high-risk histology (ductal or lobular atypia, etc.) are advised to begin screening at that point.

Breast Implants

Figure 20.5 demonstrates a very dense homogeneous opacity close to the chest wall. This is the appearance of a breast implant.

Implants may be placed in two different ways. Some implants are located posterior to the pectoralis major muscle (retropectoral) which can be seen curving around the implant's anterior surface, while other implants are placed anterior to the pectoralis muscle (prepectoral). From a mammographic stand point, the main problem with implants is that they obscure a considerable amount of breast parenchyma and

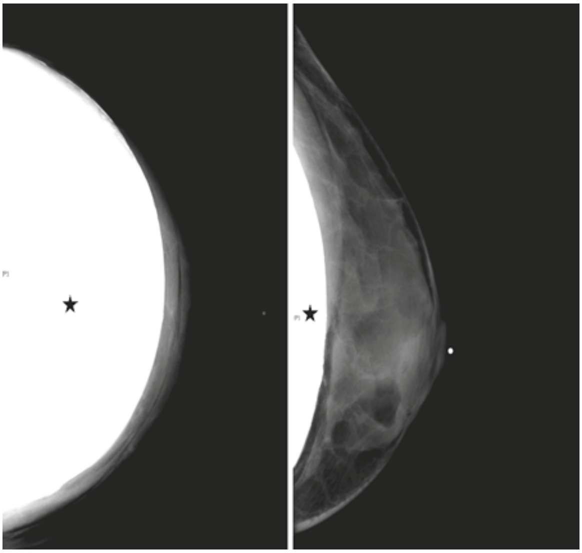

FIGURE 20.5 - BREAST IMPLANTS
The image on the *left* is a conventional CC view while the one on the *right* is an implant (*star*) displaced CC view

can make detection of early carcinomas more difficult. For this reason, patients with breast implants undergoing mammography get two full sets of mammograms (both CC and MLO). One set is the conventional type while the other set is taken with the implant displaced.

Mammographic Findings

To detect breast cancer at its earliest stage, radiologists evaluate the images for subtle changes in the density and architecture of the breast tissue, as well as microcalcifications. The breast density varies by individual, and generally decreases with age as fat replaces the fibroglandular tissue. Density affects the sensitivity of mammography for early breast cancer detection (see Dense Fibroglandular Breast Tissue – Fig. 20.3).

Calcifications are frequently observed. Based upon their imaging characteristics, radiologists have classified calcifications into benign types and types that are worrisome for malignancy. The following four figures provide examples of microcalcifications that are suggestive of malignancy, as well as several types of classic benign calcifications (Figs. 20.6–20.9).

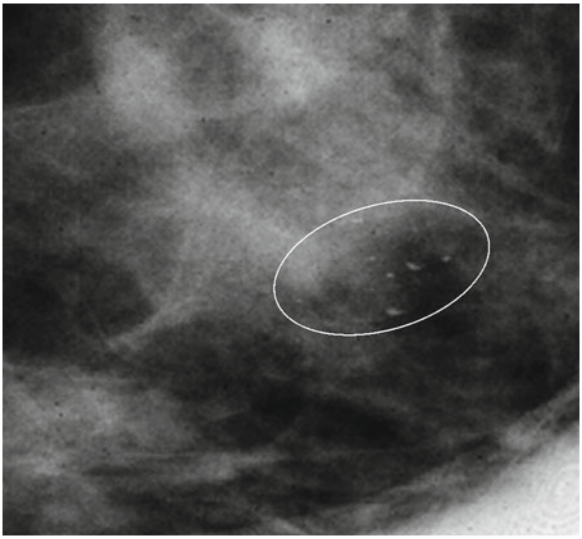

FIGURE 20.6 - BENIGN CALCIFICATIONS
Milk of calcium layering out in a gravity-dependent fashion, demonstrated with 90° positioning of the breast

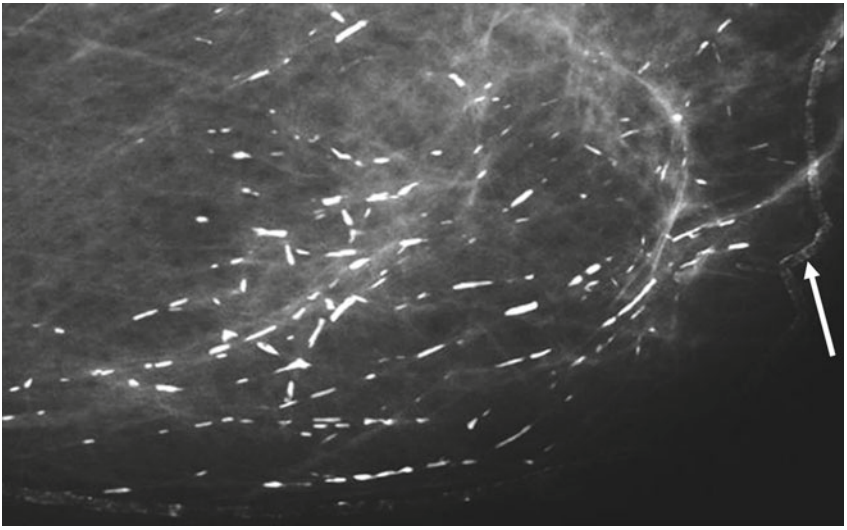

FIGURE 20.7 - BENIGN CALCIFICATIONS
Two examples of benign calcifications. First, the large, rod-shaped calcifications scattered throughout the breast. Second, vascular calcifications common with age (*arrow*)

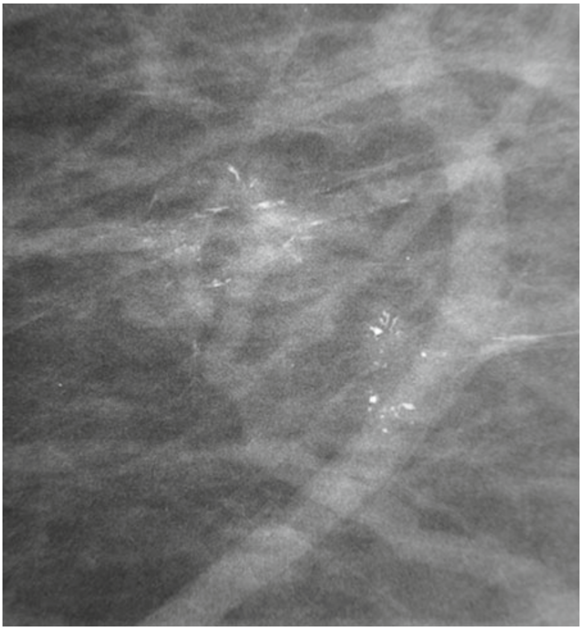

FIGURE 20.8 - MICROCALCIFICATIONS
Spot magnification compression views showing pleomorphic, fine branching microcalcifications related to DCIS

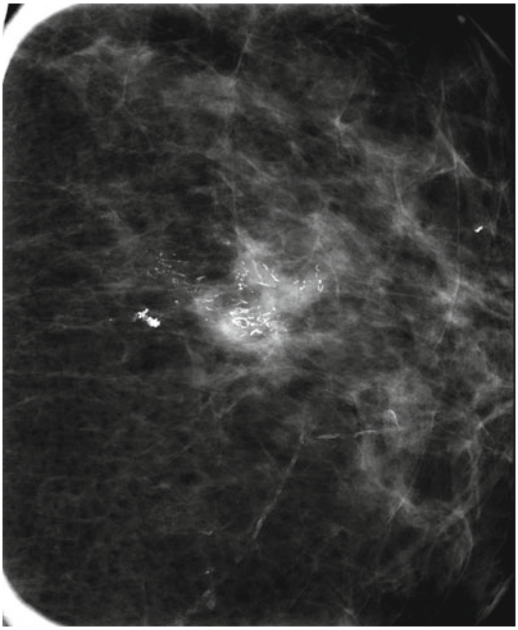

FIGURE 20.9 - MICROCALCIFICATIONS
Spot magnification compression views showing classic pleomorphic, linear branching calcifications associated with a spiculated mass in coexisting invasive ductal carcinoma and DCIS

Figure 20.10 demonstrates two examples (a and b) of well circumscribed masses called fibroadenomas. In Fig. 20.10b the mass contains coarse "popcorn" calcifications characteristic of a degenerating fibroadenoma. Fibroadenomas are one of the most common benign tumors of the breast.

In contrast to the benign fibroadenomas, Figs. 20.11a, b demonstrates a mass characteristic of carcinoma as seen on the standard two view mammogram.

Radiation Dosage

The dosage to the breast for a two-view examination (four total exposures) is approximately 200–300 millirads. The exposure is less for some digital imaging, measuring approximately 85–150 millirads. This is approximately three to ten times the dosage of a PA chest radiograph (25 millirads) depending on the technology used. At the stated dose level, mammography carries the hypothetical risk for

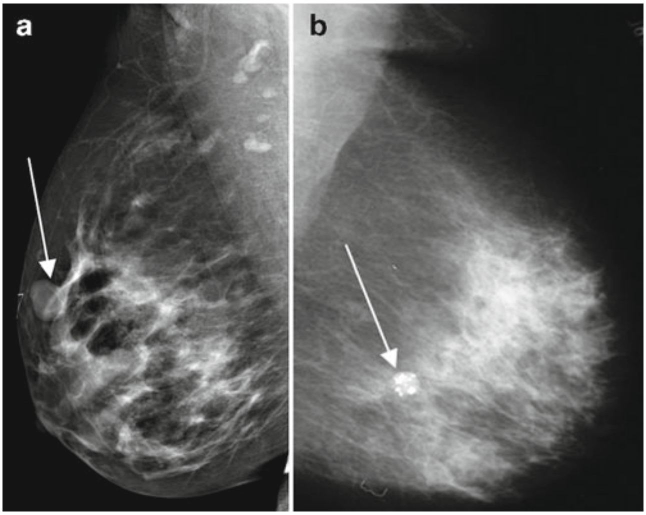

FIGURE 20.10 - FIBROADENOMA
Two different examples (**a**, **b**) of fibroadenomas. Both are smoothly marginated. Note how the one on the *right* contains coarse calcifications which is characteristic of a degenerating fibroadenoma

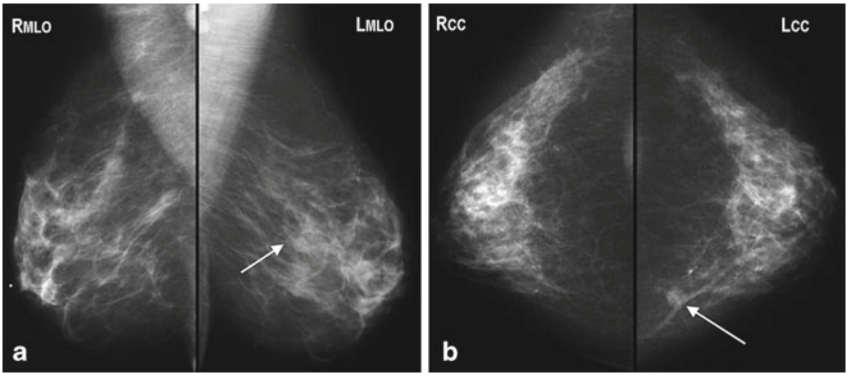

FIGURE 20.11 - BREAST MASS
(**a**) Breast mass MLO views. Mass in the left breast suspicious for carcinoma. (**b**) Breast mass CC views. Mass in the left breast seen in the MLO views, suspicious for breast carcinoma

approximately one excess cancer case per year per million women examined. If one assumes 50% breast cancer mortality, the hypothetical risk would be one excess death per two million women examined. The term hypothetical is used because, at such low increased risk, a large number of patients followed for a long period of time would be required to statistically demonstrate an effect. Because of the large population size needed for valid research, the actual research study has never been performed, and the statistics are extrapolations of patients exposed to higher dosage levels from other sources. Background radiation contributes more exposure to each of us each year, particularly those who fly frequently. It is important to keep these relationships in mind, since you will be asked frequently by patients about the safety of mammography.

The overall sensitivity of mammography for detecting breast carcinoma is approximately 90%. However, this sensitivity can be diminished substantially, and can be as low as 40% in young patients with dense breasts.

Ultrasound Utilization in Breast Imaging

Breast ultrasound is advocated for focused evaluations of abnormalities on physical examination, mammograms and after breast MRI. Whole breast ultrasound alone has not been proven to be sensitive and efficient enough to use as a screening test for breast cancer. Ultrasound has been proven to identify additional cancers as a complementary procedure to screening mammography in the early detection of breast cancer particularly in high-risk women.

When a circumscribed (smoothly marginated) breast mass is discovered on mammography, the differential diagnosis includes breast carcinoma, benign tumor of the breast such as fibroadenoma, and simple breast cyst. To avoid performing biopsies on women with breast cysts and other clearly benign lesions, ultrasound may be employed as it is excellent in discriminating cystic from solid lesions and characterizing masses.

Figure 20.12 demonstrates a mammogram of a palpable mass highlighted by a skin marker. This lesion was subsequently imaged by ultrasound as depicted in Fig. 20.13. The ultrasound shows a focal area which is free of echoes and smoothly marginated. This corresponds in location to the opacity seen on the conventional mammogram depicted in Fig. 20.12. The lesion represents a simple cyst and no further workup is required.

Breast MRI

Contrast of different soft tissues is 10–100× greater on MRI images than on conventional X-ray imaging. But, MRI is expensive, not readily available and sensitive but not specific, limiting its use as a screening modality. MRI is used in the screening of

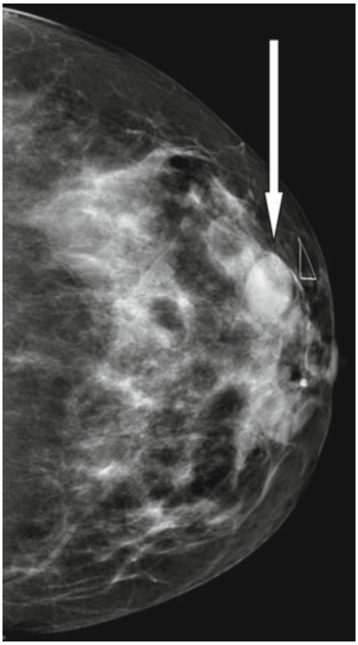

FIGURE 20.12 - PALPABLE MASS
Skin marker (the metallic *triangle*) used to indicate a palpable mass (*arrow*)

high-risk women for breast cancer in addition to, not in place of, mammography. MRI does not detect the small calcifications which can be associated with cancer. Other applications are evolving.

MRI is indicated in any woman with a new diagnosis of breast cancer. Its primary strength is near 100% sensitivity in the detection of breast cancer and definition of the extent of disease in the preoperative setting. Surgical planning also depends on accurate evaluation of skin, chest wall, and regional lymph nodes (Fig. 20.14).

Image-Guided Biopsy

Suspicious findings identified by any imaging modality can be easily biopsied with image guidance. Mammographic findings such as microcalcifications are best approached with stereotactic mammographic guidance. Images of the breast are obtained at 15° off center and this "stereo pair" is used to calculate the *x*, *y*, and *z* coordinates of the location of the abnormality in the breast. After the administration

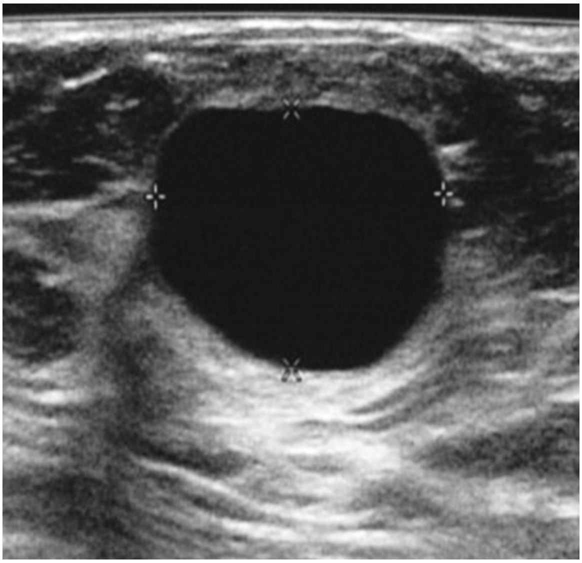

FIGURE 20.13 - SIMPLE BREAST CYST
A simple cyst is defined as anechoic, well circumscribed, with well-defined borders, and posterior acoustic enhancement

of local anesthesia, a probe is then positioned at these coordinates for sampling. Lesions at the chest wall are difficult to reach with this method and may require other modalities to biopsy.

As mentioned above, ultrasound is often used to evaluate the site of a palpable mass or mammographic abnormality. It is also an ideal modality for guiding biopsy. It is a more comfortable and cost-effective examination for the patient, and lesions in any part of the breast can be approached.

BI-RADS®

The following table shows the BI-RADS® Classification used by breast radiologists to communicate findings to other clinicians in a standard and consistent form. BI-RADS stands for Breast Imaging-Reporting and Data System and is a quality assurance tool published by the American College of Radiology. At the end of every mammogram report one of these numbers is listed (Table 20.1).

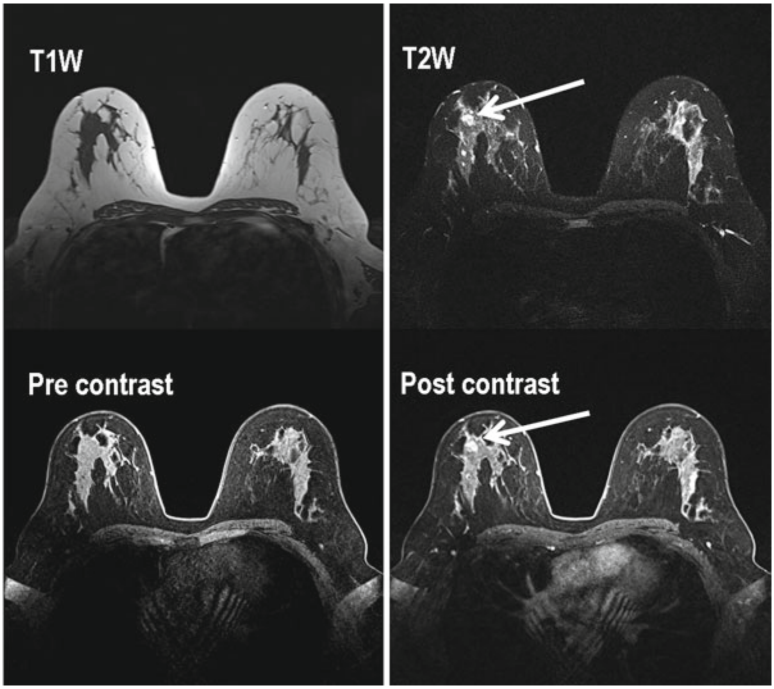
T1W
T2W
Pre contrast
Post contrast

FIGURE 20.14 - BREAST MRI
A breast MRI showing enhancement in a breast cancer (*arrows*)

Table 20-1 BI-RADS® classification (BI-RADS® is a registered trademark of the American College of Radiology, Reston, VA)

Category	Assessment	Explanation
0	Incomplete	Your mammogram or ultrasound did not give the radiologist enough info to make a diagnosis. Follow-up imaging is necessary
1	Negative	There is nothing to comment on; routine screening is recommended
2	Benign finding(s)	A definite benign finding; routine screening is recommended
3	Probably benign findings – initial short-interval follow-up suggested (findings with <2% risk of malignancy)	Findings that have a high probability of being benign (>98%); 6 month short interval follow-up
4	Suspicious abnormality-biopsy should be considered	Not characteristic of breast cancer, but reasonable probability of being malignant (3–94%); biopsy should be considered
5	Highly suspicious of malignancy-appropriate action should be taken (>95% probability)	Lesion that has a high probability of being malignant (>95%); take appropriate action
6	Known biopsy proven malignancy-appropriate action should be taken	Lesions known to be malignant that are being imaged prior to definitive treatment; assure that treatment is completed

Additional Reading

Pisano E, Gatsonis C, Hendrick E, et al. Diagnostic Performance of Digital versus Film Mammography for Breast Cancer Screening – The Results of the American College of Radiology Imaging Network (ACRIN) Digital Mammographic Imaging Screening Trial (DMIST). NEJM. 2005 Oct 27;353(17):1773–83

21

WOMEN'S ULTRASOUND

Objectives:

1. Understand how different imaging modalities contribute to evaluating conditions and diseases unique to women.
2. Name several causes of abnormal uterine bleeding and appreciate their ultrasound characteristics.
3. Name several masses seen in the ovary and appreciate their ultrasound characteristics.
4. List imaging modalities and applications in the evaluation of fertility and pregnancy.

Women's imaging is a subspecialty area of radiology devoted to the diagnosis and treatment of conditions and diseases which are unique to women. Women's imaging uses all imaging modalities to evaluate gynecologic and obstetrical conditions, breast health, and contributes to urologic evaluations and overall health. Discussions about some of these modalities and application are further addressed in specific chapters on breast imaging and women's health interventional procedures.

Ultrasound plays the primary role for much of women's imaging applications with fluoroscopy studies, CT, MRI, and nuclear medicine studies performed to assist in the subsequent evaluation. Ultrasound does not produce ionizing radiation and examinations rarely require sedation, making it a desirable modality for women of all ages.

H Singh and JA Neutze (eds.), *Radiology Fundamentals: Introduction to Imaging & Technology*, DOI 10.1007/978-1-4614-0944-1_21,

© Springer Science+Business Media, LLC 2012

Evaluation of Premenstrual Females

Women's imaging can begin before puberty. Ultrasound is used to evaluate a variety of problems in girls. Indications include evaluation for congenital abnormalities of the uterus, vaginal bleeding, precocious puberty and palpable pelvic masses. Ultrasound abnormalities often prompt further evaluation with laboratory information, CT, MRI, and sometimes direct visualization (surgery).

Evaluation of the Uterus and Uterine Bleeding

Abnormal uterine bleeding is bleeding unrelated to normal menstruation and can occur in women of any age. Organic causes of abnormal uterine bleeding include problems related to pregnancy, medication, benign and malignant masses, and systemic disease. Dysfunctional uterine bleeding (DUB) is defined as abnormal bleeding which does not have an organic cause and is commonly related to anovulation and abnormal function of the hypothalamic–pituitary–ovarian axis. Common dysfunctional uterine bleeding terms include menorrhagia (prolonged bleeding), metromenorrhagia (irregular bleeding) and spotting (intermenstrual bleeding).

Ultrasound is commonly used to begin the evaluation of abnormal uterine bleeding. Ultrasound may identify structural causes for the abnormal bleeding such as fibroids and polyps which extend into the endometrial cavity. Ultrasound can assess the thickness and contour of the endometrial lining and determine if the bleeding may be the result of a thin atrophic endometrium or a thick endometrium which may reflect hypertrophy or cancer. Ultrasound may identity structural changes in the endometrium from drugs such as tamoxifen. Pelvic ultrasound can contribute to the evaluation of amenorrhea such as seen with polycystic ovarian syndrome and pregnancy.

Transabdominal ultrasound is commonly performed first to evaluate the pelvis as it provides an "overview" of pelvic structures. The urine-filled urinary bladder is used as an acoustic window to best evaluate pelvic structures. Transvaginal ultrasound is performed with an ultrasound probe which is cleaned and covered with a sterile probe cover, and inserted into the vagina; the transvaginal approach provides more detail of the uterus, the endometrium and the ovaries. Transvaginal pelvic ultrasound evaluation is similar to a speculum pelvic examination and the patient does not have the discomfort of maintaining a full bladder (Fig. 21.1a–d).

Additional imaging may be prompted by ultrasound findings. MRI may be performed to further evaluate the myometrium and endometrial–myometrial junction. MRI can be used to evaluate for adenomyosis, a process where endometrium is deposited into the endometrial myometrial junction and myometrium CT may follow an ultrasound if a pelvic mass is identified and there is concern for more extensive disease. Diagnostic imaging does not always explain the cause of the cause of abnormal uterine bleeding but may direct the indication and location for biopsy, hysteroscopy, surgery or follow-up.

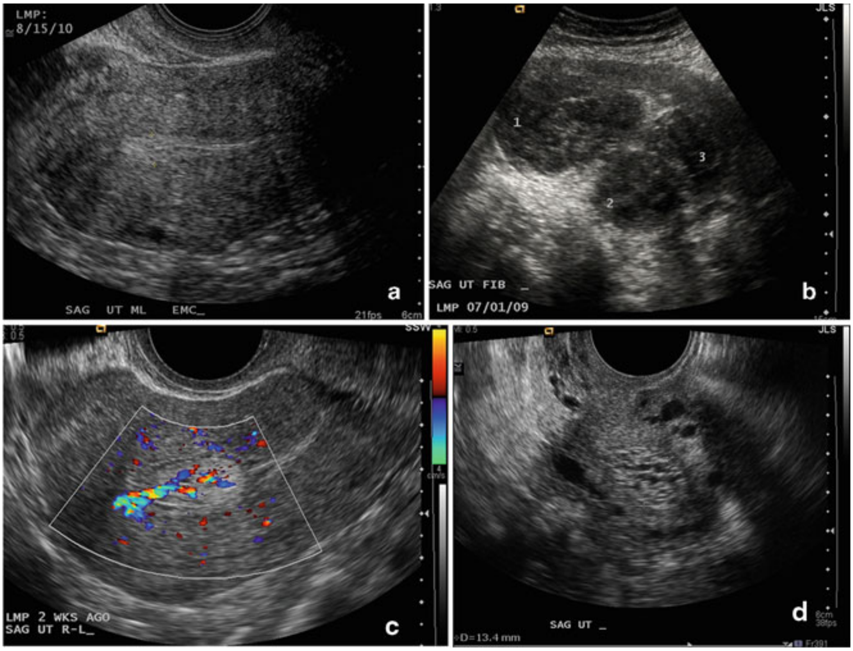

FIGURE 21.1 - EXAMPLES OF TRANSVAGINAL ULTRASOUNDS
(**a**) normal endometrium, with bright walls and central cavity delineated by *white line* (**b**) multiple hypoechoic fibroids, (**c**) echogenic polyp with central vascular stalk, and (**d**) cystic changes of endometrium from tamoxifen

Evaluation of the Ovaries

Imaging commonly is an adjunct to physical examination of the adnexa. It may be difficult to tell if a “full” adnexa is merely stool-filled bowel or pathology in the ovaries or in surrounding structures. Ultrasound commonly begins the evaluation. While there are some “classic” ultrasound findings of ovarian structures such as normal functional follicles, hemorrhagic cysts and endometriomas, many ovarian masses have nonspecific findings (Figs. 21.2a–d). A complex cystic mass in the adnexa is particularly hard to manage because the differential diagnosis is extensive and includes benign and malignant cystic neoplasm, atypical cyst, endometrioma, dermoid, torsed ovary, abscess, hydro- and pyosalpinx, as well as nongynecologic masses such as mesenteric cysts. Clinical evaluation is essential to determine if the process needs immediate intervention such as antibiotics or surgery. If patient is not acutely ill, follow-up ultrasound in 2–3 menstrual cycles is commonly recommended and performed. If follow-up ultrasound remains concerning, MRI may further char-

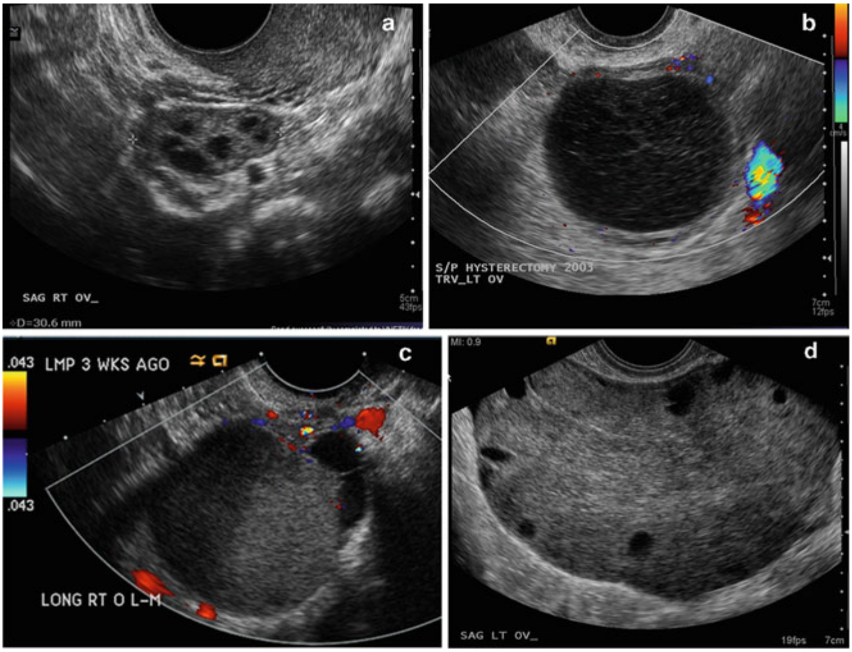

FIGURE 21.2 - EXAMPLES OF OVARIAN ULTRASOUNDS
(**a**) normal ovary, (**b**) hemorrhagic cyst with reticulated mesh-like echoes, (**c**) endometrioma with homogeneous echoes, and (**d**) enlarged torsed ovary with peripheral follicles

acterize the ovarian mass but the patient and her physician may elect to go to laparoscopy for visual and pathologic diagnosis (Fig. 21.3a, b). CT may be performed to determine extent of disease such as the presence of ascites or peritoneal metastases.

Pregnancy

An evaluation of pregnancy may begin with infertility. Fallopian tube patency can be assessed with hysterosalpingography in which contrast is instilled into the uterine cavity under fluoroscopy. If the fallopian tubes are patent, contrast will spill out of the tubes into the peritoneal cavity. Hysterosalpingography, ultrasound and MRI can assess the contour of the cavity itself and look for problems that might affect pregnancy such as large fibroids, congenital anomalies, and scarring of the cavity. The male partner may be evaluated for problems which may affect fertility such as varicoceles and testicular pathology with scrotal ultrasound.

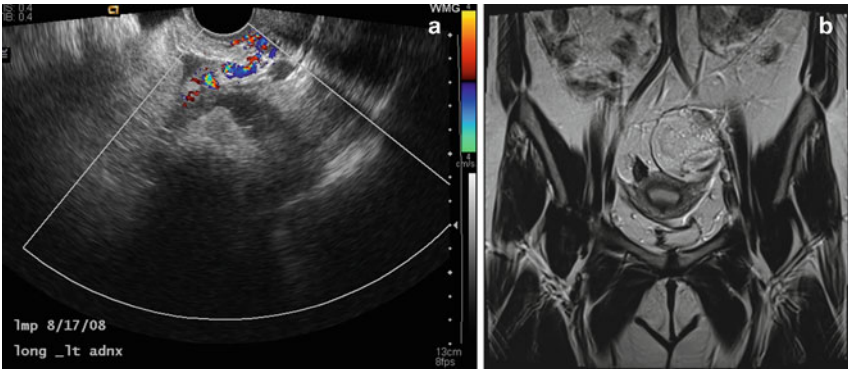

FIGURE 21.3 - "TIP OF THE ICEBERG" CONFIGURATION OF AN OVARIAN DERMOID (CYSTIC TERATOMA) ON ULTRASOUND
(**a**); the multiple types of tissue that make up a dermoid such as hair, blood, fat, cartilage, and calcifications create an acoustic shadow, which blocks all sound waves and the mass is essentially obscured. The corresponding MRI (**b**) shows the extent and complex nature of the mass. Fat identified in an ovarian mass on CT or MRI is classics for dermoid

Ultrasound is used to assess for the presence of intrauterine pregnancy initially and then for appropriate fetal growth and well being. Ultrasound is commonly used to assess for ectopic pregnancy when the patient has a positive pregnancy test and may have vaginal bleeding and/or pain. It is important to interpret the ultrasound results in conjunction with the patient's quantitative serum B-HCG levels. That is, sometimes the ultrasound is performed so early that an intrauterine pregnancy cannot be indentified and the differential includes very early intrauterine pregnancy, ectopic pregnancy, and early pregnancy loss. Ultrasound is used in the evaluation of retained products of conception and gestational trophoblastic disease (Fig. 21.4a–d).

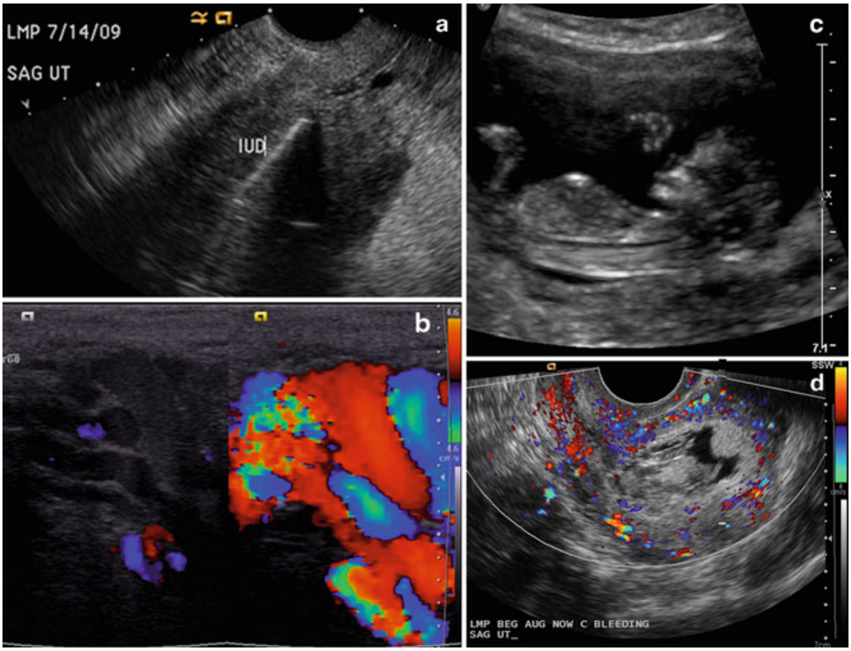
LMP 7/14/09
SAG UT
IUD
a
b
c
7.1
d
LMP BEG AUG NOW C BLEEDING
SAG UT_

FIGURE 21.4 - ULTRASOUND FINDINGS IN FERTILITY
(**a**) bright echogenic IUD in endometrial cavity, (**b**) hypervascular varicocele which increased in size and vascularity with Valsalva maneuver (**c**) intrauterine fetus, and (**d**) irregular heterogeneous tissue with degeneration of gestational trophoblastic disease (molar pregnancy)

22

WOMEN'S HEALTH INTERVENTIONS

Objectives:

1. Describe which three interventional procedures are considered part of Women's Health Interventions.
2. Understand the indications for each of the procedures.
3. Describe the basics of how each procedure is performed.

Introduction

"Women's health interventions" is a newly coined term in Interventional Radiology. It describes the group of Interventional Radiology procedures that are related to female pelvic structures and includes Uterine Artery Embolization (UAE) or Uterine Fibroid Embolization (UFE), Ovarian Vein Embolization for Pelvic Congestion Syndrome (PCS), and Fallopian Tube Recanalization. Each procedure will be discussed separately.

Uterine Artery or Fibroid Embolization

Of the approximately 600,000 hysterectomies performed in the USA each year, about 200,000 are for symptomatic fibroids. Symptoms can include significant menorrhagia, dysmenorrhea, urinary frequency and/or urgency, constipation, back pain, lower extremity pain, and dyspareunia. There are many treatment methods for symptomatic fibroids including oral contraceptives, chemical menopause, myomectomy, and hysterectomy. UAE or UFE represents a specific method of treating symptomatic patients. The "ideal" patient is an approximately 45-year-old female with multiple small fibroids who has completed child bearing and has severe menstrual symptoms. Contraindications include pedunculated subserosal fibroids and

H Singh and JA Neutze (eds.), *Radiology Fundamentals: Introduction to Imaging & Technology*, DOI 10.1007/978-1-4614-0944-1_22,
© Springer Science+Business Media, LLC 2012

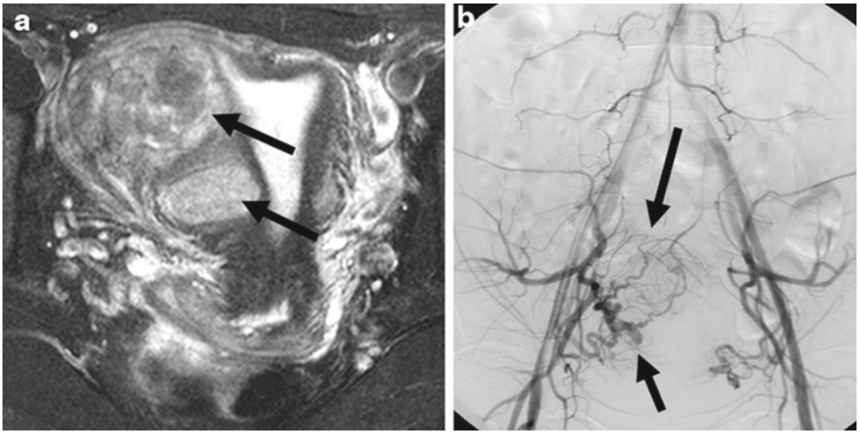

FIGURE 22.1 - UTERINE FIBROID EMBOLIZATION
On the axial image from a pelvic MRI (**a**) the fibroids (*arrows*) are seen in the right uterine wall. Note the uterine cavity appears as the white triangular shape in the midline. On the nonselective pelvic arteriogram (**b**), flow to the fibroids can easily be made out (*arrows*)

young patients still interested in future child bearing. Pelvic MRI is currently the standard of care for mapping the fibroids and identifying other possible causes of the patient's symptoms; of note, MRI alters the treatment algorithm approximately 20% of the time. UFE is performed as an outpatient procedure using conscious sedation. Via arterial access, superselective uterine arteriography is performed on each side with embolization with PVA (Polyvinyl Alcohol Particles) to occlude blood flow to the fibroid(s). This is performed on both left and right sided vessels. The patients are then admitted for a short hospital stay and have a recovery time at home of approximately 2 weeks, during which time the patients are fairly functional. Success rates are noted to be about 85% for relief or marked improvement in symptoms. That number increases to greater than 90% for bleeding symptoms and is about 75% for bulk related symptoms (Figs. 22.1a, b and 22.2a, b).

Ovarian Vein Embolization and Pelvic Congestion Syndrome

Chronic pelvic pain in women is a difficult entity to sort out because there are so many possible causes. These can include ovarian vein reflux, endometriosis, adhesions, atypical urological or menstrual pain and irritable bowel syndrome. Although noninvasive diagnostic tests are used more and more, a thorough history

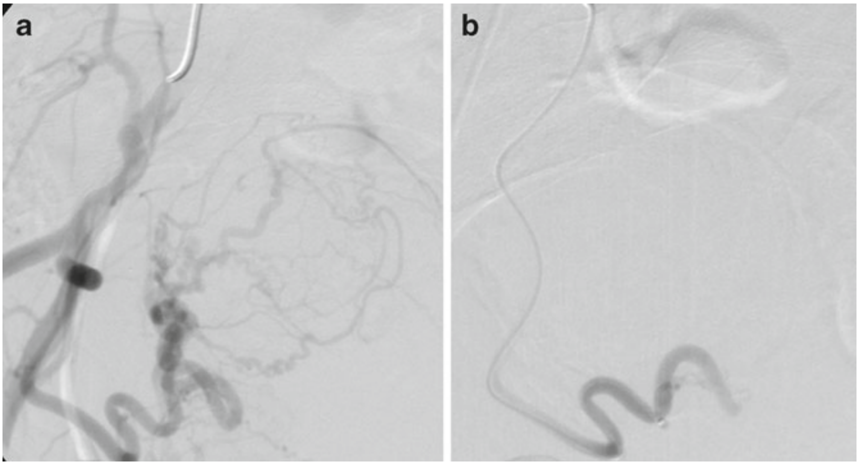

FIGURE 22.2 - UTERINE FIBROID EMBOLIZATION
Selective right uterine arteriogram showing successful embolization pre (**a**) and post (**b**) images

and physical can be very helpful. For PCS, which is a clinical diagnosis, patients relate a history of pelvic pressure that is not present first thing in the morning, gets worse as the day goes on and can be associated with varicosities of the abdominal wall and upper thighs. Spectral (or Duplex) ultrasound was the gold standard for diagnosis in the past but now pelvic MRI is a more sensitive imaging modality. More recently, with multislice CT scanners, the diagnosis of a dilated gonadal vein can be made with exquisite spatial resolution.

Definitive diagnosis is made with a gonadal venogram. For this, the patient is admitted to a CVIR short stay ward. Under conscious sedation, access to the right jugular vein is obtained and a catheter is advanced to the left renal vein. Venography that demonstrates reflux of contrast to the level of the pelvis indicates venous valvular insufficiency and with that, findings compatible with PCS. Treatment can be performed at the same time which entails embolization of the gonadal vein (and all its tributaries) starting at the level of the pelvic brim. From here, the entire gonadal vein back to the renal vein is embolized to occlusion. The right gonadal vein, a direct branch of the IVC, needs to be evaluated as well (Fig. 22.3a–c). Symptoms will take approximately 6–12 weeks to improve. Success rates are about 65% and with concomitant or subsequent internal iliac vein embolization, about 75%.

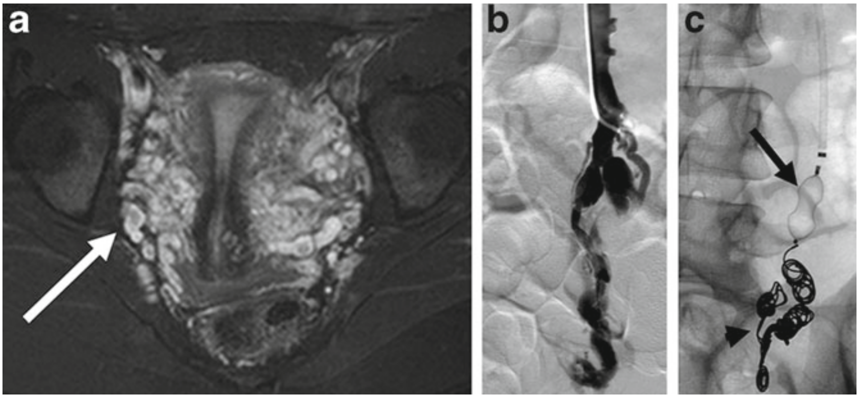

FIGURE 22.3 - PELVIC CONGESTION SYNDROME
Axial image from a pelvic MRI (**a**) demonstrates markedly dilated veins (*white arrow*) on either side of the pelvis. Injection (**b**) and embolization (**c**) on a different patient, using a combination of coils (*arrowhead*) and Amplatzer plugs (*black arrow*)

Fallopian Tube Recanalization

Fallopian tube recanalization is performed to improve a women's ability to have a physiologic intrauterine pregnancy. Fallopian tube recanalization was first accomplished in 1849 by passing a whale bone bougie through the cervix out the cornu of the uterus and out the fallopian tube. In the 1980s, with the development of microcatheters, fallopian tube recanalization took a great leap forward and has changed little since that time. A thorough gynecological history including fallopian tube surgery and a preprocedural hysterosalpingogram are very useful for identifying the possible cause of the fallopian tube obstruction with a vast majority of patients suffering from blockage by menstrual debris. Patients with a history of pelvic inflammatory disease may have a partially successful outcome while those with prior tubal ligation are the most difficult to recanalize. Patients are advised that the risk of the procedure is very low but it does increase the risk of an ectopic pregnancy by 1–2% overall.

The procedure is done as an outpatient. The patient is placed on the angiography table in the lithotomy position. The perineum is prepped as usual and a speculum is placed. The cervical os is identified and cannulated with a wire and catheter and over this combination, a 9Fr sheath is placed. Through the sheath, an angled catheter is advanced to the cornu and contrast injection performed. This sometimes is enough to clear the debris and reopen the fallopian tube. If not, through the angled catheter, a microcatheter and wire are passed out the fallopian tube. The wire should pass to the fimbrial portion of the tube. The wire is then removed and contrast injected looking for free spillage (Fig. 22.4a–c).

As devices become smaller and technology advances, patients will benefit from minimally invasive procedures. This is no more apparent than in the female patient.

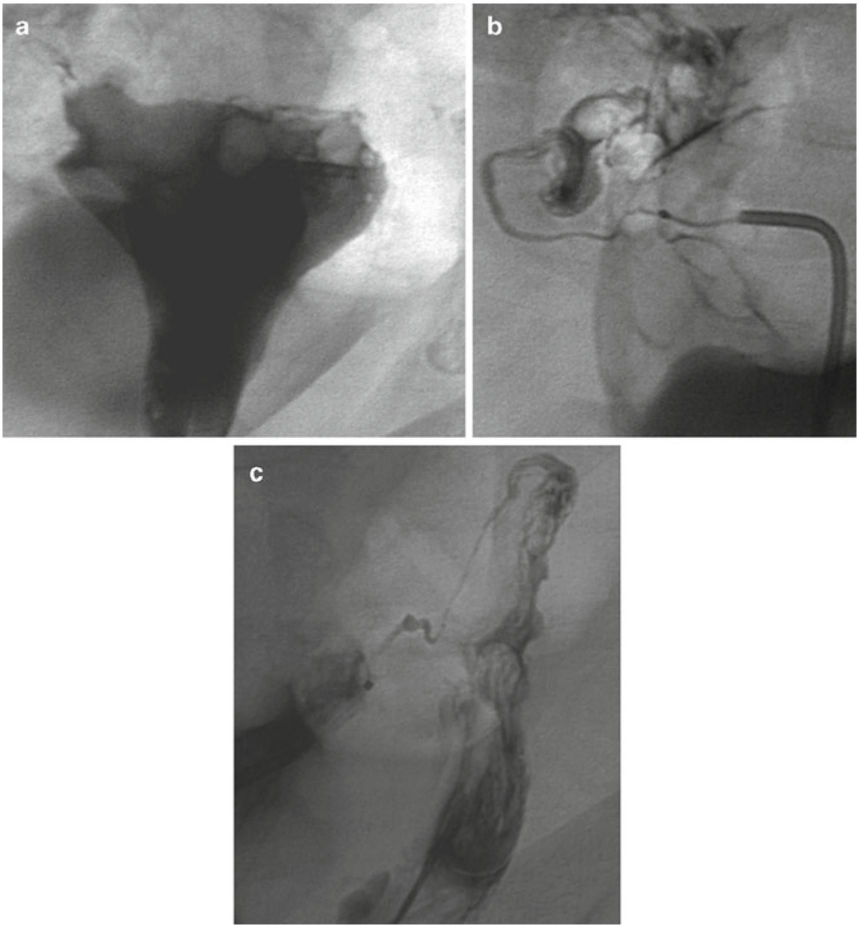

FIGURE 22.4 - FALLOPIAN TUBE RECANALIZATION
On the initial hysterosalpingogram, there is no filling of the either fallopian tube (**a**). Selective cannulation of each fallopian tube (**b**) clears debris from each tube, the most common cause. Selective injection demonstrates patency of each tube with free spillage of contrast (**c**)

23

ABDOMINAL CALCIFICATIONS

Objectives:

1. Describe the patterns of calcification and their location on radiographs for the following: chronic pancreatitis, vascular structures, uterine fibroids, appendicolith, and renal calculi.
2. Describe the usefulness of an oblique view for assessing the localization of abdominal calcifications.
3. State what percentage of renal calculi are normally visible on the plain radiograph.

Calcifications are frequently seen on radiographs of the abdomen. The purpose of this section is to demonstrate the typical appearance of the more commonly occurring calcifications. Figure 23.1 is a schematic of the lymph node distribution around the colon. Lymph nodes may calcify and be seen on abdominal radiographs as “balls” of calcium.

Chronic Pancreatitis

Figure 23.2 shows multiple calcifications of variable size in the mid upper abdomen and left upper quadrant. These are calcifications within the pancreas of a patient with chronic pancreatitis.

H Singh and JA Neutze (eds.), *Radiology Fundamentals: Introduction to Imaging & Technology*, DOI 10.1007/978-1-4614-0944-1_23,
© Springer Science+Business Media, LLC 2012

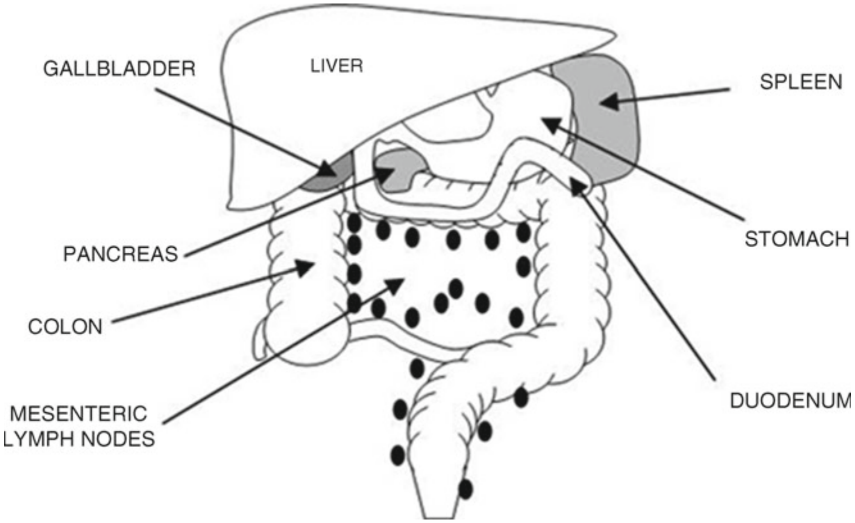
GALLBLADDER
LIVER
SPLEEN
STOMACH
PANCREAS
COLON
MESENTERIC LYMPH NODES
DUODENUM

FIGURE 23.1 - LYMPH NODES OF THE COLON
Those in the right lower quadrant are frequently seen on plain films as calcifications

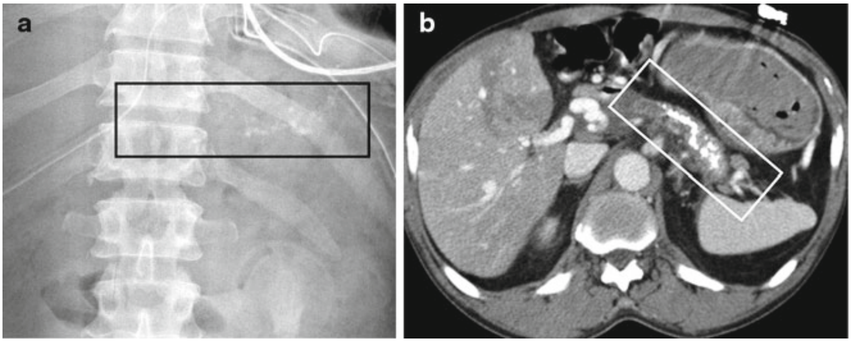

FIGURE 23.2 - CHRONIC PANCREATITIS
Supine radiograph collimated to the pancreatic bed (**a**) and corresponding axial CT slice (**b**) show pancreatic bed calcifications (*boxes*)

Vascular Calcifications

Vascular calcification takes several forms. In Fig. 23.3, numerous small, round, smoothly marginated calcifications are noted representing phleboliths within pelvic veins. Phleboliths are calcified venous thrombi. They often contain a central lucency which relates to recanalization of the occluded veins.

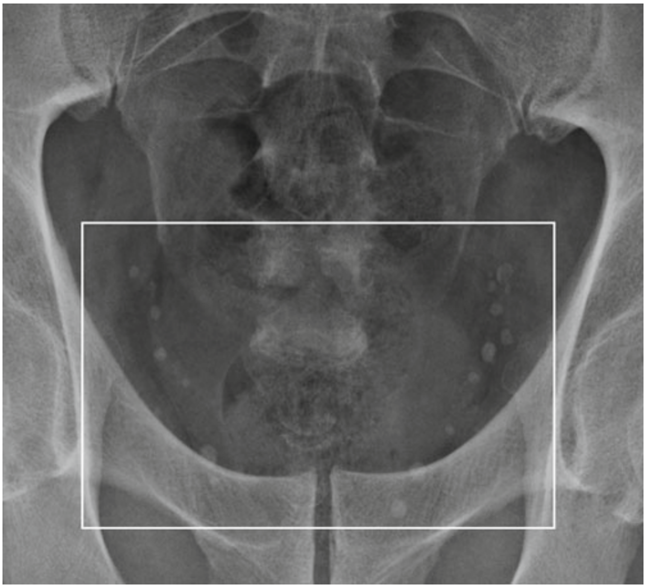

FIGURE 23.3 - PELVIC PHLEBOLITHS
Note the dense calcifications in the pelvis derived from calcified pelvic venous thrombi

Figure 23.4 shows calcification of the abdominal aorta. Sometimes the calcification is extensive enough to outline an abdominal aortic aneurysm, as in this case. Concerning calcifications on abdominal radiographs should prompt additional evaluation for abdominal aortic aneurysms with modalities such as ultrasound or CT.

Uterine Fibroids

Various tumors, both benign and malignant, may calcify. Figure 23.5 demonstrates popcorn-like calcification noted in uterine fibroids, the most common tumor found in the pelvic region. Fibroids are almost universally benign.

Appendicolith

Figure 23.6 is an abdominal radiograph and CT slice of a patient with right lower quadrant pain. A tubular calcification is seen in the right lower quadrant. This is an appendicolith, a calcified stone within the appendix. When this finding is seen in association with acute right lower quadrant pain, appendicitis should be strongly considered.

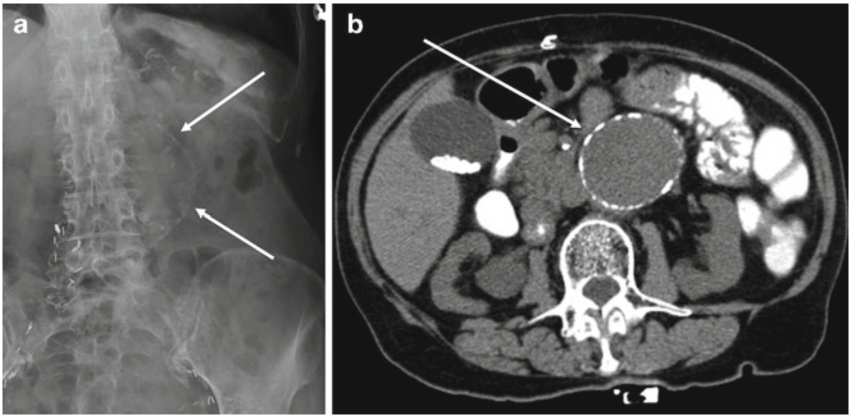

FIGURE 23.4 - AORTIC CALCIFICATION
Supine abdominal radiograph (**a**) and corresponding axial CT slice (**b**) showing a calcified aortic abdominal Aneurysm (*arrows*)

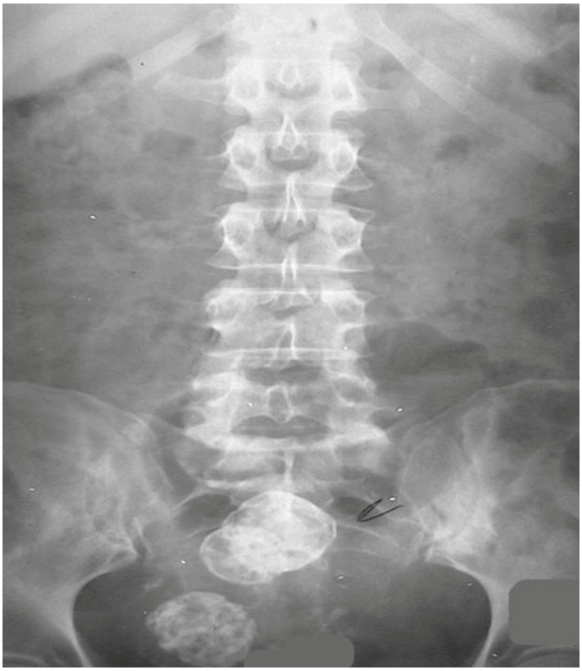

FIGURE 23.5 - CALCIFIED FIBROIDS

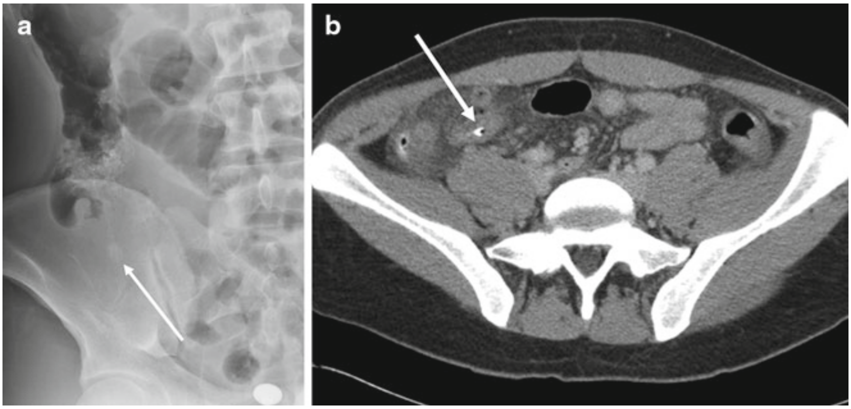

FIGURE 23.6 - APPENDICOLITH
(*arrows*) on AP abdominal radiograph (**a**) and axial CT slice (**b**)

Urinary Tract Calculi

Calcifications projected over the renal outlines or over the expected course of the ureters are often seen since 90% of renal calculi are sufficiently radiopaque for visualization on the plain radiograph (Fig. 23.7). Certain calcifications may overlie the renal outline on a frontal projection but be displaced from the renal outline on oblique views because they are anterior or posterior to the kidneys. Their exact location can be surmised by knowing the obliquity of the radiograph and the direction in which the calcifications would be expected to move with rotation.

Now CT is often the first study performed to localize and quantify calcifications in the urinary tract.

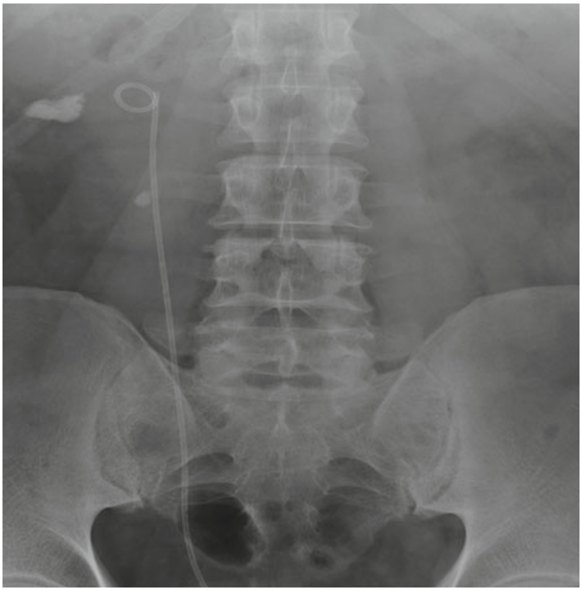

FIGURE 23.7 - RIGHT RENAL CALCULI

24

ABNORMAL AIR COLLECTIONS IN THE ABDOMEN

Objectives:

1. State the difference between an "interface" and a "line shadow."
2. State the expected radiographic findings in pneumoperitoneum in both a supine and upright patient.
3. Discuss the significance of intramural air within the bowel wall.

Pneumoperitoneum

When a hollow viscous ruptures, air (and bowel contents) is released into the abdominal cavity. "Free air" will collect in the least-dependent (highest) portion of the peritoneum.

In an upright patient, the air will collect just beneath the hemidiaphragms. In cases where a small amount of air is suspected, an upright chest radiograph, in addition to abdominal radiographs, may also be useful in detecting a pneumoperitoneum (Fig. 24.1). When the patient is not very mobile and/or there is a concern of subtle or loculated collections of "free" air outside the bowel lumen, CT is recommended.

In cases of pneumoperitoneum, the right hemidiaphragm is seen as a "line shadow." In other words, there is different radiographic density both superior and inferior to it, giving it the appearance of a line. In effect, if one was asked to measure the thickness of the right hemidiaphragm, this could be easily done when there is air beneath the hemidiaphragm. Normally, the right hemidiaphragm represents an interface, not a line shadow. This means that only its superior margin is clearly defined by the air in the adjacent lung. Inferiorly, the soft tissue of the hemidiaphragm blends imperceptibly with the soft tissue of the dome of the liver (remember the silhouette sign). The change from interface to line shadow is often a useful finding in discerning the presence of abnormal air collections within the abdomen.

H Singh and JA Neutze (eds.), *Radiology Fundamentals: Introduction to Imaging & Technology*, DOI 10.1007/978-1-4614-0944-1_24,
© Springer Science+Business Media, LLC 2012

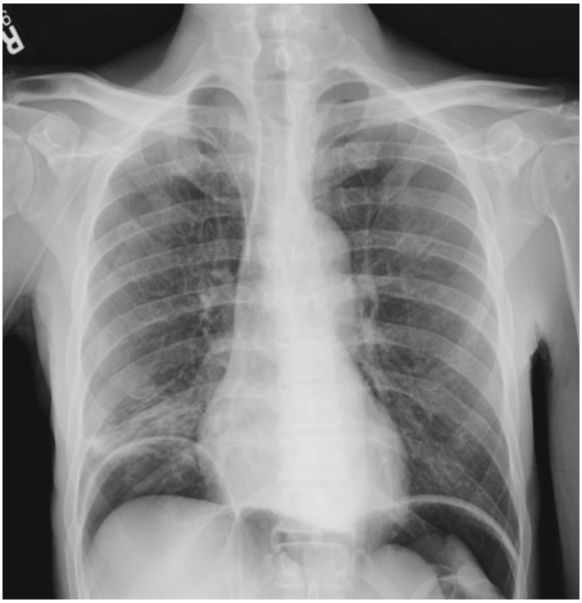

FIGURE 24.1 - PNEUMOPERITONEUM
Both the upper and lower aspects of the diaphragm are visualized secondary to the air–soft tissue interface

In an upright view of a patient's abdomen looking for a pneumoperitoneum, the bowel wall that is normally seen as an interface becomes visible as a line shadow due to the presence of air within the bowel lumen as well as free air within the peritoneum external to the bowel loop. In the supine position, air collects anteriorly within the abdomen since this, not the subdiaphragmatic region, is the highest point. For this reason, the radiographic presentation of pneumoperitoneum is different in the supine than in the upright patient.

Pneumatosis Intestinalis

Sometimes air can be found within the wall of the bowel itself. This condition is referred to as pneumatosis intestinalis and can be seen in a variety of conditions from idiopathic to benign to vascular occlusion with bowel ischemia. Figure 24.2 is an example of pneumatosis intestinalis in the cecum. Pneumatosis in infants may reflect necrotizing enterocolitis, with bowel wall ischemia, and infection.

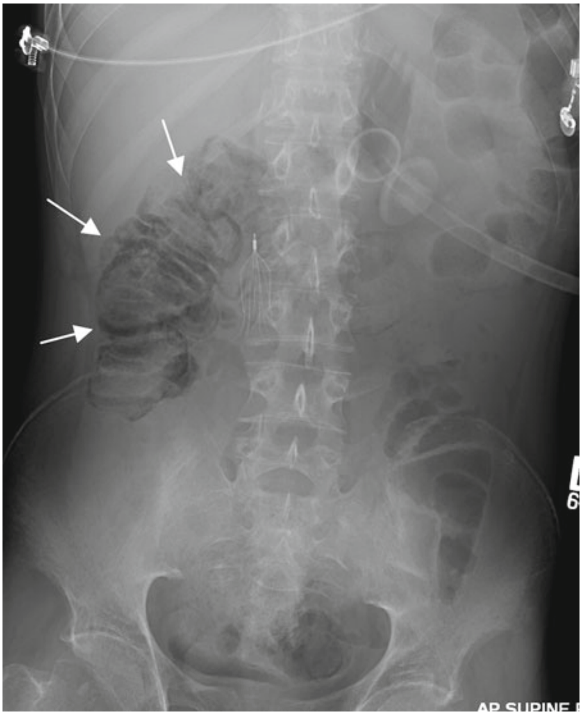

FIGURE 24.2 - PNEUMATOSIS INTESTINALIS

25

BARIUM STUDIES OF THE UPPER GI TRACT

Objectives:

1. Identify normal anatomy on a “Barium Swallow” and “Upper GI” series.
2. Be able to differentiate mucosal vs. extramucosal lesions based on radiographic findings.
3. Describe the radiographic features of malignant esophageal lesions.
4. Know the common locations for esophageal diverticuli and their radiographic appearance.
5. Name two separate methodologies for imaging the small bowel.

Barium sulfate is commonly employed for radiographic visualization of the gastrointestinal (GI) tract. For the upper GI (UGI), the barium sulfate mixture is swallowed and traced radiographically as it passes through the oropharynx, hypopharynx, esophagus, and more distal GI tract. When there is a concern of perforation or obstruction, water soluble contrast should be used.

Fluoroscopy

GI studies are observed fluoroscopically (real-time imaging) so that peristalsis and the rate of flow of barium can be ascertained. Close-up images of small anatomic areas are obtained at the time of fluoroscopy for the purpose of recording any specific abnormalities. Finally, static images (called overhead images) which are large images covering a large region of the GI tract, are acquired at the end of the study for the purpose of giving a geographic perspective to the barium distribution within the GI tract.

H Singh and JA Neutze (eds.), *Radiology Fundamentals: Introduction to Imaging & Technology*, DOI 10.1007/978-1-4614-0944-1_25,
© Springer Science+Business Media, LLC 2012

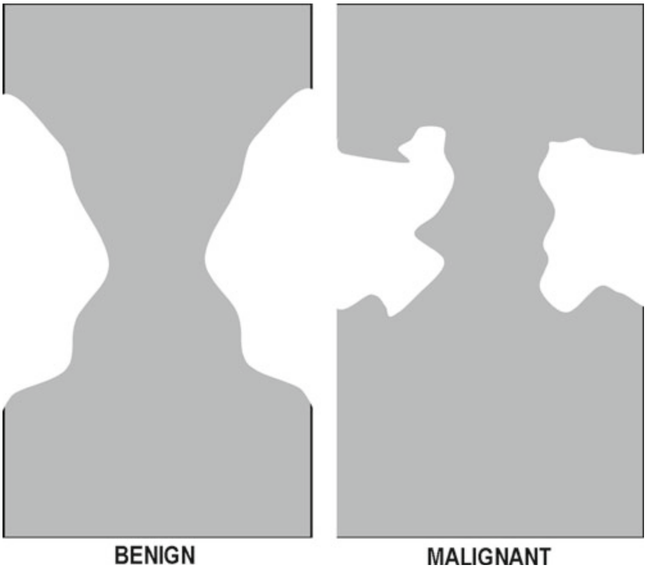

FIGURE 25.1 - BARIUM ESOPHAGRAM
On barium swallow studies, benign (*left*) and malignant (*right*) lesions have a different appearance. Note the gradual narrowing with smooth margins of the benign lesion vs. the overhanging edges and abrupt appearance of the malignant lesion

Normal Esophageal Motility

Swallowed barium is propelled by peristaltic waves, which are visible as smooth, segmental and progressive narrowing of the esophagus. These should not be confused with fixed abnormalities which may represent pathologic lesions (Fig. 25.1).

Figure 25.2 demonstrates a single image from a normal fluoroscopic exam of the esophagus. Sometimes abnormalities of esophageal motility may manifest as so-called tertiary contractions. These appear as multiple disorganized small indentations of the barium column within the esophagus and generally are related to abnormalities of the neurologic plexus which propagate the peristaltic wave. They are commonly seen in older individuals.

When the neurologic plexus in the distal esophagus degenerates, spasm without relaxation of the lower esophageal sphincter may occur, producing a condition termed achalasia. This results in distension of the proximal esophagus with collections of ingested food and secretions. A complication of achalasia is aspiration pneumonia.

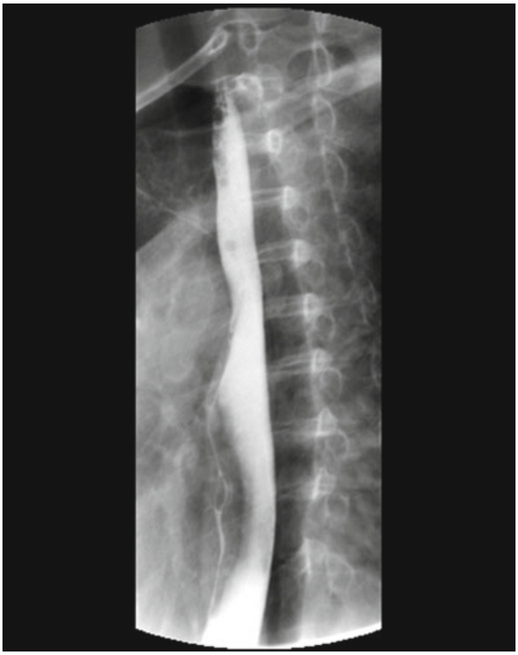

FIGURE 25.2 - UGI BARIUM STUDY
UGI Barium study demonstrating normal esophageal peristalsis

Esophageal Carcinoma

Esophageal carcinomas are fixed narrowings, often with mucosal ulceration and overhanging edges or "shouldering" of the barium column.

Esophageal carcinomas occur most commonly in the mid to lower esophagus (Fig. 25.3). It may be difficult to distinguish an esophageal stricture caused by gastric acid reflux from one caused by a carcinoma. Endoscopic biopsy is often required.

Esophageal Diverticuli

Diverticuli of the esophagus take two forms, traction diverticuli and pulsion diverticuli. Traction diverticuli most commonly arise in the region of the carina. They result from retraction of the inflamed subcarinal lymph nodes as they pull on the esophageal mucosa via fibrous adhesions. Pulsion diverticuli occur when the peristaltic waves

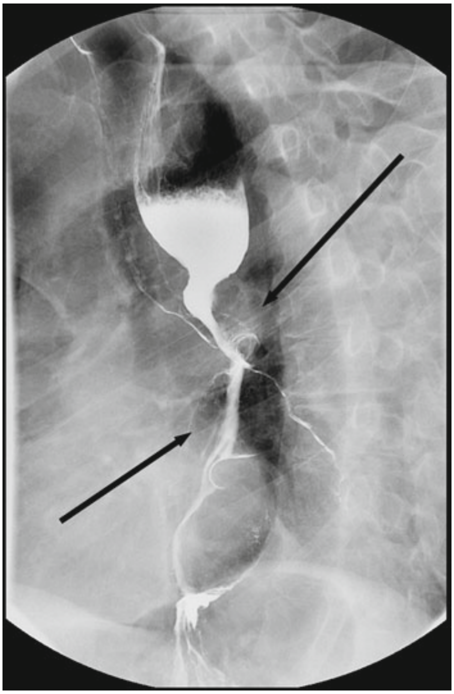

FIGURE 25.3 - ESOPHAGEAL CARCINOMA
Note the irregularity and overhanging edges (arrows)

exert a positive pressure within the esophageal lumen. Any weakness in the esophageal wall may lead to a "ballooning out" of the mucosa. A common location for an esophageal wall weakness is in the upper esophagus posteriorly where the constrictor muscles do not quite overlap to completely cover the esophageal wall. This is known as Killian's dehiscence. The pulsion diverticulum formed in this area is termed a Zenker's diverticulum and may be present as a mass in the upper neck. Another common location for pulsion diverticula is just above the lower esophageal sphincter. These diverticula are called epiphrenic diverticula.

Double and Single Contrast GI Studies

Standard UGI studies include tailored evaluations of the esophagus, stomach, and duodenal bulb.

In a double contrast study, barium and air are the two contrast agents. Within the stomach, the barium is made to coat the gastric mucosa and the air distension allows the mucosal folds of the stomach to be clearly evident (Fig. 25.4).

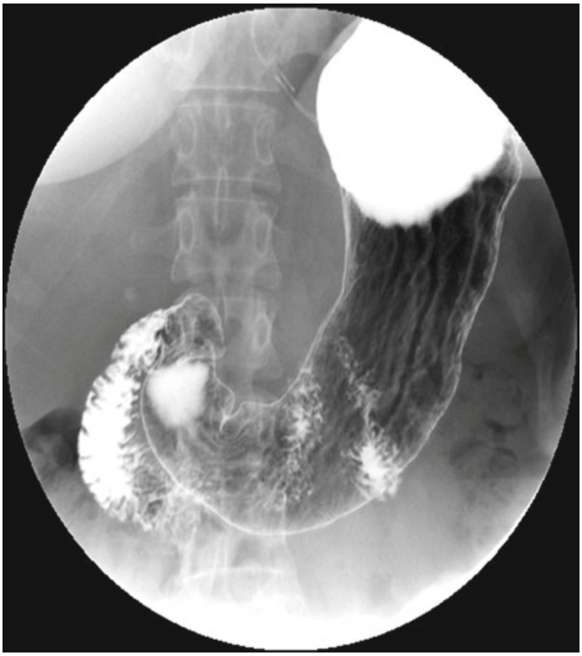

FIGURE 25.4 - DOUBLE CONTRAST GASTRIC STUDY
Note the detail of the gastric mucosa and duodenum

In a single contrast UGI series, barium is the only contrast agent. The stomach is nearly filled with contrast material and the mucosal detail is not as evident. Single contrast studies are faster to perform and result in less radiation exposure. But, less diagnostic information is obtained.

Generally, static images of the duodenal bulb and proximal loop ("C" loop) of the duodenum as it curves around the head of the pancreas are then obtained. The duodenal bulb and post-bulbar portion of the duodenum are common places for ulceration and diverticuli formation. The duodenum ends anatomically at the ligament of Treitz which should be at the same craniocaudad level as the duodenal bulb and lies to the left of the midline.

Filling of ulcer craters with barium produces small collections of contrast within the gastric wall. Gastric folds may radiate toward the ulcer as a result of inflammation. Ulcers may be malignant or benign and endoscopic biopsy is often required for evaluation.

Adenocarcinoma is the most common gastric malignancy and can present as an irregular solitary filling defect or as a diffuse infiltrative lesion which narrows the gastric body and antrum and makes it rigid, termed "linitis plastica."

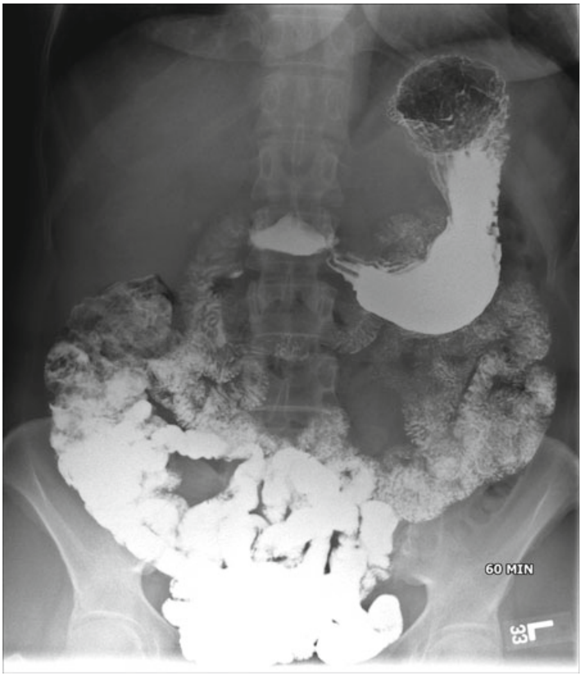

FIGURE 25.5 - SMALL BOWEL FOLLOW THROUGH
Note as the bolus of barium passes through the small bowel, mucosal detail can be seen

Small Bowel Follow Through

A single contrast study of the barium column may be followed through the small bowel as it passes distally through the GI tract, termed “a small bowel follow through” (Fig. 25.5). This will reveal gross abnormalities such as mucosal masses, strictures, and mass effect displacing the small bowel loops. The small bowel follow through terminates when contrast is seen within the cecum of the colon, having passed through the terminal ileum and the ileocecal valve.

Conventional Enteroclysis

A double contrast study of the small bowel, termed an “enteroclysis,” may be performed for the purpose of further elucidating small bowel anatomy. By placing an enteric tube distal to the ligament of Treitz, occluding the jejunal lumen with a balloon and injecting soluble barium and methyl-cellulose as a “solid column,” the double contrast effect is achieved. Multiple single exposure images of the small

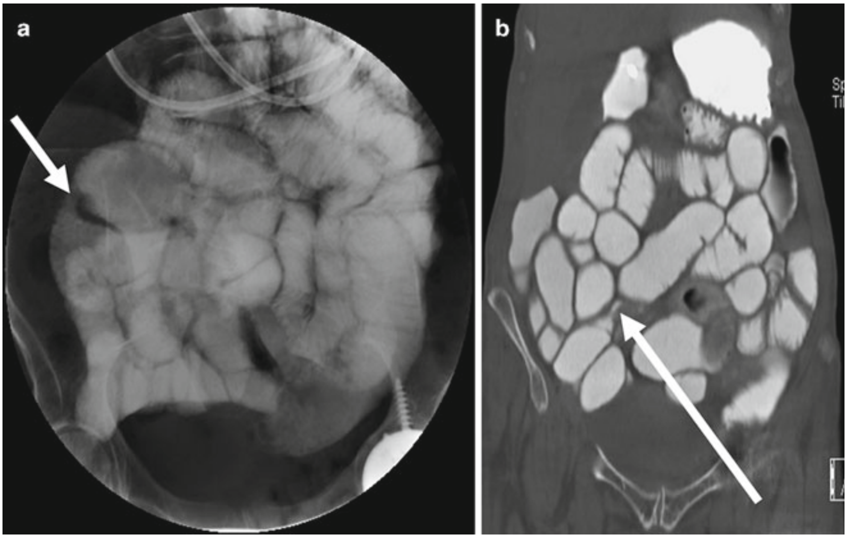

FIGURE 25.6 - CONVENTIONAL VS. CT ENTEROCLYSIS
(**a**) Conventional enteroclysis demonstrates a focal area of narrowing in the distal ileum (*arrow*). (**b**) Coronal image from a CT enteroclysis of the same patient demonstrates the focal area of narrowing in the distal ileum in the same location as the narrowing seen on conventional enteroclysis (*arrow*). CT enteroclysis had the added advantage of being able to demonstrate multiple different areas of narrowing in this patient (not shown) as well as evaluating bowel wall thickness and extraluiminal pathology

bowel are obtained with the fluoroscopy machine. The study is concluded once contrast reaches the cecum.

Small bowel malignancies may be either primary or metastatic and usually will appear as focal narrowing or strictures of the small bowel and/or nodular filling defects. This study is also useful for detecting low-grade small bowel obstruction secondary to Crohn's disease and postoperative adhesions (Fig. 25.6). Active Crohn's disease can also be detected with this type of examination.

This study is more difficult for the radiologist to perform and for the patient to tolerate. Therefore, it is used only in selected situations.

CT Enteroclysis

This type of study evaluates the small bowel in a similar manner to conventional enteroclysis. However, barium and methyl-cellulose are not used as contrast agents. This study may be performed in two different ways, depending on the indication for the study.

If the main problem to be evaluated is small bowel strictures and low-grade small bowel obstructions or small bowel masses, diluted gastrografin (1 part gastrografin: 6 parts water) is used. Approximately 1,200 mL of this diluted gastrografin is injected through the enteroclysis tube at a rate of approximately 60–90 mL/min. Again, multiple images are obtained while observing the column of contrast pass through the small bowel to the cecum. Once contrast reaches the cecum, the patient is taken to the CT scanner and an additional 200–300 mL of the diluted gastrografin is injected, prior to scanning the patient's abdomen and pelvis. CT is very useful in detecting mild caliber changes of small bowel, suggesting mild strictures and detecting acute angulation changes suggesting adhesions. CT enteroclysis also has the added advantage of being able to evaluate loops of small bowel that overlap. This is somewhat challenging with conventional enteroclysis.

If the main indication for the CT enteroclysis is to evaluate for active Crohn's disease, the study is modified. A negative or "neutral" contrast agent is used, such as water, to distend the small bowel. A total of 1,200 mL of water is injected through the enteroclysis tube. As the patient is being scanned in the CT scanner, intravenous contrast (Omnipaque 300) is injected. If there is active Crohn's disease, small bowel mucosal enhancement will be seen.

CT Enterography

Another study that may be used to evaluate the small bowel is called CT enterography, which is also used to evaluate for active Crohn's disease. The patient is instructed to drink a diluted barium drink (1% barium sulfate) called Volumen® (E-Z-EM). The patient also receives intravenous contrast to demonstrate mucosal enhancement in active Crohn's disease. If there is active Crohn's disease, there will be mucosal enhancement, as well as thickening of the wall of the small bowel (Fig. 25.7).

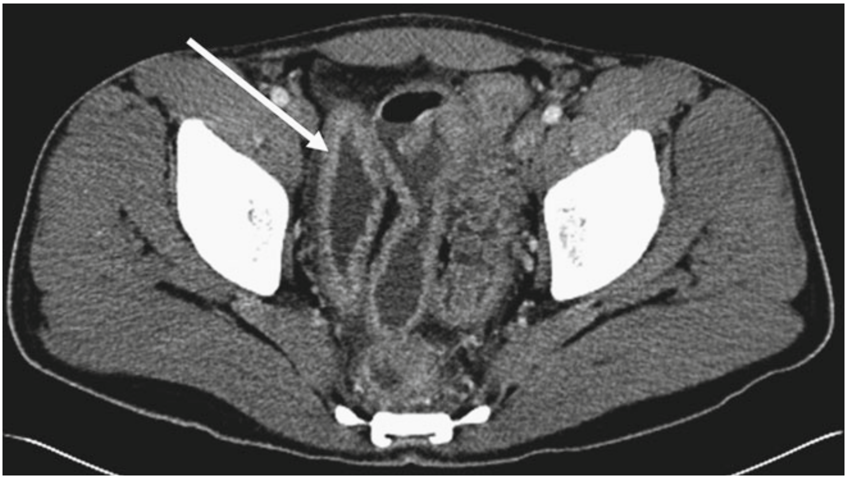

FIGURE 25.7 - CT ENTEROGRAPHY
Axial image from a CT enterography on a patient with known Crohn's disease. There are several loops of small bowel with marked mucosal enhancement and wall thickening (*arrow*), compatible with active Crohn's disease

26

BARIUM ENEMA AND CT COLONOGRAPHY

Objectives:

1. Explain the difference between a single and double-contrast barium enema.
2. List the typical findings seen in colonic malignancies.
3. Describe the radiographic appearance of colonic diverticuli and polyps.
4. Define intussusception.
5. Develop a basic understanding of the principles of CT colonography ("Virtual Colonoscopy").

As with the upper GI series, the barium enema can be performed in either a single- or double-contrast fashion. In single-contrast studies the colon is filled only with barium. This demonstrates an extrinsic displacement of the colon, such as might be seen in a pelvic mass in a patient with a gynecological malignancy, to the greatest advantage. Strictures and large intraluminal filling defects may also be identified Fig. 26.1. Double-contrast studies involve partially filling the colon with barium followed by insufflation with air (or carbon dioxide) via a rectal tube placed in the rectum for the purpose of elucidating polyps, early carcinomas and mucosal abnormalities such as inflammatory bowel disease. If there is a concern of obstruction or perforation, single-contrast water soluble enema should be performed (Fig. 26.2a).

An important part of the barium enema study is thorough bowel preparation for the examination. Barium studies cannot be performed without adequate preparation and this is often quite difficult for the patients. Patients who undergo barium enemas ingest a clear liquid diet and take preparatory agents which induce diarrhea the day or two before the examination for the purpose of clearing the GI tract of stool.

H Singh and JA Neutze (eds.), *Radiology Fundamentals: Introduction to Imaging & Technology*, DOI 10.1007/978-1-4614-0944-1_26,
© Springer Science+Business Media, LLC 2012

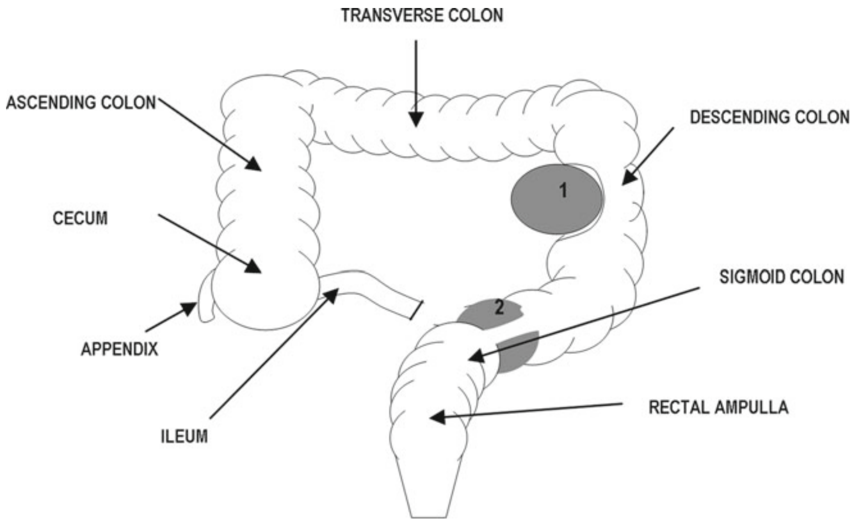
TRANSVERSE COLON
ASCENDING COLON
DESCENDING COLON
1
CECUM
SIGMOID COLON
2
APPENDIX
RECTAL AMPULLA
ILEUM

FIGURE 26.1 - SEGMENTS OF THE COLON
Note the different segments of the colon. Also note the different effect an extrinsic or mural mass (1) will have on the colon vs. an intrinsic/mucosal lesion (2)

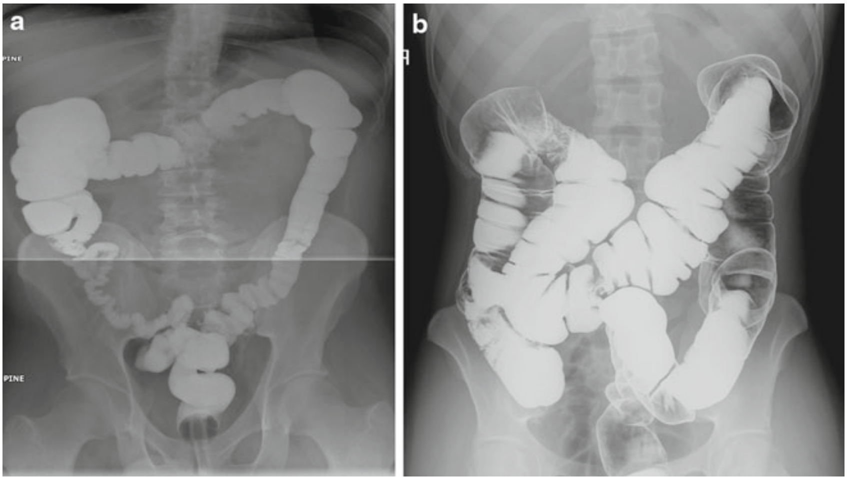

FIGURE 26.2 - (a) SINGLE-CONTRAST BARIUM ENEMA AND (b) DOUBLE-CONTRAST BARIUM ENEMA
Although a single contrast study may be easier to perform, mucosal detail is better seen on the double contrast study

Figure 26.2b is a single image from a normal double-contrast barium enema (DCBE) study. On the normal barium enema study, you should be able to identify the rectal ampulla, the sigmoid colon, descending colon, transverse colon, ascending colon and cecum. Filling of the appendix is variable, even when normal and present.

Note that the barium column is impinged upon by regularly occurring mucosal folds called haustra. These haustra are somewhat less prominent in the rectosigmoid region. Loss of normal haustral markings may indicate pathology.

Abnormalities of the colon may be intrinsic (mucosal) or extrinsic. Figure 26.3 demonstrates a large extrinsic deviation of the sigmoid colon in a patient with a pelvic mass. Figure 26.3 demonstrates a focal area of extrinsic compression of the transverse colon in a patient with gallbladder carcinoma. Contrast the radiograph of Fig. 26.3 with Fig. 26.4, which demonstrates a typical apple core lesion of the sigmoid colon, in this case a colonic adenocarcinoma.

This was a fixed abnormality on fluoroscopy and did not represent normal colonic peristalsis. There are overhanging edges and there is disruption of the normal mucosal pattern within the narrowed segment. The rectosigmoid region is the most common site of colonic carcinoma.

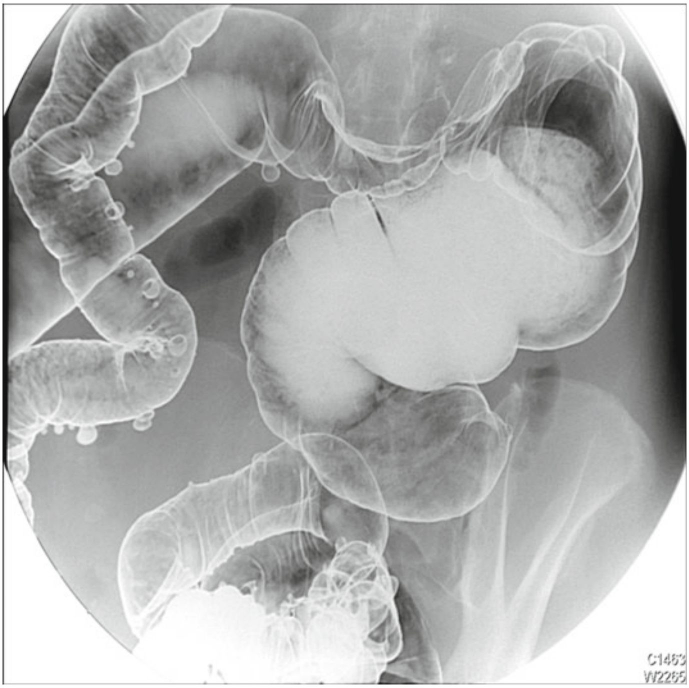

FIGURE 26.3 - COLONIC MASS
Single image from a double contrast barium enema demonstrates focal extrinsic compression of the midtransverse colon from adjacent gallbladder carcinoma

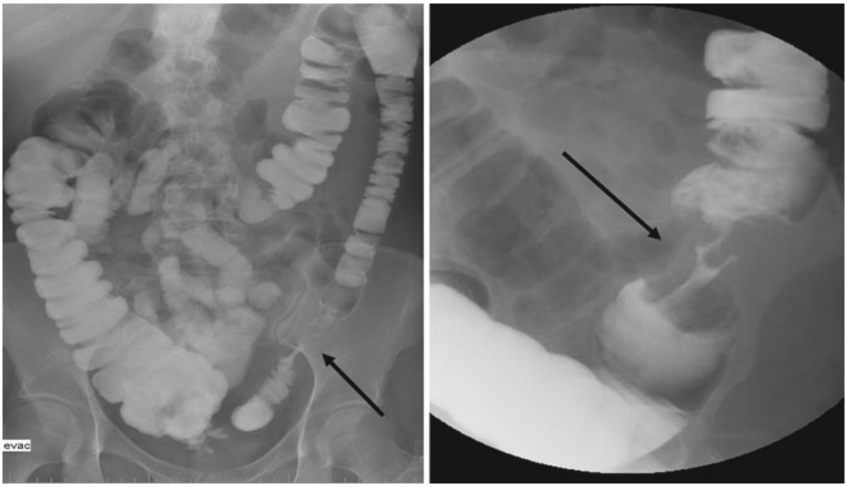

FIGURE 26.4 - APPLE CORE LESION OF THE SIGMOID COLON
Again note the abrupt caliber change and the irregular margins (*arrow*)

Colonic Diverticuli and Polyps

Figure 26.5 demonstrates numerous colonic diverticuli in the region of the sigmoid colon. Diverticuli are outpouchings of colonic mucosa between weak taenia coli muscles. They are more common with age.

Many types of polyps are felt to be premalignant lesions. Barium enema, especially a DCBE, is a relatively low cost, low-risk procedure for detection of these polyps. Please note that DCBE is less sensitive than colonoscopy at detecting small polyps. Colonoscopy, however, is more expensive and carries a higher risk of complications, including perforation.

Crohn's Disease

Crohn's disease (CD) is a chronic transmural inflammatory process thought to be an immunologic disorder that involves the GI tract anywhere from the mouth to the anus, but mainly affects the terminal ileum and colon. However, other systems may also be affected. Crohn's typically has a characteristic discontinuous pattern known as "skip lesions," where parts of the small bowel are involved with intervening normal small bowel mucosa. Crohn's characteristically causes crypt inflammation and abscesses, and tiny aphthoid ulcers. These mucosal ulcers may develop into deep serpiginous ulcers. Occasionally the bowel may have crossing deep ulcers with only small "islands" of normal mucosa left between the inflamed mucosa. This gives a characteristic "cobblestone" appearance (Fig. 26.6a) to the bowel mucosa.

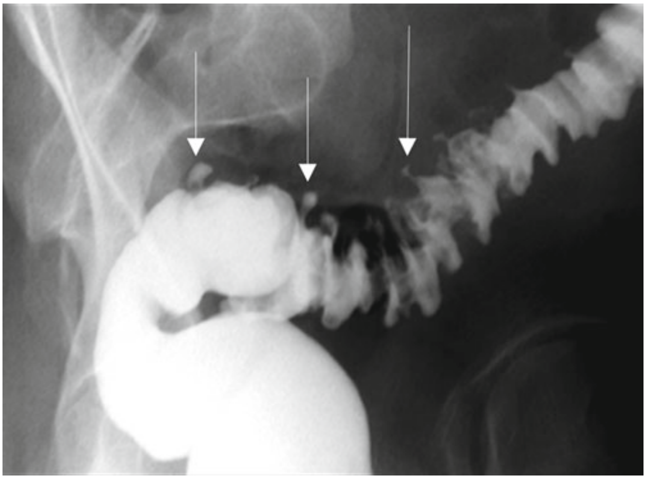

FIGURE 26.5 - SIGMOID DIVERTICULI
Multiple diverticular outpouchings within the sigmoid colon consistent with diverticulosis

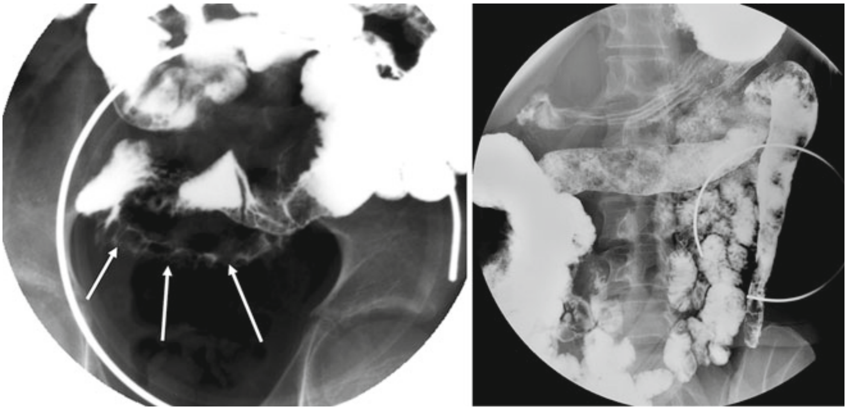

FIGURE 26.6 - CROHN'S DISEASE
(**a**) Abdominal radiograph obtained 24 h after a small bowel follow through was performed in a patient with Crohn's disease (CD). Note the lucent areas in the descending colon giving it a "cobblestone" appearance (*white arrows*), with normal mucosa opacified by the barium. The transverse and ascending colon are relatively spared. (**b**) Single-contrast enema in a different patient with a long history of CD shows the "lead pipe" appearance of the descending colon (*white arrow*) characteristic of long-standing Crohn's disease. Small ring-shaped metallic structures are from a mesh for hernia repair

At a more chronic stage, CD may cause diffuse fibrosis and spasm of the longitudinal muscles of the wall of the affected colon, giving a characteristic "lead pipe" appearance (Fig. 26.6b) due to obliteration of the normal colonic haustral folds, and typically involving the descending colon. Complications of CD include: enterocutaneous and ileo-colic fistulas, abdominal abscess formation, small bowel strictures, bowel obstruction, and even perforation.

Intussusception

Intussusception can be defined as the invagination of a segment of bowel (the intussusceptum) into a more distal loop of bowel, the intussuscipiens. There are four different types of intussusception: ileo-colic, ileo-ileal, ileo-ileo-colic, and colo-colic. 90% are ileo-colic and ileo-ileo-colic intussusceptions, 90% have no pathologic lead point, and 10% have a lead point in children, due to a Meckel's diverticulum, polyp, other tumors (Burkitt's lymphoma), or enteric duplication cysts. In contrast, intussusception in adults is commonly associated with a lead point.

The intussusceptum is pulled further into the distal segment of bowel by peristalsis, pulling the mesentery along with it and trapping the vessels. If not reduced, edema, ischemia, and bowel obstruction (usually partial) ensue with necrosis of bowel.

Intussusceptions can be reduced by using positive contrast, i.e., water soluble contrast like Omnipaque® or negative contrast (carbon dioxide). Successful reduction is noted by (1) free flow of contrast into the terminal ileum or (2) progressive reduction of ileo-colic intussusception to the ileo-cecal valve under fluoroscopic visualization. Barium is not used because, if the bowel perforated during the reduction attempt, barium would leak into the peritoneal cavity and form concretions with the bowel contents, a mess to clean up surgically. Contraindications to reduction include perforation and peritonitis. If reduction is unsuccessful with enema, the patient will require surgery.

Figure 26.7 shows a single-contrast water soluble enema performed in an attempt to reduce the intussusception. The very end of the intussusception did not completely reduce (black arrow). The patient was taken to surgery and found to have a large Burkitt's lymphoma of the distal ileum which acted as the lead point for the intussusception to develop and prevented its reduction.

CT Colonography ("Virtual Colonoscopy")

DCBEs are becoming increasingly obsolete studies in the evaluation of the colon, because of the relatively lower sensitivity in detecting colonic polyps compared to optical colonoscopy.

There is a relatively new screening tool that is almost as sensitive as optical colonoscopy in the detection of small polyps >5 mm in diameter. This tool is called computed tomography colonography (CTC) or "virtual colonoscopy." Several

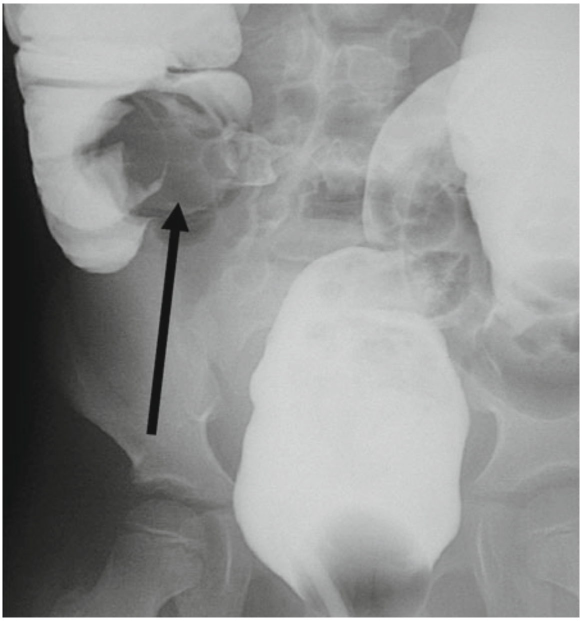

FIGURE 26.7 - INTUSSUSCEPTION
Single-contrast water soluble enema performed in an attempt to reduce the intussusception. *Arrow* points out the nonreducing distal end which was a Burkitt's lymphoma

multicenter studies have shown that CTC is almost as sensitive (98–99% sensitivity) in the detection of polyps greater than 5 mm as optical colonoscopy.

For this type of study, the large bowel is prepped in the same way as for an optical colonoscopy. The patient is placed in the CT scanner and a rectal tube is inserted in the rectum, and the colon is distended with carbon dioxide via a special insufflation pump. The CT scanner is used to obtain very thin slices through the abdomen and pelvis and images are reconstructed in axial, coronal, and sagittal planes. The patient is then rescanned in the prone position (Figs. 26.8–26.10).

The CT images are then reviewed using special software in either 2D mode (axial, coronal, or sagittal) or in 3D mode ("virtual colonoscopy") or both. Colonic polyps are considered significant if they measure >5 mm from the base of the stalk to the top of the polyp. In general, polyps <5 mm on CTC are not reported, or if they are reported, a recommendation of follow-up colonoscopy (optical or CT) in 5–7 years can be made.

There is some controversy over how polyps measuring between 6 and 9 mm should be managed. Ultimately it is the patient and treating physician preferences and any associated comorbid conditions that dictate how these polyps will be dealt with. In general, if there are 1–2 polyps measuring 8–9 mm and the patient is young,

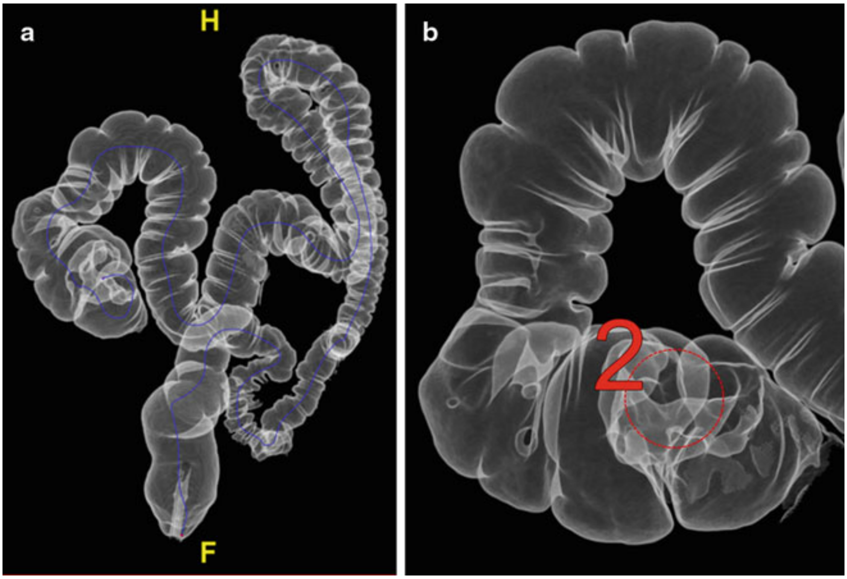

FIGURE 26.8 - CT COLONOGRAPHY
(**a**) This demonstrates a "double-contrast" image obtained by the CT scanner, and is used as a "road map" during the virtual colonoscopy portion of the study. (**b**) This is a magnified "double-contrast" view of the cecum. There is a large filling defect in the cecum

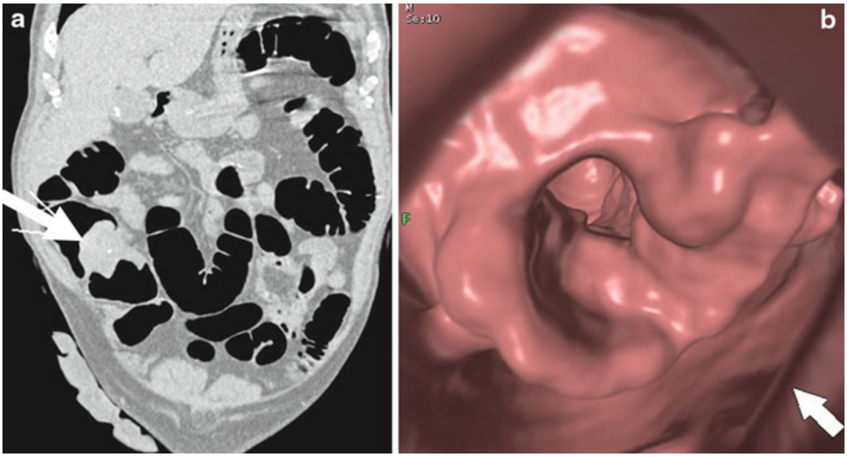

FIGURE 26.9 - CT COLONOGRAPHY
(**a**) Coronal 2D CT image of the colon demonstrates a large irregular filling defect in the cecum (*arrow*). (**b**) This is a 3D CT image of a "virtual colonoscopy" study demonstrating the same large mass in the cecum (*arrow*) as seen in (**a**). Biopsy specimen of this large mass came back as invasive adenocarcinoma, T4

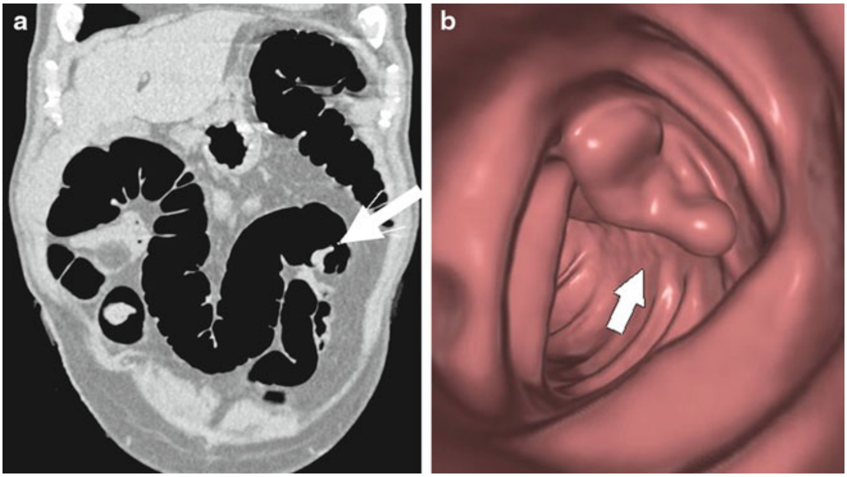

FIGURE 26.10 - CT COLONOGRAPHY
(**a**) Coronal 2D CT image of the colon also shows a polyp in the transverse colon in the same patient (*arrow*) as in Figs. 26.8 and 26.9. (**b**) This is a 3D CT image of a "virtual colonoscopy" study in the same patient, demonstrating the polyp in the transverse colon (*arrow*). Biopsy specimen of this polyp came back as benign adenoma

optical colonoscopy with polypectomy is recommended. In a young patient with <3 polyps between 6 and 7 mm, follow-up in 3 years by colonoscopy (optical or CT) is recommended. If there are >3 polyps, polypectomy is recommended, no matter what the age of the patient. Polyps >10 mm at any age should be removed by optical colonoscopy and sent for pathology evaluation.

If the patient is 50 years and CTC is negative for significant polyps or masses, optical colonoscopy is recommended in 5 years. If the patient is 55 years and optical colonoscopy is negative for polyps or masses, follow-up every 10 years by colonoscopy (endoscopy or CT) is recommended.

27

BOWEL OBSTRUCTION

Objectives:

1. Describe the radiologic findings of large and small bowel obstruction.
2. List criteria used to distinguish bowel obstruction from ileus.
3. Define the term "air–fluid" level.

Gas is normally present in the stomach and colon. Small accumulations of gas may be found in the duodenum and upper portion of the jejunum. Scattered collections of gas may be present throughout much of the small intestine in bedridden patients, patients on narcotics for pain relief, and those who swallow large amounts of air habitually. Air can be seen as individual accumulations of rounded or ovoid shaped air. If a single loop of normal intestine can be recognized because of gas filling, the shadow is seldom more than 5–8 cm in length. More often, the gas does not form any specific loop pattern.

Small Bowel Obstruction

When individual segments of small intestine are dilated 3–4 cm in transverse diameter, one should consider the possibility that the gas pattern is abnormal. Radiographic findings in small bowel obstruction develop over time as fluid and gas build up proximal to the obstructing process.

The gas is visualized readily in supine radiographs, but the presence of fluid can only be confirmed on upright or decubitus views. In the upright view, the gas rises above the fluid and the interface between gas and fluid forms a straight horizontal margin: an air–fluid level. Figure 27.1 demonstrates an air–fluid level in the small bowel.

H Singh and JA Neutze (eds.), *Radiology Fundamentals: Introduction to Imaging & Technology*, DOI 10.1007/978-1-4614-0944-1_27,
© Springer Science+Business Media, LLC 2012

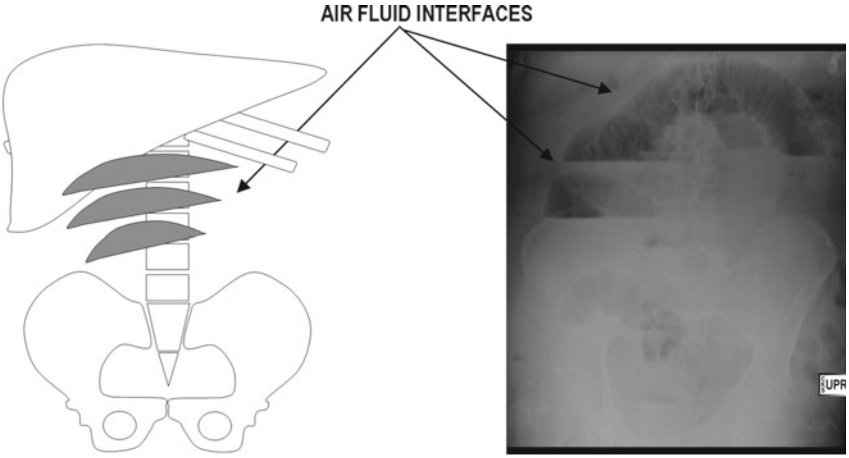
AIR FLUID INTERFACES
UPR

FIGURE 27.1 - AIR–FLUID LEVELS
The gas rises above the fluid in the bowel lumen creating a gas–fluid interface. This can be seen normally in the stomach, but not in the small bowel

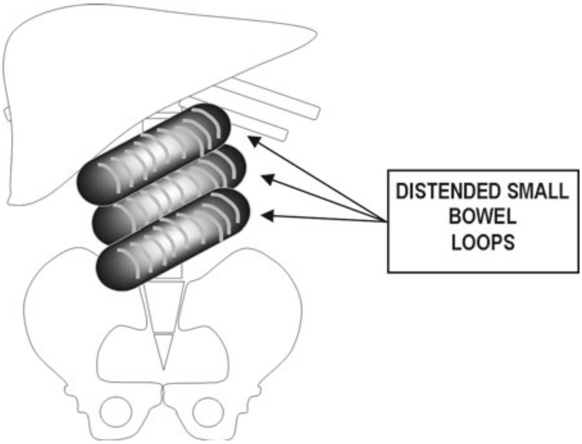
DISTENDED SMALL
BOWEL
LOOPS

FIGURE 27.2 - DISTENDED BOWEL LOOPS
As the loops of small bowel distend, they begin to lie on top of each other. The mucosal markings, called valvulae conniventes, cross the small bowel in their entirety

Air–fluid levels are generally considered to be abnormal in the small intestine. (Note that an air–fluid level is normally observed in the stomach because swallowed air is almost invariably present.)

Air–fluid levels may be seen in the first portion of the duodenum where air may be trapped temporarily when the patient assumes the upright position. In the early stage of obstruction, only one or two such gas distended segments are visualized. With increasing time, more distended loops may become visible. For this reason, serial examinations may be necessary for the diagnosis of small bowel obstruction. As distension increases, more loops become visible and they tend to lie transversely, with air–fluid levels at different levels, so-called fighting loops. Gas-filled loops may be recognized as small intestine rather than colon when they occupy the central portion of the abdomen rather than the periphery. Also, the pattern of mucosal folds in the small bowel, the valvulae conniventes, is finer and closer together than the colonic haustra. Unlike the haustral markings of the colon, these folds traverse the entire width of the bowel loop (Fig. 27.2).

When two gas-filled loops of bowel lie adjacent to one another, the soft tissue density between them represents a double thickness of intestinal wall. Thus, information concerning wall thickness is available. In a simple obstruction, a double thickness of intestine wall seldom amounts to more than a few millimeters in width, since the walls are thinned considerably by the distension. Inflammatory changes in the wall or fluid in the peritoneal cavity interposed between the bowel loops results in a thickening of this soft tissue shadow. Abnormal thickening of the bowel walls is an important sign that the bowel obstruction you are dealing with is not a simple one. If obstruction of the small intestine is complete, little or no gas will be found in the colon, a valuable differential point between mechanical obstruction and ileus.

If the obstruction is very proximal in the small intestine or if the patient has been decompressing the obstruction by vomiting, or if a nasogastric tube is used, the gas and fluid which would normally accumulate above an obstruction may not be present and the typical findings may not be seen on the radiograph.

Large Bowel Obstruction

As has been said previously, gas is normally present in the colon. Because of this, the diagnosis of colonic obstruction (large bowel obstruction) may be made only when the colon is thought to be dilated from the cecum to the level of the lesion, which is usually found more distally within the large bowel. Usually the abnormally distended colon ends abruptly at the level of the lesion with the colon distal to the lesion being free of gas. This is similar to what was previously discussed for the small bowel, and the principle is the same. Namely, distended bowel is found proximal to the obstruction. There is a paucity of gas distal to the obstruction with time. The large bowel is considered pathologically dilated when the diameter is greater than 10 cm.

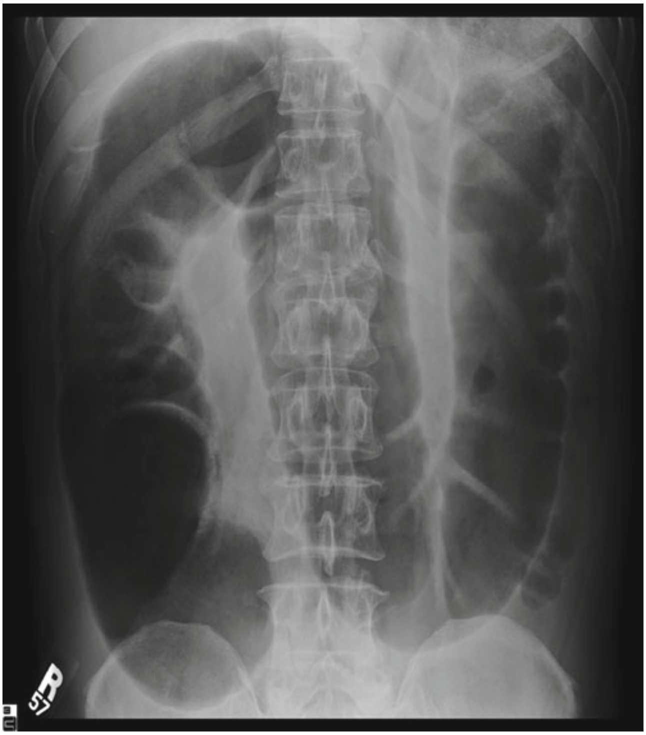

FIGURE 27.3 - TOTAL COLONIC OBSTRUCTION
Note the dilated, air-filled colon from the cecum to the proximal sigmoid. The cecum measures roughly 10 cm transversely

Figure 27.3 shows the plain abdominal radiograph of a patient with a total colonic obstruction. Can you estimate the point within the large bowel at which the colon is obstructed? (Answer: likely splenic flexure.)

The most likely site for obstruction of the large bowel, as might be expected, is in the rectosigmoid region since this is the most common site for colon carcinoma. The cecum undergoes the greatest distension in colonic obstruction and is the most likely site for perforation even when the obstruction is in the more distal colon. When the ileocecal valve is incompetent and the colon can decompress into the ileum and jejunum, there is less likelihood of perforation. When the cecum distends to ten or more centimeters, perforation becomes a very likely possibility. Fluid levels are of less significance in the diagnosis of colonic obstruction than they are in the small bowel.

Evaluation for Obstruction

Computed Tomography (CT) is generally considered the study of choice for the evaluation of obstruction. CT may show extent of obstruction, the cause of obstruction, transition points, free air, free fluid, and other pathology such as ischemic bowel and abnormal lymph nodes.

Contrast fluoroscopic evaluation is tailored to the area of concern. If the location of the obstruction is not known, the colon is studied first. Often, water soluble contrast is used so that if there is a perforation, barium does not leak into the abdomen with uncontained stool and bowel content.

If small bowel obstruction needs to be ruled out, and a fluoroscopic study is requested, barium can be given orally. Water soluble contrast tastes bad and is not well tolerated by the patient. The dilated loop of bowel, which is hard to see with water soluble contrast due to dilution of the contrast and the site of obstruction, may not be easy to identify. Barium will be diluted in the small bowel by small bowel fluid and will not cause concretions. If there is a concern of small bowel perforation, however, water soluble contrast is the contrast of choice if a fluoroscopic study needs to be performed.

Ileus

Next, turn your attention to Fig. 27.4. These are upright and supine views of a patient with ileus. There are many conditions which may reduce the motility of the large and small bowel. When this occurs, gas will accumulate within the bowel, giving a distended appearance both clinically and radiographically. Note on the upright view, however, air–fluid levels are at equal levels ("nonfighting" loops). Also note that the stomach, large, and small bowel are all affected in equal proportion suggesting a diffuse rather than focal abnormality. These findings may be useful in distinguishing ileus from bowel obstruction, although certainly this differentiation can be difficult in some patients. You will also note that this patient has "free air" under the right hemidiaphragm, suggesting that the ileus was as a result of recent abdominal surgery.

Mucosal Edema

Finally, the bowel wall may become edematous either in the presence of or the absence of obstruction. This is characterized by mucosal edema termed "thumbprinting."

Figure 27.5 demonstrates a prominent transverse colon with thickened haustra. This usually indicates edema of the bowel wall and that perforation may be imminent. The acute development of these findings may represent a surgical emergency

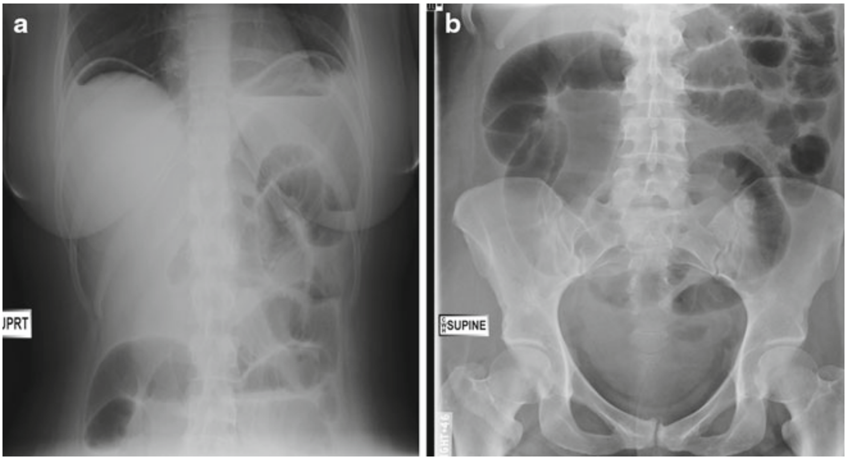

FIGURE 27.4 - ILEUS
Upright (**a**) and supine (**b**) radiographs of a patient with ileus. Noted are multiple dilated, gas-filled small bowel measuring up to 5.5 cm in diameter throughout the abdomen and the upper portion of the pelvis. Equally distended loops of large bowel are seen. Multiple air/fluid levels are noted on the upright film. The cause of ileus in this patient is recent abdominal surgery, which also explains the air under the right hemidiaphragm

and extreme vigilance must be maintained in performing any further diagnostic studies such as a barium enema. Conditions that can cause bowel edema include vascular ischemia, inflammation, infection, and hemorrhage from any cause. Hence, as in all radiographic interpretations, the clinical history is essential.

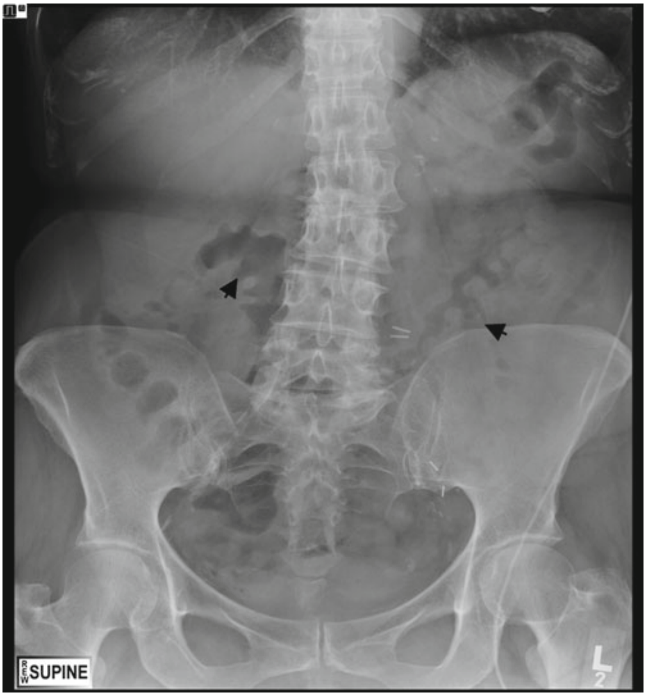

FIGURE 27.5 - LARGE BOWEL THUMBPRINTING
There is the suggestion of bowel wall thickening with thumbprinting of the transverse and descending colon

28

INFLAMMATORY BOWEL DISEASE

Objectives:

1. Know the radiographic manifestations of Crohn's disease and ulcerative colitis on both plain radiographs and contrast studies.
2. Realize that there is considerable overlap in the radiographic findings found in these processes and that biopsy may be necessary for definitive diagnosis.
3. Understand the significance of toxic megacolon with respect to acute complication of these two processes.

The two most common inflammatory bowel diseases (IBDs) are Crohn's Disease (CD) and ulcerative colitis (UC). Both of these processes are important chronic medical disorders of uncertain etiology (Fig. 28.1).

Crohn's Disease

In Crohn's disease, also termed regional enteritis, bowel inflammation is transmural (involving the entire thickness of the bowel wall), may be discontinuous (with intervening skip areas of normal bowel between affected segments) and involve the GI system from the mouth to the anus. The distal ileum and colon are most commonly involved. The earliest radiographic findings on double-contrast examinations of the colon are tiny aphthous ulcers which appear as white "pinpricks" in the mucosa as barium fills the tiny ulcers. These are very difficult to visualize with single-contrast technique. A double-contrast barium enema can detect the more subtle surface changes and thus detect early Crohn's disease with a high degree of accuracy. CT scanning does not show the mucosal abnormalities as well as fluoroscopy studies but can show distribution and extent of disease.

H Singh and JA Neutze (eds.), *Radiology Fundamentals: Introduction to Imaging & Technology*, DOI 10.1007/978-1-4614-0944-1_28,
© Springer Science+Business Media, LLC 2012

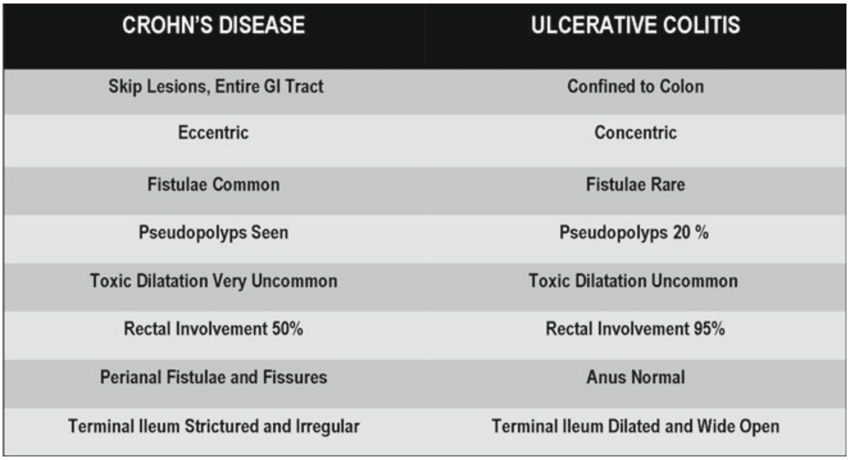

CROHN'S DISEASE	ULCERATIVE COLITIS
Skip Lesions, Entire GI Tract	Confined to Colon
Eccentric	Concentric
Fistulae Common	Fistulae Rare
Pseudopolyps Seen	Pseudopolyps 20 %
Toxic Dilatation Very Uncommon	Toxic Dilatation Uncommon
Rectal Involvement 50%	Rectal Involvement 95%
Perianal Fistulae and Fissures	Anus Normal
Terminal Ileum Strictured and Irregular	Terminal Ileum Dilated and Wide Open

FIGURE 28.1 - CROHN'S DISEASE VS. ULCERATIVE COLITIS
There are several distinguishing characteristics separating the two entities, helping to distinguish them radiographically

Crohn's Cobblestoning

Deep linear ulcers may form in Crohn's disease creating an intersecting network of ulceration which results in a characteristic appearance called "cobblestoning". Figure 28.2 demonstrates this. Note how the ulcers are larger and deeper, not aphthous any longer. Cobblestoning may also occur in advanced ulcerative colitis, an example of the radiographic overlap in appearance between ulcerative colitis and Crohn's disease. Notice that patches of ulceration are often separated by completely normal mucosa commonly referred to as "skip" areas. With advanced disease, the bowel wall thickens and become fibrotic, sometimes with stricture formation. Again, strictures may form in either ulcerative colitis or Crohn's disease, another example of the radiographic similarity which may be present in these two processes.

The "String Sign"

Narrowing of the terminal ileum, often referred to as the "string sign," also occurs in Crohn's disease and is related to both spasm, as well as stricture formation. Fistulas are a frequent complication of Crohn's disease and may extend from the cecum and ascending colon to the terminal ileum or the sigmoid colon. There is also a significant increase in the frequency of ileo-ileal fistula. Fistulas are best shown by single-contrast examination. Other complications of Crohn's disease are perforation, hemorrhage, and colonic malignancy.

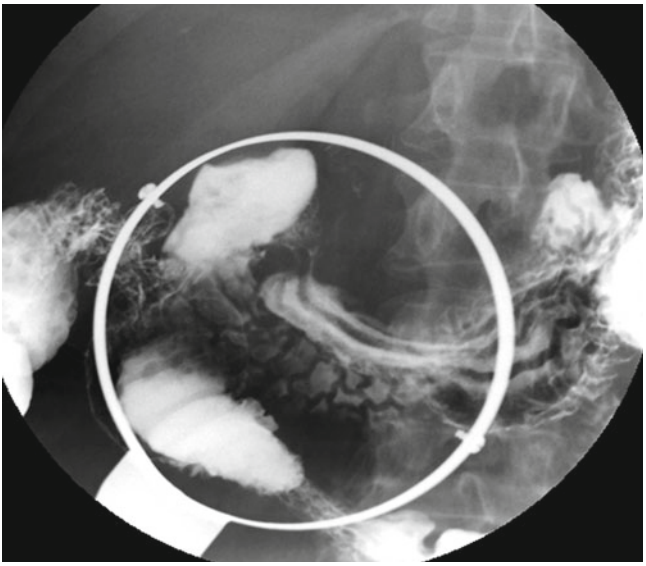

FIGURE 28.2 - CROHN'S COBBLESTONING
Cobblestone appearance of the second and third portion of the duodenum in a patient with known Crohn's disease. The ulcers fill with white barium and show up as white cobblestones

Ulcerative Colitis

Ulcerative colitis begins in the rectum and progresses proximally. The rectum is spared in about 5% of patients. The colonic involvement is relatively uniform and symmetric. During the early stages of ulcerative colitis, the mucosa loses its normal even texture and demonstrates a finely stippled appearance through the barium coating of the mucosa. This is related to multiple shallow ulcerations with surrounding edema, which provide a granular appearance. In ulcerative colitis, inflammation involves the mucosa only and does not extend throughout the bowel wall. For this reason, fistula formation is much less common in ulcerative colitis than in Crohn's disease.

Polypoid Changes in Inflammatory Bowel Disease

Three types of polypoid changes may be seen in both ulcerative colitis and Crohn's disease.

1. Pseudopolyps are islands of inflamed edematous mucosa seen between denuded and ulcerated areas of bowel wall.

2. Inflammatory polyps are areas of inflamed mucosa resulting in polypoid elevation.
3. Postinflammatory polyps are seen in the quiescent phase of ulcerative colitis and may be composed of normal or inflamed mucosa.

These “polyps” are thought to have originated from ulcerations of the mucosa with severe undermining. Long finger-like outgrowths, called filiform polyps are thought to be related to a reparative process. With healing, the colon may regain a normal appearance or may lose its haustra and shorten, resulting in the “lead pipe” colon, a sign of “burned-out colitis.”

Ulcerative Colitis and Colon Cancer

Patients with extensive, long-standing ulcerative colitis are at an increased risk of developing colorectal carcinoma. The incidence begins to rise steeply after 10 years of active disease. The risk is greatest when total colitis is present. Carcinoma in patients with ulcerative colitis is more likely to occur in multiple sites.

Rather than producing an intraluminal mass, colon carcinoma associated with IBD may infiltrate and spread along the bowel wall giving rise to deceptively benign-appearing strictures. Colon cancer is also more difficult to diagnose in patients with chronic ulcerative colitis because it is associated with symptoms related to or mimicked by the underlying disease. Colonoscopy and biopsy are used for long-term follow-up in patients with chronic pancolitis. In some patients, prophylactic colectomy may be performed.

Toxic Megacolon

Figure 28.3 shows a patient with toxic megacolon. Toxic megacolon is an acute nonobstructive dilation of the colon which is seen in different kinds of IBD. This patient, with a diagnosis of ulcerative colitis, presented with fever, bloody diarrhea, and abdominal distension.

The diagnosis of toxic megacolon is manifested here by a dilated transverse colon, paucity of haustral markings and some thickening of the bowel wall. Attempts should be made to identify this condition on plain radiograph because of the high risk of perforation if a subsequent barium enema is attempted. One of the most dramatic and ominous signs that may develop in the course of ulcerative colitis is this rapid development of extensive colonic dilatation and edema.

Note that since the underlying colon is diseased, the chance of perforation is extremely high. Therefore, *barium enema is contraindicated in the presence of toxic megacolon*.

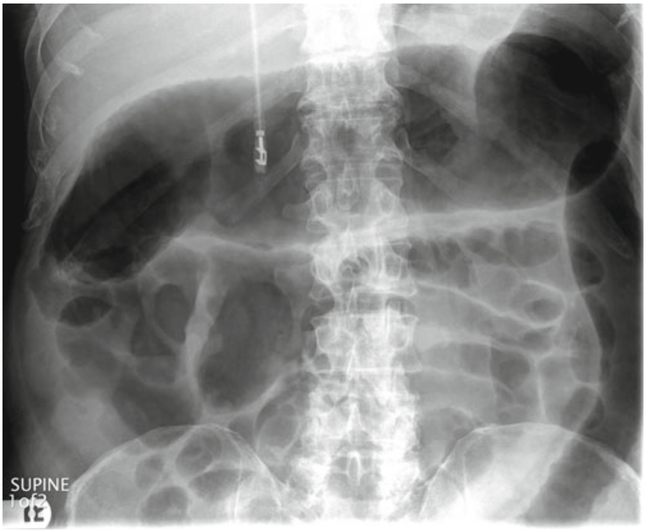
SUPINE
1 of 2

FIGURE 28.3 - TOXIC MEGACOLON
Megacolon appearance with a dilated transverse colon

29

DEFECOGRAPHY

Objectives:

1. State the indications for defecography.
2. Understand the anatomy and physiology of defecation.
3. List seven abnormal defecography findings.

Defecography is a special radiological study performed to evaluate patients with evacuatory disorders either from structural or functional abnormalities.

Indications

Defecography gives us important information about physiological and structural abnormalities of the pelvic floor muscles. There are several indications which may prompt a defecography study, which include but are not limited to chronic constipation, rectal prolapse, rectoceles, and solitary rectal ulcer syndrome.

Technique

The patient is instructed to drink a 240-mL bottle of thin barium 1 h prior to the actual study. The patient is positioned in the left lateral decubitus position. A specially constructed radiolucent plastic commode (Fig. 29.1) is positioned and fixed to the table immediately beneath the patient. A total of approximately 120 mL of semisolid barium sulfate paste (EZ paste® EZ-EM, US) is injected into the rectum via two 60-mL syringes with short plastic tubing attached to the syringes. The anal verge is marked using a small skin BB marker sticker.

H Singh and JA Neutze (eds.), *Radiology Fundamentals: Introduction to Imaging & Technology*, DOI 10.1007/978-1-4614-0944-1_29,
© Springer Science+Business Media, LLC 2012

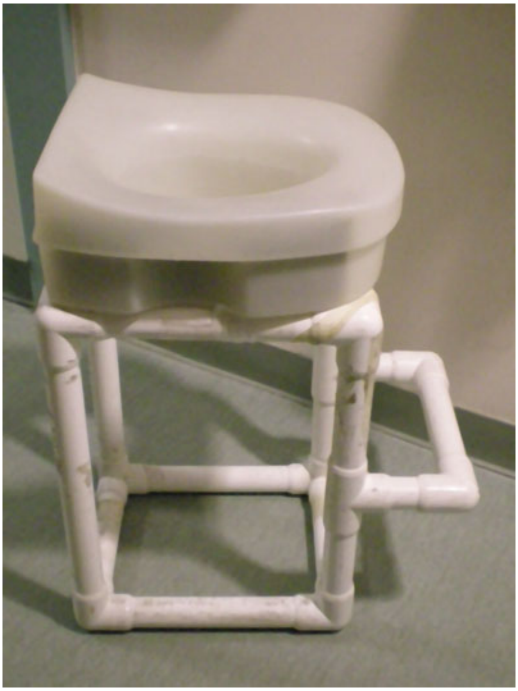

FIGURE 29.1 - COMMODE USED IN DEFECOGRAM

With the patient still in the left lateral decubitus position, the patient is instructed to perform several maneuvers and these are marked appropriately with numbers on the radiological image: rest, cough, squeeze or Kegel, and Valsalva. The table is repositioned into the upright vertical position, with the patient seated on the commode. The patient is then instructed to evacuate the barium paste as completely as possible. A digital fluoroscopy cine clip is obtained of the evacuation event.

Anatomy

The pelvic floor (levator ani) is composed of three main muscles: the puborectalis, iliococcygeus, and pubococcygeus muscles. These muscles play a crucial role in the defecation process. The puborectalis muscle forms a sling around the rectum. Fecal continence is maintained by contraction of the internal anal sphincter, external anal sphincter, and puborectalis muscle, which maintain high anal canal pressure and prevent the passage of stool.

Physiology

The defecation process involves the following steps: urge to sit or squat, Valsalva, straightening of the ano-rectal angle, increased abdominal pressure to overcome the internal anal sphincter pressure, pressure of feces on rectum causing elevated intrarectal pressure, and finally inhibition of the external anal sphincter with fecal bolus passage.

At rest, there is resting tone in the puborectalis and internal anal sphincter which help maintain continence (Fig. 29.2a). On performing the Kegel ("squeeze") maneuver (Fig. 29.2b), the puborectalis muscle contracts and the ano-rectal angle becomes more acute than at rest. On performing the Valsalva maneuver (Fig. 29.2c), the puborectalis muscle relaxes, and the ano-rectal angle becomes more obtuse than at rest. The normal radiological appearance during defecation may be summarized as (1) rapid initiation, (2) pelvic floor descent, (3) loss of puborectalis impression, (4) increase in ano-rectal angle, (5) shortening of the anal canal, and (6) anal canal opening widely.

Abnormal Defecography Findings

There are seven main abnormalities that may be demonstrated on defecography:

1. Incontinence: Spillage of barium paste from the anal canal prior to initiation of defecation (Fig. 29.3).
2. Rectocele: Bulge of the anterior rectal wall during straining or evacuation (Fig. 29.4).
3. Enterocele: Descent of the small bowel below the level of the pubococcygeal line (defined as a line joining the superior aspect of the pubic symphysis to the tip of the coccyx) during Valsalva or defecation (Fig. 29.5).
4. Dyskinesia: Muscular contraction of the pelvic floor muscles (usually the puborectalis) during defecation (Fig. 29.6).
5. Internal intussusception of the rectum: Rectal wall invagination that descends toward the anal canal (Fig. 29.7).
6. Sphincter dyssynergia: Failure of external sphincter to relax while attempting to defecate (Fig. 29.8).
7. Anismus: Failure to evacuate more than two-third of the barium paste in less than 30 s. This denotes impaired rectal evacuation secondary to a functional disturbance in defecation.

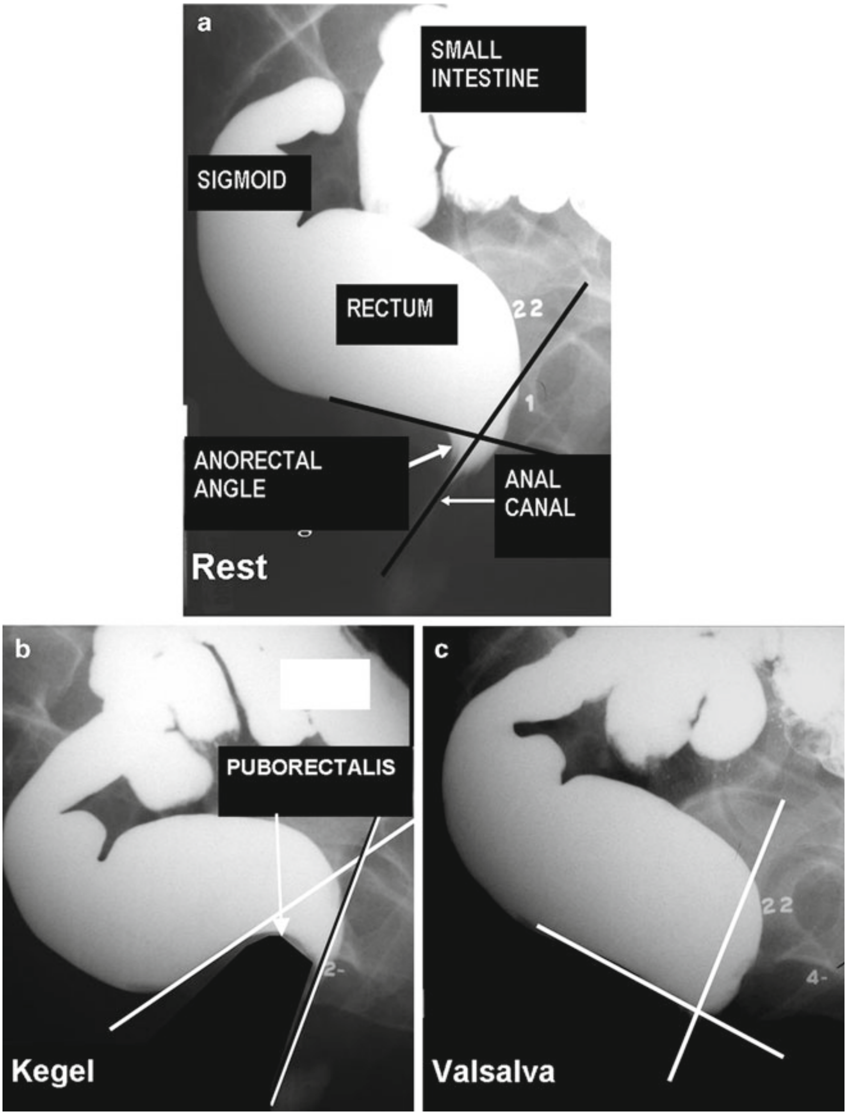
a
SMALL INTESTINE
SIGMOID
RECTUM
2 2
1
ANORECTAL ANGLE
ANAL CANAL
Rest
b
PUBORECTALIS
2-
Kegel
c
2 2
4-
Valsalva

FIGURE 29.2 - DEFECOGRAM STUDY
X-ray images of a defecogram study with patient at rest (**a**), during Kegel maneuver (**b**), and during Valsalva maneuver (**c**). Notice the change of the ano-rectal angel to an acute angle during the Kegel maneuver with impression of the puborectalis muscle on the rectum (**b**), and obtuse angle of the ano-rectal angle during Valsalva maneuver (**c**)

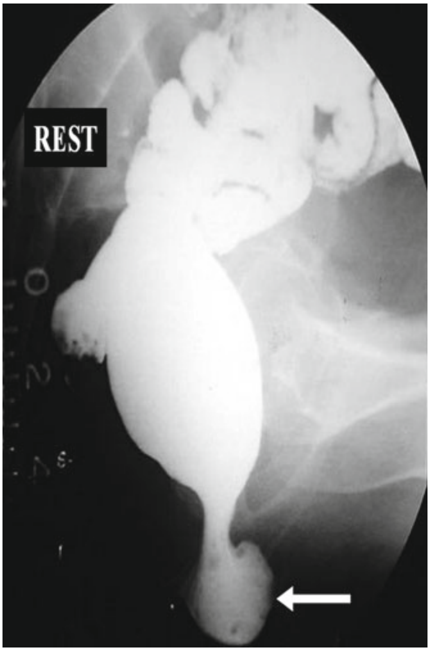

FIGURE 29.3 - INCONTINENCE
Spillage of anal canal before defecation

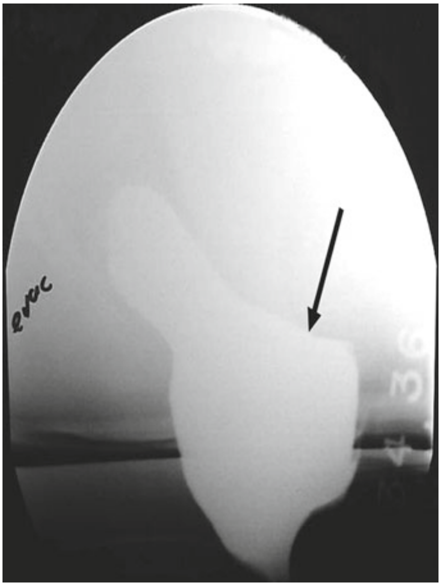

FIGURE 29.4 - RECTOCELE
Bulge of the rectal wall (usually anterior) during straining or defecation

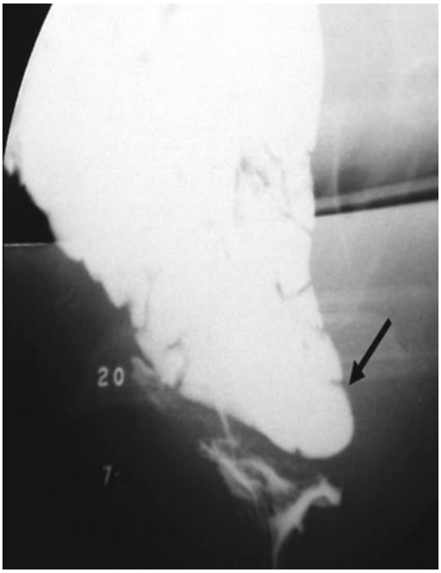

FIGURE 29.5 - ENTEROCELE
Descent of the small intestine during straining or defecation

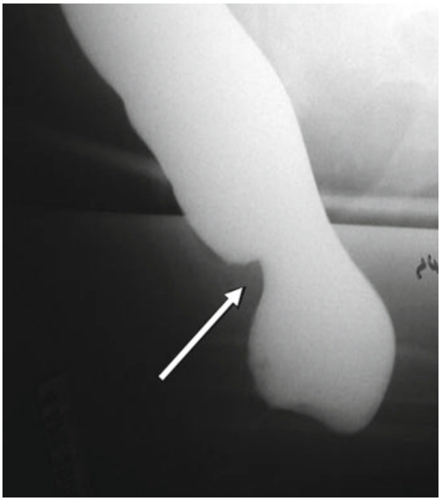

FIGURE 29.6 - DYSKINESIA
Muscular contraction of the pelvic floor muscles (usually the puborectalis) during defecation

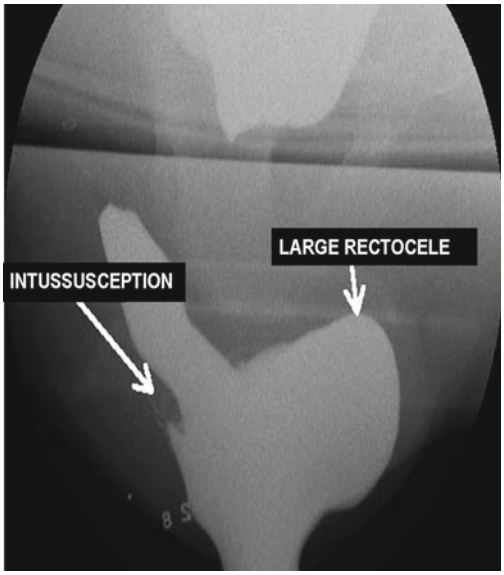
LARGE RECTOCELE
INTUSSUSCEPTION
8 S

FIGURE 29.7 - INTERNAL INTUSSUSCEPTION
An example of internal intussusception showing the rectal wall infolding into the lumen of the colon as well as a rectocele

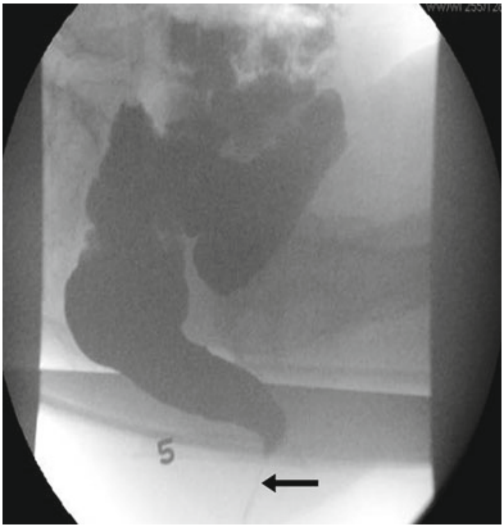

FIGURE 29.8 - SPHINCTER DYSSYNERGIA
Example of a patient trying to defecate but the sphincter is not relaxing

30

INTRA-ABDOMINAL LYMPHADENOPATHY

Objectives:

1. List the various radiographic modalities which may be employed for the purpose of detecting abdominal or pelvic lymphadenopathy.
2. List two limitations of computerized tomography in the evaluation of abdominal lymphadenopathy.
3. Identify the following structures on a normal abdominal CT scan: aorta, inferior vena cava, kidneys, liver, pancreas, and spleen.
4. State the indications for intravenous and/or gastrointestinal contrast prior to an abdominal CT scan.

Lymphadenopathy

Lymph node enlargement (lymphadenopathy) may be found in many conditions, both benign and malignant. Benign lymph node enlargement can occur in response to different infections such as tuberculosis and fungal disease. Malignant lymphadenopathy can occur in primary lymphatic diseases such as Hodgkin's and non-Hodgkin's lymphoma, as well as other malignancies which metastasize to regional lymph nodes, such as breast cancer.

In the past, the presence of intra-abdominal lymph node enlargement could only be surmised by the extrinsic mass effect of the enlarged lymph nodes on various contiguous structures seen on radiographs or barium studies of the abdomen. Now CT scanning is used to identify locations and size of abdominal lymph nodes (Fig. 30.1).

H Singh and JA Neutze (eds.), *Radiology Fundamentals: Introduction to Imaging & Technology*, DOI 10.1007/978-1-4614-0944-1_30,
© Springer Science+Business Media, LLC 2012

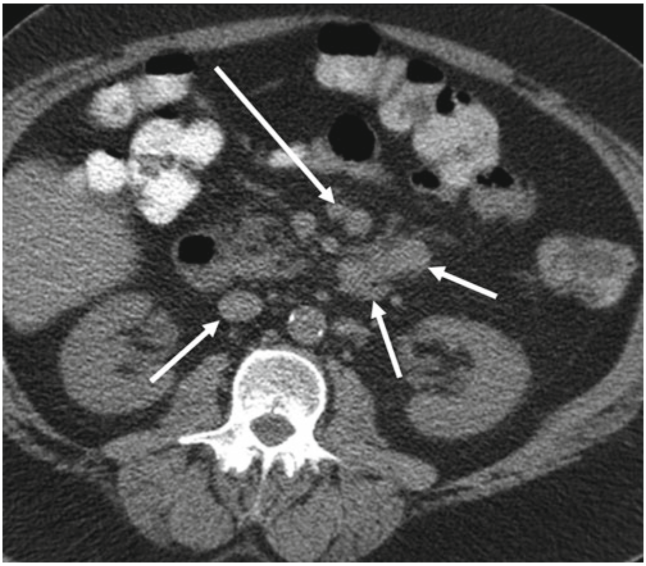

FIGURE 30.1 - ABDOMINAL LYMPH NODES
Mesenteric lymph nodes and para-aortic lymph nodes can be seen if they calcify on plain film or as abnormal soft tissue densities on CT scan (arrows)

Lymphangiogram (Historical Perspective)

The lymphangiogram was performed by cannulating the lymphatics located in the web spaces between the toes of the feet and injecting an oily contrast material directly into the lymphatic vessels. It was a 2-day examination. On the first day of the examination, contrast could be seen within the lymphatic vessels themselves. By day 2, the uptake of contrast by the lymph nodes made them directly visible. The problem with the lymphangiogram is that it is extremely uncomfortable and time consuming for the patient. We now have imaging modalities that allow us to detect lymphadenopathy noninvasively and with minimal discomfort to the patient.

Computerized Tomography Scanning

Computerized Tomography (CT) scanning is an extremely useful method for detecting lymph node enlargement. Lymph nodes appear as round or ovoid soft tissue structures surrounded by fat (Fig. 30.1).

Lymph nodes are considered abnormal on CT when they are enlarged. Normal size criteria for a lymph node depends on its location within the body. One of the limitations of CT is that some lymph nodes may be replaced with tumor but not enlarged. Hence, there will be some false negatives where disease has replaced nodal tissue but has not enlarged the nodes. Similarly, not all enlarged nodes herald a malignancy; thus, false-positive cases may be encountered. Another limitation of CT scanning relates to the presence or absence of intra-abdominal fat. Since fat has a very low density on CT scan, it serves to separate and define the normal abdominal structures. In patients who are very thin or have a paucity of intra-abdominal fat, it may be difficult to distinguish the borders of normal anatomic structures from enlarged lymph nodes, thus limiting the study. The injection of intravenous contrast or the placement of contrast within the GI tract either orally or per rectum may help to define bowel loops and normal anatomic structures from abnormal masses. For this reason, patients are asked to drink a low-density barium mixture prior to a scan for the detection of abnormal lymph nodes. Normal barium as used in an upper GI series would be too dense and create artifacts on the scan.

Esential for the detection of abnormal lymph nodes in the abdomen is the ability to define normal anatomic structures. You should be able to detect abnormal lymph nodes as extra densities by knowing which structures in the abdomen represent normal anatomy. Small blood vessels in the abdomen and pelvis can be confused with lymph nodes on single axial images. With the ability to electronically scroll through the examination, ovoid/round lymph nodes can easily be differentiated from linear vessels. Because of its capacity to distinguish different tissue densities such as soft tissue, air, fat, and bone, CT is the primary modality of choice in patients in whom an abdominal mass lesion or lymphadenopathy is suspected (Fig. 30.2a, b).

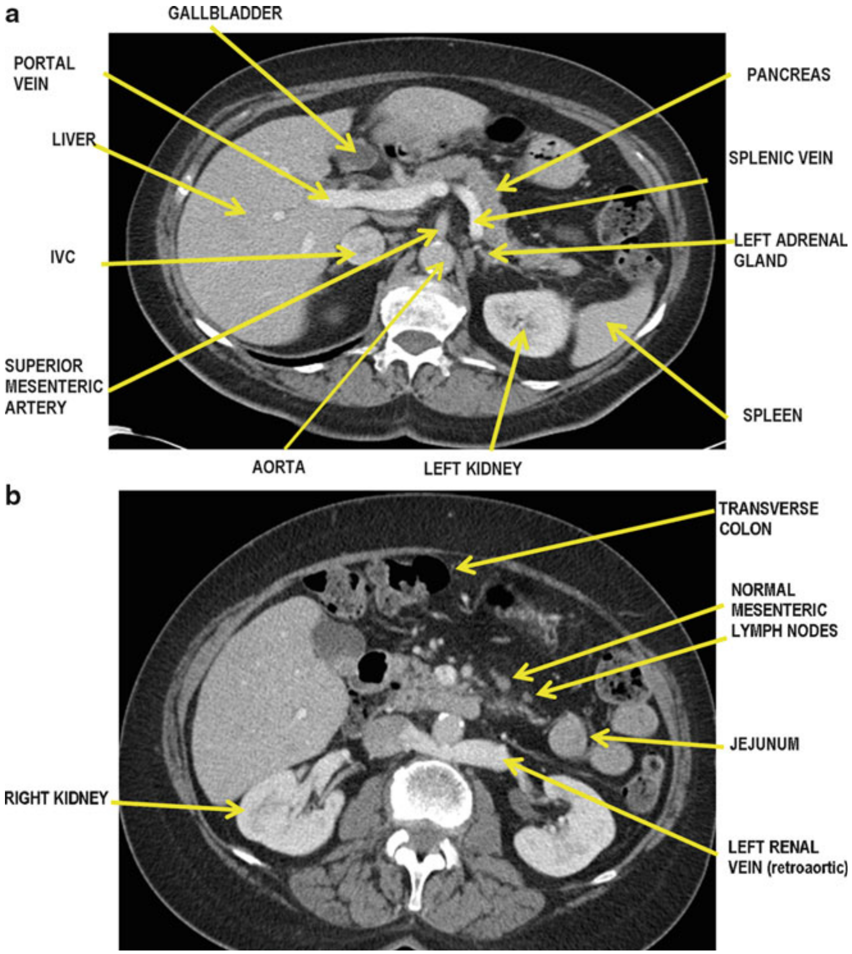
a
GALLBLADDER
PORTAL VEIN
LIVER
IVC
SUPERIOR MESENTERIC ARTERY
PANCREAS
SPLENIC VEIN
LEFT ADRENAL GLAND
SPLEEN
AORTA
LEFT KIDNEY
b
TRANSVERSE COLON
NORMAL MESENTERIC LYMPH NODES
JEJUNUM
RIGHT KIDNEY
LEFT RENAL VEIN (retroaortic)

FIGURE 30.2 - (A, B) NORMAL ANATOMY ON CT
You should be familiar with normal cross-sectional anatomy in order to help identify abnormalities such as lymphadenopathy

31

THE GALLBLADDER

Objective:

1. State the strengths and weaknesses of each of the following radiographic tests used for evaluation of the gallbladder and related structures: ultrasound, IDA scan, percutaneous transhepatic cholangiogram, ERCP and CT scan.

Right upper quadrant pain is one of the most common clinical presentations and the gallbladder is one of the most frequently imaged organs in this setting. There are numerous radiographic tests for evaluation of the gallbladder. This section discusses each of these briefly, but is certainly not complete in its coverage of the various limitations and sequencing of these tests. Of note, radiologists are not the only specialty physicians to image the gallbladder as emergency department physicians and surgeons commonly image this organ at the bedside.

The Gallbladder on Plain Radiograph

Figure 31.1 shows discreet radiopacities in the right upper quadrant of the abdomen, each measuring approximately 1 cm in size. Based on the radiographic density compared to the ribs, one can easily surmise that these are densely calcified. They represent calcified gallstones within the gallbladder. Gallstones are composed primarily of cholesterol and therefore most are lucent on abdominal radiographs. Only 10–15% of gallstones calcify sufficiently for visualization on a plain radiograph. Visible gallstones are seen as lamellated calcific densities in the right upper quadrant of the abdomen, which are usually clustered in groups. They range in size from several millimeters to several centimeters.

H Singh and JA Neutze (eds.), *Radiology Fundamentals: Introduction to Imaging & Technology*, DOI 10.1007/978-1-4614-0944-1_31,
© Springer Science+Business Media, LLC 2012

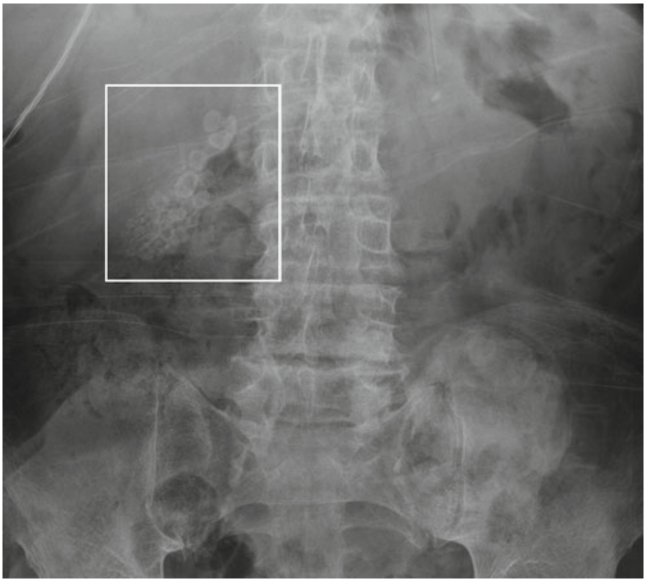

FIGURE 31.1 - GALLBLADDER STONES
The apperance and location of these calcifications are typical of gallstones

A uniformly dense calcification of the entire gallbladder wall, termed “porcelain gallbladder,” is associated with chronic gallbladder inflammation. Porcelain gallbladder is considered a premalignant condition that degenerates to gallbladder carcinoma in approximately 10% of cases.

Gallbladder on Ultrasound

Ultrasound is the preferred method for detecting the presence of gallstones. Its advantages include the fact that no ionizing radiation is employed and that the test may be performed in a single appointment. Ultrasound also identifies gallstone of all types because of density; unlike plain film or CT, a gallstone does not need to be densely calcified to be identified on ultrasound (Fig. 31.2).

Gallstones within the gallbladder are seen as bright echoes within the anechoic, bile-filled gallbladder. Distal to the bright echoes representing the gallstones, there is “shadowing” because of nontransmission of sound through the stones. This is seen as dark bands without any echoes similar in configuration to the beams of a car’s headlights and is sometimes called the “headlight sign.” Ultrasound is made more difficult in patients with copious bowel gas since sound is poorly transmitted through air. Ultrasound is also difficult in very obese patients since the sound is greatly attenuated by the thick body wall.

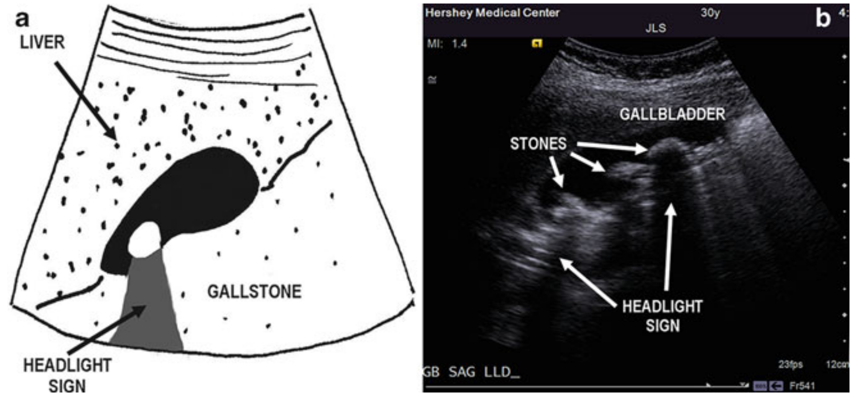

FIGURE 31.2 - GALLSTONES ON ULTRASOUND
In the above diagram (**a**) representing an ultrasound image (**b**), the gallstone in the gallbladder has an acoustic shadow behind it called the "headlight sign"

The IDA Scan

Nuclear medicine studies may also be used in evaluating possible gallbladder dysfunction. A group of compounds in the aminodiacetic acid (IDA) group are employed. Each of these is labeled to a radioactive compound and injected intravenously. The compound is then selectively extracted from the blood pool by the hepatocytes, just like bile and excreted through the bile ducts with subsequent filling of the gallbladder and spillage into the duodenum. This occurs according to a predictable time course.

Failure to visualize normal anatomic structures at the appropriate time may indicate a cystic duct obstruction (e.g., from gallstones) or some degree of physiologic dysfunction (such as seen in chronic cholecystitis). IDA scan have other applications such as evaluation for bile leak after gall bladder surgery. An example of a bile leak on HIDA scan is given (see Fig. 31.3).

Visualizing the Biliary Tree

Contrast may be used to directly opacify the biliary tree (see Fig. 31.4). This can be done from one of two approaches (see Fig. 31.5). A percutaneous transhepatic cholangiogram is performed by placing a needle through the abdominal wall directly into one of the intrahepatic bile ducts. Contrast is then injected through the biliary tree and flows distally toward the point of obstruction. This is performed by interventional radiologists. Alternatively, gastroenterologists can cannulate the ampulla of Vater and inject contrast into the biliary tree in a retrograde manner through the endoscope in a procedure called endoscopic retrograde cholangiopancreatography (ERCP). This will

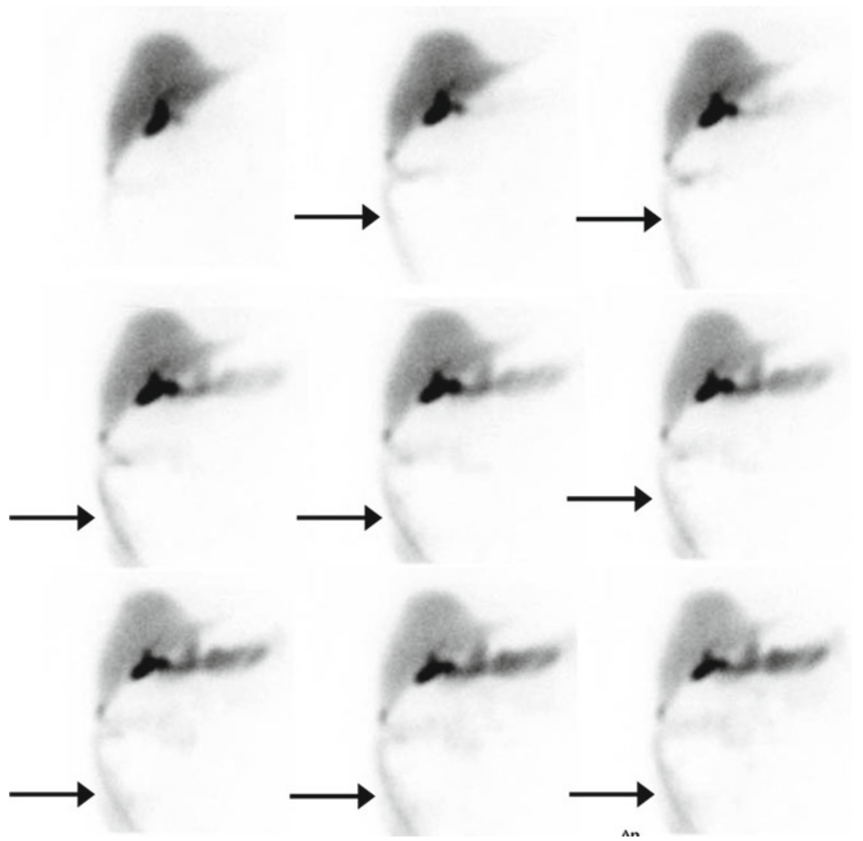

FIGURE 31.3 - BILIARY LEAK ON HIDA SCAN
There is normal hepatic extraction of radiotracer and excretion/clearance into the biliary system (*black structures*). Note the increased tracer activity within the abdominal cavity. The radiotracer tracks along the inferior edge of the right lobe of the liver. Findings are consistent with bile leak

likewise opacify the biliary tree and point out any filling defects or focal narrowing. An additional advantage of ERCP is that the pancreatic duct is often visualized.

Often, following gallbladder removal, a “T-tube” is left in place to serve as a stent and prevent bile duct obstruction immediately following surgery. When the question of a retained gallstone within the biliary tree or obstruction to biliary flow due to postsurgical stricture or edema is raised, contrast may be infused through the T-tube, opacifying the biliary tree, and demonstrating whether or not an abnormality is present (see Fig. 31.6).

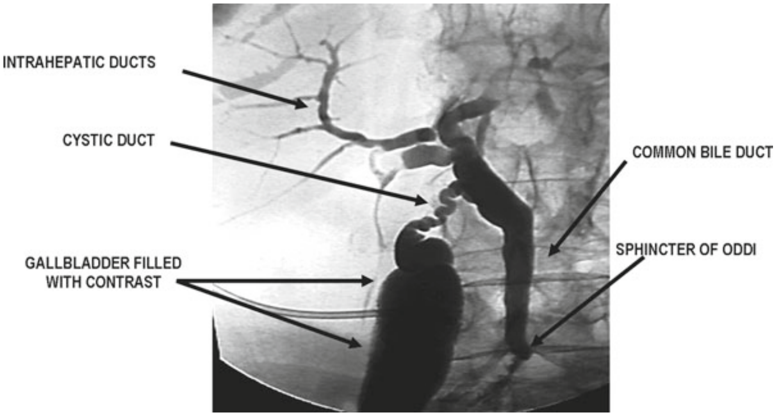
INTRAHEPATIC DUCTS
CYSTIC DUCT
GALLBLADDER FILLED WITH CONTRAST
COMMON BILE DUCT
SPHINCTER OF ODDI

FIGURE 31.4 - GALLBLADDER AND ADJACENT STRUCTURES
On this cholecystostomy study, contrast is injected via the indwelling gallbladder drain. Note the contrast-opacified gallbladder and the cystic duct, as well as the adjacent biliary structures

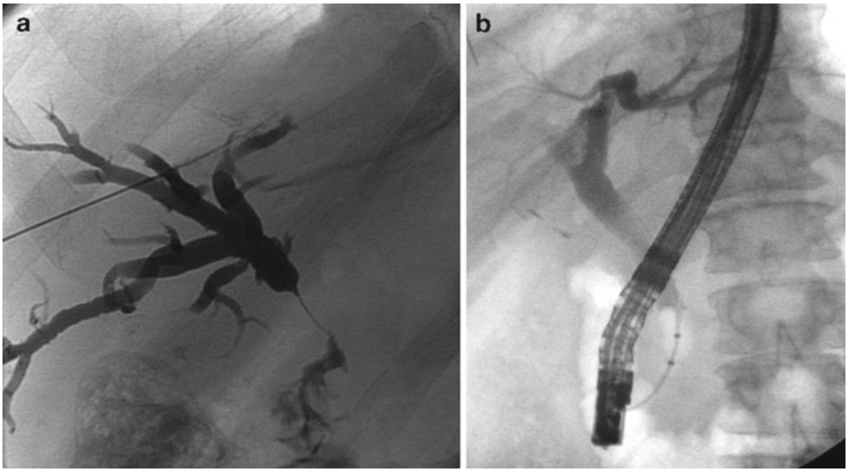

FIGURE 31.5 - PTC (A) AND ERCP (B)
In the PTC, contrast is introduced transhepatically. In the ERCP, contrast is introduced in a retrograde fashion

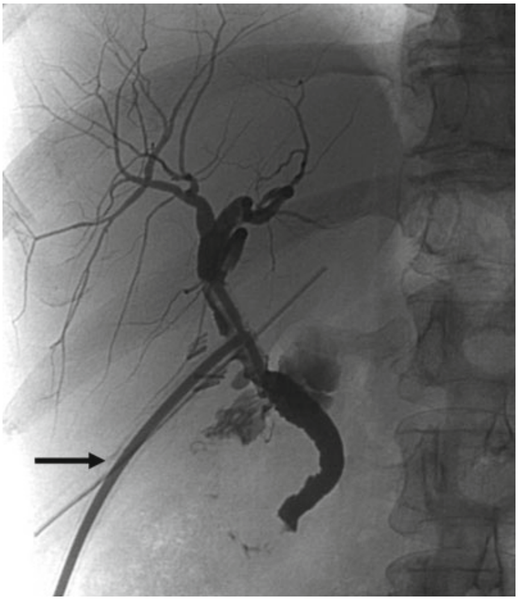

FIGURE 31.6 - CHOLANGIOGRAM
Contrast is injected through the T-tube (*arrow*) to opacify the biliary tree

Gallstones on CT

Finally, in the course of performing an abdominal CT for other reasons, gallstones may often be demonstrated as radiographically dense foci within the fluid-filled gallbladder (Fig. 31.7). Gallstones may not be seen on CT scan if they are composed mostly of cholesterol and not calcium.

Remember that the diagnosis of gallbladder disease and its complications remain complex and challenging. The use of a radiologist as a consultant to recommend and perform one or more of the appropriate studies described above will help to find the accurate diagnosis.

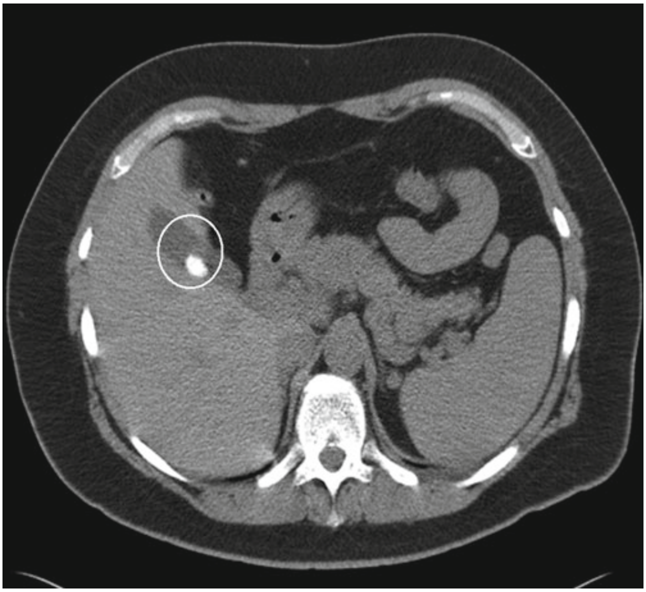

FIGURE 31.7 - GALLSTONE ON CT
Typical appearance of a gallstone on CT

32

ABDOMINAL AND PELVIC PAIN EVALUATION

Objectives:

1. Begin to understand when CT or ultrasound is an appropriate study.
2. Learn some common radiologic findings in patients with various types of abdominal or pelvic pain.

Patients with abdominal and/or pelvic pain are commonly encountered in the emergency department and throughout all of the primary care and specialty clinics. The imaging assessment of these patients depends upon their clinical presentation (acute vs. chronic pain, point tenderness vs. generalized discomfort), laboratory data (elevation of liver function tests, serum amylase, white cell count, hematocrit), age, gender, and frequently the availability of the various diagnostic imaging tests.

In the acute care setting, the most frequently utilized imaging studies are conventional radiographs, ultrasound, and CT. The most common radiograph is an abdominal series to assess for obstruction, free air, or stone disease. The most common ultrasound indications are to evaluate for obstructed biliary systems or gallbladder pathology, renal pathology, or gynecologic processes. In many institutions, CT is available 24/7 and is useful in the assessment of gastrointestinal pathology, hepatic and renal processes, and vascular disease states such as aortic dissection or mesenteric ischemia. However, CT frequently requires the injection of an intravenous contrast and may also require the use of an oral contrast agent. In addition, there is exposure to ionizing radiation with computed tomography, which should be considered when assessing children or women of reproductive age (Table 32.1).

H Singh and JA Neutze (eds.), *Radiology Fundamentals: Introduction to Imaging & Technology*, DOI 10.1007/978-1-4614-0944-1_32,
© Springer Science+Business Media, LLC 2012

Imaging of Acute Types of Pain

Ultrasound does not require the use of ionizing radiation, but due to the inherent limitations of this modality, it is routinely limited to certain abdominal/pelvic organs including liver, gallbladder, kidneys, and uterus/adnexa. Bowel gas and fecal contents will obscure visualization of other regions. Adipose tissue in large patients may also limit its use by obscuring organs and possible pathology. In addition, in many institutions, ultrasound availability off-hours may be limited.

The following tables, Table 32.2 list common causes of abdominal and/or pelvic pain organized by age group. As you will see some etiologies are common in many of the groups and some are found in only one group. Figures 32.1 through 32.7 show imaging examples of some of the most common pathologies responsible for abdominopelvic pain. For instance, in small children, acute abdominal pain is likely to be caused by routine gastroenteritis in addition to other processes such as a hernia (Fig 32.4), appendicitis (Fig 32.1), intussusception, urinary tract pathology, and malrotation. In younger and middle-aged adults, acute abdominal pain is more frequently caused by gallbladder pathology (Fig 32.3), pancreatitis, trauma,

Table 32-1 Imaging of Acute Types of Pain

Indication	Recommended imaging study
Bowel abnormalities (including inflammation or ischemia)	CT
Liver abnormalities	ultrasound (u/s) or CT
Gallbladder pathology	u/s
Kidney abnormalities (including stones)	u/s or CT
Spleen abnormalities	u/s or CT
Pancreas pathology	CT
Uterus/ovarian abnormalities	u/s
Scrotal pathology	u/s
Abnormalities of the Aorta	u/s or CT

Table 32-2 Common causes of abdominal and pelvie pain by age group

Infants

1. Intussusception
2. Malrotation
3. Trauma
4. Renal obstruction
5. Reflux/pyelonephritis/urinary tract infection
6. Scrotal pathology

Young children

1. Appendicitis
2. Urinary tract infection
3. Trauma
4. Pancreatitis
5. Scrotal pathology

Older children and young adults

1. Appendicitis
2. Urinary tract infection
3. Trauma
4. Pelvic inflammatory disease
5. Bowel obstruction
6. Liver masses
7. Gallbladder disease
8. Inflammatory bowel disease
9. Pregnancy complications
10. Pancreatitis
11. Scrotal or uterine/adnexal pathology

Older adults

1. Appendicitis
2. Urinary tract pathology
3. Malignancy
4. Diverticulitis
5. Bowel obstruction
6. Aortic aneursym or dissection
7. Gallbladder disease
8. Inflammatory bowel disease
9. Mesenteric ischemia
10. Pancreatitis
11. Scrotal or uterine/adnexal pathology

Special consideration for women of child-bearing age

1. Ectopic pregnancy
2. Pelvic inflammatory disease
3. Pregnancy complications

diverticulitis (Fig 32.2), or renal pathology. In younger adults, consideration should also be given to appendicitis or inflammatory bowel disease. Older adults are more likely to have diverticulitis or bowel obstruction (related to adhesions, etc.), gallbladder disease, pancreatitis, or mesenteric ischemia. Renal stone disease can also present with groin or abdominal pain rather than flank discomfort (Fig. 32.5). Both benign and malignant neoplasms may present with acute pain.

Pelvic or groin pain in young males may be caused by acute torsion of the testicle or the appendix testis/epididymis (Fig. 32.6). It may be related to trauma, hernia, renal stone disease, or appendicitis. In young adult males, consideration should also be given to epididymitis. Diverticulitis can also cause pelvic pain.

Female patients with acute pelvic pain are more likely to have gynecologic pathology as a source of discomfort. In pediatric populations and young adults, adnexal torsion is always a consideration. Young women of reproductive age may present with pelvic pain and/or bleeding with ectopic pregnancy or abnormalities of first trimester pregnancies (including intrauterine fetal demise, placental hemorrhage/

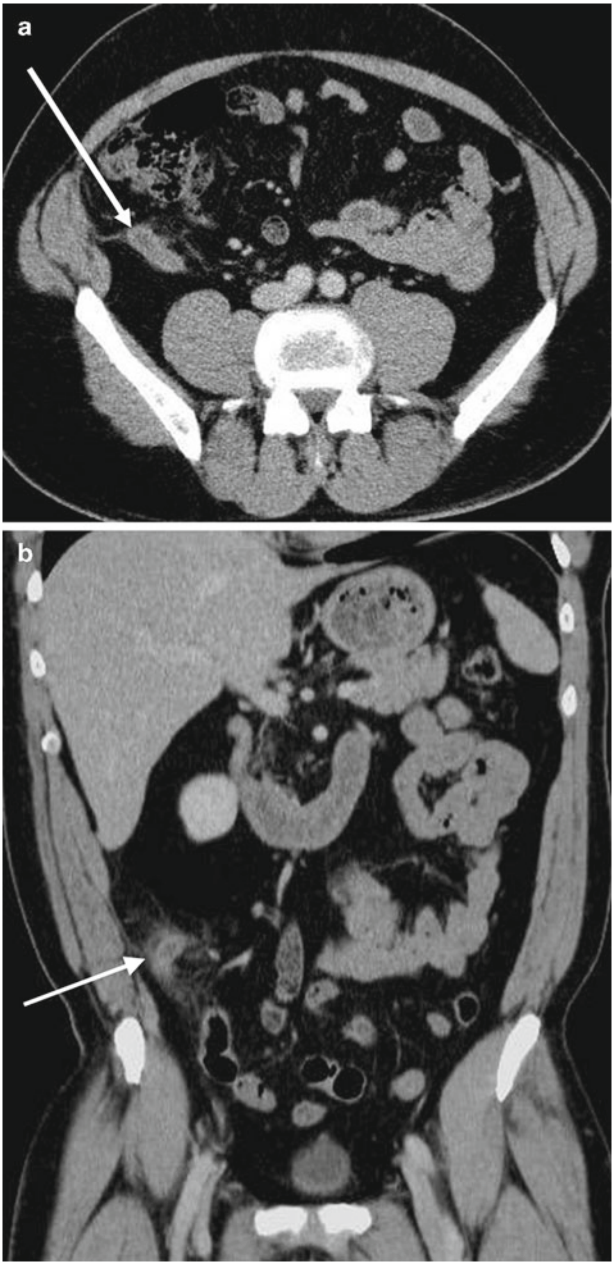

FIGURE 32.1 - APPENDICITIS
Axial (**a**) and coronal (**b**) views of appendicitis. Note the enlarged and thickened appendix and the surrounding inflammatory fat stranding

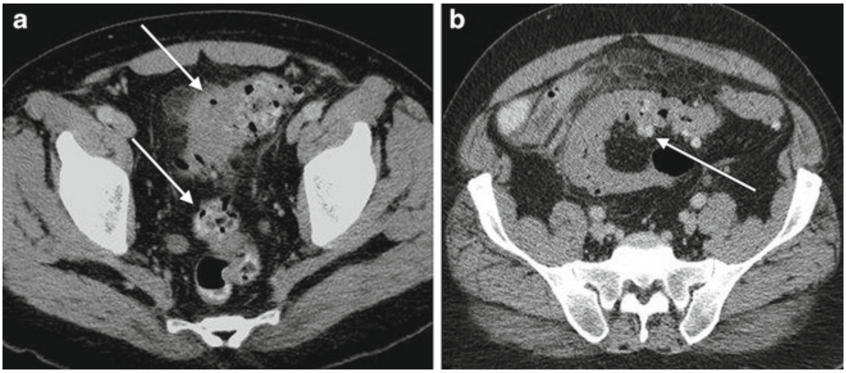

FIGURE 32.2 - DIVERTICULITIS
Axial views of diverticulitis. Note the extraluminal air, adjacent fat stranding, and several outpouchings of the colon (diverticula)

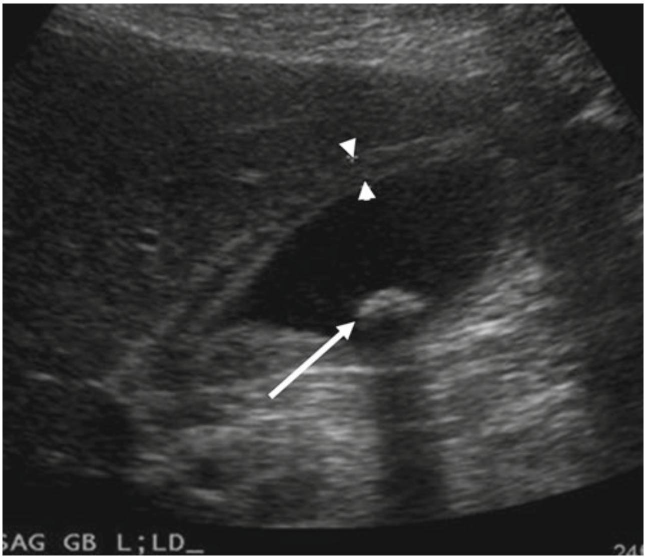

FIGURE 32.3 - CHOLECYSTITIS
Ultrasound of the right upper quadrant demonstrates a shadowing stone (*arrow*) in the gallbladder. There is also thickening of the gallbladder wall (*arrowheads*)

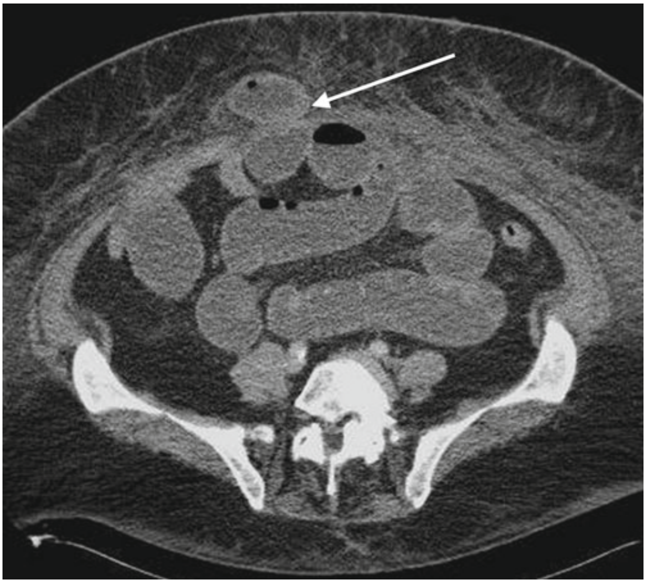

FIGURE 32.4 - VENTRAL WALL HERNIA
Axial CT image through the abdomen shows a loop of small bowel herniating across the anterior abdominal wall in this patient with abdominal pain

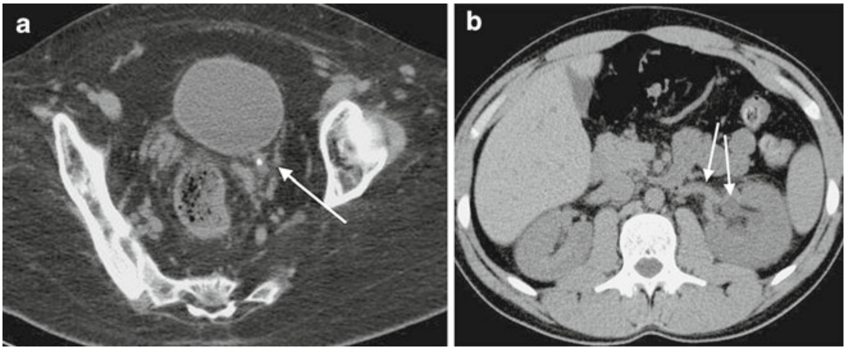

FIGURE 32.5 - RENAL CALCULUS AND SUBSEQUENT HYDRONEPHROSIS
Unenhanced axial CT slice of a ureteral calculus in the distal left ureter (**a**). Axial view of the left kidney with hydronephrosis secondary to the same calculus within the distal left ureter (**b**)

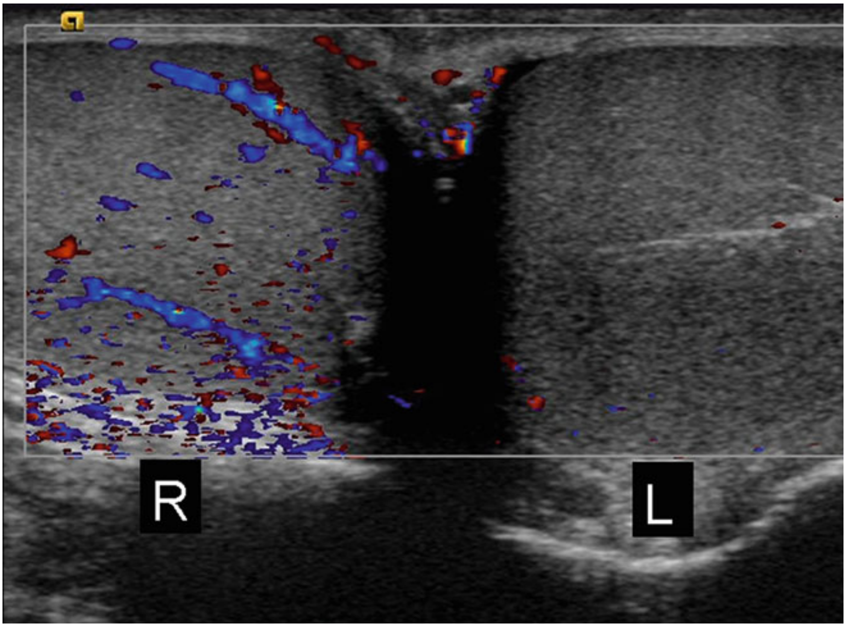

FIGURE 32.6 - TESTICULAR TORSION
Transverse image through both testicles shows asymmetry in color flow to the testes. The *left* testis (the symptomatic side) has reduced flow compared to the *right*, consistent with the diagnosis of testicular torsion

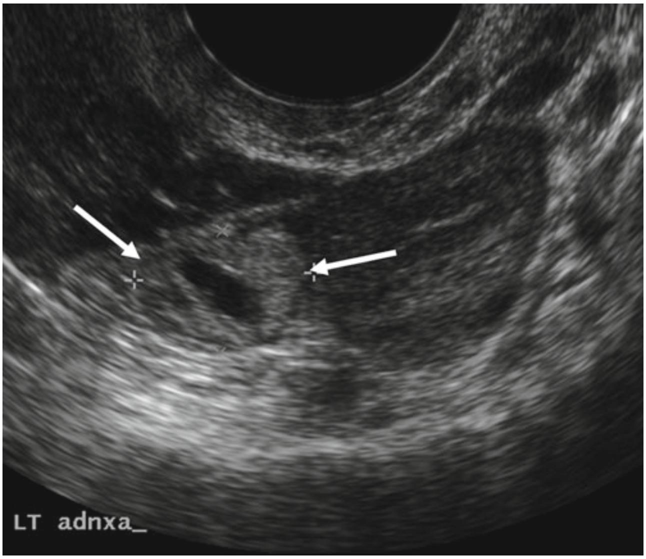

FIGURE 32.7 - ECTOPIC PREGNANCY
Transverse image through left adnexa shows a mass with echogenic donut-like rim in a woman with a positive pregnancy test (and empty uterus on ultrasound examination) which was an ectopic pregnancy (*arrows*)

abruption) (Fig. 32.7). As a result, pelvic ultrasound plays a prominent role in their work-up. However, women can also have appendicitis, diverticulitis or inflammatory bowel disease, pathology that can be better evaluated with computed tomography.

Certain acute evaluations such as the patient sustaining multiple trauma, those with possible aortic dissection or mesenteric ischemia require immediate CT. These studies are usually done with high flow bolus injections of intravenous contrast agents (to allow full evaluation of the aorta, branch arteries, and venous structures) and do not require oral contrast. When these patients suffer from underlying renal insufficiency, the CT study can be performed without intravenous contrast; however, evaluation of vascular pathology is compromised. In true emergent states, injection with special low osmolarity nonionic contrast agents and vigorous preprocedure hydration may reduce the risk of renal toxicity. Intense follow-up of renal function is always indicated in these patients and the clinical team must be prepared to support the patient with dialysis and fluids as necessary.

The following tables list common radiologic findings in various types of abdominal or pelvic pain.

Table 32-3 Some common causes of abdominal and pelvie pain and the associated imaging findings

CT findings in appendicitis (Fig. 32.1)

1. Thickened/distended appendix (with enhancing wall)
2. Periappendiceal inflammatory fat stranding
3. Periappendiceal fluid collection
4. Cecal bar (caused by edema in the cecal wall)
5. Arrowhead sign (caused by edema where the cecum meets the appendix)

Ultrasound findings in appendicitis

1. Thickened/distended appendix (with enhancing wall)
2. Hyperemia (increased flow) noted on color or power Doppler imaging
3. Periappendiceal fluid collection
4. Appendicolith

Imaging findings of ovarian torsion

1. Asymmetrically enlarged ovary; mass may be present
2. Compromised venous and/or arterial flow may be noted on Doppler evaluation
3. Due to the ovary's dual blood supply, flow may be seen within the ovary even in the cases of torsion
4. Pelvic fluid

CT findings in diverticulitis (Fig. 32.2)

1. Abnormal inflammatory fat stranding affecting a region of colon with diverticula
2. Para-colic collection
3. Para-colic extraluminal air
4. Pelvic fluid
5. Thrombus in the inferior mesenteric vein
6. Hepatic abscess formation
7. Free peritoneal air

CT findings in mesenteric ischemia

1. Clot within or occlusion or superior mesenteric artery/vein and or its branches
2. Pneumatosis intestinalis
3. Venous gas
4. Focal/segmental area of bowel showing poor enhancement
5. Thickening or thinning of bowel
6. Solid organ infarction

CT findings in inflammatory bowel disease

1. Inflammatory stranding of abdominal fat
2. Localized or free fluid
3. Abnormal thickening of bowel
4. Increased fat accumulation in the mesentery (Crohn's disease)
5. Fistula formation, abscess

CT findings in bowel obstruction

1. Dilated bowel traced to a "transition zone" where acute decrease in caliber is noted
2. Free fluid
3. Inflammatory stranding of abdominal fat

Ultrasound findings in Epididymitis

1. Abnormal enlargement of the epididymis
2. Increased flow within the epididymis (or testis if orchitis is present) on color or power Doppler imaging
3. Hydrocele
4. Heterogeneous testis (if orchitis present)
5. Decreased testicular flow if epidymo-orchitis is complicated by compromised testicular perfusion (due to testicular swelling)

U/S findings in cholecystitis (Fig. 32.3)

1. Gallbladder
2. Gallbladder wall thickening and edema
3. Fluid around gallbladder

CT findings in ventral hernia (Fig. 32.4)

1. Abdominal fat, bowel or organs across the abdominal wall mesenteric
2. Abdominal fluid
3. Inflammatory fat stranding

Ultrasound findings in Testicular torsion (Fig. 32.5)

1. Abnormal echotexture of the testis
2. No flow evident within the testis on color or power Doppler imaging
3. Hydrocele

Primary findings with renal calculi (Fig. 32.6)

1. Calcified stone within the pelvicalyceal system, ureter or bladder

Secondary findings with renal calculi

2. Asymmetric enlargement of the kidney
3. Pelvicalyceal or ureteral dilation
4. Perinephric stranding of fat
5. Perinephric fluid collection
6. Rim of ureteral mucosal edema/thickening about a stone
7. Peri-ureteric fat stranding

U/S findings in ectopicpregnancy (Fig. 32.7)

1. Complux cystitis or solid appearing mass or gestatronal sac in the ad
2. Pneumatosis intestinalis
3. Pelvic fluid seen - often complux in nature

33

IMAGING THE TRAUMA PATIENT

Objectives:
1. Understand the imaging workup of a trauma patient.
2. Become familiar with common soft tissue injuries. Seen in trauma.

Trauma patients frequently are imaged in the emergency department, as they are at high risk for significant internal injuries that would not be evident on conventional radiographs. Many institutions use "Fast" scan ultrasound (Focused Assessment with Sonography in Trauma), a way of surveying the certain portions of the abdomen and pelvis looking for free fluid, which may indicate the presence of hemorrhage. When free fluid is found, the patient is then generally evaluated with enhanced computed tomography.

In some institutions trauma patients go directly to computed tomography as it is a very sensitive way to detect significant intra-abdominal organ trauma. In general, intravenous contrast is required as it allows the detection of active bleeding and improves visualization of hypodense organ fractures/lacerations. Trauma patients can suffer any number of injuries to the chest, abdominal and pelvic organs as well as injuries to the central nervous system or musculoskeletal system. Some of the more common traumatic injuries to the chest, abdomen and pelvis are listed in Table 33.1, with references to illustrative cases.

H Singh and JA Neutze (eds.), *Radiology Fundamentals: Introduction to Imaging & Technology*, DOI 10.1007/978-1-4614-0944-1_33,
© Springer Science+Business Media, LLC 2012

Table 33-1

Chest (Fig. 33.1 and Fig. 33.2)
Hemothorax Lung contusion
Aortic dissection
Liver (Fig. 33.3)
Fluid in Morrison’s pouch or surrounding the liver Hypodense (on CT) liver laceration Subcapsular fluid or hemorrhage Liver hematoma or contusion Rupture of gallbladder
Spleen (Fig. 33.4)
Hypodense laceration Perisplenic fluid/hemorrhage Left upper quadrant rib fractures
Kidneys (Fig. 33.5)
Perirenal fluid Hypodense laceration Hematoma within the kidney Extravasation of contrast filled urine
Adrenals (Fig. 33.6)
Adrenal hemorrhage Periadrenal fat stranding
Pancreas (Fig. 33.7)
Hypodense laceration Fluid separating the splenic vein and pancreas Diffuse pancreatic enlargement/edema Pancreatic hematoma
Bowel injury (Fig. 33.8)
Bowel wall thickening Fluid adjacent to bowel Reduced enhancement of injured portion of bowel Extraluminal oral contrast Extraluminal air “Sentinel clot” in the mesentery
Duodenum (Fig. 33.9)
Fluid in the right anterior pararenal space Fluid around the duodenum Findings of bowel injury (see above) within the duodenum

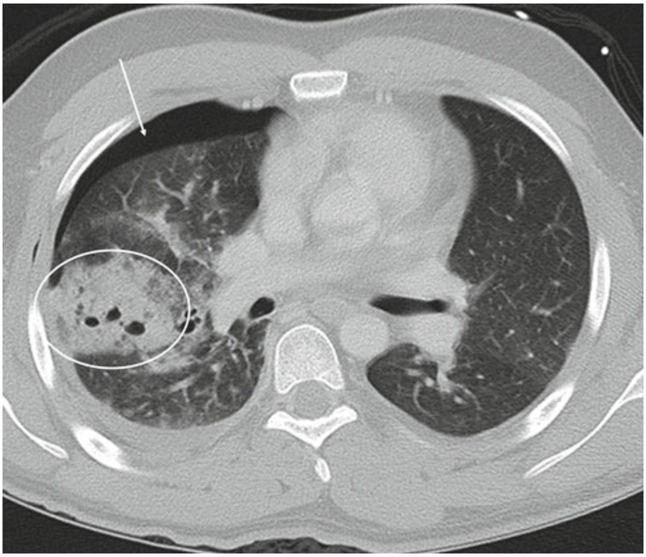

FIGURE 33.1 - TRAUMATIC INJURY TO THE THORAX
Arrow points to an anterior pneumothorax which would be difficult to appreciate on plain radiograph. *Circle* denotes an area of lung contusion

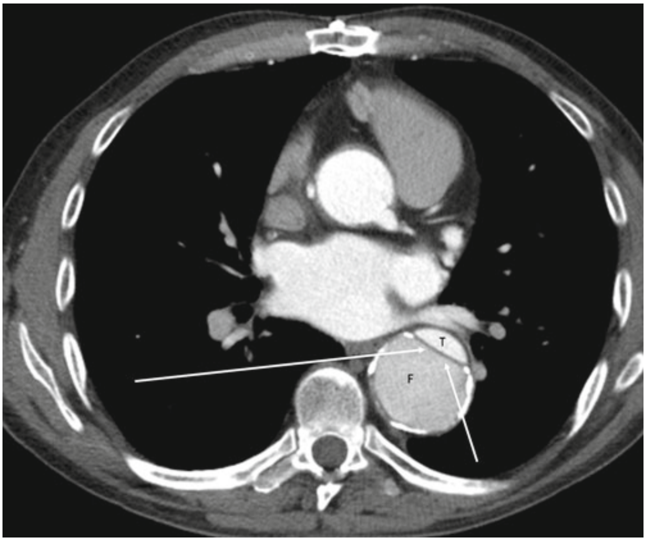

FIGURE 33.2 - TRAUMATIC INJURY TO THE THORAX
Contrast-enhanced axial CT slice shows aortic dissection as evidenced by dissection flap (*arrows*) and the two lumens, true (T) and false (F)

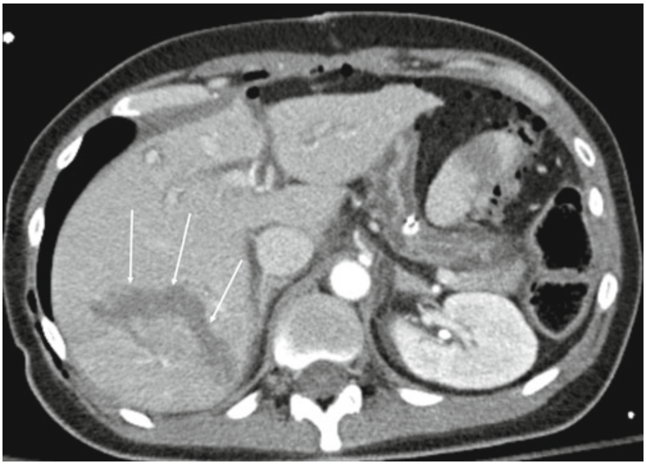

FIGURE 33.3 - TRAUMATIC INJURY TO THE LIVER
Large hypodensity (*arrows*) through the right lobe of the liver represents a large liver laceration

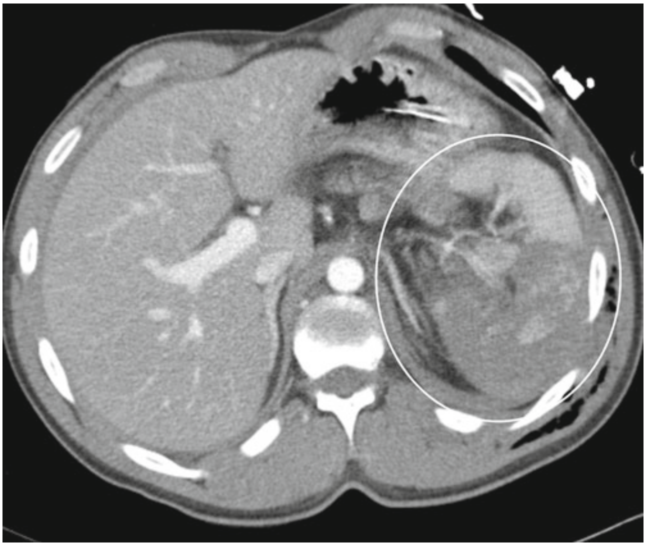

FIGURE 33.4 - TRAUMATIC INJURY TO THE SPLEEN
High grade splenic laceration. Note how hypodense the entire posterior two-thirds of the spleen is relative to the anterior one-third circle

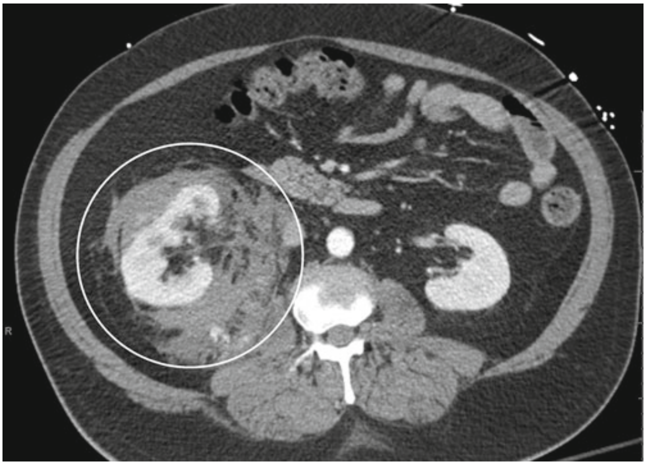

FIGURE 33.5 - TRAUMATIC INJURY TO THE KIDNEY
Extensive amount of fluid surrounding the right kidney related to recent trauma (*circle*)

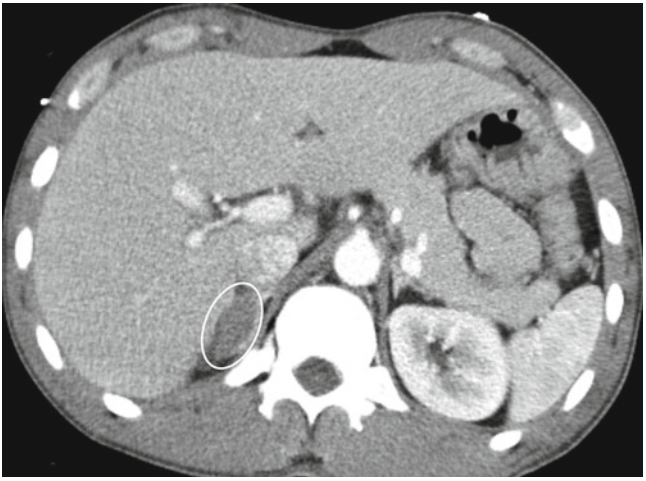

FIGURE 33.6 - TRAUMATIC INJURY TO THE ADRENALS
Hypodensity expanding the right adrenal gland represents adrenal hemorrhage related to traumatic injury (*circle*)

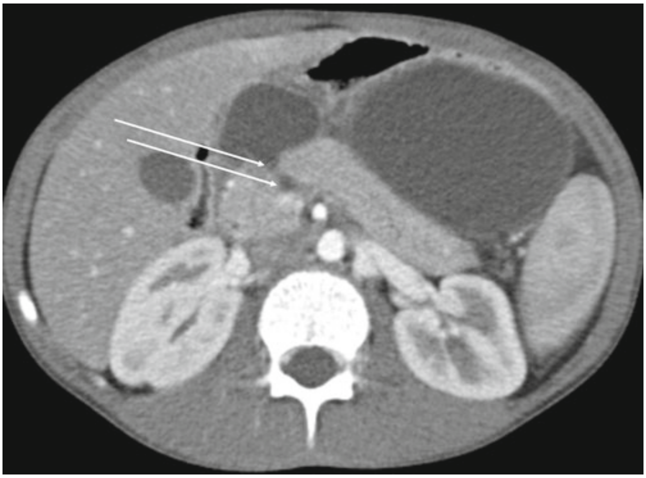

FIGURE 33.7 - TRAUMATIC INJURY TO THE PANCREAS
Hypodensity (*arrows*) through the head of pancreas represent a major pancreatic transection

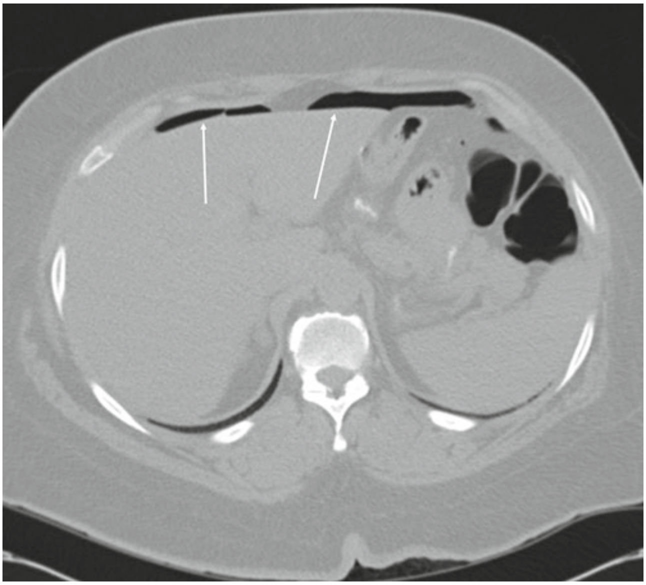

FIGURE 33.8 - TRAUMATIC INJURY TO THE BOWEL
Axial CT image of the upper abdomen on lung windows show pneumoperitoneum (*arrows*) related to bowel rupture caused by traumatic injury in this patient

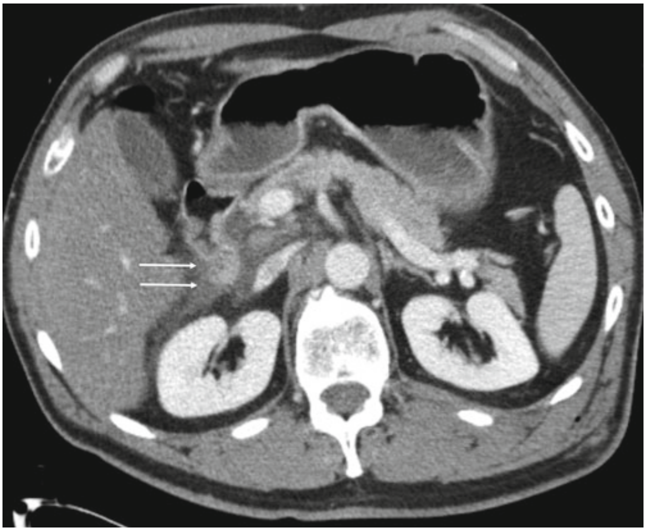

FIGURE 33.9 - TRAUMATIC INJURY TO THE DUODENUM
Fluid surrounding the third portion of the duodenum caused by traumatic injury of duodenum (*arrows*)

34

CONCERNING LESIONS

Objectives:

1. Learn to recognize potentially emergent pathologies including an abscess, pneumoperitoneum, portal venous gas, and colitis.
2. Learn to recognize other important lesions in the abdomen including an abdominal aortic aneursym, renal cell cancer, a pancreatic mass, and hepatocellular carcinoma.

Abscess

An abscess is a collection of infected fluid and inflammatory debris that has been walled off by the body's immune system. Any inflammatory process in the abdomen or pelvis such as appendicitis, diverticulitis, and Crohn's disease, can lead to an abscess. Traumatic puncture wounds and foreign bodies can also result in abscess formation. Common locations for an abdominal abscess are the subphrenic and subhepatic spaces. Abscesses can also develop in organs, such as the liver (intrahepatic abscess) or kidney (renal abscess). An abscess must be promptly treated with antibiotics and either percutaneous or surgical drainage to prevent systemic infection or sepsis.

Patients with an abscess present with increased white cell count and fever. Radiographically, an abscess appears as a loculated fluid collection with a thick enhancing wall. Free fluid tends to layer dependently while fluid in an abscess remains loculated. Characteristic features of an abscess include fluid–fluid levels, septations, and most notably, internal air (Fig. 34.1).

Sometimes you will hear the term "phlegmon" used in similar clinical scenarios. A phlegmon is also a collection of inflammatory debris, less organized physiologically than an abscess but it will resolve with antibiotics and generally does not

H Singh and JA Neutze (eds.), *Radiology Fundamentals: Introduction to Imaging & Technology*, DOI 10.1007/978-1-4614-0944-1_34,
© Springer Science+Business Media, LLC 2012

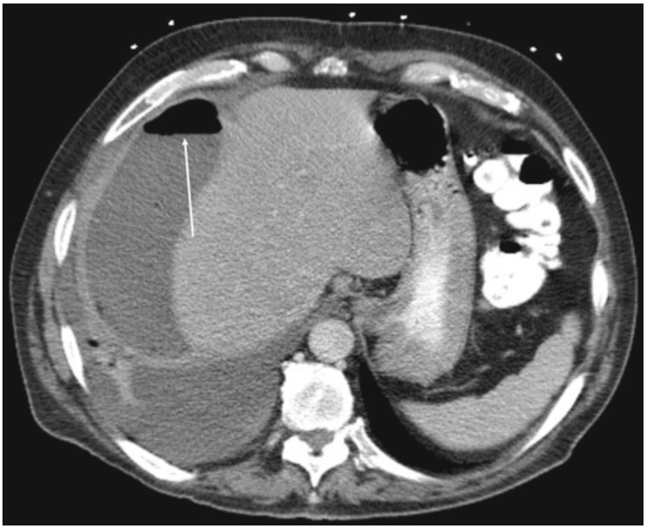

FIGURE 34.1 - SUBHEPATIC AND SUBPHRENIC FLUID COLLECTION
Note the air–fluid level (*arrow*), a classic finding of an abscess

require drainage or surgery. Disease processes such as appendicitis or pancreatitis can cause a phlegmon to develop. On CT, an abscess will demonstrate fluid density (Hounsfield units <20) while a phlegmon often demonstrates soft tissue density (Hounsfield units 20–40). A phlegmon and an abscess can be thought of as different points along the spectrum of inflammation.

Pneumoperitoneum

For a complete discussion of this very important finding see Chap. 24. Pneumoperitoneum has a broad range of etiologies from benign expected postoperative air to life-threatening hollow viscous rupture. Anytime pneumoperitoneum is identified, it needs to be explained. Often the investigation of pneumoperitoneum begins with abdominal radiographs. If free air is noted, CT is often done to further delineate the extent of free air and help determine the source (Fig. 34.2a, b).

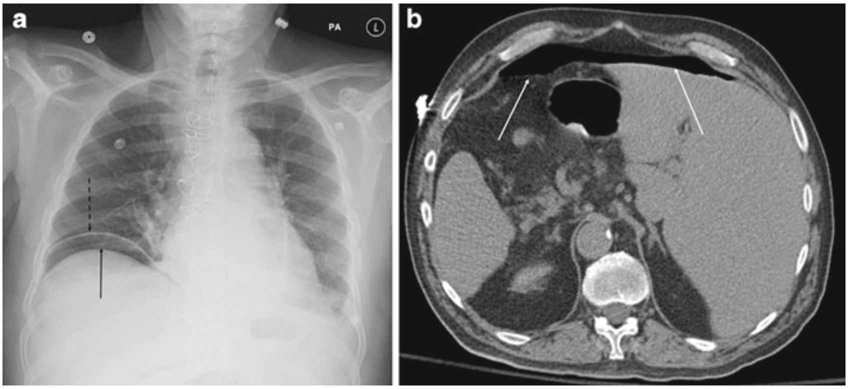

FIGURE 34.2 - PNEUMOPERITONEUM
(**a**) Note the air collection (*solid arrow*) between the liver and hemidiaphragm (*thin white line* denoted by *dashed arrow*). (**b**) Note the intraperitoneal air collection (*arrows*) due to a hollow viscous rupture in this patient

Abdominal Aortic Aneursym

Nearly 10% of the population over age 65 has an abdominal aortic aneursym (AAA). Smoking is a well-known risk factor. Guidelines state that ultrasound screening is indicated in any male over 65 years old with a smoking history. Once the abdominal aorta measures greater than 3 cm, it is considered to be an aneurysm. Ninety percent of AAA's are infrarenal (located below the renal arteries). Location is important for surgical planning as repair of an aneursym above the renal arteries is more complex.

With dissection of an aneursym, the radiologist may see an intimal flap and the subsequent development of a false lumen. Dissection involving the origin of branch vessels (for example, the celiac artery) can lead to ischemia of organs supplied by those branches. Worrisome radiographic findings include the hyperattenuating crescent sign which is a sign of impending rupture and represents acute bleeding into the wall of the aneursym (Fig. 34.3). Signs of rupture include evidence of hemorrhage in the surrounding retroperitoneal tissues or active extravasation of intravenous contrast.

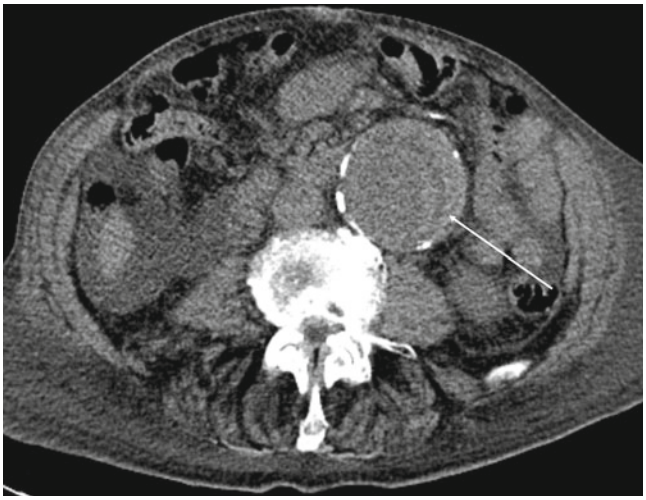

FIGURE 34.3 - RIM CALCIFIED ABDOMINAL AORTIC ANEURSYM
Arrow points out the hyperattenuating crescent sign, a sign of impending rupture

Renal Cell Cancer

Renal cell cancer (RCC) is by far the most common solid renal tumor. Smoking is a known risk factor. Other risk factors include Von Hippel Lindau syndrome and acquired renal cystic disease from chronic hemodialysis. RCC arises from the convoluted tubules in the renal cortex. The uncommon, yet classic clinical triad associated with RCC is a palpable flank mass, flank pain and hematuria.

Radiographically, the tumors are heterogeneous in appearance on CT and they appear as solid lesions or mixed cystic and solid lesions on ultrasound. The tumors show brisk enhancement after the administration of intravenous contrast. With every new diagnosis of RCC, the ipsilateral renal vein and the IVC must be examined carefully to look for tumor thrombus involvement, a relatively common occurrence with RCC. The surrounding renal hilar, pericaval, and periaortic lymph nodes should also be examined for evidence of tumor involvement. Common sites of RCC metastasis include the lungs, bones, liver, brain, and adrenal glands. RCC responds poorly to chemotherapy and radiation therapy. However, it is often curable with surgical resection when found early (Fig. 34.4a, b).

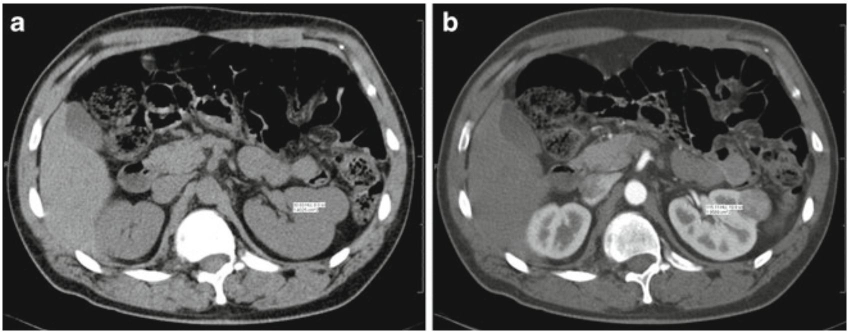

FIGURE 34.4 - LEFT RENAL MASS
(**a**) Noncontrast axial CT image shows a large isodense solid mass arising from left kidney. Hounsfield units show a value of 30. (**b**) Enhanced CT during the arterial phase shows the same renal lesion as (**a**) which demonstrates rapid arterial enhancement. Hounsfield units show a value of 115

Hepatocellular Carcinoma

Hepatocellular carcinoma (HCC) is the most common primary hepatic malignancy in patients with chronic hepatic disease; it is very uncommon in patients without chronic liver disease. Common etiologies of chronic liver disease include chronic alcohol abuse, hepatitis B and hepatitis C. Any solid hepatic mass in a cirrhotic patient is HCC until proven otherwise. HCCs develop along a pathologic continuum from a regenerative nodule to adenomatous hyperplasia to atypical adenoma hyperplasia to HCC.

Patients are often asymptomatic. The laboratory test, alpha-fetoprotein, can be used to monitor for HCC development or recurrence, in the appropriate clinical population. Radiographically, HCCs may be discrete masses but are often inconspicuous and infiltrating. The classic characteristic that assists in their identification is the fact that HCCs vigorously enhance following intravenous contrast administration (Fig. 34.5a–c). Like renal cell carcinoma, vascular invasion by tumor thrombus is relatively common. The hepatic and portal veins must be assessed for involvement of tumor thrombus on pretreatment imaging. Current treatment options consist of surgical resection, chemoembolization (generally done in Interventional Radiology), and systemic chemotherapy. A novel treatment is radiation treatment delivered by radioactive spheres deposited in a similar manner as chemoembolization.

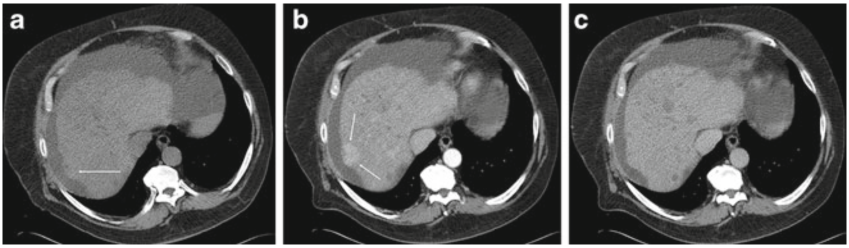

FIGURE 34.5 - HEPATOCELLULAR CARCINOMA
(**a**) Noncontrast CT shows a subtle isodense contour irregularity suggestive of a mass in the periphery of the right lobe of the liver. (**b**) Enhanced CT during the arterial phase shows avid enhancement of the mass seen in (**a**). (**c**) Enhanced CT during the venous phase shows that the mass in the periphery of the right liver has become isodense again consistent with rapid washout of contrast which is characteristic of a hepatocellular carcinoma

Portal Venous Gas

Portal venous gas is the result of dying or dead bowel and portends imminent patient demise. As the bowel necroses, gas is absorbed into the draining venous system (superior mesenteric vein and inferior mesenteric vein) and delivered to the liver via the portal vein. When this occurs, air is characteristically seen in the periphery of the liver as portal venous blood flows hepatopetally. Portal venous air must be differentiated from pneumobilia. Since bile flows out of the liver (hepatofugally) pneumobilia (air within the biliary system) is more centrally located in the liver. Etiologies of pneumobilia are more often benign and related to prior procedures such as papillotomy. When air is peripherally located in the liver, portal venous gas must be suspected and urgently communicated to the clinical team (Fig. 34.6).

Pancreatic Mass

Pancreatic adenocarcinoma has a very low 5-year survival rate despite aggressive surgical and medical treatment. The poor prognosis is due to the fact that the tumor does not manifest symptoms until late in the course of the disease. When symptoms present they often include vague abdominal pain, weight loss, and/or jaundice. Unfortunately, most tumors are not resectable at the time of diagnosis.

Pancreatic tumors are difficult to detect on imaging. Often they appear as a hypodense to isodense mass with minimal contrast enhancement on CT. Pancreatic neoplasm is difficult to diagnose with ultrasound as the gland is often obscured by overlying bowel loops and bowel gas. Sixty percent of pancreatic adenocarcinomas are located in the pancreatic head. Due to the inconspicuous nature of these tumors, indirect clues are important for determining the presence of a pancreatic tumor. The most infamous of these clues is the double duct sign (Fig. 34.7). This refers to

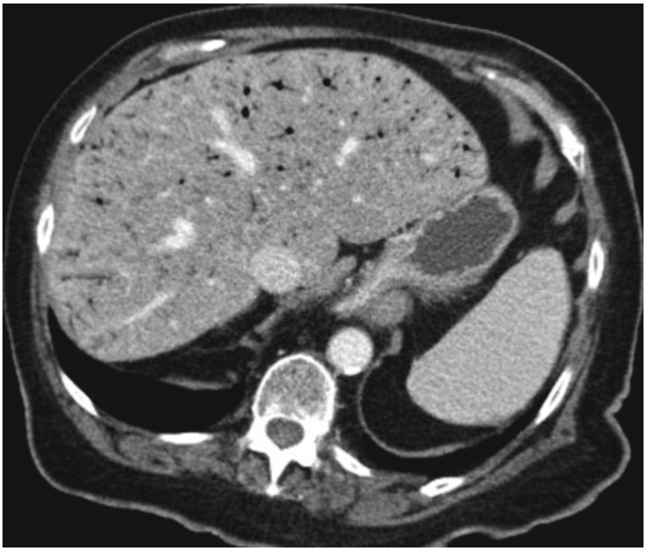

FIGURE 34.6 - PORTAL VENOUS GAS DUE TO BOWEL NECROSIS IN THIS PATIENT

Portal venous gas is distinguished from pneumobilia (air in the biliary tree) by location. As in this case portal venous gas is located in the periphery, whereas pneumobilia would be located in the center of the liver

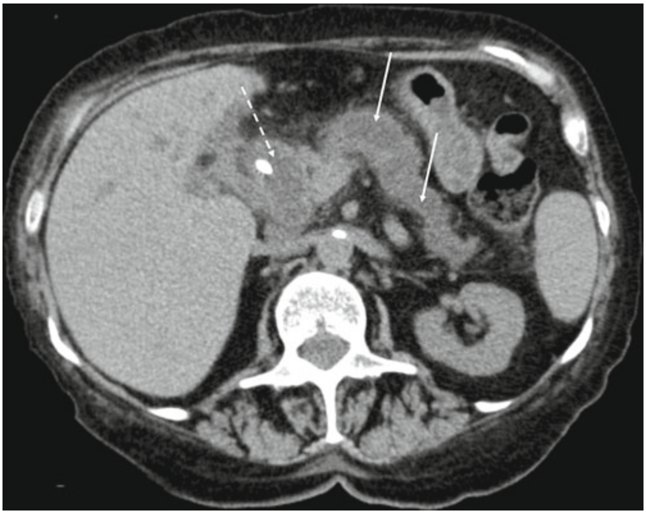

FIGURE 34.7 - THE DOUBLE DUCT SIGN CAUSED BY A PANCREATIC HEAD MASS

The *dashed arrows* denote the dilated common bile duct. The *solid arrows* point out the dilated pancreatic duct dilation of both the common bile duct and the main pancreatic duct caused by tumor in the pancreatic head compressing the distal ends of both of ducts. When evaluating a pancreatic mass, the surgeon needs to know whether the tumor is resectable. Radiographic signs of unresectable tumor include vascular involvement (celiac artery, SMA, and portal vein) and extension beyond the pancreas into other organs.

Colitis

Colitis is defined radiographically as colonic wall thickening of 3 mm or more when the bowel is distended. Often the bowel wall in colitis will enhance after intravenous contrast administration. There are three chief etiologies in the differential diagnosis of colitis: infection, inflammation, and ischemia. The bowel can be thickened by edema fluid, blood, and/or cells.

Numerous types of infection cause colitis. Two of the most severe forms are pseudomembranous colitis and typhilits. Pseudomembranous colitis is often a pancolitis. The toxin of the Clostridium difficile bacteria causes colonic mucosal ulceration which leads to the formation of pseudomembranes composed of mucin, fibrin, and inflammatory cells. Typhilitis is a neutropenic colitis that is classically seen in leukemic patients. It involves the cecum and/or ascending colon. Both of these forms of colitis are very severe and cause marked wall thickening, pericolonic inflammation, and can lead to colonic perforation (Fig. 34.8).

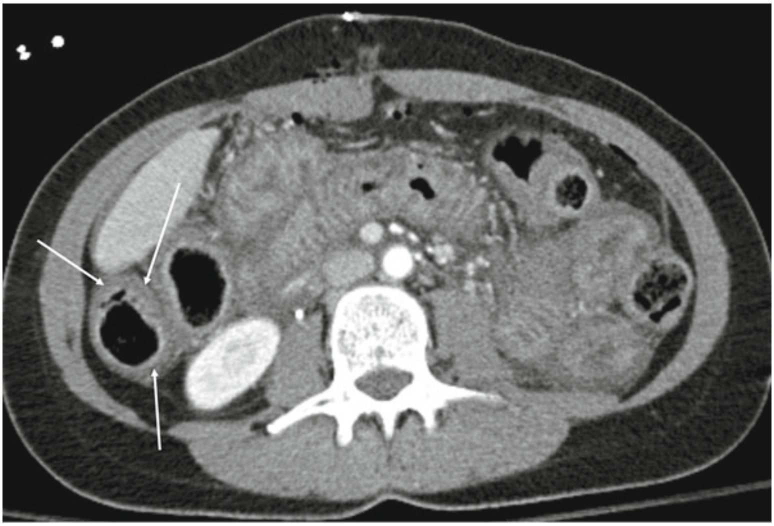

FIGURE 34.8 - CT EVIDENCE OF COLITIS
Wall thickening (***arrows***) of the ascending colon related to a nonspecific colitis

There are two common types of inflammatory colitis: ulcerative colitis and Crohn's disease. These etiologies were discussed in prior chapters. Remember that ulcerative colitis starts in the rectum and spreads retrograde in a contiguous manner and only involves the colon. Crohn's disease causes greater colonic wall thickening than UC. It is classically found in the terminal ileum, but can be found anywhere along the GI track and is famous for skip lesions.

Ischemia causes a segmental colitis. Segmental refers to the fact that only portions of the colon is affected. Ischemic colitis tends to occur at the watershed areas of vascular distribution: the splenic flexure and rectosigmoid regions.

35

INCIDENTAL LESIONS

Objective:

1. Learn to recognize several lesions found incidentally on CT scans and understand a management algorithm.

Introduction

The advent of high quality cross-sectional imaging has revolutionized medical and surgical diagnosis and treatment. However, it has also lead to the discovery of numerous incidental findings that may require evaluation to determine whether they may be safely dismissed or if further workup is required.

This chapter discusses several of the most common incidental findings and offers evidence-based management recommendations based upon the recent *Journal of the American College of Radiology* article on this subject.[1] The guidelines listed below assume a relatively healthy population with reasonable life expectancy. In patients with multiple or severe comorbidities or with limited life expectancy, these guidelines may not be appropriate and decisions should be tailored on an individual basis.

Incidental Cystic Renal Lesion

Renal cysts are some of the most commonly encountered incidental findings. The Bosniak criteria is a well-studied evidence-based approach to the management of renal cysts.[2] The Bosniak criteria describe five (I, II, IIF, III, IV) categories of renal cystic lesions based upon distinct imaging characteristics. The concept is the more

---

H Singh and JA Neutze (eds.), *Radiology Fundamentals: Introduction to Imaging & Technology*, DOI 10.1007/978-1-4614-0944-1_35,
© Springer Science+Business Media, LLC 2012

purely cystic a lesion, the more likely it is benign. The more calcification, solid components, enhancement or thickened walls a lesion has, the more likely it is to be malignant.

Categories I and II do not require follow-up and include simple cysts, cysts with fine calcifications and/or thin internal septa, and nonenhancing hyperdense cysts. Category IIF (F stands for “follow-up”) has indeterminate features and should be followed up at 6 and 12 months and then yearly for 5 years to assure stability. Categories III and IV should be referred for surgical consideration at the time of diagnosis (Fig. 35.1a, b).

Remember, size is not a determinant in renal cystic lesions.

Incidental Solid Renal Lesion

In contradistinction to cystic renal lesions, size is the primary determining factor with incidental solid renal lesions. Also, it is important to thoroughly search for fat within a solid renal lesion. If fat is identified in the lesion, then the lesion can be diagnosed as an angiomyolipoma, a benign lesion composed of vascular, muscular, and fatty elements.

Solid renal lesions that are greater than 1 cm in size and lacking fatty elements are likely malignant and should be referred to surgery at the time of diagnosis. The larger the lesion, the more likely it is malignant (Fig. 35.2). Moreover, smaller lesions that are renal cell carcinomas tend to be more indolent, lower-grade tumors. Solid renal lesions less than 1 cm in size may be observed for interval change in size at 3, 6, and 12 months, then yearly. The duration of follow-up is not well established.

Historically, biopsy of a renal lesion prior to surgical resection has not been recommended. If the imaging findings are worrisome, the sensitivity and specificity are not high enough to definitively exclude a malignant process despite a negative biopsy. Though there is discussion in the literature regarding renal biopsy, there are no current recommendations regarding biopsy of solid or cystic renal lesions.

Incidental Hepatic Lesion

Incidental hepatic lesions are very common. In fact, nearly half of patients without malignancy have benign hepatic lesions at autopsy. Any hepatic lesion in an oncology patient is extremely concerning for tumor. The recommended approach for evaluating incidental hepatic lesions involves assessing lesion size and patient risk. Despite a complex algorithm based upon these factors and imaging characteristics, the crux of the approach is that any size lesion in a high-risk patient needs further evaluation with advanced imaging (CT or MRI) and potential biopsy. The majority

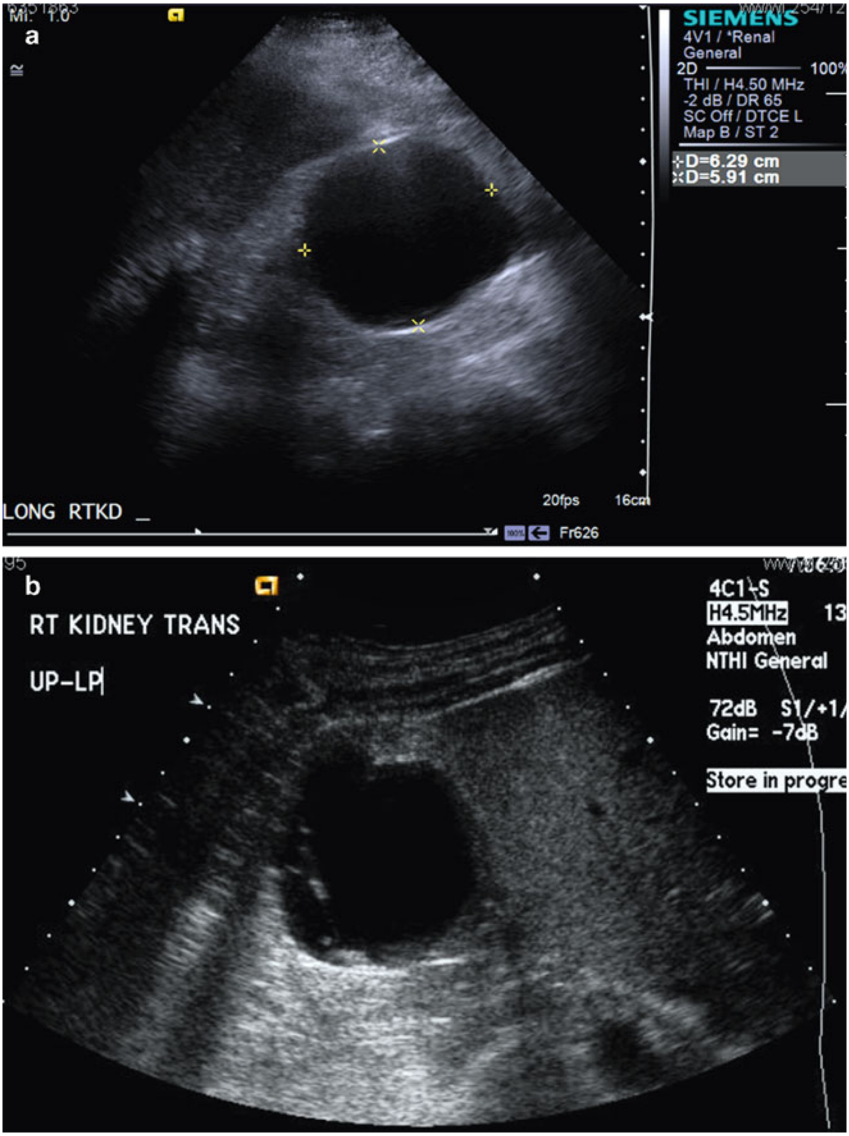
a
SIEMENS
4V1 / *Renal
General
2D 100%
THI / H4.50 MHz
-2 dB / DR 65
SC Off / DTCE L
Map B / ST 2
D=6.29 cm
D=5.91 cm
LONG RTKD
20fps
16cm
Fr626
b
RT KIDNEY TRANS
UP–LP
4C1-S
H4.5MHz
Abdomen
NTHI General
72dB
Gain= -7dB
Store in progre

FIGURE 35.1 - RENAL CYSTS ON ULTRASOUND
(**a**) Ultrasound image of a simple renal cyst Features include, well-circumscribed lesion, anechoic (*black*), well-defined wall and posterior acoustic enhancement (*whiter* behind the cyst). (**b**) Ultrasound image of a more complicated renal cyst. In comparison to image (**a**), this cyst has a nodular septation with portions of soft tissue nodularity along the wall

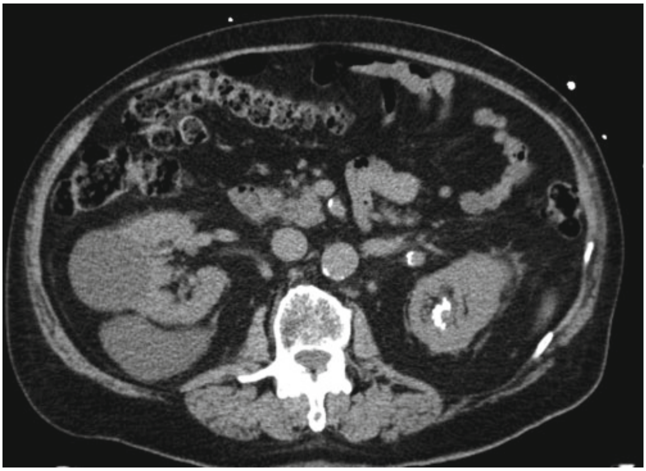

FIGURE 35.2 - LARGE SOLID RENAL LESION ARISING IN THE RIGHT KIDNEY
Given the solid appearance and the size of the lesion, it needs to be removed surgically given the probability of renal cell carcinoma

of benign lesions are hepatic cysts, hamartomas (which show no evidence for enhancement), or hemangiomas (which have a characteristic enhancement pattern). High-risk patients are those with known malignancy or cirrhosis or patients with risk factors predisposing to the development of cirrhosis (hepatitis, sclerosing cholangitis, etc.) (Fig. 35.3). In all other patients, the decision to dismiss or follow-up is based upon size and specific imaging characteristics.

Incidental Adrenal Lesion

It is estimated that 3–7% of the population has an incidental adrenal lesion. Studies indicate that the overwhelming majority are benign nonfunctioning adenomas. Therefore, it is important to definitively characterize these lesions on imaging studies.

The assessment of incidental adrenal lesions is primarily based upon imaging features. If an incidental adrenal lesion has Hounsfield units (HU) of less than 10 on a noncontrast CT exam, it can be definitively diagnosed as a benign adrenal adenoma (presumed lipid rich adenoma) (Fig. 35.4). For lesions 1–4 cm in size that are greater than 10 HU, it recommended that the patient be rescanned using a specific CT adrenal protocol. This protocol scans the patient at different time points after intravenous contrast administration to calculate a value termed "adrenal washout."

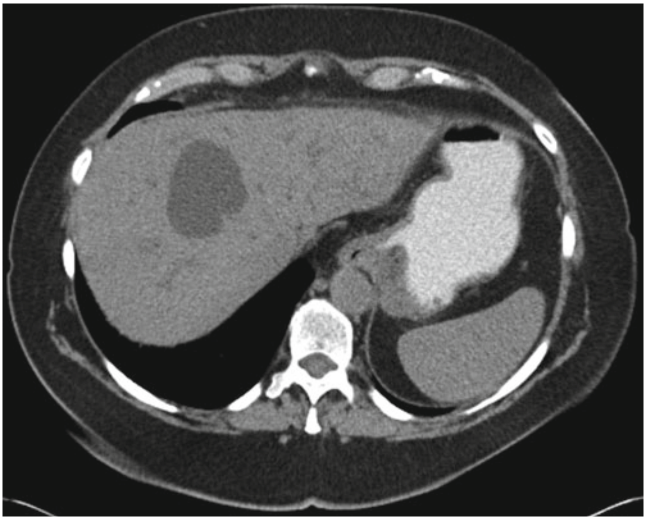

FIGURE 35.3 - LARGE HYPODENSITY IN THE CENTER OF THE LIVER
In a patient with a known malignancy this would be concerning for metastasis. However, without that history, it most likely represents a large hepatic cyst

The concept is that a benign adrenal adenoma will enhance and then quickly washout the contrast, whereas an adrenal metastasis (and presumably adrenal carcinoma) will enhance and retain the contrast (showing delayed washout). Biopsy should be recommended for a lesion with delayed washout. Lesion size and patient history of malignancy are also important factors. Lesions larger than 4 cm have a higher risk for malignant tumor; generally they are recommended for biopsy. Of note, functioning adrenal cortical tumors and pheochromocytomas are almost always associated with symptoms and elevated biochemical markers in blood or urine.

Incidental Pancreatic Lesion

Incidental pancreatic cysts in patients without clinical or laboratory findings of pancreatic disease are relatively common findings. Cystic pancreatic neoplasms are generally benign or low-grade malignancies (Fig. 35.5). There are three main categories of cystic pancreatic neoplasms: mucinous neoplasm, serous neoplasm, and intraductal papillary mucinous neoplasm (IPMN). Serous tumors are benign but can enlarge. Mucinous tumors and IPMNs have malignant potential.

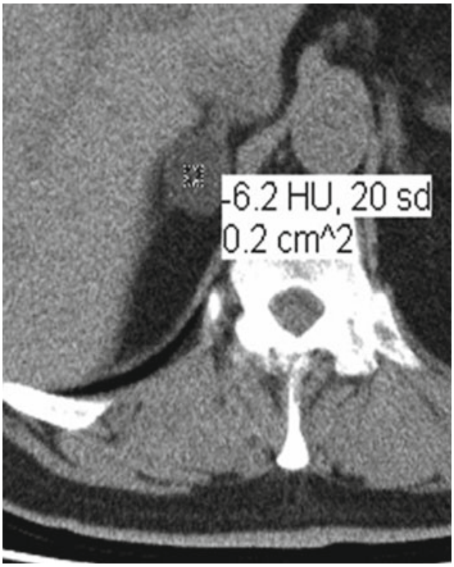

FIGURE 35.4 - LIPID RICH ADENOMA ON CT
Note the round lesion arising from the right adrenal gland. The Hounsfield units measured −6.2 which is diagnostic of a benign lipid-rich adrenal adenoma

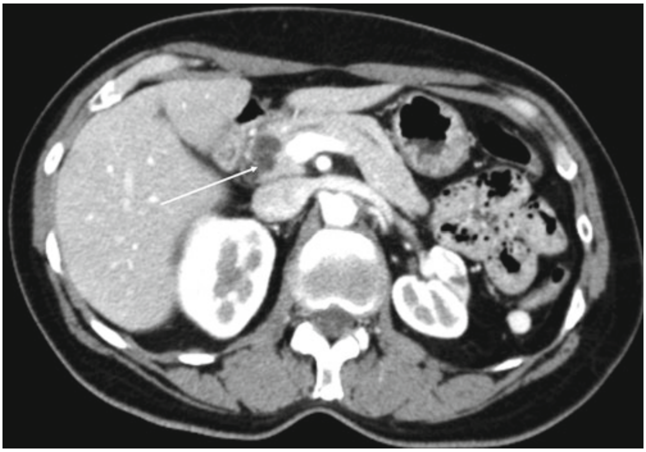

FIGURE 35.5 - PANCREATIC CYSTIC LESION
Axial CT image at the level of the pancreas showing a multicystic lesion of the pancreatic head

Size is the predominant variable used in the evaluation of incidental pancreatic lesions. Those less than 2 cm should be followed up with CT or MRI in 1 year. If the lesion is unchanged in size and appearance, no further follow-up is needed. If the lesion grows or changes on follow-up or if the initial lesion is 2–3 cm in size, MRI with MRCP (MR cholangiopancreatography) is generally recommended. If a serious lesion is diagnosed, then it should be followed every 2 years. If an IPMN is diagnosed, follow-up is recommended every 6 months for at least 2 years. If the lesion is not fully characterized, then annual follow-up is recommended. If the initial lesion is greater than 3 cm and serous neoplasm cannot be definitively diagnosed, then cyst aspiration using endoscopic ultrasound guidance should be attempted.

References

1. Berland L, Silverman S, Gore R, et al. Managing Incidental Findings on Abdominal CT: White paper of the ACR Incidental Findings Committee. JACR. 2010 Oct:7(10): 754–773.
2. Webb R, Brant W and Major N. Fundamentals of Body CT. 3rd Edition. Philadelphia: Elsevier Inc, 2006. 285–289.

36

RADIONUCLEOTIDE EVALUATION OF GI BLEEDING

Objectives:

1. To understand how red blood cells are labeled with the radionuclide Tc-99m.
2. To understand the appropriate use of Tc-99m RBC imaging in patients with gastrointestinal bleeding.

The radiopharmaceutical used in nuclear medicine to detect gastrointestinal bleeding is Technetium 99m-labeled autologous red blood cells (Tc-99m RBC). Labeling of red blood cells is possible because the radionuclide technetium 99m pertechnetate (TcO_4^-) freely crosses the red blood cell membrane via anion exchange. However, once TcO_4^- is reduced, it can no longer pass through the red blood cell membrane. Therefore, it follows that if TcO_4^- is allowed to cross the RBC membrane and subsequently reduced within the cell, Tc-99m will be trapped within the RBC. This is precisely how RBCs are labeled for a nuclear medicine GI bleeding study. The agent used to reduce TcO_4^- is tin (Sn^{+2}). The protocol involves pretreating red blood cells with tin followed by exposure to TcO_4^-. The intracellular tin reduces the TcO_4^- trapping it within the cell. The reduced technetium 99m binds to the beta chain of hemoglobin (see Fig. 36.1).

A GI bleeding scan image represents the distribution of red blood cells within a patient. Figure 36.2 demonstrates a normal Tc-99m-labeled red blood cell study. Note the intense activity at the uppermost border of the image, representing blood within the chambers of the heart. The aorta, IVC, iliac vessels, liver, and spleen are also easily identified, given the high concentration of RBCs within these structures. In vitro labeling of RBCs is 95% efficient. However, some labeling of small polypeptides occurs and these are filtered and excreted by the kidneys. Therefore, visualization of the bladder is normal and expected, and does not indicate blood in the urine.

H Singh and JA Neutze (eds.), *Radiology Fundamentals: Introduction to Imaging & Technology*, DOI 10.1007/978-1-4614-0944-1_36,
© Springer Science+Business Media, LLC 2012

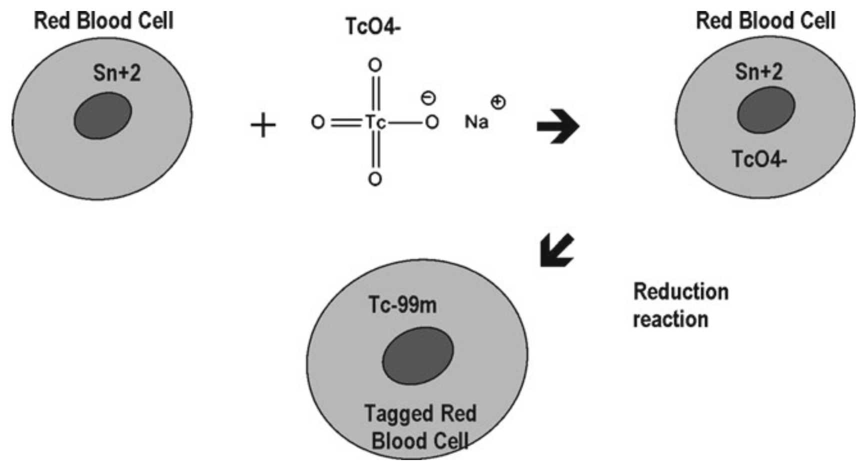
Red Blood Cell
Sn+2
TcO4-
O
O
Tc
O
O
Na
Red Blood Cell
Sn+2
TcO4-
Reduction reaction
Tc-99m
Tagged Red Blood Cell

FIGURE 36.1 - TC-99M RBC TAGGING
When technetium pertechnetate (TcO_4^-) is mixed with a RBC containing intracellular tin (Sn^{+2}), the TcO_4^- crosses the RBC membrane via anion exchange. TcO_4^- is reduced by Sn^{+2}, and subsequently trapped within the RBC bound to the beta chain of hemoglobin

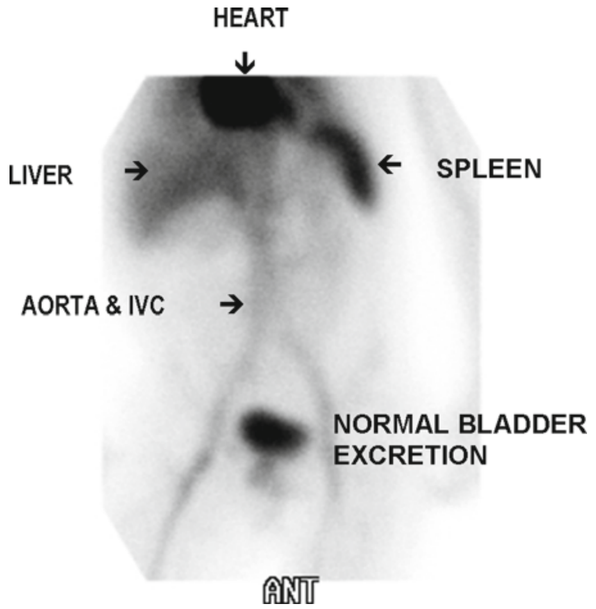
HEART
LIVER
SPLEEN
AORTA & IVC
NORMAL BLADDER EXCRETION
ANT

FIGURE 36.2 - NORMAL GI BLEEDING SCAN
Tc-99m RBCs are visualized within the heart, liver, spleen, aorta, IVC, iliac, femoral vessels, and bladder. Note that there is no activity seen in the distribution of the large or small intestine

Although a nuclear medicine GI bleeding study can diagnose upper GI bleeding, it is not indicated in the initial workup of acute upper GI bleeding. If gastric intubation and/or endoscopy are negative, a Tc-99m RBC study is indicated.

Nuclear medicine GI bleeding studies are indicated in the initial workup of acute lower GI bleeding. Lower GI bleeding is classically intermittent and difficult to evaluate clinically. Colonoscopy is of limited value. Angiography can be used to both diagnose and treat a lower GI bleed. However, to detect bleeding during angiography, the patient must be actively bleeding at approximately 1 ml/min during the few seconds it takes for the iodinated contrast to pass through the arteries. A tagged RBC study does not have this limitation, given the ability to image the patient continuously for 1–2 h intervals, over 24 h, if needed. Continuous imaging increases the likelihood of detecting an intermittent active bleed, and allows for localization of the site of bleeding (small bowel, ascending colon, transverse colon, descending colon, or rectum). The rate of bleeding is much less important in a Tc-99m RBC study. Regardless of the bleeding rate, 2–3 ml of pooled, extravasated blood is necessary for detection by a gamma camera. Typically, the strengths of nuclear medicine and angiography are used in a complementary fashion. If a nuclear medicine study is positive for active bleeding, the patient can immediately undergo angiography, if indicated, based on the site of bleeding. This sequence of studies increases the probability of locating active bleeding during angiography, and subsequent definitive treatment.

Occasionally, the origin of a GI bleed is more proximal than predicted by the clinical presentation and initial workup. Figure 36.3 shows a positive GI bleeding

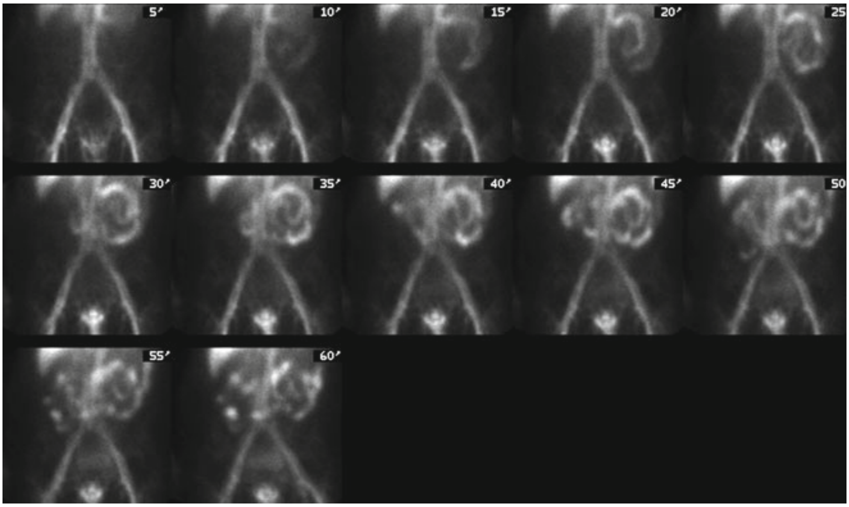

FIGURE 36.3 - POSITIVE GI BLEEDING STUDY
The 5-min image is normal. On the 10-min image, a focus of extravasation is seen in the left upper quadrant. The extravasated Tc-99m-labeled blood progresses through multiple loop of bowel from the left upper quadrant to the right lower quadrant indicating a proximal small bowel bleeding site

study. The study is positive for a proximal small bowel bleed. Initial workup with gastric lavage was negative, and the patient presented to nuclear medicine for diagnosis and localization with a Tc-99m RBC study. Given the unexpected finding of a proximal small bowel bleeding source, endoscopy was performed rather than angiography. Endoscopy subsequently revealed a bleeding duodenal ulcer.

37

RADIONUCLEOTIDE BONE IMAGING

Objectives:

1. Describe the physiologic rationale for tracer uptake on a bone scan.
2. Describe the sensitivity and specificity of the bone scan for detection of metastatic disease.
3. List three common causes of locally increased radiotracer uptake.

When technetium 99m is bound to methylene diphosphonate, the resulting compound is called technetium 99m-MDP. Administered intravenously, as much as 60% of this substance will be taken up by the skeleton through a process called chemabsorption by which the tracer is actually incorporated into the calcium hydroxyapatite crystal matrix of bone or other calcium depositions. The remainder of the tracer is excreted via the urinary tract. Gallium, another radioactive material, is not used as a primary agent for bone scans now that MDP bone scanning is available (Fig. 37.1).

Radiotracer Uptake

Actively growing bone, actively metabolizing or repairing bone, or areas of increased circulation have a particular affinity for tracer. This affinity, termed increased uptake or "hot spots," can be found in many disease processes including infection, neoplasm, metabolic disease, Paget's disease, and trauma.

If one sees an area of increased uptake, one cannot be sure of the etiology from the bone scan alone. Hence, bone scanning is quite nonspecific. It is much more sensitive, however, than conventional radiographs and thus may be very useful for detecting early metastatic disease, osteomyelitis and occult fractures. Osteoid

---

H Singh and JA Neutze (eds.), *Radiology Fundamentals: Introduction to Imaging & Technology*, DOI 10.1007/978-1-4614-0944-1_37,
© Springer Science+Business Media, LLC 2012

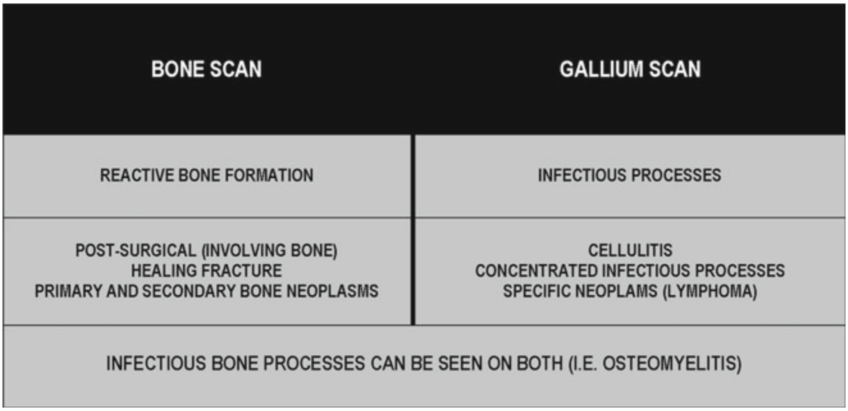

BONE SCAN	GALLIUM SCAN
REACTIVE BONE FORMATION	INFECTIOUS PROCESSES
POST-SURGICAL (INVOLVING BONE) HEALING FRACTURE PRIMARY AND SECONDARY BONE NEOPLASMS	CELLULITIS CONCENTRATED INFECTIOUS PROCESSES SPECIFIC NEOPLAMS (LYMPHOMA)
INFECTIOUS BONE PROCESSES CAN BE SEEN ON BOTH (I.E. OSTEOMYELITIS)	

FIGURE 37.1 - INDICATIONS FOR BONE SCAN AND GALLIUM SCAN

osteoma, a benign bone neoplasm which is often quite small and difficult to see especially in the spine, may be detected much more readily with bone scanning. It should be noted that when a lytic lesion such as a bone tumor or osteomyelitis shows increased uptake on a bone scan, it is reactive bone formation, specifically the osteoblasts around the lesion, which cause increased tracer activity in the area.

Figure 37.2 demonstrates a normal bone scan in a young adult. Note the characteristic areas of increased uptake in the knees, sacroiliac joints and hip joints. These are areas of active bone growth and increased blood supply. The symmetry is useful in excluding pathology in these situations.

The spine is seen best in the posterior view and the sternum best in the anterior view. This is because the bones are closer to the imaging detector in this situation and a greater percentage of photons emitted from the bones are effectively gathered by the detector. Remember, radionuclide imaging differs from conventional radiographs in that the source of radiation which creates the image is within the patient.

Figure 37.3 shows the classic appearance of metastatic disease. Markedly increased radiotracer activity is noted in the T10 vertebral body, extending to involve the posterior elements. Also, there is a large round lesion of moderately increased radiotracer uptake involving the left posterior parietal/occipital region. Finally, markedly increased radiotracer activity is noted in the posterior medial aspect of the left iliac bone. In combination, these findings are most consistent with metastatic disease.

The equilibrium concept of lytic and blastic bone lesions (Fig. 37.4) shows why both lesions show increased uptake on the bone scan since obsteoblastic activity is present in both processes.

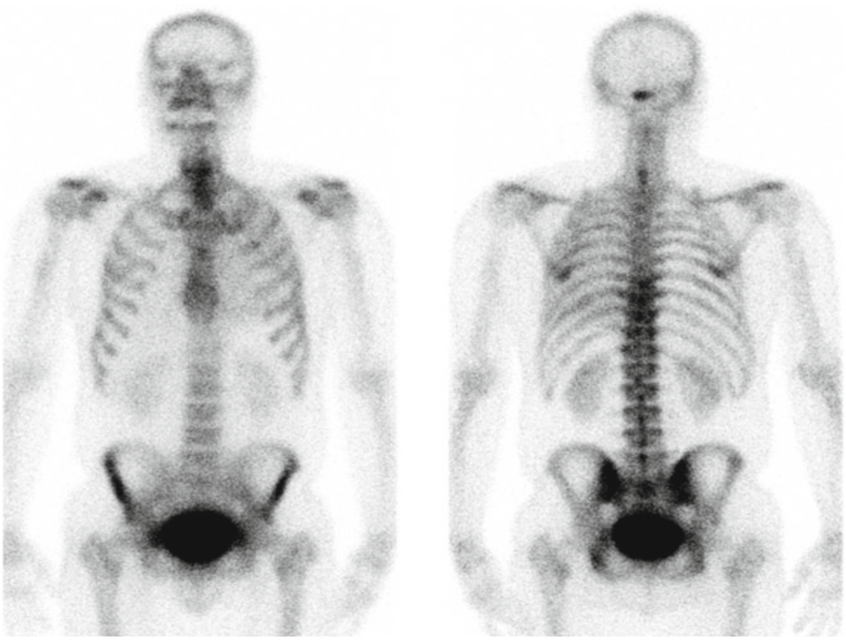

FIGURE 37.2 - NORMAL BONE SCAN
Example of a normal bone scan showing normal physiologic uptake

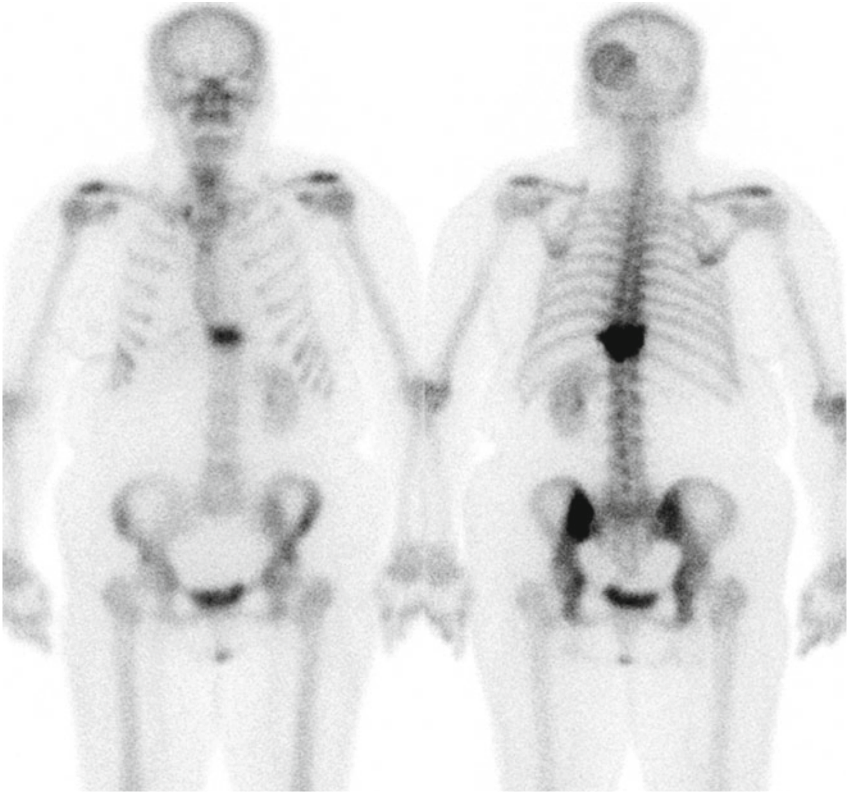

FIGURE 37.3 - ABNORMAL BONE SCAN
Three foci of abnormal radiotracer uptake involving the T10 vertebral body, left ilium, and left parietal/occipital region of the skull. In combination, these findings are most consistent with metastatic disease

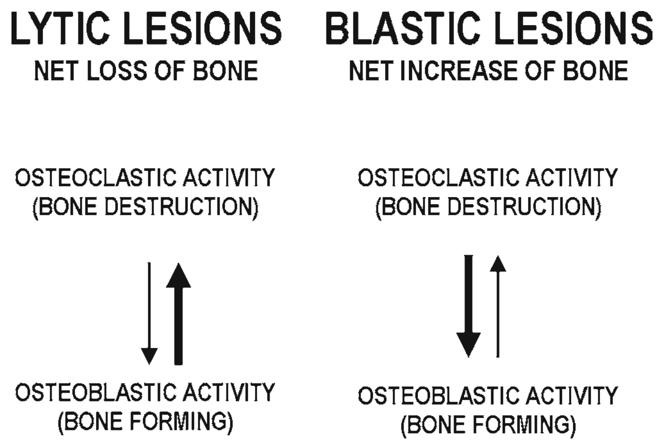
LYTIC LESIONS
NET LOSS OF BONE
OSTEOCLASTIC ACTIVITY
(BONE DESTRUCTION)
OSTEOBLASTIC ACTIVITY
(BONE FORMING)
BLASTIC LESIONS
NET INCREASE OF BONE
OSTEOCLASTIC ACTIVITY
(BONE DESTRUCTION)
OSTEOBLASTIC ACTIVITY
(BONE FORMING)

FIGURE 37.4 - LYTIC VS. BLASTIC LESIONS
Although osteoclasts and osteoblasts are both involved, the type of bone lesion determines which one is dominant

38

LUNG VENTILATION AND PERFUSION IMAGING

Objectives:

1. Name the agents used in lung perfusion and ventilation scans and the physiologic rationale for this examination.
2. Describe the probability of pulmonary embolism for each of the following V/Q scan reports: High, Moderate, Indeterminate, and Low Probability.

Ventilation and perfusion scans are used for detecting pulmonary oxygenation abnormalities.

To perform a ventilation scan, the patient inspires radioactive Xenon gas and images are obtained. Those portions of the lung which are ventilated will be imaged by the tracer. The tracer levels will gradually decrease during the washout phase of the study as the patient breathes pure oxygen.

To obtain a lung perfusion scan, technetium 99m is first bound to microaggregated albumin (MAA). The particle size of MAA can be adjusted, in this case, to a particle size of 10–40 μm. The average diameter of a human capillary is 7 μm, so these particles will not pass through the capillary bed of the lung, but remain trapped there, in essence forming many small "emboli." Only 1 in 1,000 capillaries are occluded during this study, which is usually quite safe. An exception is in patients who have pulmonary arterial hypertension, in which the relative number of functioning arterioles is markedly reduced. Pulmonary artery hypertension is a relative contraindication to radionuclide perfusion imaging.

Figure 38.1 represents a normal ventilation/perfusion study of the lung. If no perfusion defect is identified on a six position scan, the ventilation scan is not needed. An area of decreased ventilation (due to pneumonia, atelectasis, etc.) will also have reduced perfusion so as to minimize intrapulmonary shunting.

It is important that when we see an area of decreased perfusion to make sure that there isn't decreased ventilation to the same area before we ascribe to it the

---

H Singh and JA Neutze (eds.), *Radiology Fundamentals: Introduction to Imaging & Technology*, DOI 10.1007/978-1-4614-0944-1_38,
© Springer Science+Business Media, LLC 2012

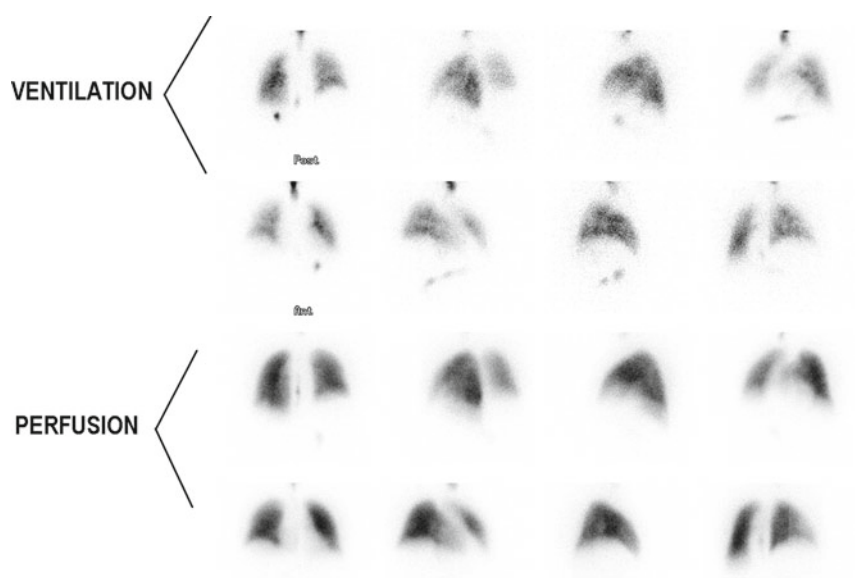

FIGURE 38.1 - NORMAL V/Q SCAN
This study is suggestive of a very low (0–5%) probability for pulmonary embolus

diagnosis of pulmonary embolism. For this reason, ventilation/perfusion scans are usually read in conjunction with a recent chest radiograph which may be useful in delineating areas of pulmonary disease such as pneumonia or pleural effusion which could affect the study.

Figure 38.2 shows an abnormal lung perfusion scan. Findings are interpreted using PIOPED criteria (Fig. 38.3).

Interpreting Lung Ventilation–Perfusion Study Results

Spiral CT is now supplanting V/Q scanning to diagnose pulmonary embolism. CT scan is usually available around the clock and can be performed shortly after being ordered. V/Q scanning may take several hours to be performed if ordered after regular clinic hours, as a technician often needs to be called in from home and radiopharmaceuticals newly prepared and administered. Contraindications to CT scan include contrast allergy and renal insufficiency.

Pulmonary angiography still remains the gold standard for the diagnosis of pulmonary embolism and may be necessary if the diagnosis is still in doubt after a V/Q or CT scan is performed.

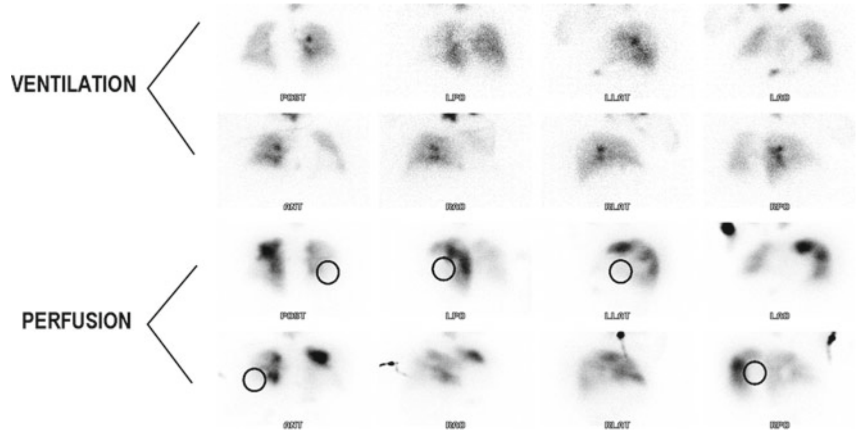
VENTILATION
POST
LPO
LLAT
LAO
ANT
RAO
RLAT
RPO
PERFUSION
POST
LPO
LLAT
LAO
ANT
RAO
RLAT
RPO

FIGURE 38.2 - V/Q SCAN SUGGESTIVE OF HIGH PROBABILITY FOR PULMONARY EMBOLUS
There are multiple mismatched segmental perfusion defects (*circles*) in both lungs making the study high probability for pulmonary embolism

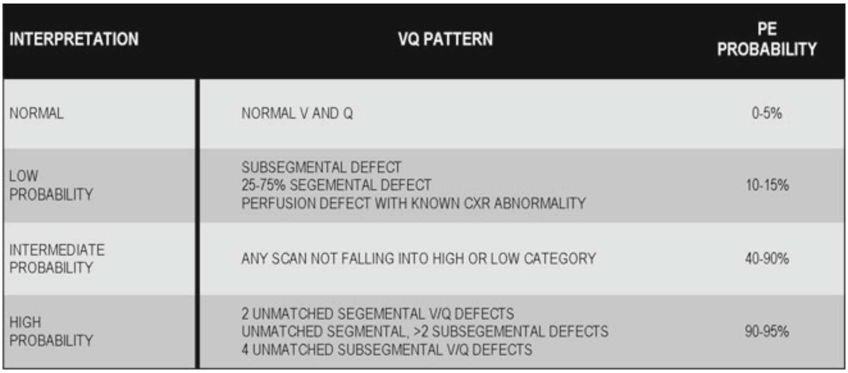

INTERPRETATION	VQ PATTERN	PE PROBABILITY
NORMAL	NORMAL V AND Q	0-5%
LOW PROBABILITY	SUBSEGMENTAL DEFECT 25-75% SEGEMENTAL DEFECT PERFUSION DEFECT WITH KNOWN CXR ABNORMALITY	10-15%
INTERMEDIATE PROBABILITY	ANY SCAN NOT FALLING INTO HIGH OR LOW CATEGORY	40-90%
HIGH PROBABILITY	2 UNMATCHED SEGEMENTAL V/Q DEFECTS UNMATCHED SEGMENTAL, >2 SUBSEGEMENTAL DEFECTS 4 UNMATCHED SUBSEGMENTAL V/Q DEFECTS	90-95%

FIGURE 38.3 - INTERPRETATION OF V/Q SCAN RESULTS

39

RADIONUCLEOTIDE CARDIAC IMAGING

Objectives:

1. Describe how radionuclide imaging can be used to calculate the left ventricular ejection fraction and to evaluate left ventricular wall motion.
2. Describe the physiologic rationale for thallium stress imaging of the myocardium.

Radionucleotide imaging is an important part of the diagnostic arsenal used in evaluation of the heart. This is because, in addition to displaying anatomic features, radionucleotide images are also a graphic representation of normal and abnormal myocardial physiology. In this unit, we will consider two important uses of radionucleotide imaging with regard to the heart.

The first topic we will discuss is the utilization of radionucleotides for calculation of the left ventricular ejection fraction. Focus your attention on Fig. 39.1. You will notice a graphic plot representing the volume of radioactively labeled blood (radioactive "counts") detected within a region of interest representing the left ventricle (*y*-axis) vs. time (*x*-axis). Using a computer, an area of interest corresponding to the anatomic boundaries of the left ventricular cavity is established.

Using red blood cells that are labeled with radioactive tracer, the volume (represented by the number of radioactive "counts") within the left ventricle at any time can be determined. As demonstrated by the graph, the maximum number of counts (red blood cells) in the left ventricular cavity is present at end diastole. The minimum number of counts is present at end systole. The ratio of the difference between the end diastolic and end systolic number of counts to the number of counts at end diastole is then used to calculate the ejection fraction. In general, any value greater than 50% is considered within normal limits. The accuracy of this test has been shown to be reliable with respect to ejection fractions calculated from a more invasive ejection fraction test that can be performed during cardiac catheterization.

H Singh and JA Neutze (eds.), *Radiology Fundamentals: Introduction to Imaging & Technology*, DOI 10.1007/978-1-4614-0944-1_39,

© Springer Science+Business Media, LLC 2012

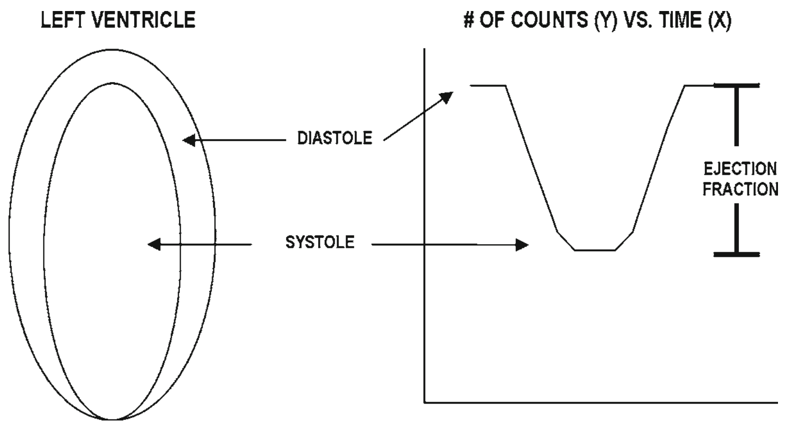

FIGURE 39.1 - LEFT VENTRICULAR EJECTION FRACTION
The image on the (*left*) depicts the left ventricular wall kinetics during systole and diastole. The image on the (*right*) represents the number of radioactivite "counts" and stroke volume between systole and diastole

Therefore, the radionucleotide ejection fraction calculation may be used to follow the contractility of the myocardium over a period of time in patients in whom changes might be expected. Examples are patients with degenerative muscle diseases and patients receiving chemotherapy which might be toxic to the heart such as adriamycin.

Radionucleotide imaging may also be employed to localize sites of myocardial ischemia and/or infarction. The radionucleotide most commonly used for this purpose is thallium. Thallium is a radioactive potassium analog that is distributed to myocardial cells, assuming that they are adequately perfused. The rationale for thallium imaging of the myocardium is that, under stress, poorly perfused (i.e., ischemic) myocardial cells will receive less thallium and therefore show less uptake of the radioactive tracer. Of note, imaging of obese patients is better accomplished using the radionucleotide Technetium-99 labeled to either sestamibi or Myoview™ which are physiologically similar to thallium in that they are taken up by viable myocardial cells. The images produced for interpretation are very similar when using thallium or technetium-99.

The patient exercises on a treadmill until he/she develops symptoms or to maximal exercise tolerance, if no ischemic symptoms are displayed. Then, thallium is injected intravenously. Ischemic areas in the left ventricle will be displayed as areas of decreased intensity (lower number of radioactive counts detected) on the image. The patient is then allowed to rest, and the left ventricle is reimaged. Areas that are ischemic under maximal stress will now perfuse and may show uptake similar to the remainder of the myocardium (redistribution). If frank infarction has occurred, no change in the region of diminished thallium uptake will occur and the area will have less intense radioactivity. This is because this region will be composed of fibrosis rather than viable myocardium. Fibrotic cells do not have the same affinity for thallium as the normal myocardium (Fig. 39.2).

It is important to note that the evaluation of radionuclide images is highly computerized and that although these visual displays demonstrate changes which may occur, computer analysis of the data with respect to the number of counts per unit area is much more sensitive and forms the main basis for evaluation of the data.

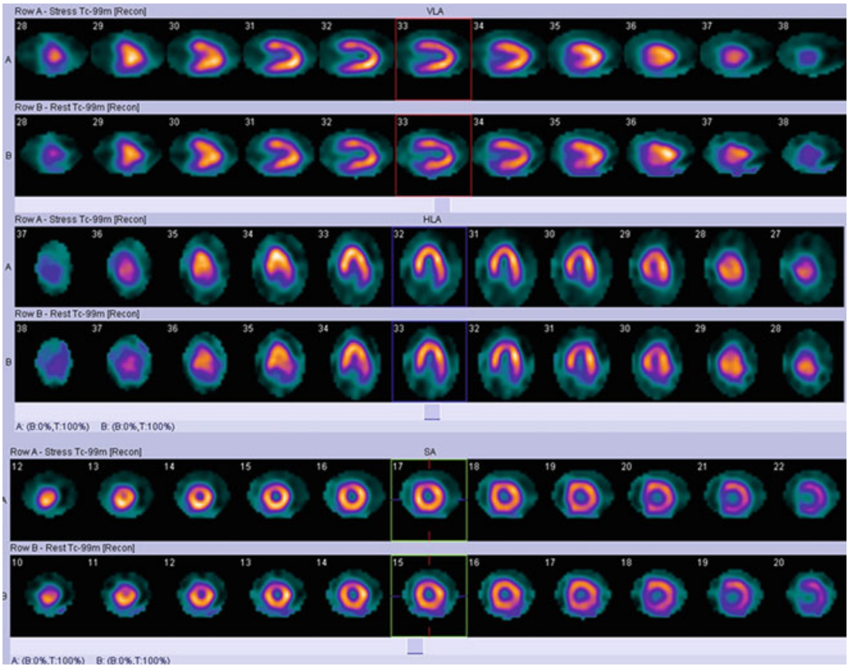
Row A - Stress Tc-99m [Recon]
VLA
28 29 30 31 32 33 34 35 36 37 38
A
Row B - Rest Tc-99m [Recon]
28 29 30 31 32 33 34 35 36 37 38
B
Row A - Stress Tc-99m [Recon]
HLA
37 36 35 34 33 32 31 30 29 28 27
A
Row B - Rest Tc-99m [Recon]
38 37 36 35 34 33 32 31 30 29 28
B
A: (B:0%,T:100%) B: (B:0%,T:100%)
Row A - Stress Tc-99m [Recon]
SA
12 13 14 15 16 17 18 19 20 21 22
Row B - Rest Tc-99m [Recon]
10 11 12 13 14 15 16 17 18 19 20
A: (B:0%,T:100%) B: (B:0%,T:100%)

FIGURE 39.2 - THALLIUM-LABELED MYOCARDIAL PERFUSION STUDY
Stress and rest images represent an example of a normal nuclear medicine stress test

40

F-18 FDG POSITRON EMISSION TOMOGRAPHY

Objectives:
1. To understand the chemistry and physiology of the F-18 FDG molecule.
2. Describe the patient preparation required for this type of imaging study.
3. State the use of PET in oncology.
4. State several PET pitfalls.

Overview

The radiopharmaceutical used in positron emission tomography is Fluorine-18 fluorodeoxyglucose (F-18 FDG).

F-18 decays by positron emission (Fig. 40.1). A positron is emitted from the F-18 nucleus and undergoes an annihilation reaction with an electron. This results in two 511 keV photons traveling in opposite directions. These photons strike the PET scanner's ring of detectors 180° apart, and an image is created. The PET scanner detectors can identify and localize millions of annihilation events per second. The 511 keV photons have too much energy for the sodium iodide crystal of a standard nuclear medicine gamma camera. Therefore, imaging with F-18 FDG requires a separate dedicated PET machine. Virtually all F-18 FDG PET studies are performed on hybrid PET/CT machines, which combine the anatomic and diagnostic data of CT with the metabolic data of FDG PET (Fig. 40.2).

Glycolysis is derived from the Greek words "glykys" (sweet) and "lysis" (splitting). Glycolysis is the sequence of reactions that convert glucose into pyruvate with the concomitant production of ATP (the universal currency of free energy in biologic systems). ATP is the cell's energy source for synthesis and cell division. Fluorodeoxyglucose (FDG) is a glucose analog. FDG crosses the cell membrane via the glucose transporter, and enters the glycolytic pathway. However, after undergoing

H Singh and JA Neutze (eds.), *Radiology Fundamentals: Introduction to Imaging & Technology*, DOI 10.1007/978-1-4614-0944-1_40,
© Springer Science+Business Media, LLC 2012

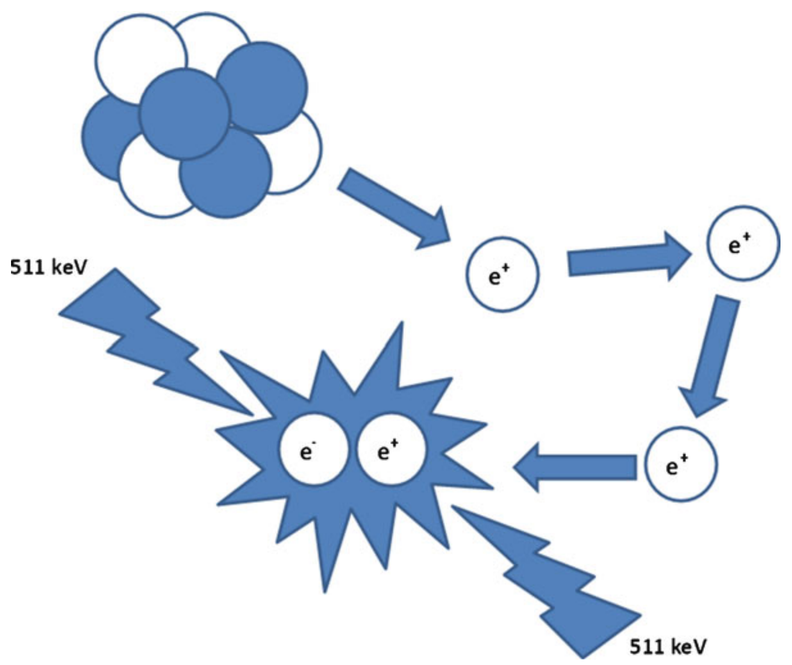

FIGURE 40.1 - POSITRON REACTION
Positron emission and resultant annihilation reaction. A positron is emitted from the F-18 nucleus and undergoes an annihilation reaction with an electron. The mass of the positron and electron are converted to energy in the form of two 511 keV photons ($E = MC^2$)

one phosphorylation by hexokinase, FDG-6-P is trapped and cannot progress any further along the glycolytic pathway (Fig. 40.3).

An F-18 FDG PET scan image is a snapshot of the distribution of cellular metabolism of glucose (Fig. 40.4). The majority of cancer cells are hypermetabolic relative to normal cells, and this is the basis for the usefulness of F-18 FDG imaging in oncology.

Patient Preparation

Three days prior to an FDG PET study, patients are encouraged to maintain a low carbohydrate diet to decrease or eliminate left ventricular myocardial uptake of FDG (the myocardium uses fatty acids as an energy source under these dietary conditions).

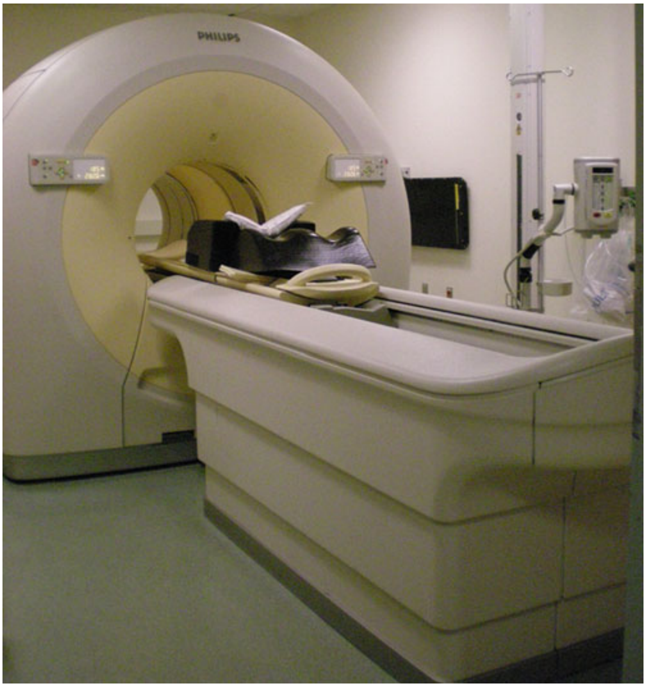

FIGURE 40.2 - F-18 FDG PET/CT SCANNER
There are two gantries; one for CT and the other for FDG PET

Patients are NPO for 12 h prior to the study. This prevents both competitive inhibition of FDG by endogenous glucose and redistribution of FDG into skeletal muscle by endogenous insulin. Diabetics must take no insulin for 6 h prior to the study and must have a blood glucose level below 200. Patients are encouraged to avoid physically strenuous activity for 24 h prior to the study to prevent muscular uptake of FDG secondary to muscle repair and replenishment of glycogen stores. Activation of brown adipose tissue results in significant uptake of FDG predominantly in the fat of the neck and paraspinous region. Therefore, patients are encouraged to wear warm comfortable clothing. Finally, claustrophobic patients are given anxiety medications as needed.

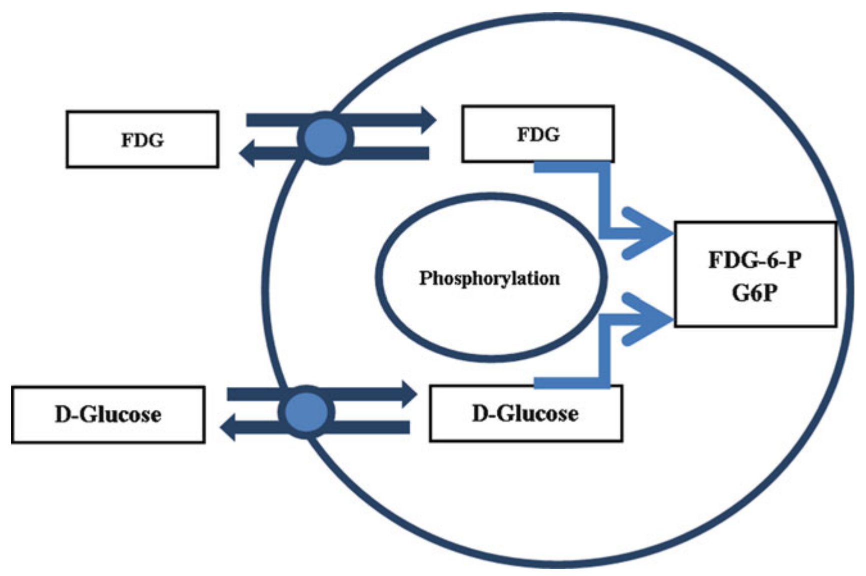

FIGURE 40.3 - PHYSIOLOGY OF FDG
FDG and D-glucose are transported across the cell membrane and enter the glycolytic pathway. After the first phosphorylation, FDG is trapped in the cell

Application in Oncology

FDG PET is a useful tool in patients with cancer. It is used to diagnose stage and restage a variety of malignancies. After radiotherapy and chemotherapy, FDG PET is helpful to evaluate a tumor's response to therapy.

Figure 40.5 is an FDG PET study in a 38-year-old, nonsmoking male with no history of malignancy or hemoptysis. A CT of the chest showed a 2.1-cm lobulated noncalcified left upper lobe nodule. The PET study was performed as a diagnostic tool to evaluate the posttest probability of malignancy. If the FDG PET were negative, the posttest probability of malignancy would be 2%. However, the PET study was positive indicating a 65% probability of malignancy. Subsequent biopsy revealed a non-small cell carcinoma. Left upper lobectomy and lymph node resection confirmed a metastatic node in the left side of the mediastinum.

Figure 40.6 is an FDG PET study of a 56-year-old female with known lung cancer. The study was performed to restage her lung cancer. CT of the chest showed hilar and mediastinal adenopathy. The FDG PET study revealed diffuse metastasis

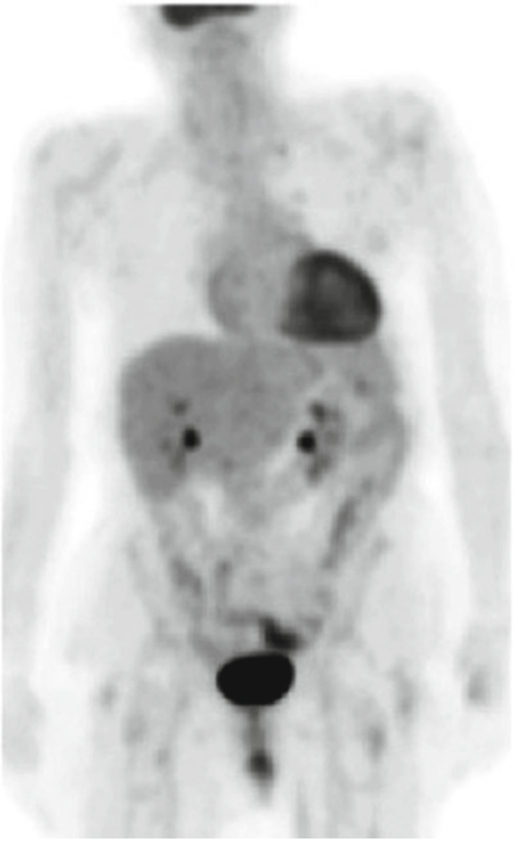

FIGURE 40.4 - NORMAL F-18 FDG PET STUDY
There is physiologic activity in the heart, liver, kidneys, liver, spleen, bowel, bladder, bone marrow, and cerebellum

within the lymph nodes of the neck, chest, abdomen, and pelvis, as well as bone, lung, and liver metastasis.

Figure 40.7 shows prechemotherapy and postchemotherapy FDG PET studies in a patient with lymphoma. The study was done to evaluate response to chemotherapy. PET changes the clinical management in approximately 25% of patients with lymphoma. A metabolic response to therapy indicates that therapy is effective and provides prognostic information. Patients with an excellent metabolic response to therapy stay in remission longer and are at lower risk for relapse.

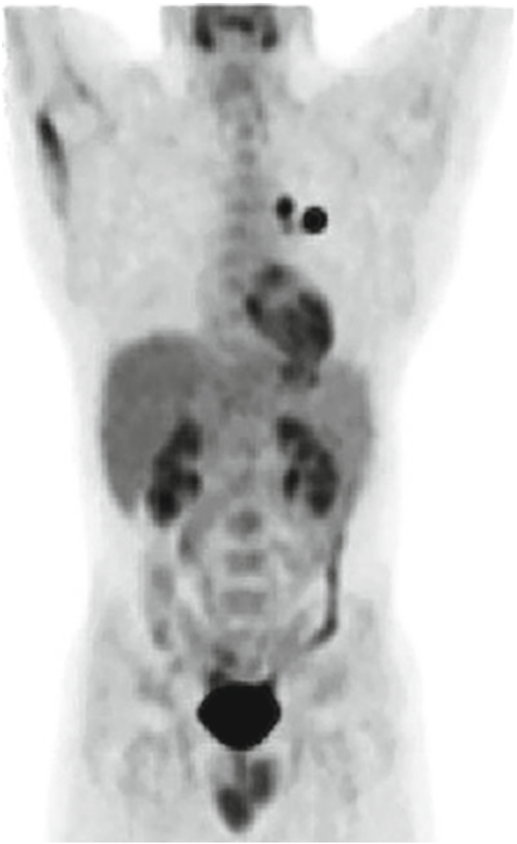

FIGURE 40.5 - MALIGNANT EXAMPLE
Left upper lobe non-small cell lung cancer with a metastatic mediastinal lymph node

PET Pitfalls

False-positive FDG PET studies result from intense inflammatory reactions secondary to infection, trauma, surgery, radiation, and inflammatory diseases. False-negative studies occur because some tumors are not FDG avid. Bronchoalveolar cell carcinoma and carcinoid of the lung, MALT lymphoma, and mucinous colonic neoplasms are sometimes non-FDG avid. Tumors less than 8 mm in size may not be well seen with FDG PET.

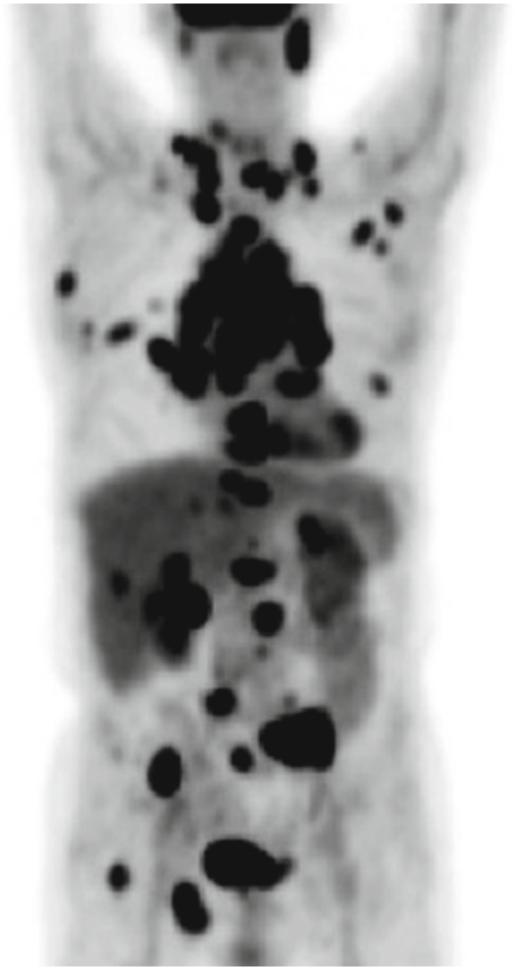

FIGURE 40.6 - RESTAGING OF LUNG CANCER
FDG PET of a 56-year-old with known lung cancer. Note the extensive lymph node metastasis. There are also bone, lung, and liver metastasis

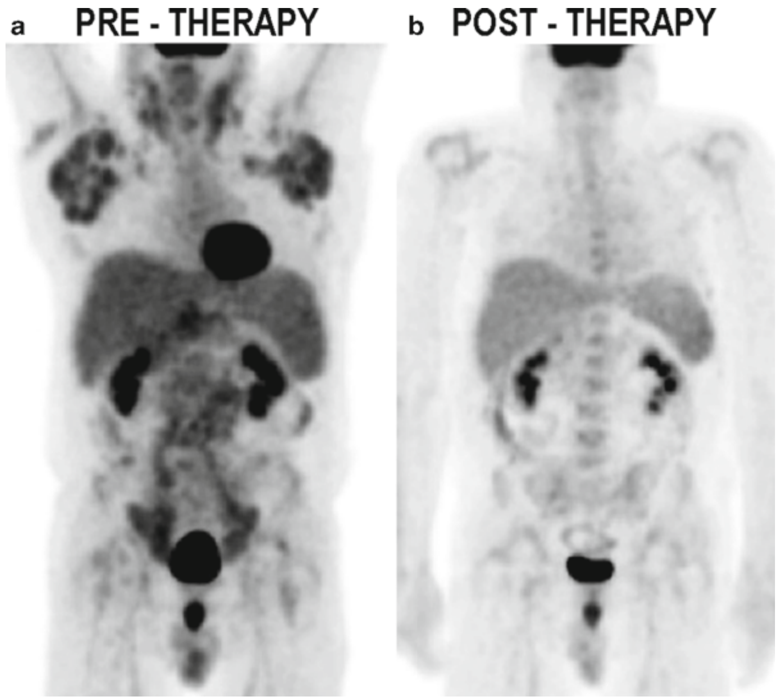

FIGURE 40.7 - RESPONSE TO THERAPY
Note the extensive FDG avid lymphadenopathy in the neck, axilla, abdomen and pelvis on the pretherapy study (**a**). After three cycles of chemotherapy, there is no detectable disease indicating an excellent metabolic response to therapy (**b**). (Incidentally, the intense left ventricular activity on the pretherapy study which is not present on the posttherapy study does not indicate treated lymphoma. Rather, it simply reveals that the patient failed to follow a low carbohydrate diet prior to the pretherapy study)

41

DIAGNOSTIC ARTERIOGRAPHY

Objectives:
1. Describe in detail the technique for arterial groin and arm punctures.
2. Discuss how catheter design helps in the performance of arteriography.
3. Discuss the complications of arteriography and their relative frequency.

Arteriography involves the placement of a catheter into the arterial system with injection of contrast while obtaining X-ray images. Various catheters and wires are used in combination to cannulate the desired arteries (Fig. 41.1).

Femoral and Brachial Artery Access

Access to the femoral or brachial artery is performed at the level of the femoral head or in line with the humerus above the elbow, respectively. Access is achieved at either of these points for two reasons. First, the artery in these locations is easy to palpate and therefore easier to locate and puncture. Second, the artery is adjacent to a bony structure; when the catheter is removed, hemostasis can be achieved by compressing the artery against the bone directly behind it (Fig. 41.2).

Once access to the artery is obtained, a floppy-tipped guide wire is advanced under fluoroscopy. The stiffer portion of the guide wire follows for an adequate distance. The needle is then exchanged over the wire for either a catheter or a vascular sheath. A vascular sheath is a device which has a hemostatic valve proximally that stays in place in the artery through which catheter exchanges can be accomplished with minimal blood loss. A disadvantage is its larger outer diameter and the larger hole it makes in the artery compared to a catheter alone.

H Singh and JA Neutze (eds.), *Radiology Fundamentals: Introduction to Imaging & Technology*, DOI 10.1007/978-1-4614-0944-1_41,
© Springer Science+Business Media, LLC 2012

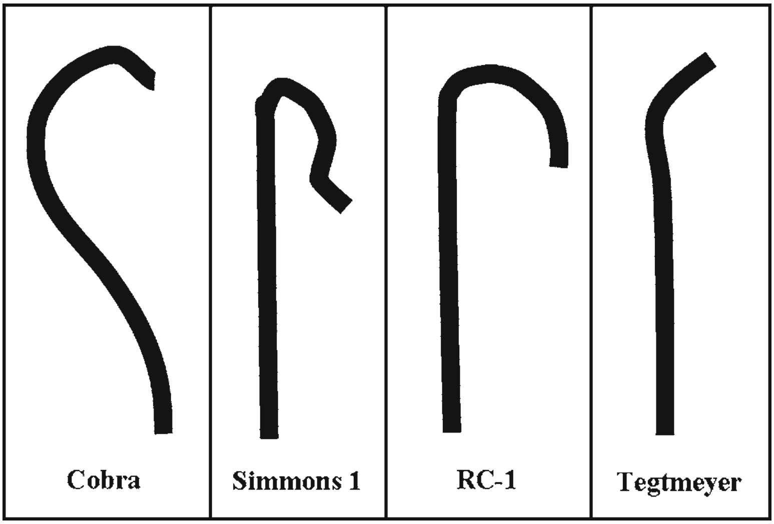
Cobra
Simmons 1
RC-1
Tegtmeyer

FIGURE 41.1 - CATHETERS AND WIRES
Various catheters and wires are used in combination to cannulate the artery in question

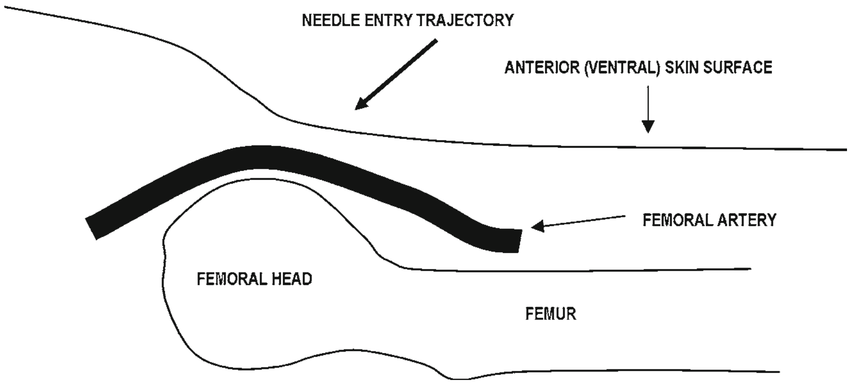
NEEDLE ENTRY TRAJECTORY
ANTERIOR (VENTRAL) SKIN SURFACE
FEMORAL ARTERY
FEMORAL HEAD
FEMUR

FIGURE 41.2 - COMMON FEMORAL ARTERY ACCESS
In the lateral view, the femoral artery lies just on top of the femoral head. At this point, it is easy to palpate and easy to compress after the catheter is removed

If "flush" arteriographic studies are to be performed, particularly of large vessels, a catheter with multiple side holes is used to evenly distribute the contrast in the blood pool. A typical example of this would be aortography using a "pigtail" or "tennis racket" catheter. If selective arteriography is needed, then an appropriately shaped catheter, usually with a single end hole, is used with a guide wire to select the desired arteries.

Once the catheter is in appropriate position, contrast is injected either by hand or with a power injector using a known rate and pressure. Images are obtained with digital subtraction angiography (DSA) imaging. Diagnostic images are reviewed. Either the study is concluded at that time or an intervention is undertaken, if appropriate.

At the completion of the procedure, the catheter or sheath is removed and hemostasis is obtained at the puncture site by compressing the artery against the underlying bony structure. Compression is held for 15–20 min. Once hemostasis is obtained, the patient must lie flat for 6 hours (or maintain the elbow extended after an arm puncture) and the groin or antecubital fossa must be checked frequently to make sure no bleeding has occurred.

Arteriography Complications

Complications of arteriography include the following:

1. *Groin or arm hematoma*

   In the groin, a hematoma which requires additional treatment is not uncommon, occurring up to 5% of the time. In the arm, it can be much more dangerous because of possible compression of the vessels and nerves in the neurovascular bundle and should be addressed immediately.
2. *Infection*

   Infection is almost unheard of in arteriography. Because of the small access points and the sterile draping and technique, it occurs in less than 1% of all cases.
3. *Contrast reaction*

   Injection of contrast media in anyone may result in a contrast reaction. The most common reaction clinically is the onset of itching and hives. Treatment is nearly always successful using known drug algorithms. Death occurs in only about 1 in 40,000 contrast injections. If a patient has a known contrast allergy, he or she must be pretreated with oral or intravenous steroids, (e.g., oral prednisone 50 mg) at 13, 7, and 1 hours before the procedure. The patient must also be given Benadryl® 50 mg IV or PO 1 hours prior to the procedure. The most important steroid dose is the dose given 13 hours before the procedure. The mechanism of protection is thought to be the stabilization of mast cell membranes by preventing the degranulation and release of histamine.

4. *Contrast-induced nephrotoxicity* (*CIN*)

   Current literature suggests the main risk factors for CIN include pre-existing renal insufficiency, diabetes mellitus, and in some cases, severe congestive heart failure.

5. *Vessel dissection or pseudoaneurysm formation*

   Any time a blood vessel is entered traumatically (as with a puncture for arteriography), there is the definite but small risk of vessel injury, pseudoaneurysm, or AV fistula formation.

42

PULMONARY ARTERIOGRAPHY AND IVC FILTER PLACEMENT

Objectives:

1. List the indications for pulmonary arteriography.
2. Describe the technique for pulmonary arteriography including the contraindications.
3. Describe the technique for inferior vena cava filter placement including what is appropriate for an inferior cava larger than 28 mm.

Although still considered the gold standard for the diagnosis of pulmonary embolism, pulmonary arteriography has largely been supplanted by pulmonary CT scan angiography (CTAP). Nevertheless, pulmonary arteriography may still be indicated in patients with a high clinical suspicion for pulmonary embolism and

1. A low probability or indeterminate V/Q scan or CTAP.
2. An indeterminate V/Q or CTAP and contraindication to anticoagulation.

Conventional pulmonary arteriography is accomplished from the right common femoral vein or right internal jugular vein. Access is obtained in a fashion similar to that described in the arteriography section. Once access has been obtained, a pulmonary artery catheter is advanced to the level of the right atrium. The catheter is gently advanced across the tricuspid valve and, while pushing forward, is rotated. As it crosses through the right ventricle to the pulmonary outflow tract, it is gently pushed farther, usually into the left pulmonary artery (Fig. 42.1). The catheter position in each pulmonary artery is confirmed with a minimal amount of contrast and pulmonary artery pressures are recorded. The contrast injection is tailored, based on the pulmonary artery pressures. If the pressures are normal or only mildly elevated, a standard pulmonary arteriogram is performed. If the pressures are elevated, the contrast injection volume is decreased or a subselective angiogram is performed. Once images have been obtained on the left, the catheter is then manipulated to the right side.

H Singh and JA Neutze (eds.), *Radiology Fundamentals: Introduction to Imaging & Technology*, DOI 10.1007/978-1-4614-0944-1_42,
© Springer Science+Business Media, LLC 2012

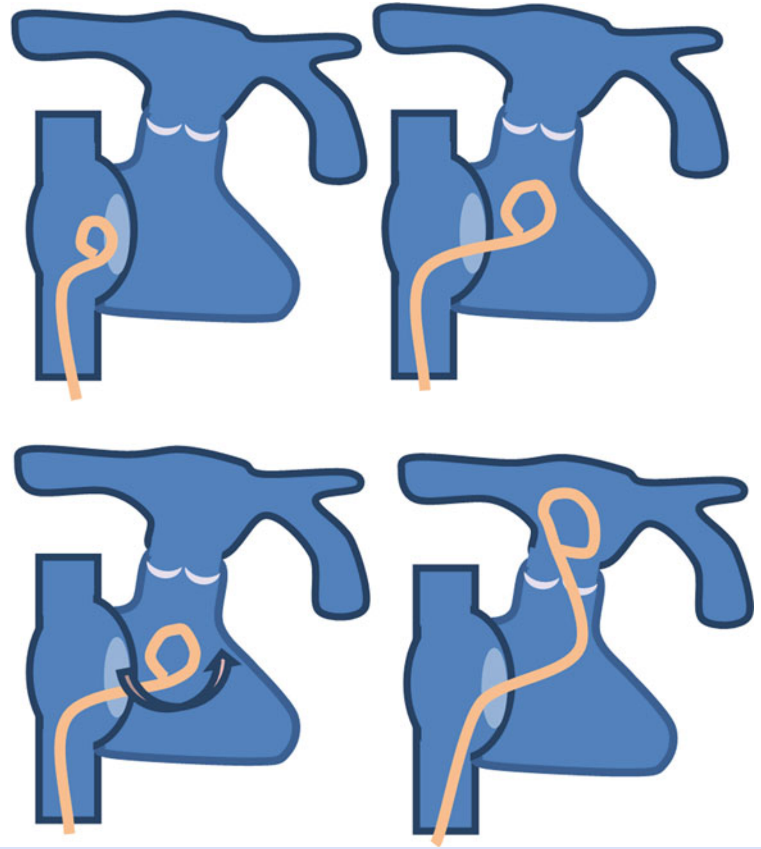

FIGURE 42.1 - PLACEMENT OF A PULMONARY ARTERY CATHETER
Manipulations used to advance a catheter through the heart and into the pulmonary artery

Images are obtained in the AP and opposite oblique (i.e., for a left pulmonary arteriogram, an AP and right anterior oblique study are performed). If there remains a question, selective magnification views of the area of concern can be performed. Angiographic findings of acute pulmonary embolism include “worm-like” filling defects (clots that are casts of the lower leg veins) that are often draped over vessel bifurcation points, tram-tracking of contrast around clots that are nearly occlusive in the vessel, and complete vessel occlusions characterized by cutoffs with a meniscus.

IVC Filter Placement

Although often thought of as separate entities, deep vein thrombosis (DVT) and pulmonary embolism (PE) are the beginning and ultimate final end result of a single disease process known as venous thromboembolic disease (VTED). The primary treatment of choice of VTED is anticoagulation therapy. Anticoagulation therapy prevents new clot formation and allows the body's own mechanisms to dissolve the blood clot. It is a generally safe, effective and affordable means of preventing a DVT from progressing to a PE.

Inferior vena cava (IVC) filters are metallic devices placed in the IVC that present a mechanical barrier that prevents an embolus from traveling from the lower extremities or pelvis to the pulmonary arteries. Although IVC filters are effective in preventing PE, they remain as second line therapy for several reasons:

1. IVC filters do nothing to help resolve existing clot, and in some cases, may worsen underlying DVT.
2. IVC Filters are associated with complications that become more likely the longer that the device stays in place. These include
   (a) Filter fracture.
   (b) Perforation of filter elements through the cava and into adjacent structures.
   (c) Filter migration/embolization.
   (d) Caval thrombosis.
3. Some studies suggest that over time, IVC filters lose their protective value.[1] After 2 years, when compared with patients who receive anticoagulation, patients with IVC filters have the same rate of recurrent PE with twice the rate of recurrent DVT.

Indications for the placement of an IVC filter in patients with VTED include

1. Contraindication to anticoagulation.
2. PE despite adequate anticoagulation (failed anticoagulation therapy).
3. Significant risk of complication from anticoagulation therapy (e.g., fall risk, planned elective surgery).
4. Trauma with injury patterns known to place the patient at high risk for VTED, such as long bone fracture and spinal cord injuries.

Many different filter designs are available in the North American and European markets, but in general, they all fall into one of two categories: permanent and retrievable (Fig. 42.2). A permanent filter, as the name implies, is intended to stay in place permanently. A retrievable filter (also sometimes referred to as an "optional" filter) can be used as a permanent device but has design features that allow it to be removed using percutaneous techniques. These devices are sometimes referred to as "optional" filters because they are permanent devices with the option to be removed.

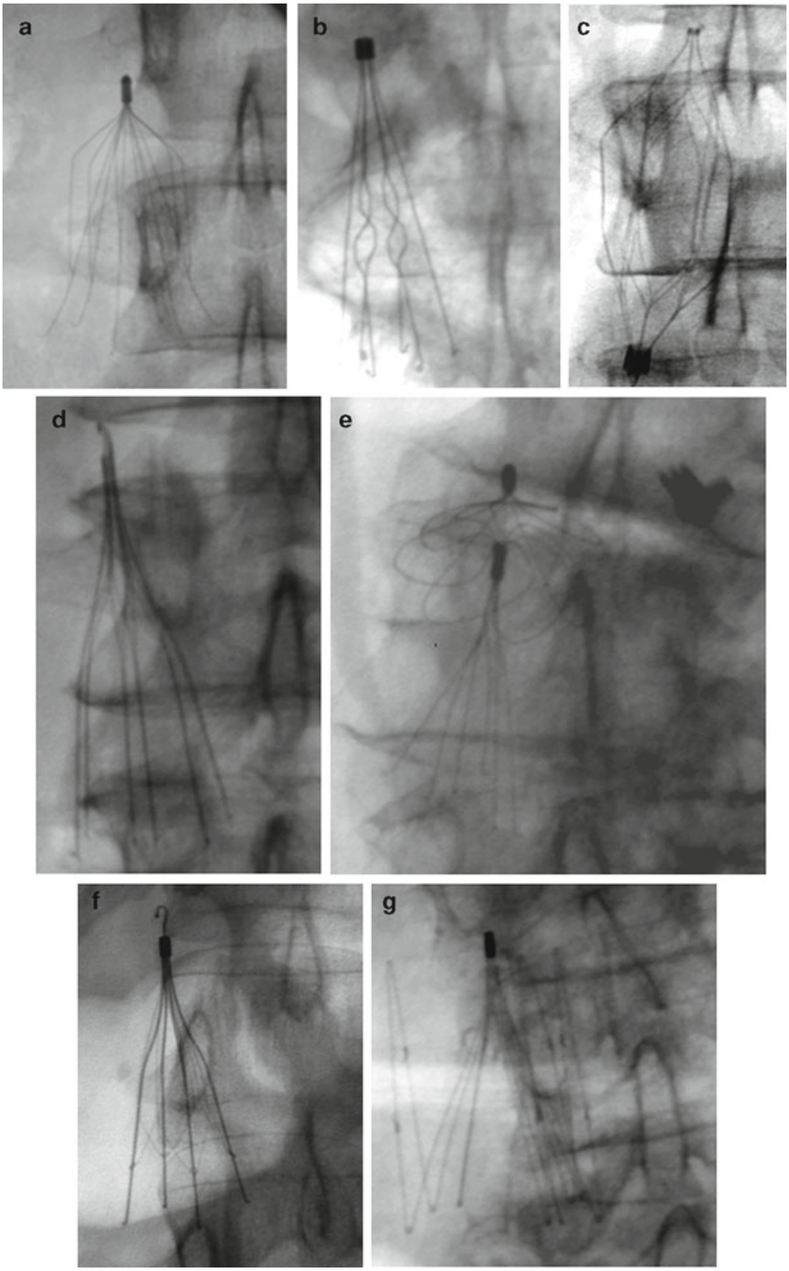

FIGURE 42.2 - EXAMPLES OF SEVERAL IVC FILTERS AVAILABLE TODAY (**a**) G2 (removable), (**b**) Greenfield (permanent), (**c**) Optease (removable), (**d**) Option (removable), (**e**) Simon Nitinol (permanent), (**f**) Tulip (removable), and (**g**) Vena Tech LP (permanent)

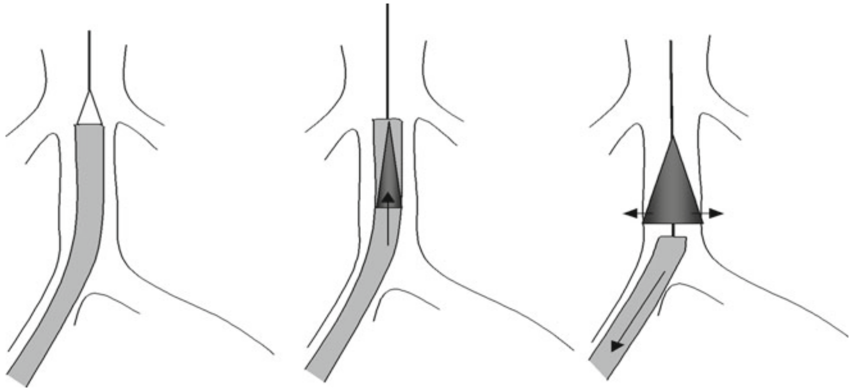

FIGURE 42.3 - DEPLOYMENT OF A VENA CAVA FILTER
On the left, a deployment sheath with the introducing cannula is advanced over a wire. The cannula is then removed and inside the sheath, the filter is advanced to the tip of the sheath. The sheath is then pulled back (important) and the filter self-deploys. It is very important to know exactly where the renal veins, accessory renal veins and the iliac vein confluence are so that optimal deployment is possible

The rational for having such a device is simple. Because IVC filters are good at preventing PE in the short term but lose their effectiveness while increasing their complication rate over time, it makes sense to have a device that can be placed to protect a patient during a period of high risk that can then be removed once the risk returns to normal.

IVC filters are placed via common femoral vein or internal jugular vein access. A marker catheter (a catheter with radiopaque markers at an exact distance, usually 20 mm) is placed in the right common iliac vein and a power-injection IVC study is performed, paying close attention to the iliac vein confluence and the inflow from the renal veins. Most IVC filters are designed to be stable in vena cavas 28 mm or less in diameter. The marks on the catheter serve as a reference distance and allow for accurate measurement of the caval diameter accounting for magnification. The appropriate filter is chosen (based on caval size and configuration) and delivered into position inside of a long deployment sheath. Rather than being pushed out the end of the sheath, the filter is deployed by withdrawing the outer sheath, allowing the filter to expand in place, usually just below the renal veins (Fig. 42.3). A follow-up study is performed to confirm the filter's position.

Reference

1. Decousus H, Leizorovicz A, Parent F, et al. A clinical trial of Vena Caval Filters in the Prevention of Pulmonary Embolism in Patients with Proximal Deep Vein Thrombosis. NEJM. 338 (7). 1998. 409–415.

43

PERCUTANEOUS NEPHROSTOMY PLACEMENT

Objectives:

1. Identify the relevant anatomy of the kidney and how it relates to deciding on access to the kidney.
2. Describe why air is important to the performance of a nephrostomy tube placement.
3. Describe a Cope loop.

Percutaneous drainage of the kidney is performed for several reasons, the most common of which is obstruction from nephrolithiasis, kidney stone disease. Obstructive uropathy secondary to a ureteral stone can be a medical emergency, particularly if there is evidence of urosepsis from ureteral obstruction. In those cases, percutaneous drainage may be a life-saving measure.

Frequently, renal ultrasound or abdominal CT scan has already been performed to evaluate the cause of the patient's flank pain, fever, etc. These studies are then reviewed carefully to help localize the kidney and any possible intervening structures such as colon, spleen or liver prior to drainage.

The three most common methods for initial puncture of the kidney include using anatomic landmarks, using ultrasound guidance, and using a small dose of intravenous contrast to generate a faint nephrogram. The initial access is achieved with a 22-g Chiba needle.

Once the needle is in the renal pelvis, urine is withdrawn and sent for culture. A small amount of contrast is used to confirm access to the renal pelvis. The renal pelvis can be opacified with contrast (although this may require a large amount of contrast and may distend the collecting system unnecessarily) or air. The air will fill the nondependent posterior calyces that can then be targeted under fluoroscopy for definitive access. Once the appropriate calyx is chosen, the angle of entry should be determined. The kidney should be accessed along Brodel's avascular line, a plane between the posterior and anterior segmental arteries.

H Singh and JA Neutze (eds.), *Radiology Fundamentals: Introduction to Imaging & Technology*, DOI 10.1007/978-1-4614-0944-1_43,
© Springer Science+Business Media, LLC 2012

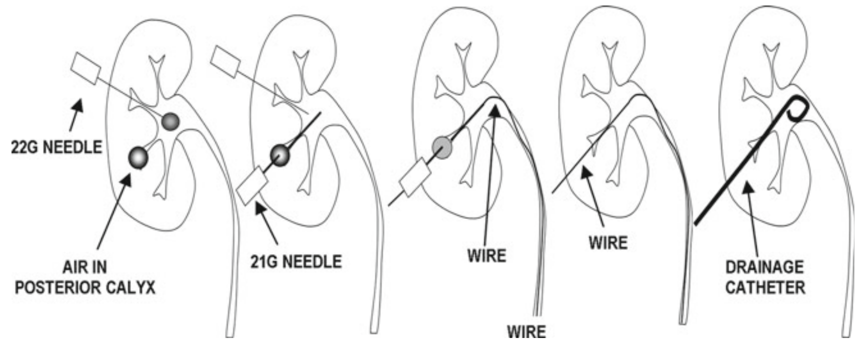

FIGURE 43.1 - PERCUTANEOUS NEPHROSTOMY TUBE PLACEMENT
In the first image, a small caliber needle (22 g) is advanced in to the renal collecting system. The system is opacified with contrast and air is instilled to demonstrate a posterior calyx. This is then accessed with a larger needle (21 g) which accepts an 0.018″ wire. The needle is then removed, the tract dilated over the wire, and a drainage catheter advanced into place. The tip is drawn back by an internal string system, which helps keep the catheter locked in the collecting system

Once the calyx has been accessed, a wire is advanced into the renal collecting system through the access needle. The needle is removed and over the wire, the tract is dilated to an appropriate caliber. Once the tract is dilated, a stiffer wire is advanced into place and over the wire, a drainage catheter is advanced into the collecting system and locked in place. The catheter is placed to external drainage and the output is recorded carefully (Fig. 43.1).

Once the kidney is decompressed, various catheters are available for long-term drainage, including nephroureteral stents, and internal double J stents. The possible combinations are quite extensive (Figs. 43.2 and 43.3).

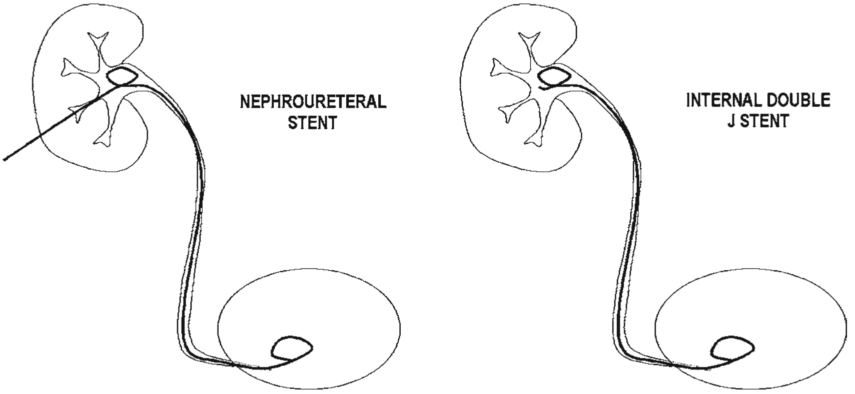

FIGURE 43.2 - TWO TYPES OF UROLOGICAL CATHETERS
On the left, the percutaneous nephrostomy tube has been converted to a nephroureteral catheter, from the kidney down to the bladder. On the right, there has been percutaneous placement of an internal double J catheter

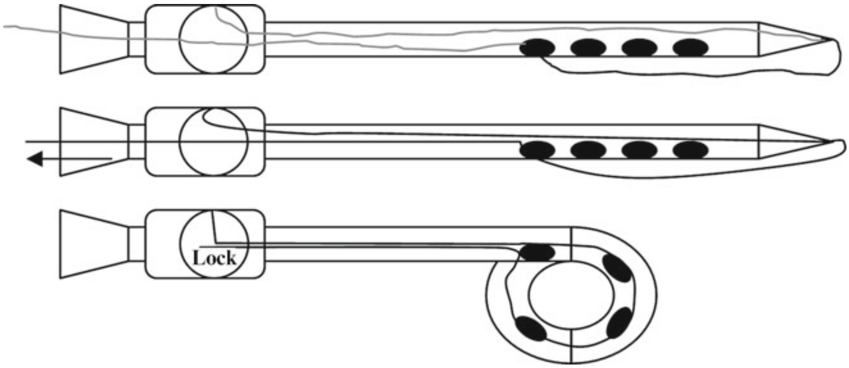

FIGURE 43.3 - COPE LOOP
In the first catheter at the top, there is a string extending loosely from the hub, through the end of the catheter and back into a sidehole. Once the catheter is in place, tension is placed on the string which then draws the tip of the catheter back on itself, forming the distal Cope loop. The string is then locked at the hub and the excess string is trimmed

44

TIPS

Objectives:

1. List the indications for TIPS.
2. List the contraindications for TIPS.
3. Describe the steps needed to create a TIPS.
4. Discuss how TIPS placement alters long-term survival.

The Transjugular Intrahepatic Portosystemic Shunt (TIPS) is a percutaneous procedure designed to decompress the portal system in patients with portal hypertension (Table 44.1).

Table 44-1 TIPS indications and contraindications

TIPS shunt indications
Variceal hemorrhage which is refractory to medical management
Prophylaxis for recurrent variceal bleeding
Ascites which is refractory to medical management
Budd–Chiari Syndrome
TIPS contraindications
Severe hepatic insufficiency
Poorly controlled encephalopathy
Portal vein occlusion
Polycystic liver disease
Hypervascular hepatic tumor
TIPS relative contraindications
Active bleeding
Active infection

H Singh and JA Neutze (eds.), *Radiology Fundamentals: Introduction to Imaging & Technology*, DOI 10.1007/978-1-4614-0944-1_44,
© Springer Science+Business Media, LLC 2012

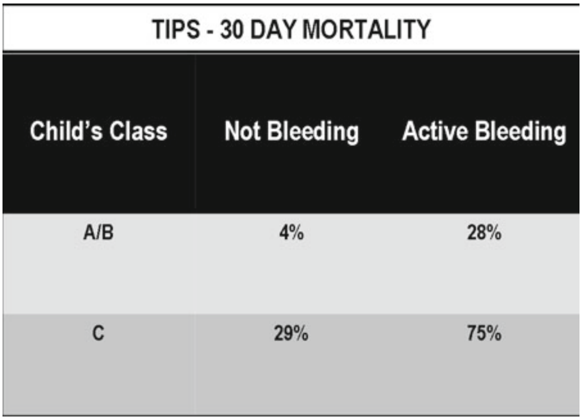

TIPS - 30 DAY MORTALITY

Child's Class	Not Bleeding	Active Bleeding
A/B	4%	28%
C	29%	75%

FIGURE 44.1 - TIPS – 30-DAY MORTALITY

Once the TIPS shunt has been deemed appropriate, several questions must be answered. Is the portal vein patent by ultrasound or CT scan? If the varices are actively bleeding, TIPS is relatively contraindicated because of the high mortality associated with placement of a TIPS shunt in an actively bleeding patient. Sometimes, however, it is the patient's only option (Fig. 44.1).

TIPS Placement

For placement of the TIPS shunt, the right internal jugular vein is used for access. Once access has been obtained, a large, long sheath (10 French) is placed with its tip in the right atrium. Using an angled catheter, access is obtained to the right hepatic vein (or sometimes the middle hepatic vein). Simultaneous pressures are obtained between the hepatic vein and the right atrium. Next the catheter is "wedged" as peripherally as possible in the hepatic vein. A wedged hepatic vein pressure to right atrial pressure gradient (similar to inflating the balloon of a Swan Ganz catheter to obtain left atrial pressures) is determined. A hepatic venogram is then obtained. The angled catheter is exchanged for one of several transhepatic needle access systems.

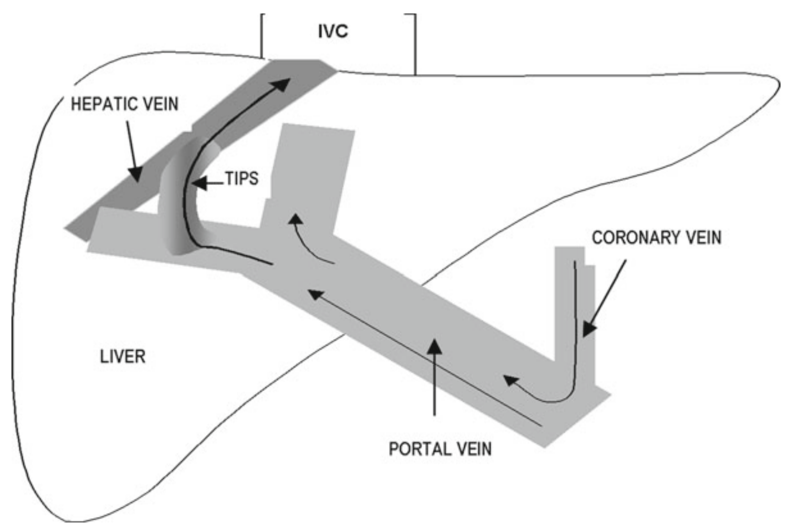

FIGURE 44.2 - DIAGRAM OF A TIPS SHUNT
Through a percutaneous access from the internal jugular vein, the right hepatic vein is "connected" to the right portal vein branch via a transparenchymal tract. This tract is supported open utilizing a metallic stent. This allows the portal venous flow to decompress into the hepatic venous system and the associated varices to bypass the diseased liver

A large, hollow, directional needle is used to gain access through the liver and, via the needle, a wire is advanced into the portal vein. True simultaneous pressures are obtained across the liver in the hepatic vein and the portal vein. The tract is predilated with an 8-mm balloon. A stent of appropriate length is deployed across the liver and dilated. Simultaneous gradients are then obtained. A target gradient of 9–11 mmHg is set for variceal bleeding and 5–7 mmHg for refractory ascites. If the gradient is too low there can be a significant "steal" phenomenon from liver perfusion. If the gradient is too high, improvement in the varices or ascites may be inadequate. Pressure gradients greater than 12 mmHg are associated with an increased rate of variceal bleeding. If the pressure gradient remains elevated after TIPS placement, the stent may need to be dilated to a larger diameter to reduce the gradient to an acceptable level (Fig. 44.2).

An ultrasound is obtained prior to the patient's discharge, and at subsequent regular intervals, for follow-up after discharge to ensure patency of the TIPs shunt.

Long-Term Survival

Although TIPS placement is successful in 96% of cases, it does not significantly alter long-term survival. Long-term survival is primarily related to the hepatic reserve. TIPS placement does not alter the underlying liver disease. It only alters the manifestations of portal hypertension. The best predictor of survival is the patient's Child–Pugh Score. Since it does not alter the underlying liver disease, TIPS is best used as a bridge to transplantation (Figs. 44.3 and 44.4).

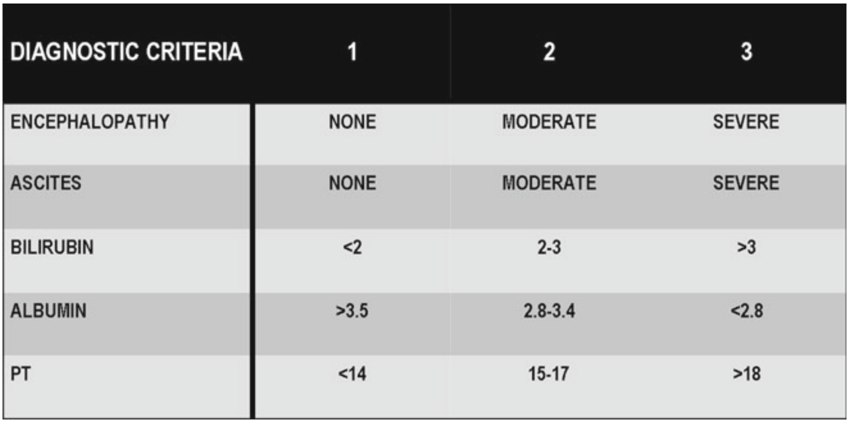

DIAGNOSTIC CRITERIA	1	2	3
ENCEPHALOPATHY	NONE	MODERATE	SEVERE
ASCITES	NONE	MODERATE	SEVERE
BILIRUBIN	<2	2-3	>3
ALBUMIN	>3.5	2.8-3.4	<2.8
PT	<14	15-17	>18

FIGURE 44.3 - CHILDS SCORE
This classification scheme is used to assess the prognosis of chronic liver disease. To calculate a score, add the points from each category together. A is 5–6 points, B is 7–9 points, while C is greater than 10 points

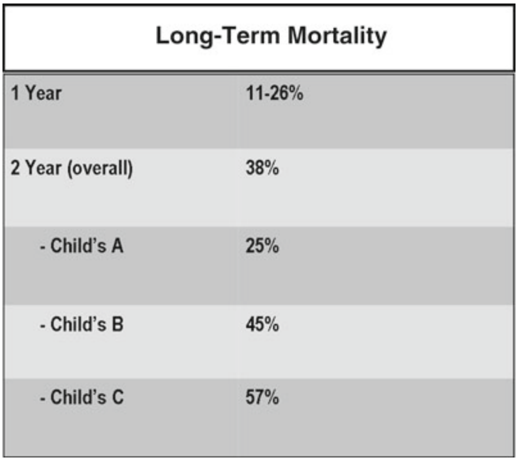

Long-Term Mortality	
1 Year	11-26%
2 Year (overall)	38%
- Child's A	25%
- Child's B	45%
- Child's C	57%

FIGURE 44.4 - LONG-TERM MORTALITY FOLLOWING TIPS PLACEMENT

45

CENTRAL VENOUS ACCESS

Objectives:

1. List the types of devices available and their indications for placement.
2. List the different methods of central venous access.

Maintenance of venous access is the cornerstone of many medical therapies. Durable venous access into the central venous systems is essential for most cancer regimens, extended antibiotic therapies, parenteral nutrition, and inotropic therapies. Durable central venous access for patients who require hemodialysis serves as a bridge until a dialysis fistula or graft is established or as a means of last resort when a graft or fistula is no longer possible. Increasingly, the placement of a long-term central venous access device is performed using ultrasound and fluoroscopic image guidance and is most commonly performed by Interventional Radiology.

There is a great deal of confusion concerning the different types of venous access devices. This situation is complicated by the common practice of referring to catheters by trade names, which are often ambiguous as to form and function. In general, catheters are classified by two attributes: nontunneled vs. tunneled and infusion vs. exchange. An exception to this is subcutaneous devices (ports) which are almost always used for infusion therapy and can remain in place for extended periods of time (Fig. 45.1).

Nontunneled catheters are generally intended for short-term use (days to weeks). These catheters have no subcutaneous tunnel and their entry site goes directly through the skin and into the access vein. As the name implies, tunneled catheters have a subcutaneous tunnel between the skin entry site and the vein entry site. Often, these devices include one or more cuffs that are positioned along the tunnel and serve to provide a barrier to infection and eventually assist in anchoring the catheter in place (Fig. 45.2). The tunnel and cuff system allow the device to stay in place for weeks to months (Fig. 45.3).

H Singh and JA Neutze (eds.), *Radiology Fundamentals: Introduction to Imaging & Technology*, DOI 10.1007/978-1-4614-0944-1_45,
© Springer Science+Business Media, LLC 2012

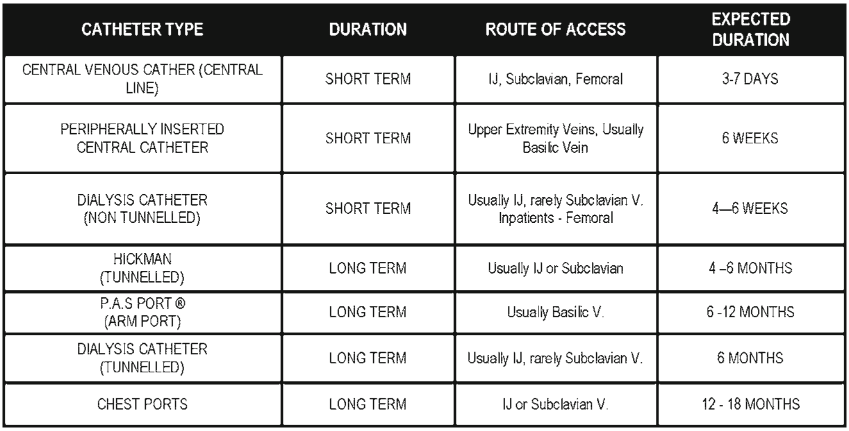

CATHETER TYPE	DURATION	ROUTE OF ACCESS	EXPECTED DURATION
CENTRAL VENOUS CATHER (CENTRAL LINE)	SHORT TERM	IJ, Subclavian, Femoral	3-7 DAYS
PERIPHERALLY INSERTED CENTRAL CATHETER	SHORT TERM	Upper Extremity Veins, Usually Basilic Vein	6 WEEKS
DIALYSIS CATHETER (NON TUNNELLED)	SHORT TERM	Usually IJ, rarely Subclavian V. Inpatients - Femoral	4—6 WEEKS
HICKMAN (TUNNELLED)	LONG TERM	Usually IJ or Subclavian	4 –6 MONTHS
P.A.S PORT ® (ARM PORT)	LONG TERM	Usually Basilic V.	6 -12 MONTHS
DIALYSIS CATHETER (TUNNELLED)	LONG TERM	Usually IJ, rarely Subclavian V.	6 MONTHS
CHEST PORTS	LONG TERM	IJ or Subclavian V.	12 - 18 MONTHS

FIGURE 45.1 - CENTRAL VENOUS ACCESS
Indications and route of access for various central venous catheters

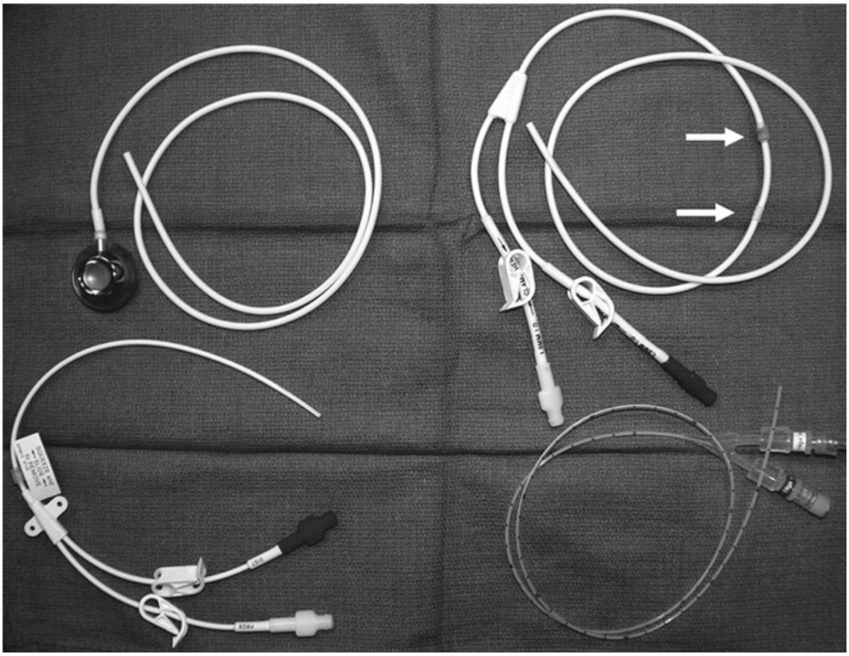

FIGURE 45.2 - EXAMPLES OF INFUSION CATHETERS
From left to right and top to bottom they include a subcutaneous port, a tunneled infusion catheter, a nontunneled infusion catheter (Hohn), and a percutaneously inserted central catheter (PICC). Note the fabric cuffs on the mid shaft of the tunneled catheter (*arrows*)

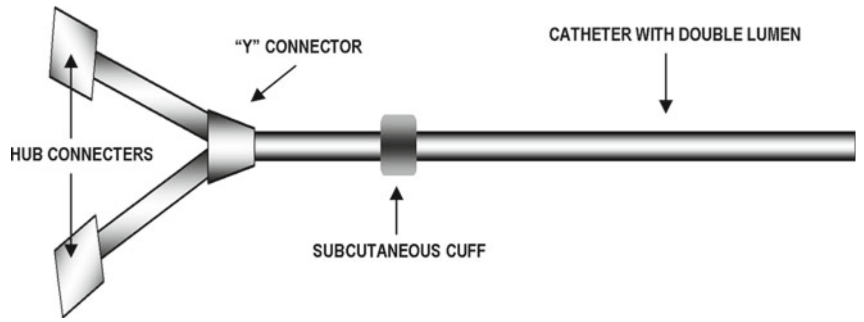

FIGURE 45.3 - TUNNELED CATHETER GENERAL DESIGN
In this dual lumen catheter, the main catheter has an extruded dual lumen. These are divided at the Y connector. The hub connectors are used for access, each equipped with a luer lock device. The key portion is the subcutaneous cuff which seals the subcutaneous access tunnel when the surrounding tissues grow into the cuff, preventing movement of the catheter and preventing the advancement of skin flora up the tract into the central venous system

Subcutaneous infusion catheters (a.k.a. "ports") consist of an infusion catheter attached to a reservoir hub. The entire device is placed under the skin and when used (a.k.a. "accessed"), a special needle is placed through the skin into the reservoir. Once accessed, the port functions like any other infusion catheter. When not accessed, the port requires little care. These attributes make it ideal for patients whose therapies are characterized by episodes requiring continuous venous access separated by periods where venous access is not required, e.g., chemotherapy.

Catheters intended for infusion therapy are generally small in diameter (5–10 Fr), may have one to three lumens and have simple end-hole designs. Catheters intended for exchange therapy, such as hemodialysis or plasmapheresis catheter, are much larger in diameter (11–16 Fr), have at least two lumens (one to withdraw and one to return) and have specially designed tips that prevent the blood that is returned from the catheter from being reaspirated through the other lumen (Fig. 45.4). During exchange therapy, blood flows sometimes up to 600 ml/min are required through these devices.

The subclavian vein is often used for short-term venous access because of the relative distance of the vein to the mouth reduces the likelihood of infection. Anatomically, the subclavian vein passes through a narrow space at the junction of the first rib and clavicle. This space is further compressed with movement at the shoulder. This compression combined with the presence of the catheter is associated with a high incidence of venous stenosis and even catheter fracture (so-called catheter pinch-off syndrome). Since subclavian vein stenosis may have long-term implications for future venous and hemodialysis access, the preferred site for long-term central venous access is the internal jugular vein.

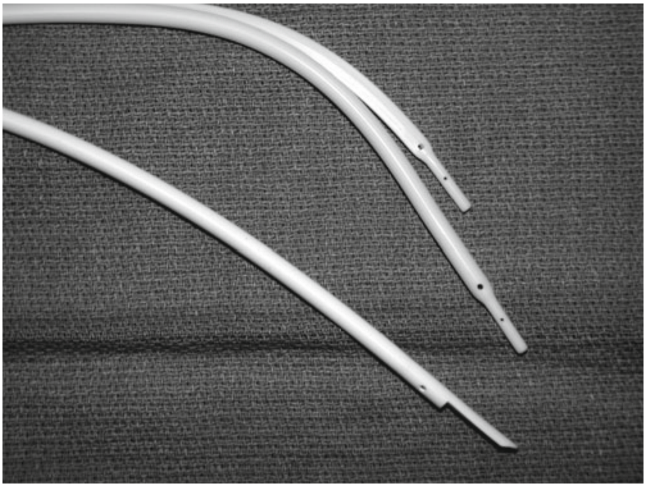

FIGURE 45.4 - EXCHANGE CATHETERS
Two examples of specially designed tips on exchange catheters that prevent recirculation of blood that has already been processed during dialysis or plasmapheresis

The procedure for placement of central venous access is quite straight forward. A preliminary ultrasound of the vein to be accessed is performed to confirm its patency. The neck and the ipsilateral chest are then prepped appropriately. Access is obtained to the vein using vascular ultrasound guidance (most commonly). Once venous access is established, an appropriate tunnel area is chosen. The tunnel is formed under the skin using a tunneling device and the catheter is advanced through the tunnel. Finally, the catheter is advanced into the vein. The ideal catheter tip position is at the cavoatrial junction, which is typically 3–4 cm below the carina on chest radiograph.

In unusual circumstances, when a patient may no longer have patent veins in the chest, central venous catheters can still be placed in other locations. Using similar techniques as described above, catheters can be placed in the common femoral veins or even directly into the inferior vena cava through the back. Trans-organ venous access can also be performed percutaneously through the kidneys or liver. Catheters placed in these sites carry high rates of complications and are therefore used as options of last resort for venous access.

46

FRACTURES: PART I

Objectives:
1. List five major categories of description when evaluating a fracture.
2. List the Salter–Harris classification of fractures in children.
3. State the radiologic features of the "battered child syndrome."
4. Define the phrase pathological fracture.

Fractures are ubiquitous in medical practice. Radiographs have been used to evaluate fractures from the earliest days of diagnostic radiology and remain a cornerstone of clinical care in the diagnosis and treatment of skeletal trauma.

The Simple Fracture

Figure 46.1 demonstrates an acute fracture of the fourth proximal phalanx in the left foot. Note the presence of a linear lucency, sharp edges without marginal sclerosis, and soft tissue swelling.

Fracture Nomenclature

It is important to be able to verbally describe a fracture since you will often be called upon to communicate what you are looking at on a radiograph to a referring physician. Features that must be mentioned include the following:

1. *Location*: the name of the bone involved and the part of the bone involved. In long bones, the fracture can involve the epiphysis, metaphysis, diaphysis, and

H Singh and JA Neutze (eds.), *Radiology Fundamentals: Introduction to Imaging & Technology*, DOI 10.1007/978-1-4614-0944-1_46,
© Springer Science+Business Media, LLC 2012

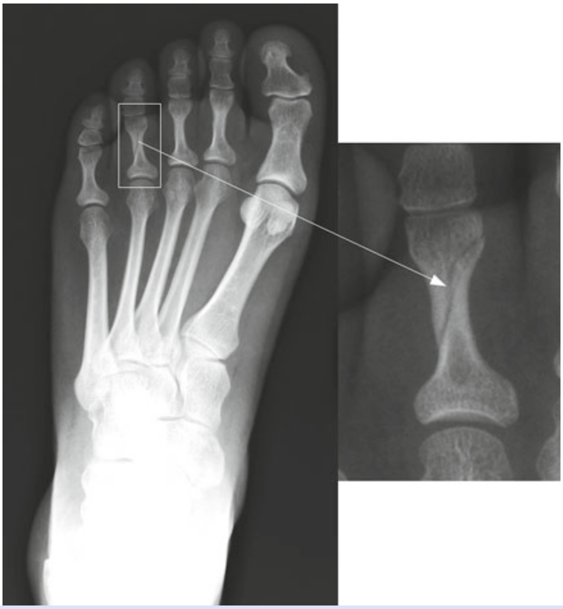

FIGURE 46.1 - SIMPLE FRACTURE
Oblique, nondisplaced fracture of the fourth proximal phalanx for the left foot

even the physis (growth plate). Other designations such as head, neck, body, waist, etc. (depending on the bone), may be employed (Fig. 46.2).

2. *Type of fracture*: transverse, oblique, spiral, butterfly are all appropriate descriptors. Comminuted is used when there are multiple fracture fragments. It is also important to note any intra-articular extension of the fracture (extension into the joint) (Fig. 46.3).
3. *Displacement* (*nonalignment of periosteal surfaces of the bone*): Displacement is described using the location of the distal fragment with respect to the proximal fragment. Hence, if the distal fragment is medially displaced the fracture is medially displaced. Open or compound fractures are fractures which penetrate the skin.
4. *Angulation of the "apex" of the fracture*: the direction that the angle of the fracture points is used to describe the fracture position. A common phrase used would be "the apex of the fracture is directed laterally."
5. *Rotation of the distal fragment*: if the distal fragment is rotated relative to the proximal fragment, this should be included in the description (Fig. 46.4).

Note that at least two views are required to completely visualize and therefore describe the position of a fracture. An example of a complete description of a

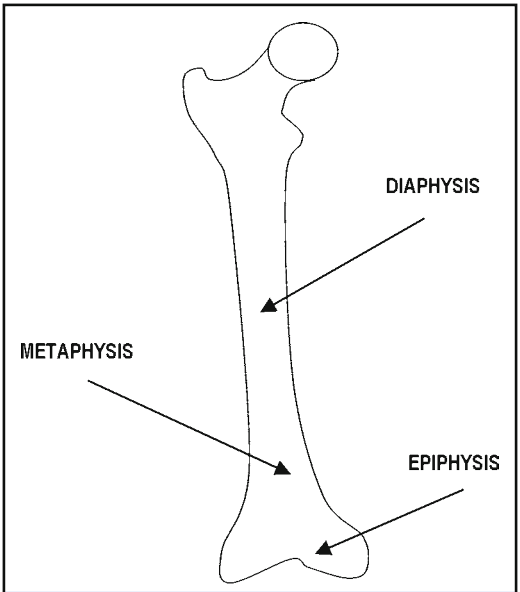
DIAPHYSIS
METAPHYSIS
EPIPHYSIS

FIGURE 46.2 - BASIC LONG BONE ANATOMY
It is important to have a certain level of familiarity with the long bone anatomy

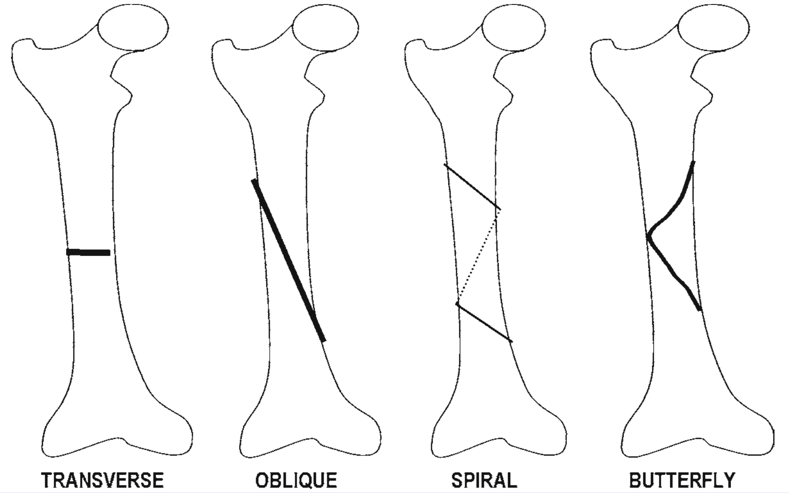
TRANSVERSE
OBLIQUE
SPIRAL
BUTTERFLY

FIGURE 46.3 - FRACTURE NOMENCLATURE
In describing fractures, the referring physician should be able to visualize the fracture without the X-rays. Knowing the nomenclature greatly facilitates this communication

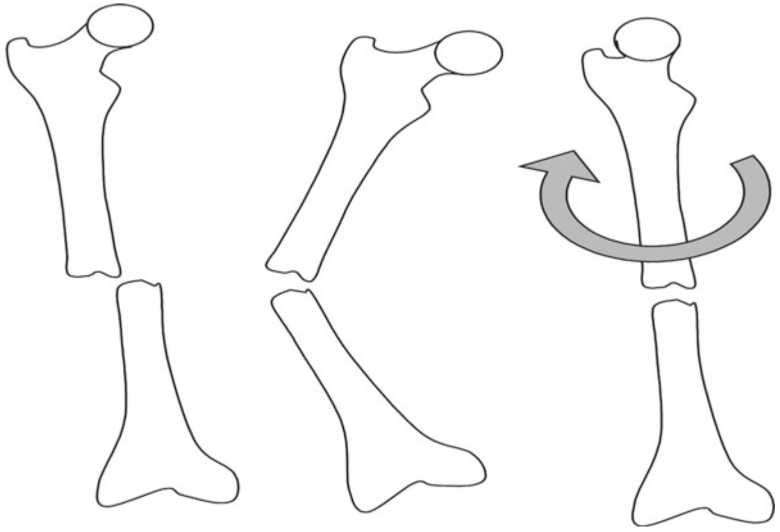

FIGURE 46.4 - FRACTURE FRAGMENT ORIENTATION
In the image on the *left*, there is one shaft width displacement of the distal fracture fragment. In the *middle* image, there is medial angulation of the distal fracture fragments. In the image on the *right*, there is rotation of the fracture fragments

fracture would be "There is a comminuted fracture of the diaphysis of the left femur with medial displacement of the distal fragment, apex lateral angulation, and internal rotation of the distal fragment."

Pediatric Fractures

There are significant differences between the bone of children and adults that are pertinent when discussing skeletal trauma:

1. Bones in children are actively growing and posses growth plates. These growth plates or physes may undergo premature fusion if injured, resulting in growth deformities.
2. The bones of children are more "plastic" than the bones of adults. In addition, their periosteum is thick and durable and may not be torn just because the underlying bone is broken. This may result in a torus (buckle) or greenstick fracture.
3. Fractures in the Salter–Harris classification, by definition, involve the growth plate (physis). A graphic depiction of the nomenclature can be found in Fig. 46.5.

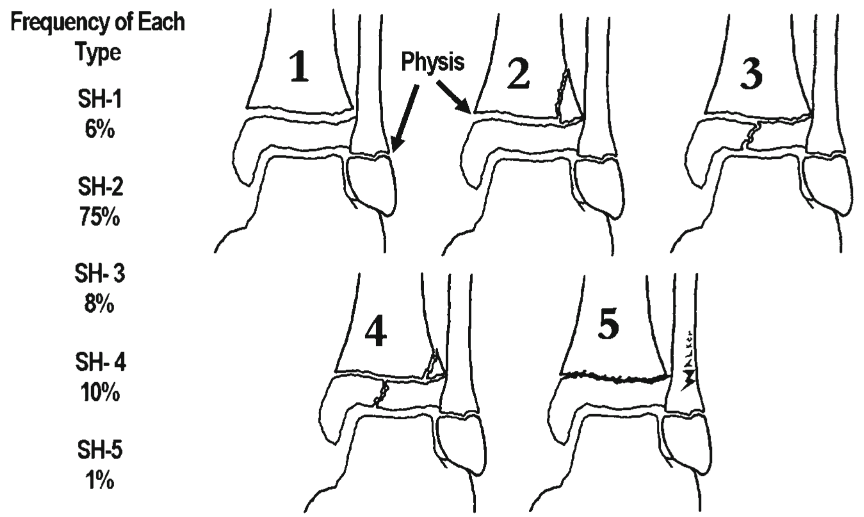

FIGURE 46.5 - SALTER–HARRIS SYSTEM FOR PEDIATRIC FRACTURE CLASSIFICATION
In Salter–Harris 1, the growth plate (physis) is injured and the epiphysis and metaphysis remain intact. As you go farther up the classification, the higher the likelihood of growth plate injury and limb growth retardation. In Salter–Harris 5, the growth plate is crushed (Salter and Harris 1963). Images drawn by Dr. Walker

Salter–Harris Fracture Classification

Salter–Harris 1 – A fracture involving only the growth plate. Since the growth plate is composed of rapidly proliferating cartilage that is transparent radiographically, the diagnosis is made by noting displacement of the epiphysis from the metaphysis. The fracture may not be displaced at the time the radiograph is taken, but the diagnosis is suggested by noting either (1) that the apex or maximum point of soft tissue swelling is directly adjacent to the growth plate or (2) by clinical exam if the patient is tender specifically in the region of the physis.

Salter–Harris 2 – This fracture involves the growth plate and the metaphysis. This fracture is more likely than a Salter–Harris 1 fracture to result in premature closure of the physis with resultant limb shortening or deformity.

Salter–Harris 3 – This involves the growth plate and the epiphysis. Note this is of “higher grade” than Salter–Harris 2 because it involves the articular surface.

Salter–Harris 4 – This involves the growth plate, the metaphysis, and the epiphysis.

Salter–Harris 5 – This is a crush injury to the growth plate. The growth plate will almost certainly go on to premature closure, thereby limiting the growth of the involved limb.

In general, the higher the number in the Salter–Harris classification of pediatric fractures, the greater the likelihood of resultant premature arthritis, physis closure, and/or limb deformity.

Greenstick and Torus Fractures in Children

Because the bones of children are more plastic than those of adults and the periosteum is more durable, torus fractures and greenstick fractures are commonly seen. A greenstick fracture is aptly named because it simulates a break noted when one breaks a freshly cut branch. One side breaks while the other side does not. A torus fracture is often referred to as a "buckle fracture" because there is slight deformity of the cortex on one or both sides of the bone. However, the alignment of the fracture fragments is near anatomic due to the tough periosteum (Fig. 46.6).

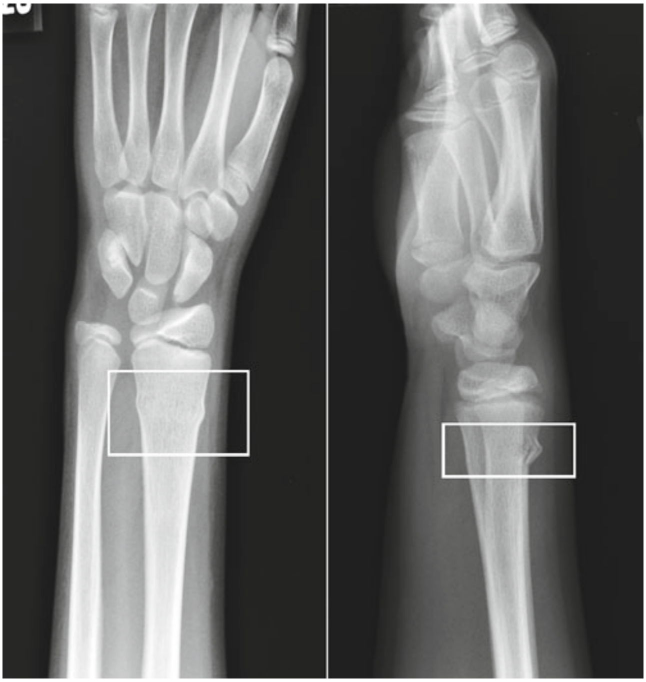

FIGURE 46.6 - TORUS FRACTURE
PA and lateral radiographs demonstrate a buckle fracture of the left distal radial metaphysis

Battered Child Syndrome

The radiologist often plays an important role in making the diagnosis in the "battered child syndrome." The radiographic findings that should alert you to the potential of a battered child are as follows:

1. Multiple fractures at various stages of healing.
2. Fractures of unusual locations like ribs or of unusual mechanism like legs of children who are not yet walking.
3. Spiral fractures.
4. Metaphyseal fractures.
5. Subperiosteal hematomas.
6. Subdural hematoma.

Pathologic Fracture

Figure 46.7 is of a patient with a lytic lesion in the bone as a result of multiple myeloma. Because this has thinned the cortex of the bone and weakened it structurally, a fracture has occurred. This is termed a pathologic fracture. A pathologic

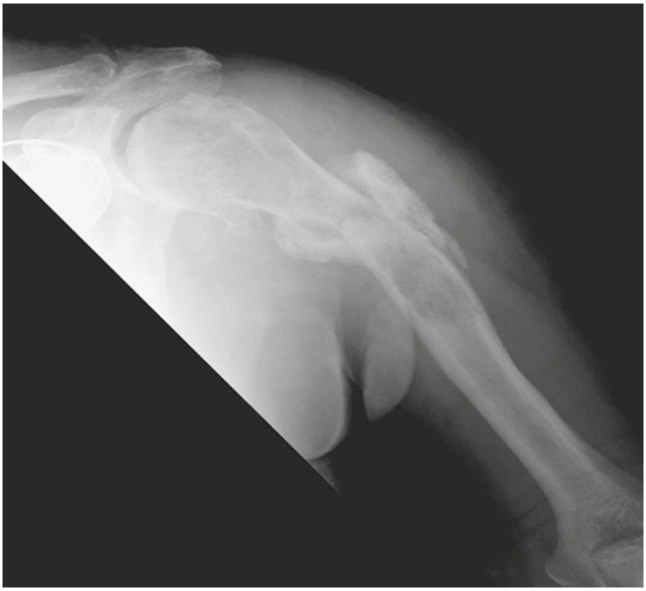

FIGURE 46.7 - PATHOLOGIC FRACTURE
Lytic lesion in the mid left humeral diaphysis with a comminuted proximal pathologic fracture and significant periosteal reaction and callus formation. These findings are consistent with the patient's history of multiple myeloma

fracture is the result of normal stresses in an abnormal bone. The pathologic process can be benign or malignant.

A useful mnemonic for remembering which tumors spread to bone is PB KTL (Lead Kettle – remember lead's symbol is Pb).

P = *P*rostate
B = *B*one
K = *K*idney
T = *T*hyroid
L = *L*ung

Osteoporosis

Osteoporosis refers to thinning of the bones which is most often associated with aging. Screening for osteoporosis is accomplished with a modality called dual energy X-ray absorptiometry (DEXA). All women over age 65 are counseled to get a baseline DEXA exam. It is also recommended that men with a history of vertebral fracture or long-term corticosteroid use get a DEXA scan. A DEXA scan uses approximately 1/10th the radiation dosage of a chest X-ray. Figure 46.8 shows an example of an osteoporotic vertebral column. Note how lucent the vertebrae appear. Figure 46.9 shows an example of a DEXA scan printout.

The patient's bone mineral density (BMD) is compared to two norms. These are calculated as T-scores and Z-scores and reported as standard deviations. T-scores compare the patient's BMD to a healthy 35-year-old's BMD. Meanwhile, Z-scores compare a patient's BMD to an age-matched control. While a Z-score is often measured, the T-score is the number used to define osteopenia and osteoporosis. On the scale, anything above zero is normal. Negative 1 to negative 2.5 is considered osteopenia, which means low bone density. Anything more negative than negative 2.5 is considered to be osteoporosis. A general rule of thumb is that for every standard deviation below normal, the risk of fracture doubles (T-score of negative 1 has double the risk, T-score of negative 2 has four times the risk).

There are three abnormal types of calcifications that you should be familiar with:

1. *Heterotopic ossification* is an abnormal deposition of true bone within soft tissues. It is formed by dormant osteoprogenitor cells in the soft tissue that are caused to differentiate into osteoblasts by a variety of bone morphogenic proteins (BMPs).
2. *Dystrophic calcification* refers to an accumulation of calcium salts in dying tissues (any area of necrosis, AVN, damaged heart valves). This calcification can become heterotopic. Serum calcium is normal.

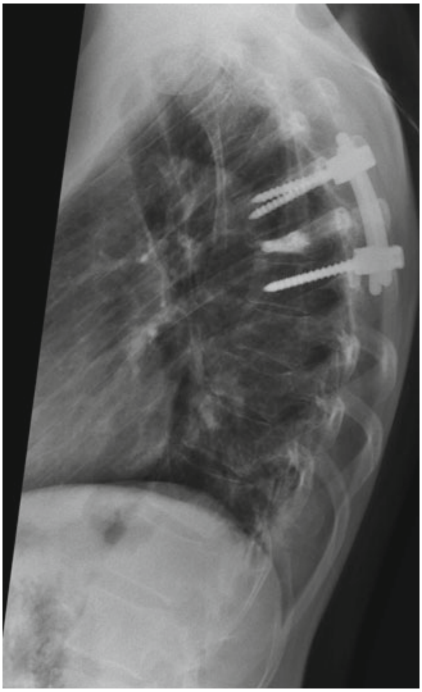

FIGURE 46.8 - OSTEOPOROSIS
Note the lucency of the vertebral column

3. *Metastatic calcification* refers to the deposition of calcium in tissues secondary to hypercalcemia. This may be due to increased parathyroid hormone, destruction of bone by tumors, chronic renal failure, increased vitamin D (Fig. 46.10a–c).

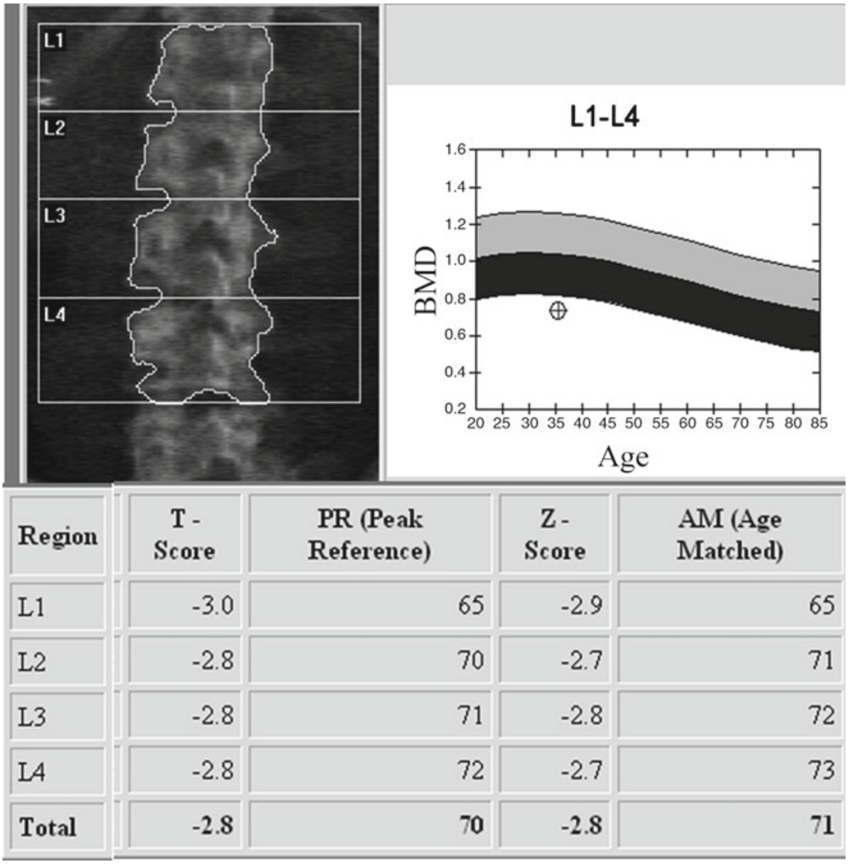
L1
L2
L3
L4
L1-L4
BMD
1.6
1.4
1.2
1.0
0.8
0.6
0.4
0.2
20 25 30 35 40 45 50 55 60 65 70 75 80 85
Age

Region	T - Score	PR (Peak Reference)	Z - Score	AM (Age Matched)
L1	-3.0	65	-2.9	65
L2	-2.8	70	-2.7	71
L3	-2.8	71	-2.8	72
L4	-2.8	72	-2.7	73
Total	**-2.8**	**70**	**-2.8**	**71**

FIGURE 46.9 - DEXA SCAN
Both T- and Z-scores are reported. Note that the risk of fracture is high in this patient

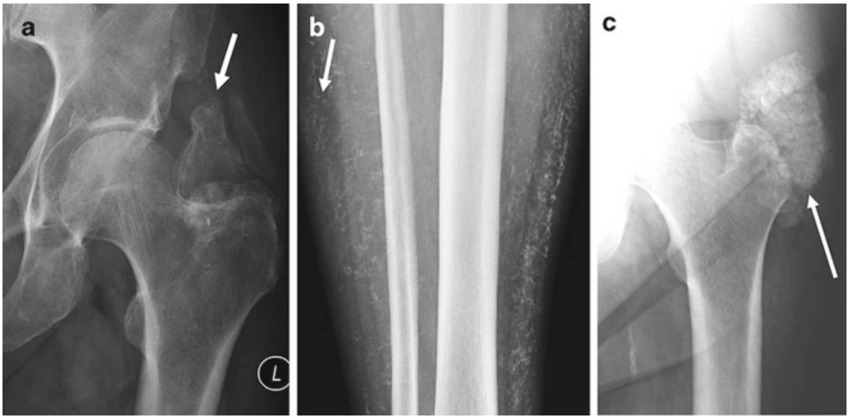

FIGURE 46.10 - SEVERAL TYPES OF CALCIFICATION
(**a**) Heterotopic ossification (*arrows*). (**b**) Dystrophic calcifications are noted in the skin of a patient with peripheral vascular disease. (**c**) Metastatic calcification (tumoral calcinosis) is present above the greater trochanter in a patient with chronic renal failure on dialysis (*arrow*)

Reference

Salter RB, Harris WR. Injuries involving epiphyseal plates. Journal of Bone and Joint Surgery [AM] 1963;45:587–622

47

FRACTURES: PART 2

Objectives:

1. Be able to identify internal and external rotation views of the shoulder.
2. Be able to define normal and abnormal anatomy on the "Y" view of the shoulder.
3. Discuss the significance of a joint effusion in the elbow in the presence of acute trauma.
4. State the mechanism of injury in a Colles' fracture.
5. Discuss the concept of the "Scottie Dog" in evaluating the lumbar spine.
6. Describe the "bony ring" principle and relate its importance to acute trauma involving the pelvis.
7. Describe the classification of femoral neck fractures.
8. Describe the radiographic features of a suprapatellar knee joint effusion.
9. Discuss the imaging of tibial plateau fractures and the significance of a fat fluid level within the knee joint space.
10. List the two main mechanisms of injury in ankle fractures.
11. Define Boehler's angle and its pathologic significance in regard to fractures of the calcaneus.

Shoulder Views

Figure 47.1 shows a normal two view study of the shoulder as might be obtained in the emergency room.

Note the difference between the internal and external rotation views. On internal rotation views the appearance of the humeral head is similar to the smooth round top of an ice cream cone (*I*ce cream = *I*nternal). On external rotation views, the greater tuberosity may be seen clearly in profile. These two views will usually suffice to

H Singh and JA Neutze (eds.), *Radiology Fundamentals: Introduction to Imaging & Technology*, DOI 10.1007/978-1-4614-0944-1_47,
© Springer Science+Business Media, LLC 2012

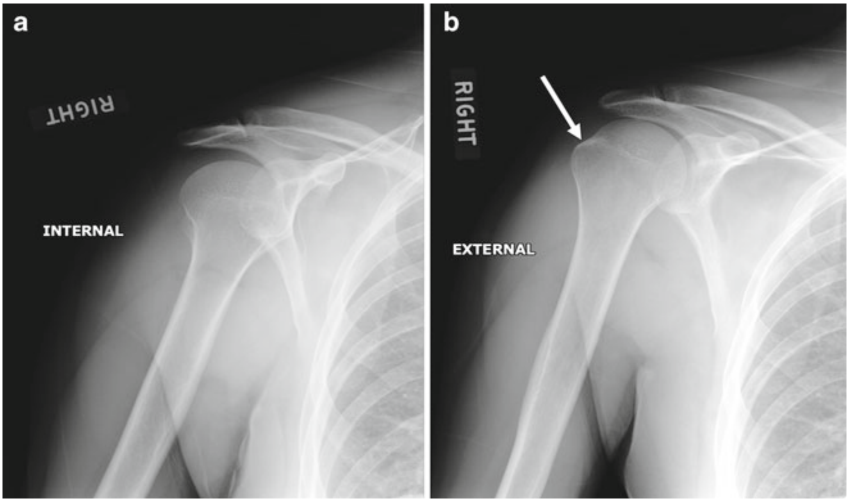

FIGURE 47.1 - (A) INTERNAL AND (B) EXTERNAL ROTATIONAL VIEWS OF THE RIGHT SHOULDER
Arrow shows the greater tuberosity of the humeral head

exclude a fracture. However, dislocation may be more difficult to exclude without views from another projection.

Figure 47.2 is an axillary and scapular "Y" view of the shoulder. Imagine that you are looking upward through the axilla toward the ceiling in a standing patient. You should be able to visualize the clavicle and acromion process anteriorly, the acromio-clavicular joint, and the glenohumeral articulation. Because of the projection of the axillary view, anterior or posterior dislocations are usually well demonstrated. The problem with this view is that it is often very uncomfortable for a patient with an acutely injured shoulder.

A different way of imaging the shoulder in a plane perpendicular to the anterior–posterior projection is called a Y view. In this case, the patient is obliqued slightly and a "lateral view" of the shoulder is obtained. The stem of the Y is the scapular body, while the two upper arms of the Y are the acromion and coracoid processes. At the center of the Y is a circle corresponding to the glenoid fossa. The humeral head should project over the confluence of the three arms of the Y. If the humeral head is posterior to the intersection of the arms of the Y, a posterior dislocation may be diagnosed. Again, remember that posterior dislocation may look normal in the AP view. Note that the scapular "Y" view is not as good as the axillary lateral view for assessing dislocations or subluxation.

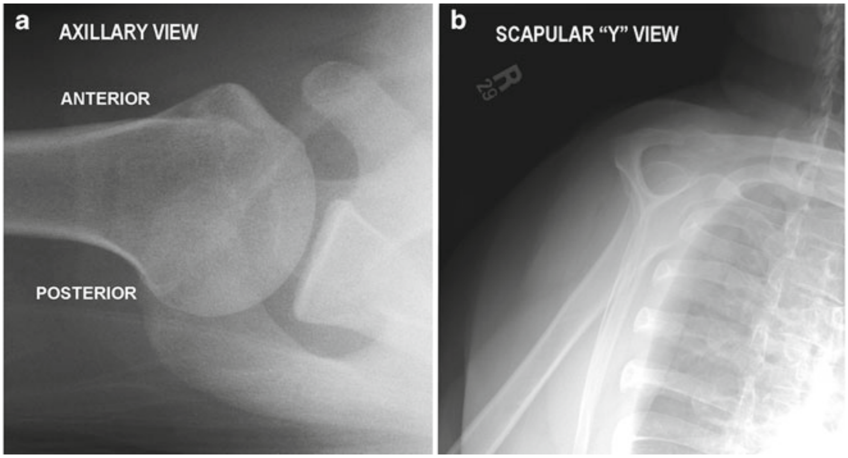

FIGURE 47.2 - ADDITIONAL VIEWS OF THE SHOULDER (A) AXILLARY AND (B) SCAPULAR "Y" VIEWS OF THE RIGHT SHOULDER
Demonstrating appropriate position of the humeral head

Shoulder Dislocation

Figure 47.3 shows a typical anterior (most common) dislocation of the humerus. In anterior dislocation, the humeral head moves inferiorly under the coracoid and slightly medially. This can usually be identified on the routine anterior views (a). The axillary view (b) demonstrates the humeral head anterior to the glenoid.

Figure 47.4 demonstrates a typical posterior dislocation of the humerus. The dislocation is hard to appreciate on the AP view (a), but in posterior dislocations the humerus is always internally rotated (patient cannot externally rotate). Image (b) shows the axillary view with the humeral head posterior to the glenoid. The Grashey view (c) reveals overlap of the humeral head at the glenohumeral joint.

Fat Pad Sign

Figure 47.5 shows a normal and abnormal lateral view of the elbow. In the image on the right, note the presence of the triangular-shaped lucency just anterior to the distal humerus representing the anterior fat pad of the elbow. Fat pads serve as markers for elbow joint effusions. Fluid or blood within the joint will displace them. Elbow joint effusions in the face of acute trauma almost always indicate a fracture. In the image on the right, no obvious fracture is seen. However, there is evidence of

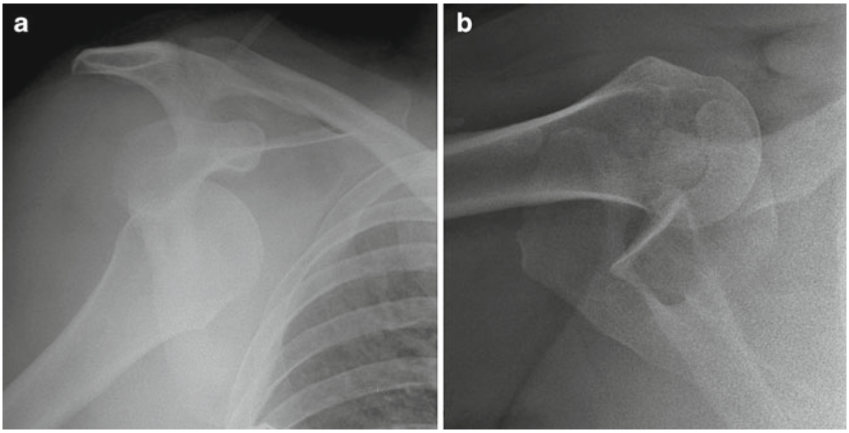

FIGURE 47.3 - ANTERIOR DISLOCATION OF THE SHOULDER
(**a**) Anterior and (**b**) axillary views

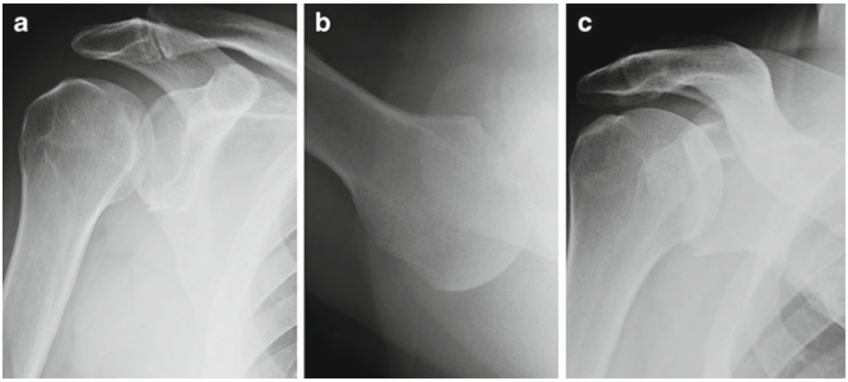

FIGURE 47.4 - POSTERIOR DISLOCATIONS OF THE SHOULDER
(**a**) AP, (**b**) axillary, and (**c**) Grashey views

an elbow joint effusion since the anterior fat pad is displaced (compare to normal). In addition, a posterior fat pad along the posterior aspect of the distal humerus is seen. This always indicates the presence of a joint effusion and usually indicates a fracture, in the proper clinical situation. It is important to understand that while an anterior fat pad sign is more sensitive for joint pathology, a posterior fat pad sign is more specific for occult fracture.

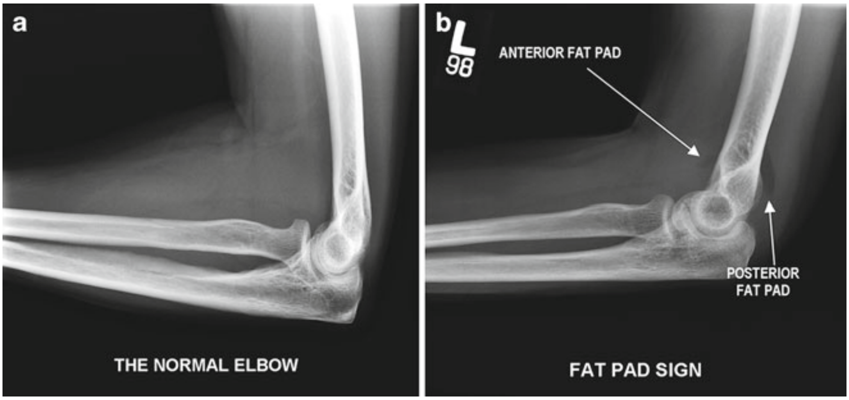

FIGURE 47.5 - (A) THE NORMAL AND (B) ABNORMAL VIEWS OF ELBOW AND FAT PAD SIGN
The image on the *left* is a normal lateral elbow. The triangular lucencies anterior and posterior to the humerus on the *right* image represent displaced fat (fat pad sign) when there is fluid in the elbow joint. Fluid in the joint can be seen in inflammatory conditions. In the setting of trauma, displaced fat pads have a high association with fracture even if the fracture is not immediately visualized

Note that the elbow is not the only joint in which fat pads can be useful. For instance, ankle injuries may reveal a fat pad anterior to the joint between the talus and tibia which may suggest fracture.

These fractures may be occult radiographically. Occasionally, a small fracture of the radial head can be demonstrated with further or follow-up views. Again, whenever an elbow joint effusion is seen in the setting of acute trauma and in the absence of other preexisting reasons for an elbow joint effusion (rheumatoid arthritis, hemophilia) the patient should be treated as if a fracture is present.

Colles' Fracture

Figure 47.6 demonstrates one of the most common wrist injuries. The Colles' fracture is defined as a transverse fracture of the distal metaphysis of the radius with dorsal angulation of the distal fragment commonly caused by falling on an outstretched hand. By the previously described nomenclature, we should say that this fracture has apex volar (palmar) angulation. However, in the case of a fracture near an articular surface we use the direction of the articular surface to describe angulation. Often a Colles' fracture will have an associated fracture of the ulnar styloid process.

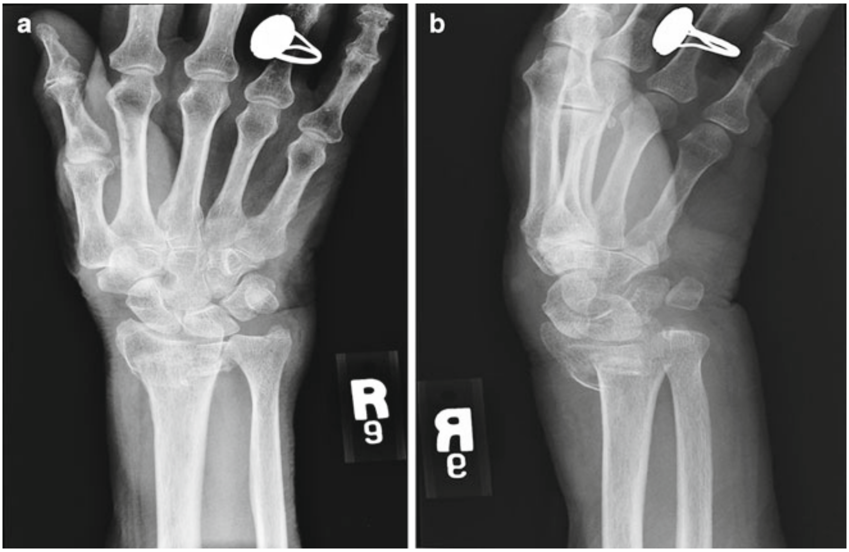

FIGURE 47.6 - COLLES' FRACTURE
(**a**) AP and (**b**) lateral views of the right wrist demonstrate a comminuted, impacted, and intra-articular fracture of the right distal radius, with approximately 20° of dorsal angulation of the distal fragment. Note that there is also deformity and marked soft tissue swelling at the site of injury

The Scottie Dog

Another term you should be familiar with is the Scottie Dog. This refers to the outline of a dog that can be seen on an oblique view of a lumbar vertebra. The eye of the dog corresponds to the pedicle, the snout – the transverse process, the neck – the pars interarticularis, the ear – the superior articular facet and the front leg – the inferior articular facet (Fig. 47.7).

It is important to evaluate these structures, especially the pars interarticularis. A fracture or congenital defect in this region will manifest itself as a lucent (dark) line in the neck of the dog (it looks like a dog collar). This is termed spondylolysis. Spondylolysis can lead to spondylolisthesis which is a slippage of the superior vertebra on the inferior one, most often in the anterior direction. There is a grading system based upon what percentage of the vertebra has slipped forward, but for now, just understand the concept.

Roughly 5% of the population have L5 spondylolisthesis and of those, roughly 5% are symptomatic. In general, spondylolysis with spondylolisthesis is more likely to be symptomatic.

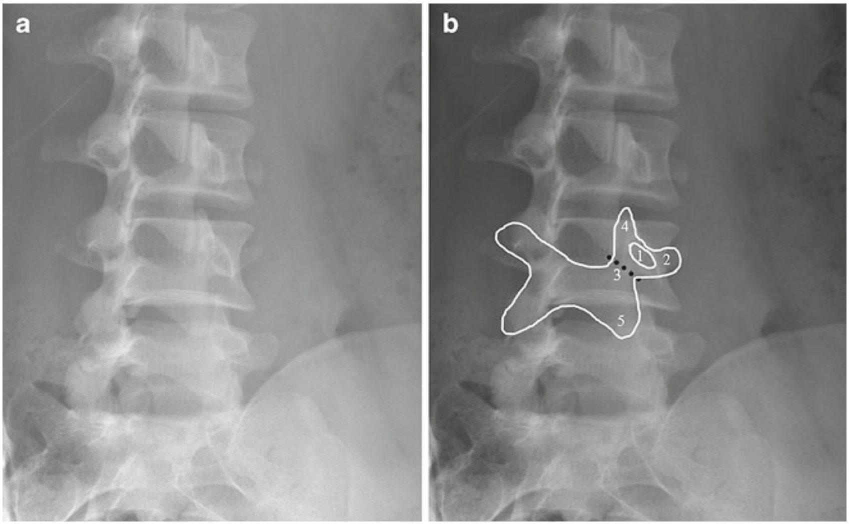

FIGURE 47.7 - (A, B) THE SCOTTIE DOG CONCEPT
(**a**) Oblique lumbar radiograph (**b**) Drawing of the scottie dog on the radiograph. 1 – pedicle, 2 – transverse process, 3 – pars interarticularis, 4 – superior articular facet, and 5 – inferior articular facet. The *dashed line* through the neck that looks like a collar represents what a pars fracture would look like

Pelvic Fractures

Evaluation of the pelvis is often a part of the radiographic evaluation of patients who have undergone acute trauma. One helpful principle in looking for fractures of the pelvis is the “bony ring” concept. Can you break a pretzel ring in only one place? It will always break in two places. This is also true of the pelvis. A fracture or separation in a bony ring is usually associated with at least one other fracture in that ring. Figure 47.8 illustrates this principle. Remember, pelvic fractures also occur in the elderly with much less force secondary to osteoporosis.

Femoral Neck Fractures

The femoral neck is a very common site for acute skeletal trauma. Femoral neck fractures range from quite obvious both clinically and radiographically to very subtle abnormalities radiographically. Fractures are classified according to the site of the fracture within the proximal femur. The most common locations for femoral neck fractures are in the intertrochanteric area extending between the greater and lesser trochanters, and in the subcapital region, that area of the femoral neck just

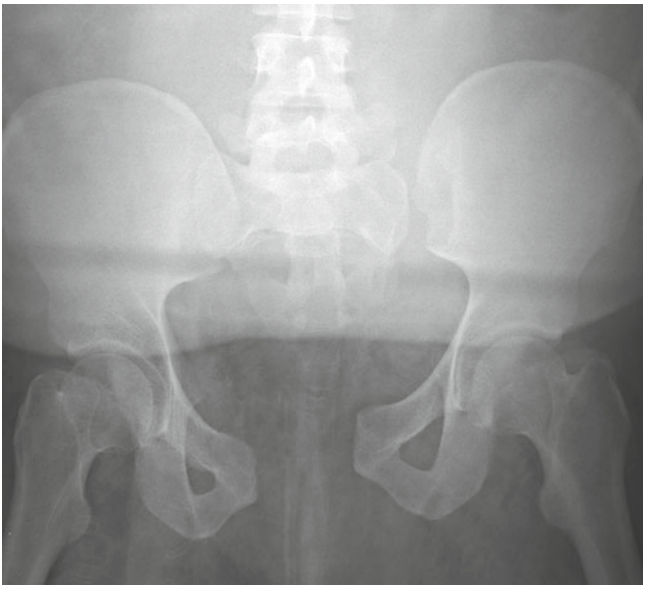

FIGURE 47.8 - PELVIC FRACTURE
There is marked widening of the left sacroiliac joint and the pubic symphysis. Also note that there is extensive soft tissue density in the pelvis consistent with hematoma

distal to the femoral head. Mid-cervical or basi-cervical femoral neck fractures are less common. Internal rotation of the hip will improve evaluation of the femoral neck (Fig. 47.9).

Fractures of the hip may be more extensive than is evident on plain radiograph alone and further imaging, commonly with computed tomography, is often performed. Of course, as with all fractures, two plain film views are required to assess the fracture. A commonly used view with hips is called the cross-table lateral view. An example of this view is shown in Fig. 47.10.

Knee Joint Effusion

Many abnormalities of the knee are associated with a knee joint effusion. The relationship of effusion to fracture is certainly not as strong as that discussed in the last chapter in relation to the elbow. However, the presence of a knee joint effusion may be the only manifestation of a cartilaginous or ligamentous injury in the absence of fracture. On the lateral view, the suprapatellar fat pad is a dark triangle with its apex

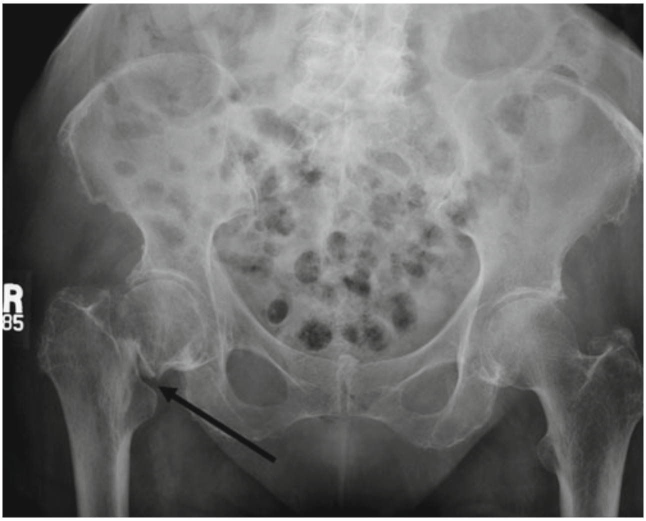

FIGURE 47.9 - FEMORAL NECK FRACTURE
Displaced subcapital fracture in an osteopenic elderly female (*arrow*). Femoral necks would be better evaluated if the hips were internally rotated

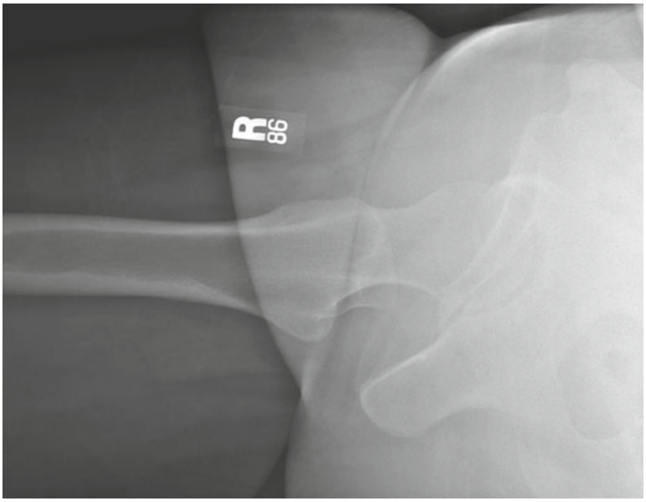

FIGURE 47.10 - CROSS-TABLE LATERAL OF HIP
This gives the radiologist a new view of the femoral neck

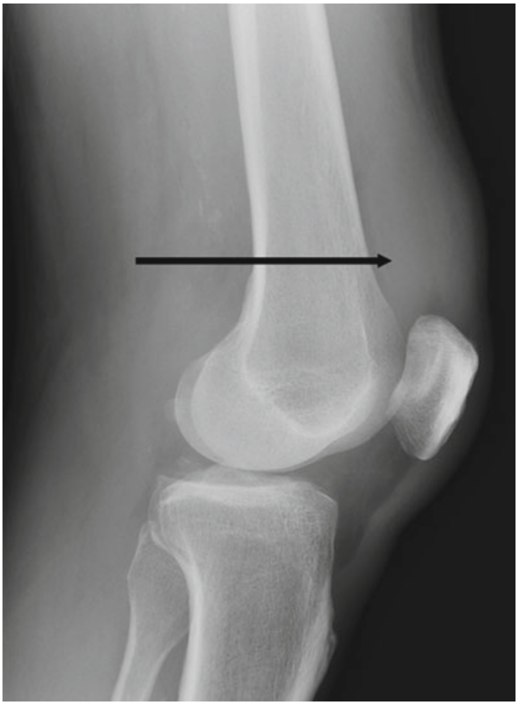

FIGURE 47.11 - KNEE JOINT EFFUSION
Large left knee joint effusion with associated soft tissue swelling (*arrow*)

directed superiorly and its base situated along the superior aspect of the patella itself. The prefemoral fat pad is a broad, anteriorly convex area of decreased density based along the anterior aspect of the distal femur. The suprapatellar pouch of the knee joint is between these fat pads. When there is a knee joint effusion, these two fat pads are separated by more than 5 mm. It is important that, on the lateral view, the knee be appropriately flexed at approximately 30° and that a true lateral view (nonrotated) be obtained when evaluating for a joint effusion (Fig. 47.11).

In some patients who have undergone significant trauma involving the knee, a cross-table lateral view may be performed with the knee straight. When this occurs a transverse interface may be oriented horizontally and represents a fat fluid level. Remember that fat is less dense (darker) radiographically than fluid. Also, fat is of a lesser density than fluid and tends to rise to the top of the joint compartment while the fluid sinks to the bottom. The fat represents marrow contents which have leaked into the joint space as the result of a fracture, usually of the proximal tibia, which involves the articular surface. In patients with a fat fluid level, an intra-articular fracture will invariably be present (Fig. 47.12).

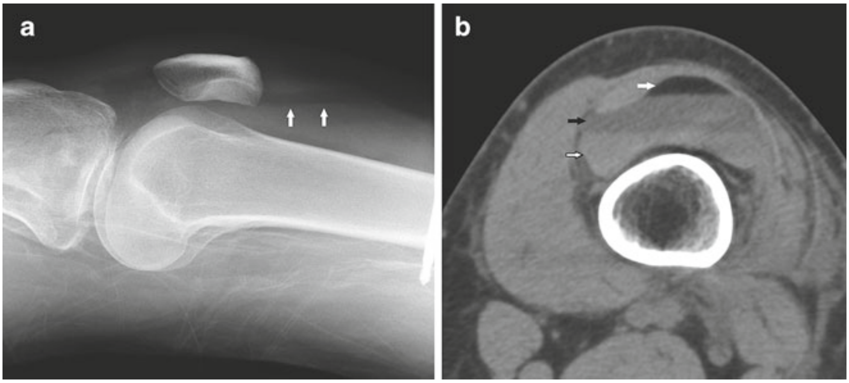

FIGURE 47.12 - LIPOHEMARTHROSIS
(**a**) Shows a cross-table lateral view demonstrating a fat fluid level (*white arrows*). (**b**) Shows the corresponding axial CT slice revealing lipohemarthrosis with fat (*top white arrow*), serum (*black arrow*), and hematocrit fluid levels (*bottom white arrow*)

Tibial Plateau Fractures

A common intra-articular fracture involving the proximal tibia is a so-called tibial plateau fracture. The lateral and medial tibial plateau may be injured by impact from the femoral condyles. This results in a depression of the plateau with subsequent fracture of the underlying bone. The radiographic features of a tibial plateau fracture may be quite subtle with only a small cortical irregularity or plateau depression noted on plain radiographs. Further imaging with computerized tomography is commonly performed to delineate the true extent of the fracture which may be much more extensive than appreciated on the radiograph alone (Fig. 47.13).

Ankle Fractures

Figure 47.14 shows a trimalleolar fracture. There is an oblique fracture of the lateral malleolus (distal fibula), a transverse fracture of the medial malleolus, and seen best on the lateral film, a fracture of the posterior malleolus. In some cases, there may only be a tear of the deltoid ligament (medial aspect of ankle). In these cases, only nonspecific soft tissue swelling may be seen on the radiograph.

During the injury process, different types of rotation stress can result in fractures of the mid or even high fibula. High fractures of the fibula are especially common in eversion (or pronation) type injuries, are called Maisonneuve fractures, and can easily be missed if only ankle radiographs are taken. For this reason, understanding the mechanism of injury is important in deciding which radiographs should be performed.

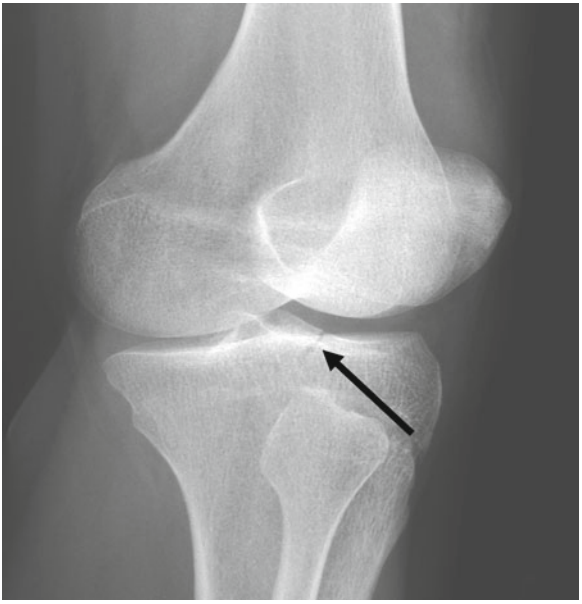

FIGURE 47.13 - TIBIAL PLATEAU FRACTURE
Nondisplaced intra-articular fracture of the lateral tibial plateau

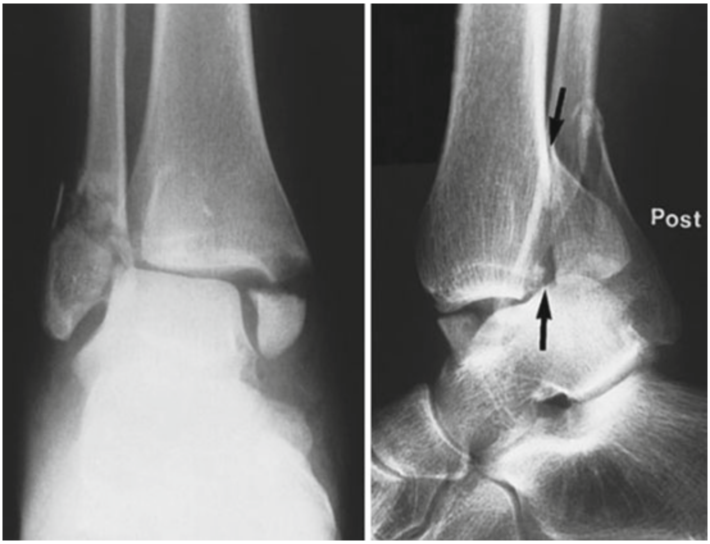

FIGURE 47.14 - TRIMALLEOLAR ANKLE FRACTURE
Note that all three malleoli are fractured

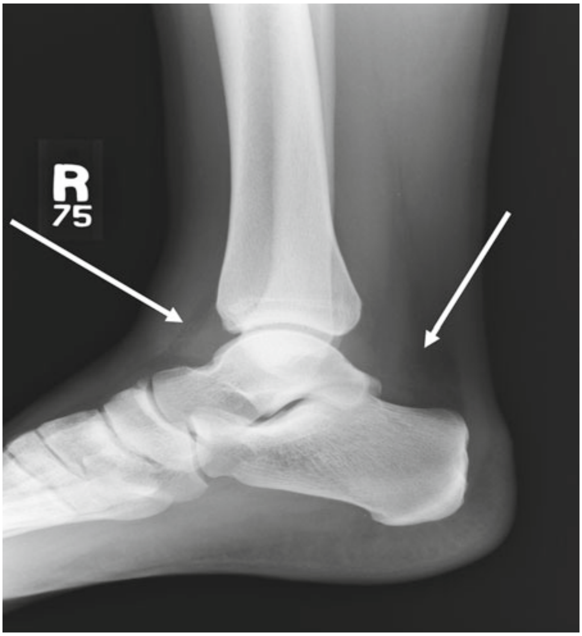

FIGURE 47.15 - ANKLE SPRAIN
This patient presented following an ankle sprain with significant swelling. The *arrows* denote the significant soft tissue swelling over the anterior and posterior-lateral aspects of the ankle joint

Ankle injuries may be divided into inversion and eversion types. One can further subdivide these fractures into inversion (adduction) with or without rotation and eversion (abduction) with or without rotation. The most common type of "twisted ankle" is the inversion injury with rotation. From the location and appearance of the injuries, the mechanism of injury can be ascertained (Fig. 47.15).

There are four areas that are always important to check on a foot or ankle view because fractures can easily be missed in these areas:

1. Base of the fifth metatarsal
2. Lateral talus
3. Superior part of the talus/talar neck
4. Anterior calcaneus

Another term important to be familiar with is Lisfranc injury or fracture. The Lisfranc ligament connects the medial cuneiform to the bases of the first and second metatarsals. Lisfranc injuries tend to be quite difficult to evaluate with plain films. As with most radiographs, it is important to provide a good clinical history which can greatly help the radiologist when attempting to determine if an injury or fracture has occurred.

Since ankle injuries are so common and often imaged, the Ottawa Ankle Rules were developed.[1] These are recommendations to determine when radiographs are necessary to evaluate an ankle injury based on physical exam findings. These recommendations have a sensitivity of nearly 100%. These rules do not apply to pregnant females, children under the age of 18, or patients that cannot follow the test commands (intoxication, etc.)

Ankle radiographs are indicated if there is any pain in the malleolar zone and any one of the following:

1. Bone tenderness along the distal 6 cm of the posterior edge of the tibia or tip of the medial malleolus.
2. Bone tenderness along the distal 6 cm of the posterior edge of the fibula or tip of the lateral malleolus.
3. An inability to bear weight for four steps.

The Ottawa foot rules are followed for assessing whether a foot X-ray series is indicated. Foot radiographs are indicated if there is any pain in the midfoot zone and any one of the following:

1. Bone tenderness at the base of the fifth metatarsal (for foot injuries)
2. Bone tenderness at the navicular bone (for foot injuries)
3. An inability to bear weight for four steps.

A common foot injury occurs when a patient jumps from a high location, landing on his feet. Often the bone that bears the brunt of the initial impact is the calcaneus. The calcaneus may be evaluated on the lateral view by calculating Boehler's angle, normal between 20° and 40°. The angle is reduced when a fracture is present (Fig. 47.16). The fracture itself may not be evident merely by searching for fracture lines within the bone.

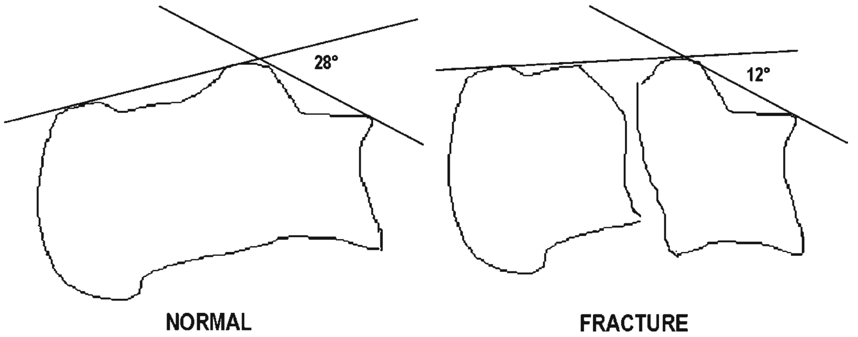

FIGURE 47.16 - BOEHLER'S ANGLE
On the *left*, the diagram demonstrates the normal angle of 28° formed by the intersection of the anterior and the posterior aspect of the calcaneus. With axial-loading injuries (i.e., landing feet first), the calcaneus is fractured. The angle then is reduced and is noted to be less than 28°

Note that calcaneal injuries are often bilateral and can be associated with other axial-loading injuries such as tibial plateau or thoracolumbar spine fractures.

Reference

1. *Wofle M, Uhl T, Mccluskey L. Management of Ankle Sprains. Am Fam Physician.* 2001 Jan 1;63(1):93–105.

48

ARTHRITIDES

Objectives:

1. List four features which allow distinctions between rheumatoid arthritis/rheumatic variants and osteoarthritis.
2. List three findings seen in the skeleton in gout and explain how they differ from those seen in rheumatoid arthritis.

Osteoarthritis

The typical radiographic characteristics of osteoarthritis include (Fig. 48.1)

1. *Asymmetric joint space narrowing* – This indicates loss of articular cartilage. For example, the hip migrates superiorly because of the loss of cartilage superiorly along the weight-bearing surface.
2. *Subchondral sclerosis* (*also called eburnation*) – This is caused by trabecular compression and fracture with callus formation.
3. *Osteophyte formation*.

Figure 48.2 is an example of asymmetric joint space narrowing which reflects thinning of the cartilage in the medial aspect of the joint, the area of maximal weight bearing. The body reacts to this change in its weight-bearing surface by increasing the thickness at the margins of the weight-bearing area resulting in subchondral sclerosis and reinforcement of the ligamentous support of the knee through the formation of spurs or osteophytes.

This new bone formation is what characterizes degenerative or osteoarthritis and allows it to be separated from rheumatoid arthritis and the rheumatoid variants.

H Singh and JA Neutze (eds.), *Radiology Fundamentals: Introduction to Imaging & Technology*, DOI 10.1007/978-1-4614-0944-1_48,
© Springer Science+Business Media, LLC 2012

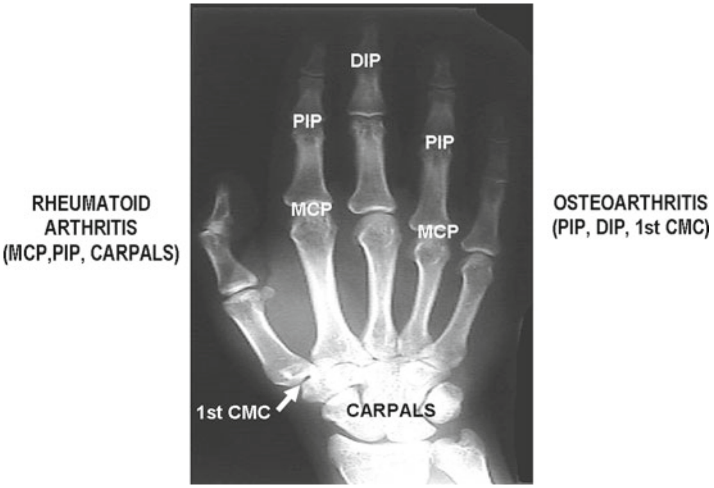
DIP
PIP
PIP
MCP
MCP
RHEUMATOID ARTHRITIS (MCP,PIP, CARPALS)
OSTEOARTHRITIS (PIP, DIP, 1st CMC)
1st CMC
CARPALS

FIGURE 48.1 - DISTRIBUTION OF OSTEOARTHRITIS VS. RHEUMATOID ARTHRITIS
Osteoarthritis, characterized by joint space narrowing, subchondral sclerosis (also called eburnation), and osteophyte formation tends to affect the proximal and distal interphalangeal joints, as well as the first carpometacarpal joint. Rheumatoid arthritis, characterized by periarticular osteoporosis, marginal erosions, boutonniere deformity, swan neck deformity, subluxations, and dislocations, tends to affect the metacarpophalangeal joints and proximal interphalangeal joints

Rheumatoid Arthritis

Figure 48.3 demonstrates a case of rheumatoid arthritis. In rheumatoid arthritis, there is symmetric joint space narrowing and loss of bone density. These findings help distinguish rheumatoid arthritis from osteoarthritis.

In addition, look for marginal erosions along the articular surfaces. Again, these erosions help distinguish the rheumatoid type arthritides from osteoarthritis.

Distinctions Between Osteoarthritis and Rheumatoid Arthritis

Note again that in osteoarthritis (OA) there is asymmetric joint space narrowing, subchondral sclerosis, and osteophyte formation. Also note that the main areas of involvement are in the distal interphalangeal joints with relative sparing of the metacarpophalangeal joints and intercarpal joints. Osteophytes formed about the DIP

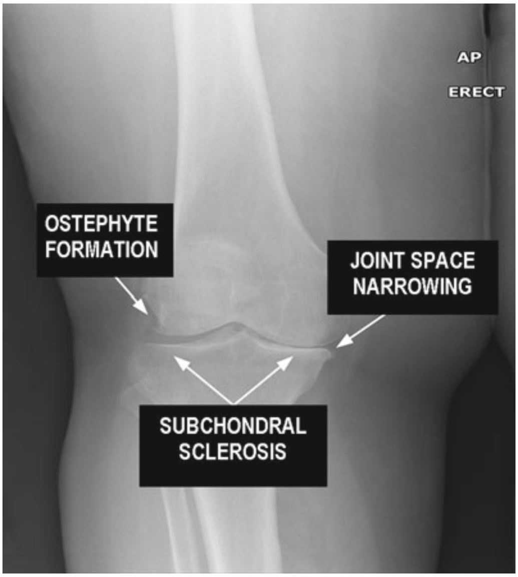
AP
ERECT
OSTEPHYTE FORMATION
JOINT SPACE NARROWING
SUBCHONDRAL SCLEROSIS

FIGURE 48.2 - OSTEOARTHRITIC KNEE
Right knee displaying osteophyte formation, joint space narrowing and subchondral sclerosis, consistent with severe osteoarthritis

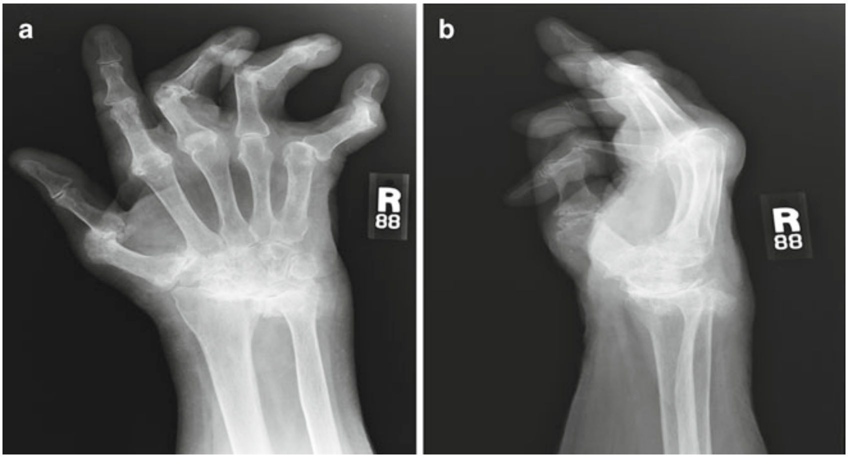

FIGURE 48.3 - SEVERE RHEUMATOID ARTHRITIS
AP (**a**) and lateral (**b**) views show a boutonniere deformity of the fifth digit, with hyperflexion at the PIP joints and hyperextension at the DIP joints. There are severe ulnar subluxations and marginal erosions. Diffuse joint space narrowing is noted at the carpal joints and the metacarpophalangeal joints

joints are referred to as Heberden's nodes while those at the PIP joints are referred to as Bouchard's nodes. Osteoarthritis begins peripherally and as it becomes more severe, progresses to involve the PIP joints. The only exception from the distal to proximal migration of osteoarthritis would be the first (thumb) carpometacarpal joint. This is a common site of osteoarthritis proximally.

On the other hand, in rheumatoid arthritis (RA) there is symmetric joint space narrowing and periarticular erosions (which can be quite subtle in the early stages). RA usually involves the intercarpal joints and metacarpophalangeal joints at an early stage. There is ulnar deviation and erosions in the late stages of RA. You should be able to distinguish osteoarthritis from the rheumatoid type arthritides in most cases. However, in very advanced disease, degenerative arthritis may be superimposed on preexisting rheumatoid type arthritis. Other arthritides, which may look like osteoarthritis, include the arthritis produced by pseudogout (calcium pyrophosphate deposition disease) and hemochromatosis. Other than rheumatoid arthritis, arthritides which produce erosions include psoriatic arthritis, and enteropathic arthritis (associated with Crohn's Disease and ulcerative colitis).

Gout

Figure 48.4 demonstrates a patient with gout. You should note the following:

1. *Soft tissue tophi*: Lumpy bumpy pattern of soft tissue swelling that may mineralize in a small percentage of cases.
2. *Pressure erosions*: These occur in the regions of soft tissue tophi. Unlike the erosions of rheumatoid arthritis, they are further from the joint (periarticular) and have characteristic sharply defined overhanging edges.
3. *Joint destruction*: This is usually late in the disease and contiguous to the tophus. The joint spaces are characteristically normal in joints that are not destroyed.

In summary, gout is a disease of the soft tissues near the joints, not of the intra-articular portions of the joint itself.

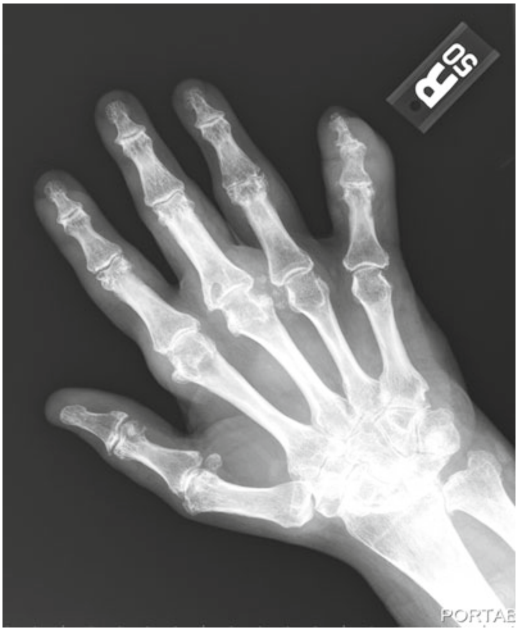

FIGURE 48.4 - GOUT
Nodular soft tissue swelling most impressive in the distal little finger, but also involving the ring, middle, and index fingers Findings are consistent with tophaceous gout

49

BONE TUMOR CHARACTERISTICS

Objectives:

1. Name the two most important variables when creating a differential for bone tumors.
2. Name three lesional characteristics that further refine a differential of bone tumors.
3. Understand the difference between aggressive/nonaggressive and benign/malignant.

This chapter is not an exhaustive description detailing the characteristics of various types of bone tumors. It does, however, provide a paradigm to evaluate and classify types of bone tumors which allows for the creation of a useful differential diagnosis when a new bone tumor is encountered in clinical practice.

The two most important aspects when evaluating a bone tumor lesion and creating a differential diagnosis is to note the age of the patient and the location of the lesion.

Skeletal maturity is the most important variable used to classify bone tumors. That is, certain tumors have a predilection for certain age ranges (less than 20 years old, between 20 and 40, and older than 40 years old). For instance, primary bone malignancies are uncommon in patients older than 40 years old. In this age group, a bony malignancy is much more likely to be a metastatic lesion or multiple myeloma.

The second most important way to classify a bone tumor is based upon the tumor's location. Most tumors have a predilection for specific locations within bone, i.e., diaphysis, metaphysis (site of rapid bone growth) and epiphysis. Axial skeleton vs. appendicular skeleton or long vs. flat bones are other important factors regarding location. As an example, a Ewing sarcoma follows the course of red marrow. Therefore in children, it is often found in the diaphysis of long bones and in young adults it has a predilection for flat bones such as the pelvis, reflecting the normal evolution of red marrow distribution.

H Singh and JA Neutze (eds.), *Radiology Fundamentals: Introduction to Imaging & Technology*, DOI 10.1007/978-1-4614-0944-1_49,
© Springer Science+Business Media, LLC 2012

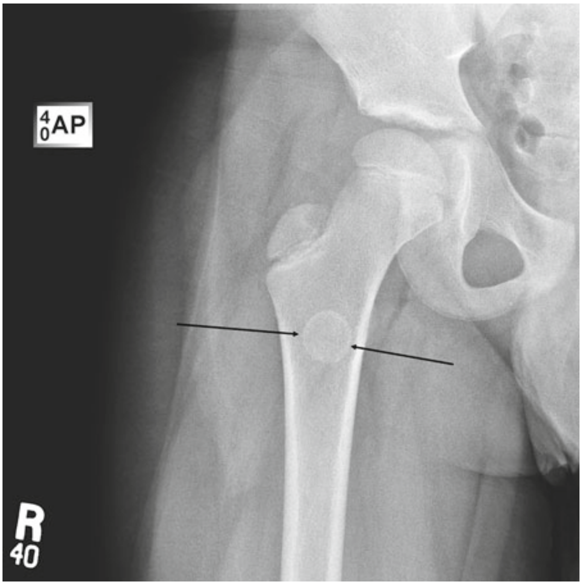

FIGURE 49.1 - NONAGGRESSIVE LESION
Thin white (sclerotic) rim margins indicate a nonaggressive lesion

Certain features of the appearance of lesion itself are quite important. Most notable are the margins of the lesion. The sharper the margins, especially if there is a sclerotic (white) rim, the less aggressive the lesion is (Fig. 49.1). The more indistinct and ill-defined the margin, the more aggressive the lesion. The most aggressive lesions have a characteristic appearance called "moth eaten" or "permeative" (Fig. 49.2). These terms refer to small, patchy, ill-defined areas of destruction.

Furthermore, the presence of periosteal reaction and its appearance is an important characteristic in evaluating a bone lesion. A solid or unilamellar periosteal reaction signifies that a tumor is slow growing, allowing the bone to "wall off" the lesion (Fig. 49.3). A multilamellated appearance, also known as "onionskin appearance," suggests an intermediate aggressiveness. Periosteal reaction that is spiculated in appearance, "hair on end," is the most aggressive periosteal appearance (Fig. 49.4a, b). A Codman triangle refers to an elevation of the periosteum away from the cortex. This term is classically associated with an osteosarcoma, but is not limited to this as any number of malignant or benign processes can cause this feature.

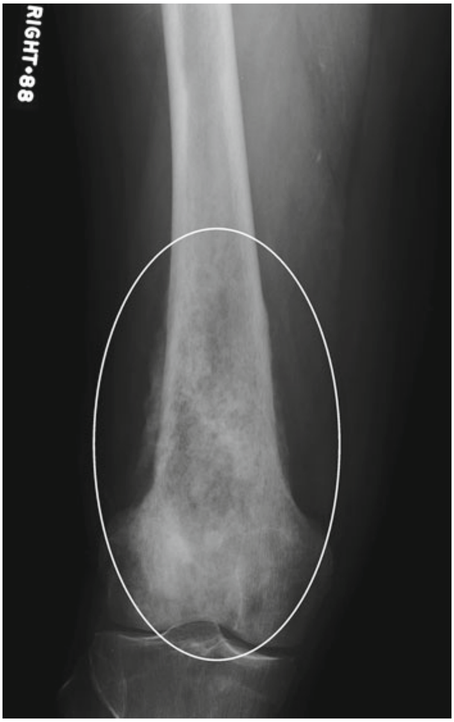

FIGURE 49.2 - AGGRESSIVE BONE LESION
Example of permeative or “moth eaten” appearance of an aggressive lesion

Evaluating the matrix mineralization of a bone tumor can help classify the lesion and further refine the differential diagnosis. A tumor producing new bone will have a fluffy or cloud-like amorphous matrix appearance (Fig. 49.5). Whereas a chondral (cartilaginous) tumor will have matrix mineralization that appears as punctate arc and ring calcifications (Fig. 49.6). CT is often better than plain film at this delineating the type of matrix mineralization.

Finally, it is imperative to understand that aggressive and nonaggressive are not synonymous with malignant and benign. Though a very aggressive-appearing lesion is more likely malignant than a nonaggressive one, certain lesions can be aggressive and benign and vice versa. For example, osteomyelitis often appears aggressive but is clearly not malignant, whereas a giant cell tumor may look nonaggressive but can be malignant.

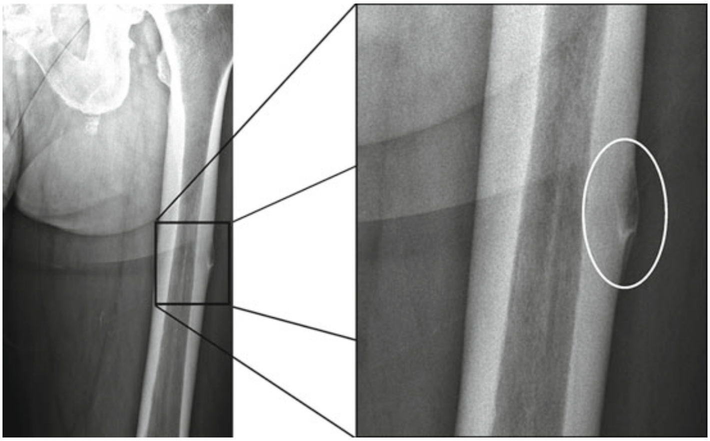

FIGURE 49.3 - SOLID PERIOSTEAL REACTION
Unilamellated or solid periosteal reaction usually found with nonaggressive lesions

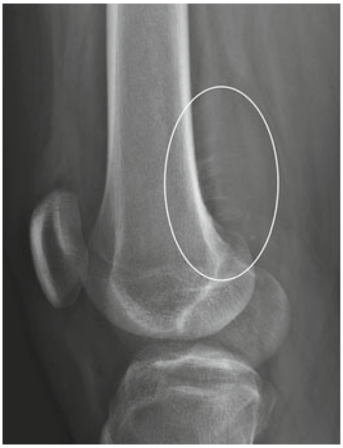

FIGURE 49.4 - AGGRESSIVE PERIOSTEAL REACTION
Radiographic appearance of the classic “hair on end” periosteal reaction characteristic of aggressive lesions

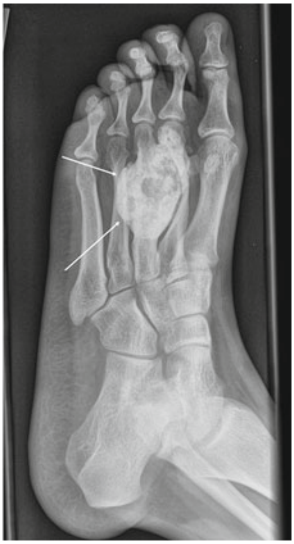

FIGURE 49.5 - OSTEOID MATRIX
Lesion arising from the second metatarsal which has an osteoid matrix characterized by the fluffy, cloud-like appearance

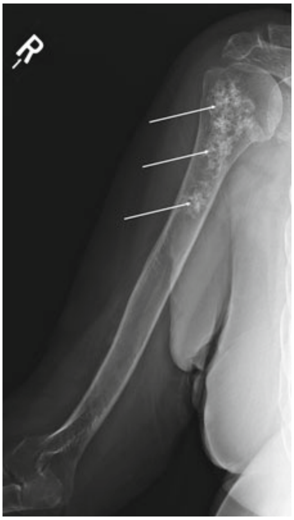

FIGURE 49.6 - CHONDROID MATRIX
Lesion arising in the proximal humerus with chondroid matrix characterized by arc and ring calcifications

50

CNS ANATOMY

Objectives:

1. Identify the important normal anatomic landmarks on brain CT and MRI.
2. Describe how you would differentiate an enhanced (intravenous contrast) from an unenhanced CT scan of the head.
3. Understand the basic principle of image formation in MRI.

Figures 50.1 and 50.2 demonstrate a normal CT and MRI of the brain. Be sure to become familiar with the labeled structures.

Note that on CT scans which are performed after administration of intravenous contrast the Circle of Willis, as well as other various cortical vascular structures, is prominently displayed. You should be able to identify the anterior cerebral artery, the middle cerebral artery, the posterior cerebral artery, and the region of the anterior and posterior communicating arteries.

MRI technology uses powerful magnets with magnetic fields several times more powerful than the Earth's gravitational field. Hydrogen atoms are normally spinning in a random fashion. When a magnetic field is applied to the atoms, the magnetic poles of the hydrogen atoms are aligned. The magnetic field is then turned off and the alignment of the hydrogen atoms degrades. With the degradation, a radiofrequency signal is given off which is then recorded and analyzed by the computer. From this information, an image is formed (see Chap. 6).

H Singh and JA Neutze (eds.), *Radiology Fundamentals: Introduction to Imaging & Technology*, DOI 10.1007/978-1-4614-0944-1_50,
© Springer Science+Business Media, LLC 2012

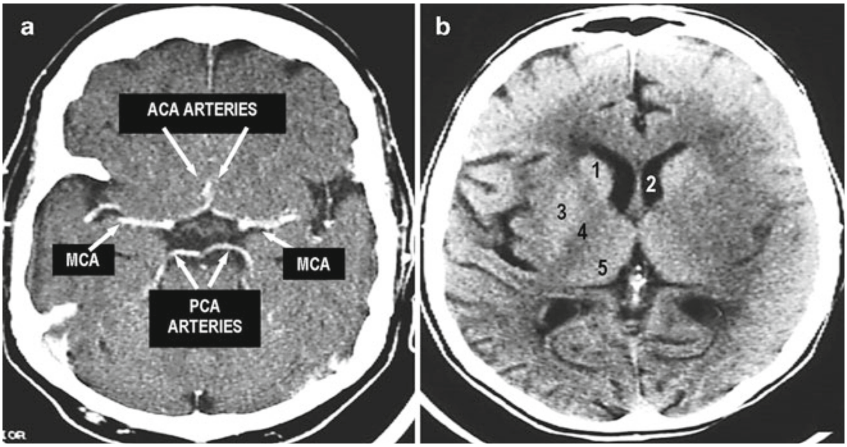
a
ACA ARTERIES
MCA
MCA
PCA ARTERIES
b
1
2
3
4
5

FIGURE 50.1 - BASIC CT NEUROANATOMY
The image on the *left* (**a**) shows the intracerebral circulation (Circle of Willis), which is clearly evident postcontrast. On the noncontrast image (**b**) the following structures have been labeled (1) caudate, (2) lateral ventricle frontal horn, (3) putamen and globus pallidus, (4) internal capsule (extends anteriorly), and (5) thalamus

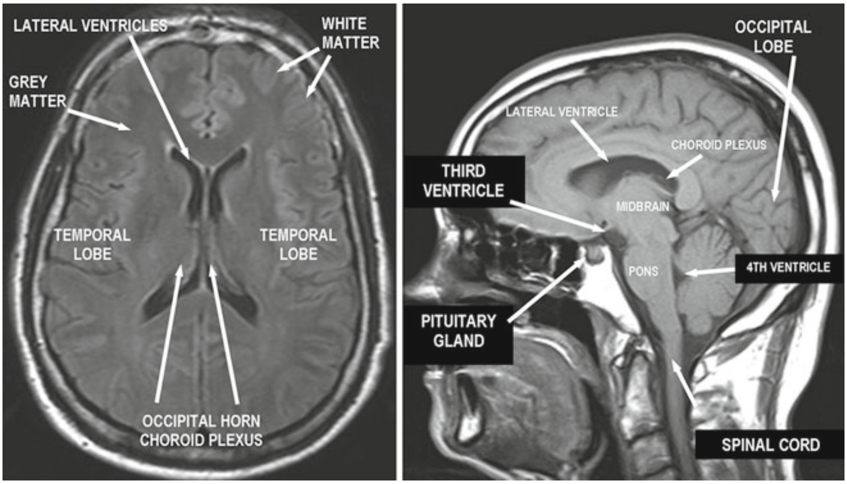
LATERAL VENTRICLES
WHITE MATTER
GREY MATTER
TEMPORAL LOBE
TEMPORAL LOBE
OCCIPITAL HORN CHOROID PLEXUS
OCCIPITAL LOBE
LATERAL VENTRICLE
CHOROID PLEXUS
THIRD VENTRICLE
MIDBRAIN
PONS
4TH VENTRICLE
PITUITARY GLAND
SPINAL CORD

FIGURE 50.2 - BASIC MRI ANATOMY
Note the tissue contrast resolution allowing for identification of many structural details

51

THE CERVICAL SPINE

Objectives:

1. To know the various imaging modalities in evaluation of the cervical spine.
2. To develop a systematic approach to evaluating the cervical spine.

Plain radiographs of the cervical spine are the initial imaging modality, where the frontal, lateral, and AP views may be supplemented by additional views (like the "open-mouth" and extension/flexion views) (Fig. 51.1). Screening in spine trauma begins with plain radiographs as traumatic injuries must be ruled out prior to moving the patient for other views and further treatment. Bony evaluation is now more commonly performed with CT which has much higher resolution and can provide multiplanar reformations. MRI is the modality of choice when spinal cord injury, ligamentous, or soft tissue injury is suspected. A systematic and thorough review as outlined in the following steps is mandatory.

Systematic Approach to Evaluating the Cervical Spine with CT or Plain Film

Step 1: Count the visualized cervical vertebral bodies. It is mandatory that all seven cervical vertebrae (both the body and posterior elements) as well as the relationship of the inferior aspect of C7 with T1 are visualized.

Step 2: Check the alignment of the anterior aspects of the vertebral bodies; the anterior vertebral line. There should be a smooth curve that is convex anteriorly as one progresses from superior to inferior in the cervical spine. Loss of this curvature may indicate muscle spasm or soft tissue injury if the curvature is straightened or reversed. If the curvature changes abruptly, a fracture is likely.

H Singh and JA Neutze (eds.), *Radiology Fundamentals: Introduction to Imaging & Technology*, DOI 10.1007/978-1-4614-0944-1_51,

© Springer Science+Business Media, LLC 2012

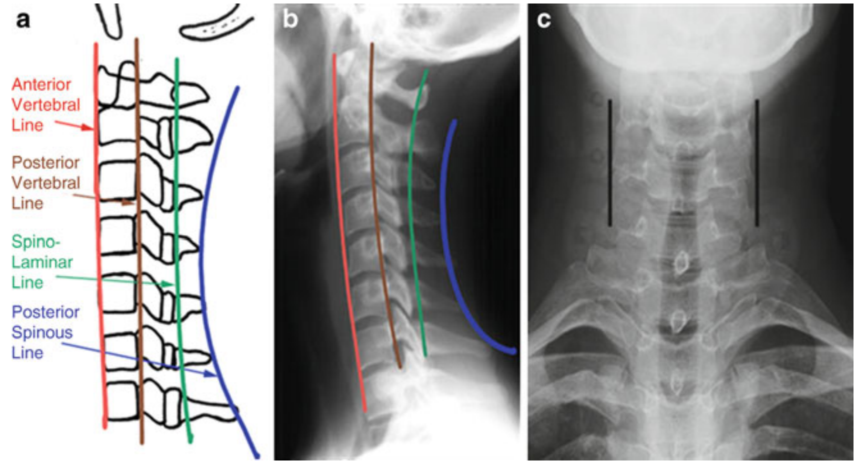

FIGURE 51.1 - (A–C) CERVICAL SPINE LATERAL AND AP VIEWS
The anatomical landmarks are labeled on the diagram (**a**) and subsequently shown on the lateral radiograph (**b**). Note the undulating, rhythmic appearance of the lateral aspects of the cervical spine, bilaterally (**c**)

Step 3: Check the alignment of the posterior aspects of the vertebral bodies (posterior vertebral line, which represents the anterior aspect of the bony spinal canal). For obvious reasons, this curvature should parallel the curvature of the anterior aspect of the vertebral bodies (Fig. 51.2). Abnormalities of this curvature have the same significance as those of the anterior vertebral body curvature.

Step 4: Check the alignment of the spino-laminar line. This is a smooth line drawn along the anterior aspect of the spinous processes (which represents the posterior aspect of the bony spinal canal). Again, any disruption of this smooth curvature should be viewed with suspicion.

Step 5: Check the distance between the posterior aspect of the anterior arch of C1 and the anterior aspect of the odontoid process. This is the atlanto-axial space (sometimes called the predental space). Any increase in this distance may represent disruption of the transverse ligament that secures the posterior aspect of the dens to the atlas. The upper limit of normal for adults is 2.5 mm. Check the prevertebral soft tissues. As a general rule, think 6 and 2: at C2 they should be maximally 6 mm wide and at C6 they should be maximally 22 mm wide. An open-mouth odontoid view is helpful to look for fractures of the odontoid process of C1 and the status of the lateral masses of C2 (Fig. 51.3).

The approach in evaluating a cervical spine CT is similar to that of a radiograph. However, with multiplanar reformats and better resolution, CT is much more sensitive than plain radiography. With the advent of multidetector CT, bony evaluation of the cervical spine has now been overtaken by CT, but the principles outlined above can be applied to any imaging modality.

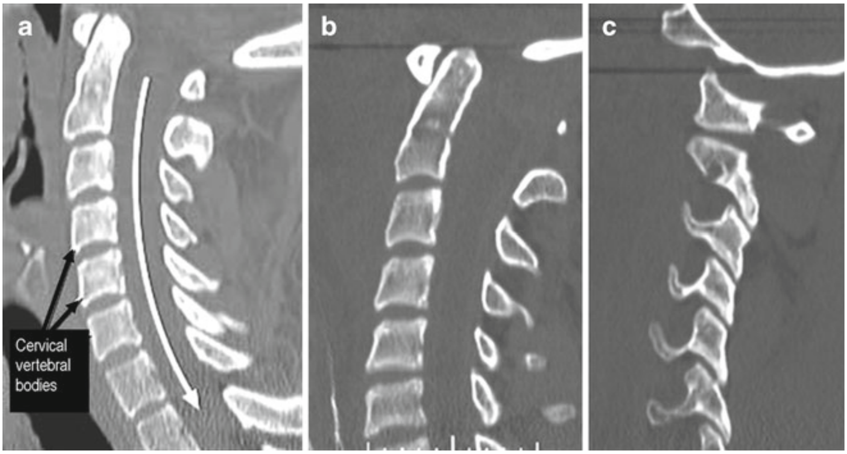
a
b
c
Cervical vertebral bodies

FIGURE 51.2 - CERVICAL SPINE CT SAGITTAL VIEWS
Midsagittal (**a**) and the parasagittal images (**b,c**) of the cervical spine with normal alignment of the vertebrae with maintained body heights and normal facet articulations

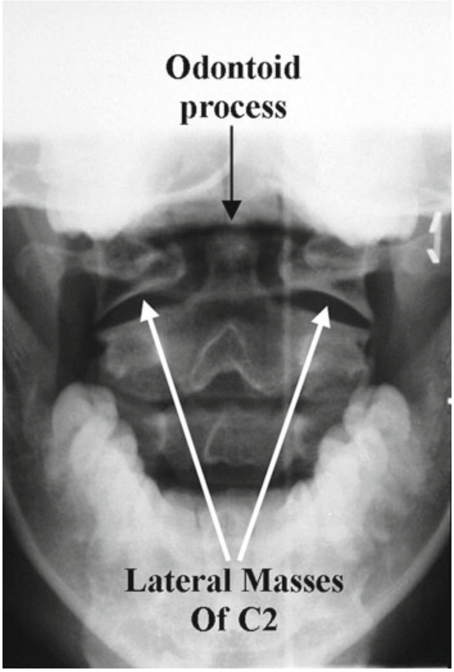
Odontoid process
Lateral Masses Of C2

FIGURE 51.3 - OPEN-MOUTH ODONTOID VIEW
The AP open-mouth odontoid view provides an unobstructed view of both the odontoid process of C2 and the lateral masses of C1

MRI in the Cervical Spine Evaluation

MRI is very useful for evaluating spinal injuries. It is especially helpful for diagnosing or ruling out spinal cord injuries and acute compression of the spinal cord when clinical examination shows muscle weakness or paralysis. MRI is able to detect subtle changes in the vertebral column that may be an early stage of fracture, infection, or tumor. The imaging modality may be better than CT scanning for evaluating tumors, abscesses, and other masses near the spinal cord (Fig. 51.4).

Evaluation of cervical spine MRI begins with the assessment of alignment, vertebral body heights and presence abnormal marrow signal. Disc and ligaments are much better seen on MRI as compared to CT. The most important feature of MRI of the cervical spine is evaluation of the spinal cord. Cord compression, canal stenosis or abnormal signal within the cord can be evaluated. Finally, the pre/paravertebral soft tissues and muscles are evaluated to look for any hematoma or pathologic masses.

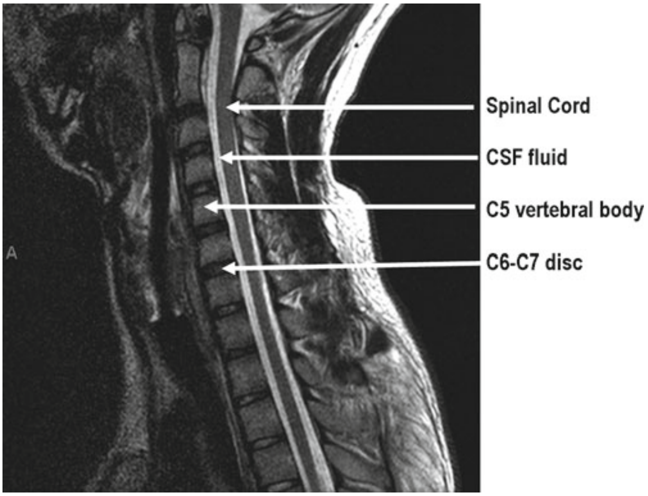

FIGURE 51.4 - SAGITTAL CERVICAL SPINE MRI
T2-weighted MRI of cervical spine shows normal alignment of the vertebrae with normal bone marrow and spinal cord signal

52

HEAD TRAUMA

Objectives:
1. Describe the role of skull radiographs in head trauma.
2. Describe the appearance of an epidural hematoma on a head CT scan.
3. Describe the appearance of a subdural hematoma on a head CT scan.
4. Describe the appearance of a subarachnoid hemorrhage on a head CT and MRI.
5. Describe the findings on CT/MRI in a patient with cerebral contusion.
6. Describe the appearance of Diffuse Axonal Injury on CT/MRI.

Skull Radiograph

With the advent of CT scans, the role of routine skull radiographs in neurologic trauma has become limited. In moderate and severe head trauma, a CT scan is the study of choice. Skull radiographs are only indicated in minor head trauma patients where a CT scan is otherwise not clinically indicated during the initial evaluation.

Skull radiographs may be helpful and can compliment other imaging modalities in the following conditions:

1. Depressed fracture is suspected clinically or by the nature of the injury
2. Penetrating injury by metal or glass is suspected
3. Radiodense foreign body is suspected

The basic skull projections used in evaluation of head trauma are the lateral and the fronto-occipital (AP) views (Fig. 52.1).

H Singh and JA Neutze (eds.), *Radiology Fundamentals: Introduction to Imaging & Technology*, DOI 10.1007/978-1-4614-0944-1_52,
© Springer Science+Business Media, LLC 2012

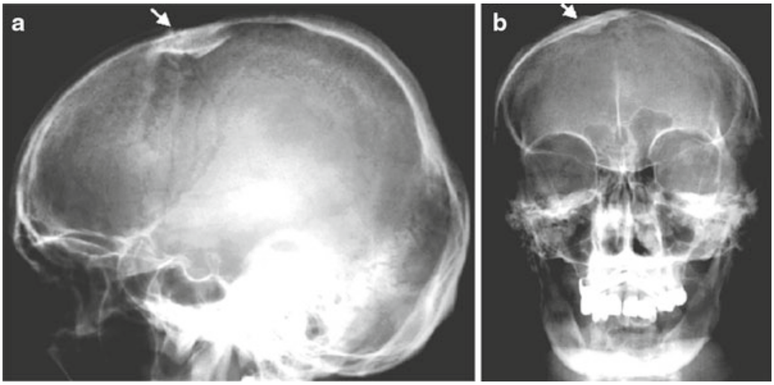

FIGURE 52.1 - SKULL RADIOGRAPH
Lateral (**a**) and AP (**b**) views show a depressed fracture of the right parietal bone with displacement of the bone fragment into the skull

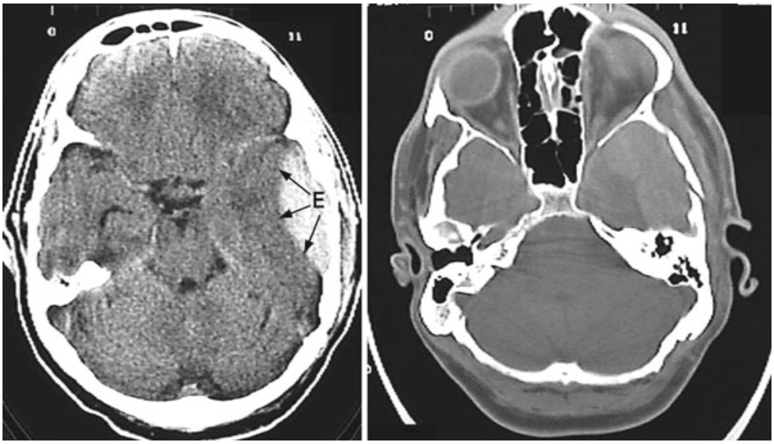

FIGURE 52.2 - EPIDURAL HEMATOMA WITH SKULL FRACTURE
In this trauma victim, there is an epidural hematoma (E). It has the typical elliptical shape. There is mass effect, centered on the bleed (*arrows*). The image on the *right* is further evidence of head trauma and the likely cause of the epidural hematoma. Did you notice the left temporal bone fracture?

Epidural Hematoma

Figure 52.2 is a CT of a patient with a known skull fracture and acute hemorrhage. Blood appears as radiodense on head CT. The biconvex appearance of the epidural blood is caused by the tight attachment of the dura to the skull. Midline shift is present secondary to the mass effect of the hematoma.

Subdural Hematoma

Figure 52.3 demonstrates a subdural hematoma which is hemorrhage under the dura. Note that the blood is free to follow the contour of the brain so that it has a flat or concave inner surface.

In the normal evolution of a subdural hematoma, the collection becomes hypodense with respect to brain tissue. As more time passes it becomes isodense (equally dense) with respect to the brain tissue. Diagnosis during this period of isodensity can be difficult. Chronic subdural hematomas that are hypodense with respect to the brain substance are referred to as subdural hygromas.

Subarachnoid Hemorrhage

Trauma is the most common cause of subarachnoid hemorrhage (SAH) overall. A large percentage of traumatic brain injuries include this type of bleeding. On CT scans, SAH appears as a high-attenuating (hyperdense), amorphous substance that fills the normally dark, CSF-filled subarachnoid spaces around the brain (Fig. 52.4). These findings are most evident in the largest subarachnoid spaces, such as the suprasellar

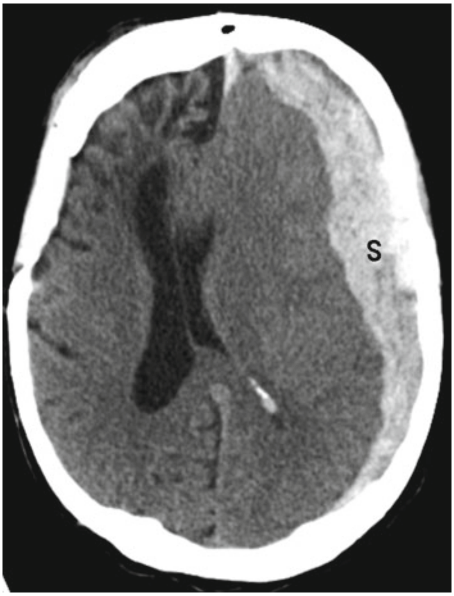

FIGURE 52.3 - SUBDURAL HEMATOMA
In this trauma victim, there is a large left holohemispheric subdural hematoma (S). It has a distinctly flat/concave inner surface which allows one to distinguish it from an epidural hematoma

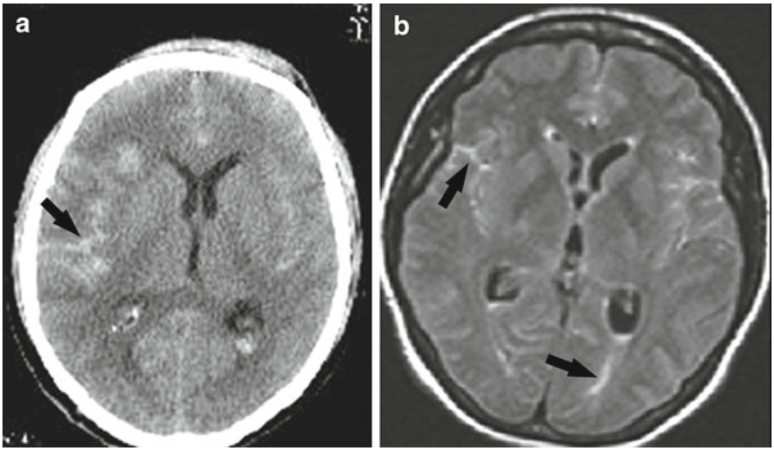

FIGURE 52.4 - (A, B) CT AND MRI OF SUBARACHNOID HEMORRHAGE
(**a**) CT shows hyperdensity within the CSF sulci spaces, most prominently along the sylvian fissures (*arrow*), consistent with subarachnoid hemorrhage. (**b**) MRI on the same patient shows corresponding areas of T2 hyperintensity within the sylvian fissures along with intraventricular hemorrhage (*arrows*)

cistern and Sylvian fissures. It can also be seen tracking along the sulci, outlining the gray matter. MRI has a higher sensitivity in diagnosing subarachnoid hemorrhage. This is especially true in the hyperacute and chronic phases where CT may be completely negative because blood in those states is equal in density to brain tissue.

Parenchymal Contusion

Figure 52.5 shows an area of generally decreased attenuation (gray) with an area of lobular increased density. There is subtle mass effect with contralateral midline shift (to the patient's right). This displacement and low density is caused by edema with the lobular areas representing hemorrhage. This is the radiographic appearance of a cerebral contusion, or literally, "a bruise of the brain." In all of the above diagnoses, there may be associated findings such as a skull fracture and associated soft tissue swelling external to the skull. These abnormalities may give you a clue as to where to look within the brain for abnormalities, as these findings can sometimes be quite subtle.

Diffuse Axonal Injury

Diffuse axonal injury (DAI) is a frequent result of traumatic deceleration injuries and a frequent cause of a persistent vegetative state (Fig. 52.6). Typically, the process is diffuse and bilateral, involving the lobar white matter at the gray–white matter

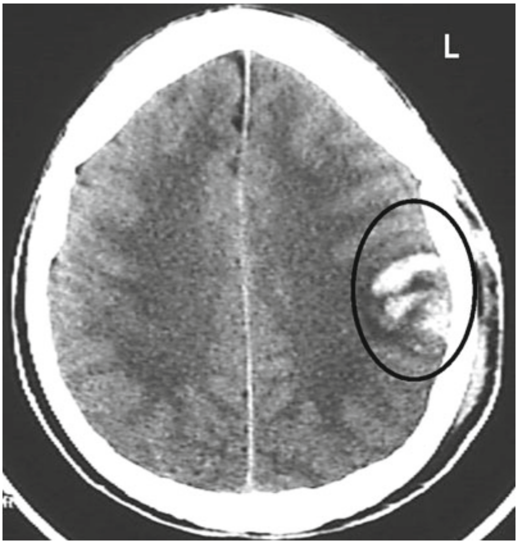

FIGURE 52.5 - PARENCHYMAL CONTUSION
In the same patient as Fig. 43.1, there is also evidence of blood in the parenchyma with some surrounding edema consistent with a contusion. Note the subtle mass effect at this level

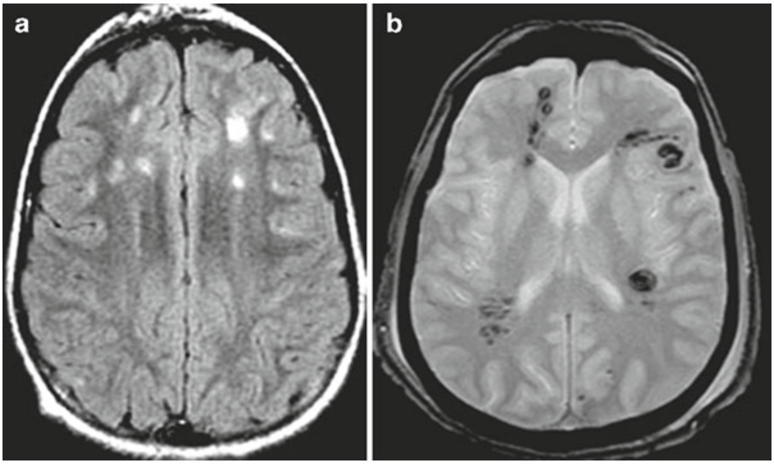

FIGURE 52.6 - HEAD TRAUMA IMAGING OF DIFFUSE AXONAL INJURY (DAI)
MRI in a young patient with trauma and negative head CT shows multiple areas of T2 hyperintensity at the gray–white matter junction (**a**). The petechial hemorrhages are seen as low signal areas on gradient images (**b**) (gradient echo is an MRI sequence which is very sensitive to blood products)

interface. The corpus callosum frequently is involved, as is the dorsolateral rostral brainstem. On CT, 60–90% of patients with DAI may have a normal CT scan on presentation. Small petechial hemorrhages located at the gray–white matter junction and corpus callosum are characteristic but only occur in about 20%. MRI is the modality of choice for diagnosing DAI. Most common MRI findings are multiple focal areas of abnormally bright signal on T2-weighted images in the white matter of the temporal or parietal corticomedullary junction or in splenium of corpus callosum. Gradient-echo sequences are very useful in demonstrating petechial hemorrhages. The paramagnetic properties of blood cause a loss of signal, represented by black areas.

53

STROKE

Objectives:
1. State the definition of stroke.
2. Understand the role of imaging in stroke.
3. Be able to describe major CT and MRI findings in stroke.

Introduction

Stroke is a clinical syndrome. It is used somewhat colloquially to refer to a group of clinical syndromes that involve mental status changes. Although most of us think primarily of cerebrovascular accident (CVA) when we hear "stroke," there are other processes which could mimic CVA, such as hemorrhage, seizure, tumors, etc.

Imaging in strokes is used to differentiate

1. Vascular process from other mimics such as hemorrhage, tumor, AVM
2. Hemorrhagic from nonhemorrhagic infarction
3. Arterial from venous infarction
4. Large territory defect (anterior or posterior) from lacunar type infarctions

In addition, if there is ischemia, more advanced CT and MRI techniques can be applied [i.e., CT perfusion (CTP), CT angiography (CTA), MRI angiography] to help further determine the course of treatment.

Imaging Findings in Stroke

When is the optimal time to image stroke? The answer generally is "as soon as possible," although this depends on the treatment options available to the patient at the medical care facility. It also depends on how long the patient has had the symptoms,

H Singh and JA Neutze (eds.), *Radiology Fundamentals: Introduction to Imaging & Technology*, DOI 10.1007/978-1-4614-0944-1_53,
© Springer Science+Business Media, LLC 2012

as duration of symptoms determines whether the patient is a candidate for thrombolytic therapy (tPA-tissue plasminogen activator). “Time is brain” and generally speaking, there is a 6-hour window after the onset of symptoms where thrombolytics can be given (assuming there is no hemorrhage or sizeable infarction on imaging). This window is somewhat flexible, depending on the vessel involved and the experience of the medical center.

Noncontrast CT is usually first obtained (Fig. 53.1). This is a very fast and widely available study. Quite a bit of information can be gained from the basic CT such as is there a discernible abnormality? Does it appear to be ischemia or something else, like a mass? Is there blood? How much brain tissue is involved? Is there herniation/mass effect that would constitute a neurosurgical emergency?

Ischemia is not always immediately evident on CT, especially if the patient is imaged very early after the onset of symptoms, or if the area of brain involved is small (lacunar infarct).

The early signs of ischemia on CT are

1. Hypoattenuation (low density) in the affected tissue
2. Loss of gray white matter differentiation (insular ribbon sign)
3. Sulcal effacement due to brain swelling
4. Hyperdensity in a large vessel (hyperdense MCA sign) or “dot sign” due to acute clot in the diseased vessel

Seeing the distribution of infarcted or ischemic tissue and knowing the arterial supply (Fig. 53.2) to the different parts of the brain, one can infer the vessel(s) affected. The vascular territories of the cerebral arteries described in the figure include ACA = anterior cerebral artery, MCA = middle cerebral artery, PCA = posterior cerebral artery.

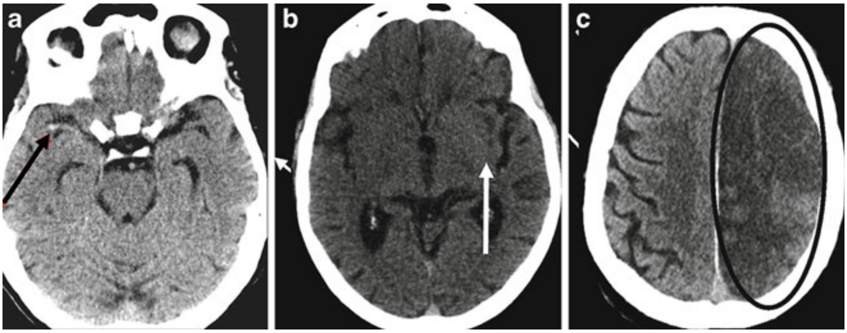

FIGURE 53.1 - CT FINDINGS OF ACUTE ISCHEMIA
The above images represent CT findings of acute ischemia. (**a**) Hyperdense MCA, (**b**) loss of gray–white matter differentiation in the insula, (**c**) sulcal effacement, and hyperdensity in the MCA territory

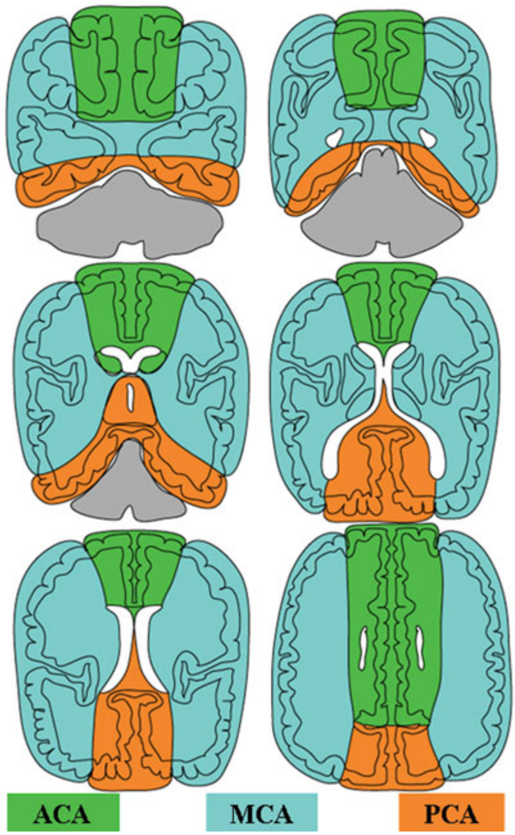

FIGURE 53.2 - VASCULAR AREAS OF CEREBRAL ARTERIES
Based on the distribution of infarcted or ischemic tissue, one can infer the vessel that is affected based on the arterial supply to the brain

Although in many instances subtle findings can be seen on CT, sometimes the study can appear essentially normal, especially early. If this is the case, the patient could clinically still have a "stroke" syndrome and should be treated as such.

MRI is more sensitive for detection of early ischemia using diffusion imaging, and is better at detecting small infarctions, especially in patients who have cerebrovascular disease and have had chronic small infarcts before (Fig. 53.3). Also, MRI is better at finding other processes which maybe causing the patient's symptoms; however, the disadvantages of MRI include less availability, higher price and longer scanning time (a major drawback given the previously discussed treatment window). In addition, MRI is not safe for some patients who have metallic foreign bodies or certain devices, most notably pacemakers, certain models of artificial valves, cochlear implants, spinal stimulators, and some IVC filters.

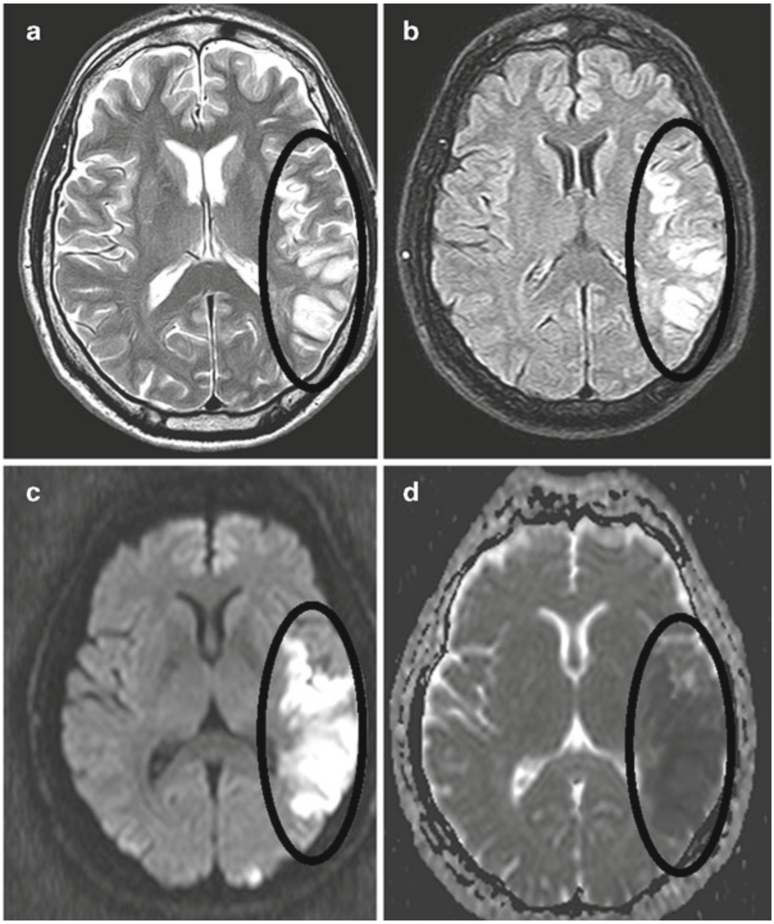

FIGURE 53.3 - ACUTE ISCHEMIA
MRI findings of acute ischemia in the left MCA distribution (**a**) T2W, (**b**) FLAIR, (**c**) DWI, and (**d**) ADC map

CTP is performed by monitoring the first pass of the contrast bolus through the cerebral circulation (Fig. 53.4). Information can be obtained at four representative levels in the brain or be obtained through a volume of brain tissue. Using this information, color maps of cerebral blood volume (CBV), cerebral blood flow (CBF), mean transit time (MTT), and time to peak (TTP) are generated. This information is used to look for areas of perfusion defect and mismatch, which, in addition to the region of the infarction core, indicate other areas of ischemia and potential infarction, the "penumbra." This may influence further treatment decisions. MRI perfusion operates on basically the same principles, except gadolinium-based contrast is used

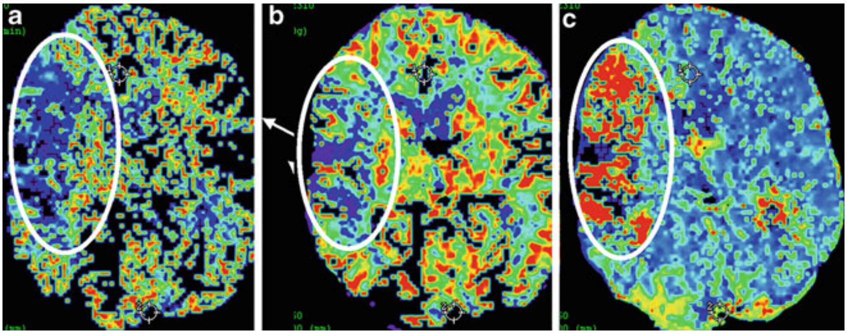

FIGURE 53.4 - CT IMAGES OF AN ACUTE INFARCT
CT Perfusion in acute right MCA infarct with all three parameters being abnormal in the affected distribution (**a**) CBV, (**b**) CBF, and (**c**) MTT

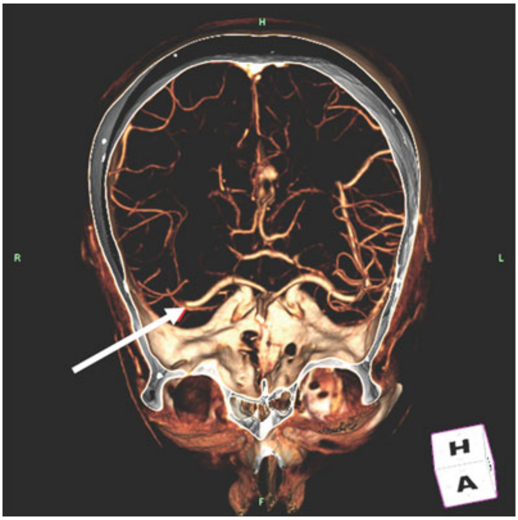

FIGURE 53.5 - OCCLUSION OF MIDDLE CEREBRAL ARTERY
CTA shows acute occlusion of the right MCA

and perfusion maps are compared with diffusion-weighted images to determine if there is tissue that can potentially be saved. Although the information is similar, CTP is much faster and therefore more commonly used in acute settings.

CTA or CT venography (CTV) are noninvasive techniques using thin section techniques and contrast to image the intracranial and extracranial (neck) vasculature. This is useful for identifying sites of occlusion, stenoses, dissection, and aneurysm (Fig. 53.5).

Although CVA is more frequently caused by arterial occlusion, venous thrombosis can also lead to ischemia and hemorrhage. Venous infarcts do not follow arterial territories, and occur more often in younger patients with hypercoagulable states. CTV or MR venography can evaluate the patency of major dural sinuses.

Summary

Imaging of stroke includes CT, CT perfusion, CT angiography, MRI and MRI angiography. Not all of these studies are indicated on every patient. CT is faster, more readily available and, in some ways, easier to interpret. MRI is more expensive, less available, slower, but more sensitive for acute ischemia and used to find other causes of patient's symptoms that may not be evident on CT. However, not every patient can safely have an MRI.

54

HEADACHE AND BACK PAIN

Objectives:

1. Understand the role of imaging in the patient with headache and back pain.
2. Be able to describe the major CT findings of subarachnoid hemorrhage.
3. Be able to state other causes of headache and back pain.

Introduction

Many disease processes manifest as headache. While headaches are mostly benign and self-limited, imaging is often obtained to exclude acute or life-threatening processes, such as a hemorrhage or mass.

Back pain is one of the most common complaints in health care. It is important to remember that back pain is not a diagnosis but a symptom of a medical condition. Most causes are benign. Imaging is often obtained when there is no response to rest, exercise, and medication to ensure there is no process that needs further intervention.

Intracranial Hemorrhage

Classically, the presentation of "the worst headache of my life" with a sudden onset is concerning for subarachnoid hemorrhage (SAH). The most common cause of nontraumatic SAH is a ruptured intracerebral aneurysm. Acute blood products are hyperdense on CT and therefore CT is useful for detection of SAH. CT angiography (CTA) is highly sensitive for diagnosis of the underlying aneurysm, although catheter angiography remains the gold standard (Fig. 54.1). CSF sampling by lumbar puncture can be done in cases of CT-negative, suspected SAH.

H Singh and JA Neutze (eds.), *Radiology Fundamentals: Introduction to Imaging & Technology*, DOI 10.1007/978-1-4614-0944-1_54,
© Springer Science+Business Media, LLC 2012

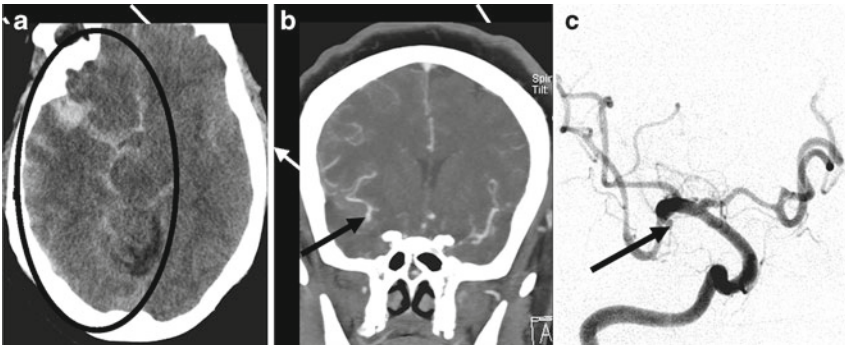

FIGURE 54.1 - SUBARACHNOID HEMORRHAGE
Image (**a**) is a CT which shows predominantly right hemispheric SAH. Image (**b**) is a coronal CTA reformat showing a very small aneurysm of the right M2 segment of the MCA while the digital subtraction image (DSA) shown in image (**c**) shows the same aneurysm

There are other types of intracranial hemorrhage which could cause headache though they are frequently associated with trauma. These include subdural and epidural hematomas and hemorrhagic contusions and are addressed in the Head Trauma section (Chap. 52).

Other Common Causes of Headache on Imaging

Any disease process which alters the intracranial pressure (ICP) or causes hydrocephalus, midline shift, or cerebral edema can cause a headache. This includes brain tumors (primary or metastatic), nonneoplastic masses which can have mass effect or obstruct the ventricles, (Fig. 54.2) or idiopathic processes such as pseudotumor cerebri, increased ICP of unknown etiology that can lead to blindness in 10–20% of the patients. Infectious processes, including meningitis and encephalitis, can present with headache but often have no or little findings on imaging with the diagnosis dependent not on imaging but on CSF and serum assay.

Back Pain

Causes of back pain include mechanical problems, injuries, neoplasm and infection. Intervertebral disc degeneration and herniation, facet arthritis, and muscle spasm are examples of mechanical problems that result in back pain. Injuries to

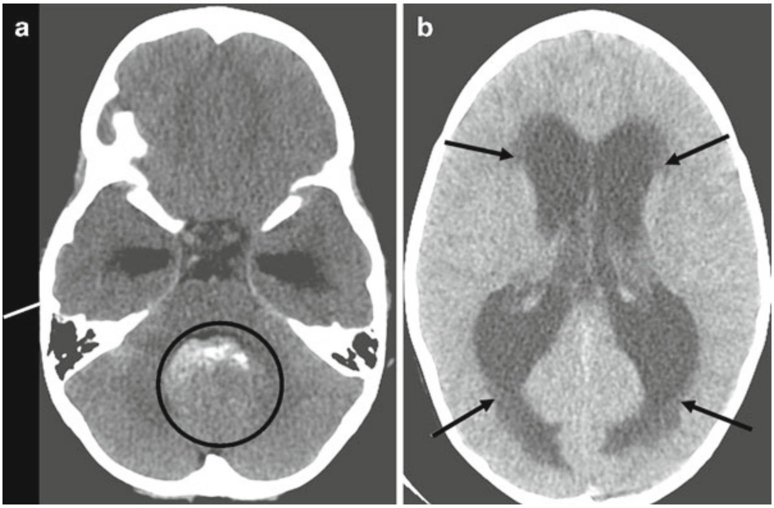

FIGURE 54.2 - HYDROCEPHALUS
CT showing a dense posterior fossa mass (**a**) causing hydrocephalus (**b**)

bones, muscles, tendons and ligaments from sports, trauma like car accidents, and improper lifting and twisting can result in back pain. Compression fractures in osteoporotic patients may manifest as back pain. Permanent and progressive conditions such as inflammatory processes and osteoarthritis, scoliosis, and fibromyalgia cause or contribute to back pain. Patients with renal calculi, pancreatitis, pregnancy, and endometriosis may have back pain. A leaking aortic aneurysm or aortic dissection may present as back pain. Osteomyelitis, discitis, primary tumors to the spinal cord or vertebral bodies and metastatic disease may also cause back pain. While most causes of back pain are physical, it should be noted that stress, anxiety, depression and insomnia can exacerbate existing back pain.

In the absence of underlying conditions such as known cancer or trauma, appropriate treatment may first be exercise, mild medication, physical therapy, and life style modification such as weight loss and treatment of stress and depression. If these interventions do not help, imaging should be considered. Plain films of the lumbar spine will demonstrate alignment, compression or traumatic fractures and disc space height, and arthritic changes. CT scan is helpful if other conditions are suspected, as it will demonstrate kidney stones, adenopathy and other masses. MRI is sensitive for the detection of bone and disc infections, spinal cord tumors, disc herniation and nerve root impingement (Fig. 54.3).

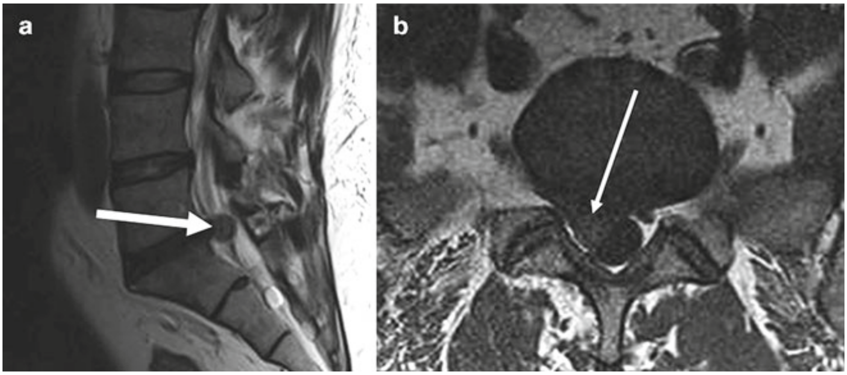

FIGURE 54.3 - LUMBAR DISC HERNIATION
Sagittal (**a**) and axial (**b**) MRI images showing a focal protrusion of the L5-S1 disc (*arrows*) causing moderate mass effect on the thecal sac

Summary

Headache is a very common complaint. Patients with simple headache often have no imaging findings. Moreover, imaging is not needed in the majority of cases of headache. Imaging is used when there is clinical suspicion for a more complicated or acute process, such as hemorrhage, mass, or hydrocephalus. Noncontrast CT is excellent for the initial evaluation of headache and can help to exclude life-threatening processes, with the caveat that some very serious disease processes, especially infectious diseases affecting the central nervous system, can have little or no imaging findings.

Back pain is also very common and imaging is not always needed in the majority of cases. Acute situations such as loss of bowel or bladder control or acute muscle weakness should prompt a consideration of imaging with CT and/or MRI. Clinical acumen remains of the utmost importance.

55

RADIOLOGY COMING SOON

Objectives:

1. Be able to describe the clinical situations where MR Enterography is a useful tool.
2. Understand the different types of tissue ablative techniques.
3. Understand which clinical scenarios are appropriate for Coronary CTA use.

Radiology, as we have alluded to many times in this text, is a fast moving field. It is likely that the three "coming soon" areas in radiology described in this chapter will be relatively common in practice by the time you read about them here. Moving at the "speed of light" is what makes this field so exciting.

MR Enterography: Michael Moore, MD

MRI is increasingly being utilized in the setting of inflammatory bowel disease, particularly Crohn's disease. Although CT is currently widely used in this setting, MRI has certain advantages including comparable diagnostic information while avoiding ionizing radiation. Decreasing radiation is of particular concern for these children, adolescents, and young adults given the chronic nature of their disease and frequent imaging. MRI is also superior to CT when evaluating perianal disease. Recent advances in MR technology allow faster acquisition times which decrease the effects of bowel motion. Typically, the patient will drink oral contrast (such as a low concentration barium solution that contains sorbitol) to provide bowel distention. Bowel wall enhancement is assessed with gadolinium administration. MRI findings in the setting of inflammatory bowel disease include bowel wall thickening,

H Singh and JA Neutze (eds.), *Radiology Fundamentals: Introduction to Imaging & Technology*, DOI 10.1007/978-1-4614-0944-1_55,
© Springer Science+Business Media, LLC 2012

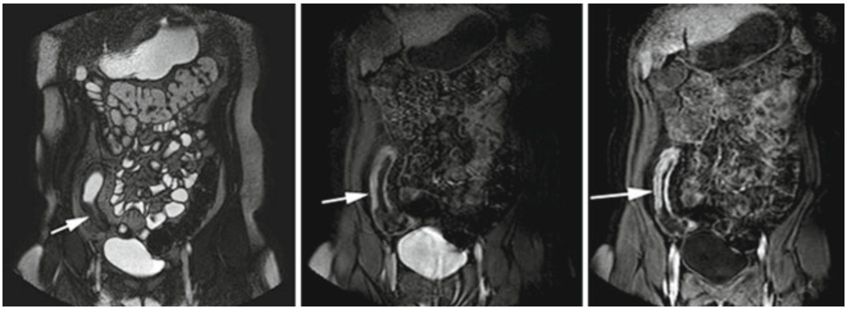

FIGURE 55.1 - MR IMAGING IN INFLAMMATORY BOWEL DISEASE
Three images from an MR Enterography study demonstrating abnormal signal in the right lower quadrant consistent with thickening and inflammation of the terminal ileum in this patient with Crohn's disease (*arrow*)

luminal narrowing, and avid enhancement in the setting of active disease. In the upcoming years, there will be increasing use of MRI in the setting of inflammatory bowel disease (Fig. 55.1).[1]

Tissue Ablation Techniques: Allene Burdette, MD

Tissue ablation techniques, using extremes of temperature, are commonly used to treat loco-regional lesions in malignant and benign diseases of the kidneys, liver, lung, breast, prostate, and bones. These temperature techniques are advances from the days of chemical ablation, where alcohol or acetic acid was injected into tumors in order to cause tissue necrosis. The temperature extremes generated by radiofrequency ablation, microwave ablation, and cryoablation result in irreversible damage to tumor cells. Radiofrequency ablation generates high temperatures using high frequency electrical currents passed through an electrode. Microwave ablation utilizes high frequency electromagnetic waves to cause rapid vibration of molecules. The friction generated by the vibration causes extreme heat. Temperatures greater than 50°C cause irreversible damage to proteins. The heat generated by these techniques disrupts cellular activity and produces coagulative necrosis. Alternatively, cryoablation freezes tissues to <−20°C. Tissue injury and death results from direct injury from ice formation, shifting of cellular solutes and solvents resulting in dehydration and cell rupture, as well as microvascular thrombosis resulting in ischemia. Each of these three techniques requires image-guided (CT, US, MRI, or fluoroscopy)

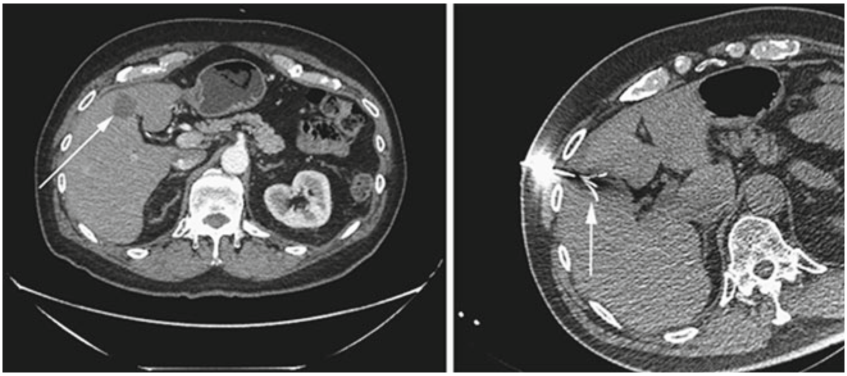

FIGURE 55.2 - RADIOFREQUENCY ABLATION PRE-PROCEDURAL AND INTRA-PROCEDURAL CT SCAN IMAGES
Two images from two different CT scans in the same patient. In the first image (left), from a pre-procedural contrast enhanced CT scan, the lesion is clearly identified anteriorly (*arrow*). On the second image (right), at a different setting, a radiofrequency (RF) probe has been inserted into the liver and the tines deployed (*arrow*) into the lesion, ready for ablation to begin

placement of one or several probes, through which either electrical current, electromagnetic waves, or a cryogen is delivered to a tumor in order to generate the desired temperature extreme for cellular destruction (Fig. 55.2).[2]

Coronary CTA

CT scanners are now able to acquire images rapidly enough to “freeze” the heart in time and clearly delineate the coronary arteries. Their utility has been focused on the differentiation of patient’s with cardiac and noncardiac chest pain with an emphasis on those patients who have low to intermediate risk for coronary artery disease without EKG changes or enzyme elevation. The patients are optimized for the coronary CT scan including the placement of a large bore IV in the right arm, given oral or IV beta blockers and finally 800 mcg of SL NTG just prior to contrast injection. Nonionic contrast is usually injected at 6 cc/s for a total of 65–75 cc. Images are acquired during diastole, when the heart is filling passively but also has the least amount of motion. The images acquired are then viewed in both standard planes as well as on a 3D workstation. Description of any plaque should include whether the plaque is noncalcified vs. calcified vs. mixed. Sensitivity and specificity for the 128 slice CT scanners are ~92 and 95%, respectively (Fig. 55.3).[3]

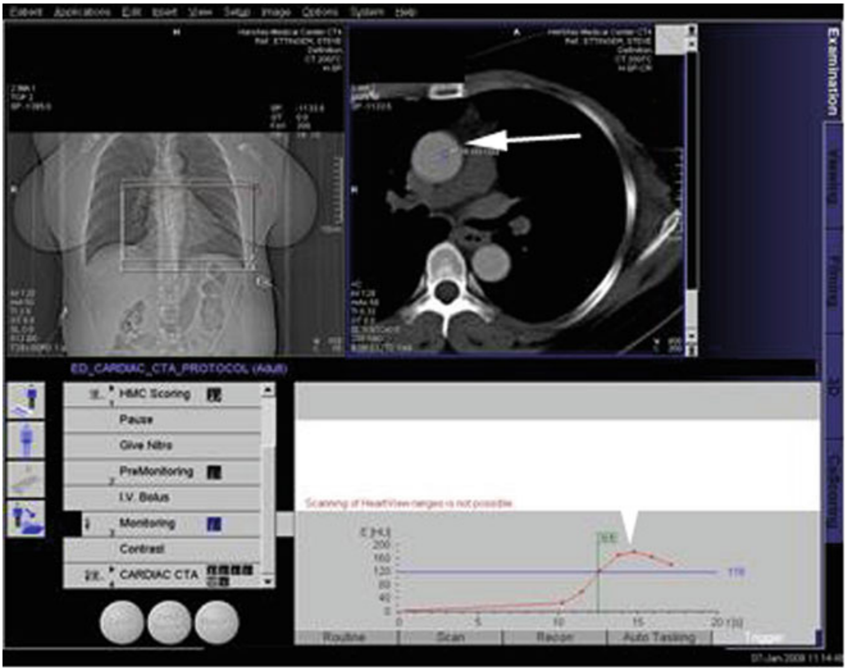
Patient Applications Edit Insert View Setup Image Options System Help
Examination
Viewing
Filming
3D
CaScoring
ED_CARDIAC_CTA_PROTOCOL (Adult)
HMC Scoring
Pause
Give Nitro
PreMonitoring
I.V. Bolus
Monitoring
Contrast
CARDIAC CTA
E [HU]
200
160
120
80
40
0
0
5
10
15
20 t [s]
Routine
Scan
Recon
Auto Tasking
Trigger
07-Jan-2008 11:14:48

Scanning of HeartView ranges is not possible

FIGURE 55.3 - CORONARY CTA PLANNING SCREEN
In the first image, a screen capture is presented demonstrating the region of interest in the ascending aorta and how the bolus tracking curve would look like to those performing the study. The second two images are a centerline reconstruction of the right coronary artery demonstrating a proximal stenosis and 3D volume-rendered images of the coronary arteries including the right coronary lesion

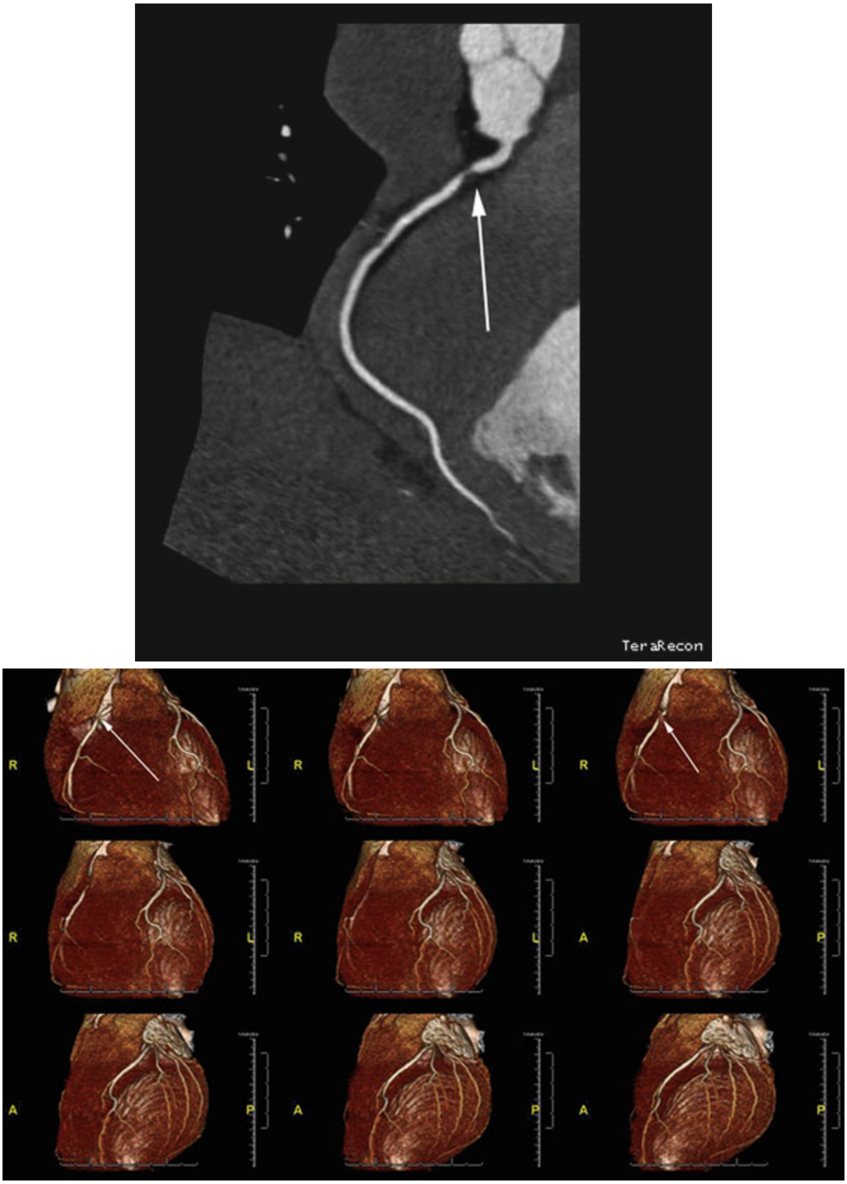
TeraRecon
R
L
R
L
R
L
R
L
R
L
A
P
A
P
A
P
A
P

FIGURE 55.3 - CONTINUED

References

1. MR Imaging of the Bowel: Pediatric Applications. Kassa Darge, Sudha A. Anupindi, Diego Jaramillo. Magn Reson Imaging Clin N Am 16 (2008) 467–478.
2. Kevin A. Smith and Hyun S. Kim, Interventional Radiology and Image-Guided Medicine: Interventional Oncology; Semin Oncol 38:151–162.
3. Hulten, Edward A., Carbonaro, Salvatore, Petrillo, Sara P., Mitchell, Joshua D., Villines, Todd C. Prognostic Value of Cardiac Computed Tomography Angiography: A Systematic Review and Meta-Analysis**.** J Am Coll Cardiol 2011 57: 1237–1247

INDEX

A
Abdominal and pelvic pain evaluation
    appendicitis, 204, 209
    causes by age group, 202–203
    cholecystitis, 205, 210
    diverticulitis, 205, 209
    ectopic pregnancy, 208, 210
    in female patients, 203
    hernia, 206, 210
    hydronephrosis, 207, 210
    imaging of, 201, 202
    testicular torsion, 207, 210
Abdominal aortic aneursym, 221, 222
Abdominal calcifications
    appendicolith, 139, 141
    chronic pancreatitis, 137–138
    lymph nodes, colon, 137–138
    urinary tract calculi, 141–142
    uterine fibroids, 139–140
    vascular calcification
        abdominal aortic aneurysm, 139
        aortic calcification, 139–140
        pelvic phleboliths, 138–139
Abnormal air collections, abdomen
    pneumatosis intestinalis, 144–145
    pneumoperitoneum, 143–144
Abscess, 219–220
Achalasia, 148
Adhesive atelectasis, 70–72
Adrenal lesions, 232–234
Air space disease
    air bronchograms, 59, 61
    air space consolidation, 59–60
    cardiogenic edema, 61
    lung acinus, 59–60
    neoplasms, 62
    pathologic process, 62
    pneumonia, 61–62
    pulmonary acinus, 59
Ankle fracture
    Boehler's angle, 312
    fibula, 309, 310
    inversion and eversion types, 311
    sprain, 311
Anteroposterior (AP) radiograph, 11–12
Appendicitis, 204, 209
Appendicolith, 139, 141
Arteriography
    catheters and wires, 263, 264
    complications, 265–266
    femoral and brachial artery access, 263–265
Arthritides
    gout, 318, 319
    osteoarthritis
        Bouchard's nodes, 318
        Heberden's nodes, 318
        knee, 315, 317
        vs. rheumatoid arthritis, 315, 316
    rheumatoid arthritis, 316, 317
Atelectasis
    adhesive, 70–72
    air space opacity, 69
    cicatrization, 70–71
    definition, 69
    passive, 71–72
    postobstructive, 70
    radiographic opacity, 73

H Singh and JA Neutze (eds.), *Radiology Fundamentals: Introduction to Imaging & Technology*, DOI 10.1007/978-1-4614-0944-1,
© Springer Science+Business Media, LLC 2012

B
Back pain, 346–348
Barium enema and CT colonography
  apple core lesion, sigmoid colon, 159–160
  CD, 160–162
  colonic diverticuli and polyps, 160–161
  colonic mass, 159
  colonic polyps, 162, 163
  colon segments, 157–158
  coronal 2D image, 163–165
  double-contrast barium enema (DCBE), 158–159
  "double-contrast" image, 163–164
  follow-up colonoscopy, 163
  intussusception, 162–163
  polypectomy, 165
  single-contrast water soluble enema, 157–158
Barium esophagram, 148
Barium studies, upper gastrointestinal (UGI) tract
  conventional enteroclysis, 152–153
  CT enteroclysis, 153–154
  CT enterography, 154–155
  double and single contrast GI study, 150–151
  esophageal carcinoma, 149–150
  esophageal diverticuli, 149–150
  fluoroscopy, 147
  normal esophageal motility, 148–149
  radiographic visualization, 147
  small bowel follow through, 152
Battered child syndrome, 293
BI-RADS®, 122, 124
Boehler's angle, 312
Bone imaging
  indications for, 241, 242
  lytic *vs.* blastic lesions, 242, 245
  T10 vertebral body, 242, 244
  in young adult, 242, 243
Bone tumor
  aggressive lesion, 322, 323
  chondroid matrix, 323, 325
  nonaggressive lesion, 322
  osteoid matrix, 323, 325
  periosteal reaction, 322, 324
Bowel obstruction
  air-fluid level, 167–169
  computed tomography (CT), 171
  distended bowel loops, 168–169
  gas-filled loops, 169
  gas visualization, 167
  ileus, 171–172
  mucosal edema
    barium enema, 172
    prominent transverse colon, 171, 173
    thumbprinting, 171
  supine radiograph, 167
  total colonic obstruction, 170
Breast imaging
  BI-RADS®, 122, 124
  breast implants, 115–116
  craniocaudad (CC) and mediolateral oblique (MLO) view, 112–113
  dense fibroglandular breast tissue, 113–115
  diagnostic mammograms, 111
  digital mammography, 111
  image-guided biopsy, 121–122
  mammographic findings
    benign calcification, 116–117
    breast mass MLO view, 118–119
    dense breast tissue, 114, 116
    fibroadenoma, 118–119
  MRI, 120–121, 123
  radiation dosage, 118, 120
  screening mammography, 111
  ultrasound utilization
    differential diagnosis, 120
    palpable mass, 120–121
    simple breast cyst, 120, 122
Breast implants, 115–116
Bronchogenic carcinoma, 101

C
Calcific pericarditis, 95–96
Cardiac imaging
  left ventricular ejection fraction, 251, 252
  red blood cells, 251
  thallium-labeled myocardial perfusion study, 252–253
Cardiovascular and interventional radiology (CVIR)
  biliary procedure, 37
  central venous access, 36
  DSA, 35–36
  gastroenteric access, 37
  genitourinary procedure, 37
Catheters
  exchange, 285, 286
  infusion, 283, 284
  tunneled, 283, 285
Cavitary lesion, 54–56
Cavitary tuberculosis, 96–97
CD. *See* Crohn's disease (CD)

Central nervous system (CNS), 327–328
Central venous access
  dialysis access catheters, 36
  exchange catheters, 285, 286
  indications, 283, 284
  infusion catheters, 283, 284
  tunneled catheter, 283, 285
Central venous catheters, 106–108
Cervical spine
  CT/plain film evaluation
    open-mouth odontoid view, 330, 331
    sagittal views, 330, 331
  MRI, 332
  plain radiographs, 329
Cholangiogram, 196, 198
Cholecystitis, 205, 210
Chronic obstructive pulmonary disease (COPD), 85–86
Chronic pancreatitis, 137–138
Cicatrization atelectasis, 70–71
Coin lesion, 53–54
Colitis, 226–227
Colles' fracture, 303, 304
Colon cancer, 178
Colonic diverticuli and polyps, 160–161
Computed tomography (CT)
  contrast studies, 26
  enteroclysis, 153–154
  enterography, 154–155
  hounsfield units (HU), 25–26
  imaging orientation, 23–24
  lymphadenopathy, 190–192
  pixels and voxels, 23–25
  specific structure visualization, 26–27
Computed tomography perfusion (CTP), 342, 343
Congestive heart failure (CHF), 83
COPD. *See* Chronic obstructive pulmonary disease (COPD)
Cope loop, 274, 275
Coronary computed tomography angiogram (CTA), 351–353
Crohn's cobblestoning, 176–177
Crohn's disease (CD), 160–162, 175
CT. *See* Computed tomography (CT)
CVIR. *See* Cardiovascular and interventional radiology (CVIR)

D

Deep sulcus sign, 92–93
Defecography
  abnormal findings
    dyskinesia, 183, 186
    enterocele, 183, 186
    incontinence, 183, 185
    internal intussusception, 183, 187
    rectocele, 183, 185
    sphincter dyssynergia, 183, 187
  anatomy, 182
  indications, 181
  physiology
    during Kegel maneuver, 183, 184
    during Valsalva maneuver, 183, 184
  technique, 181–182
Diagnostic mammograms, 111
Diffuse axonal injury, 336–338
Digital mammography, 111
Digital subtraction angiography (DSA), 35–36
Diverticulitis, 205, 209
Doppler shift, 20
Dysfunctional uterine bleeding (DUB), 126
Dyskinesia, 183, 186

E

Ectopic pregnancy, 208, 210
Endoscopic retrograde cholangiopancreatography (ERCP), 195–196
Endotracheal (ET) tube
  atelectasis, 105–107
  positioning, 105–106
  right main bronchus intubation, 105, 107
Enterocele, 183, 186
Epidural hematoma, 334
Esophageal carcinoma, 149–150
Esophageal diverticuli, 149–150
Esophageal motility, 148–149
Exchange catheters, 285, 286

F

Fallopian tube recanalization, 134–135
Fat pad sign, 301–303
Femoral neck fracture, 305–307
Fluorine–18 fluorodeoxyglucose (F–18 FDG)
  application in oncology
    lung cancer, 258–259, 261
    malignancies probability, 258, 260
    pre and postchemotherapy, 259, 262
  cellular metabolism, glucose, 256
  glycolysis, 255–256, 258
  patient preparation, 256–257
  PET pitfalls, 260
  positron reaction, 255, 256

Fracture
  ankle
    Boehler's angle, 312
    fibula, 309, 310
    inversion and eversion types, 311
    sprain, 311
  battered child syndrome, 293
  Colles' fracture, 303, 304
  fat pad sign, 301–303
  femoral neck, 305–307
  greenstick and torus, 292
  knee joint effusion, 306, 308, 309
  nomenclature
    angulation of the apex, 288
    displacement, 288
    fragment orientation, 288, 290
    long bone anatomy, 288, 289
    type of, 288, 289
  osteoporosis
    calcifications types, 294, 297
    DEXA, 294, 295
  pathologic, 293–294
  pediatric, 290, 291
  pelvic, 305, 306
  Salter-Harris fracture classification, 291–292
  Scottie Dog concept, 304, 305
  shoulder
    anterior and posterior dislocation, 301, 302
    rotational views, 299, 300
  simple, 287, 288
  tibial plateau, 309, 310

G
Gall bladder
  biliary tree visualization
    adjacent biliary structures, 195, 197
    ERCP, 195–196
    PTC, 195, 197
    T-tube, 196
  gallstones
    computed topography, 198, 199
    plain radiography, 193, 194
  IDA scan, 195, 196
  ultrasound, 194, 195
Gallstones
  computed topography, 198, 199
  plain radiography, 193, 194
Gastroenteric access, 37
Gastrointestinal (GI) bleeding
  angiography, 239
  red blood cell study, 237, 239
  TC–99M RBC taggng, 237, 238
Glycolysis, 255–256, 258
Gout, 318, 319

H
Hamartoma, 54–55
Headache and back pain
  causes of, 346, 347
  intracranial hemorrhage, 345–346
Head trauma
  diffuse axonal injury, 336–338
  epidural hematoma, 334
  parenchymal contusion, 336, 337
  skull radiograph, 333, 334
  subarachnoid hemorrhage, 335–336
  subdural hematoma, 335
Heart
  cardiac contours, 39–40
  cardiac measurement, 40–41
Hemidiaphragms, 47–49
Hepatic lesions, 230, 232, 233
Hepatocellular carcinoma, 223, 224
Hernia, 206, 210
Hounsfield units (HU), 25–26
Hydrocephalus, 346, 347
Hydronephrosis, 207, 210

I
IBD. *See* Inflammatory bowel disease (IBD)
Ileus, 171–172
Incidental lesions
  adrenal, 232–234
  hepatic, 230, 232, 233
  pancreatic, 233–235
  renal
    Bosniak criteria, 229–230
    solid renal, 230, 232
    ultrasound, 229, 231
Incontinence, 183, 185
Inflammatory bowel disease (IBD)
  CD, 175
  chronic medical disorders, 175–176
  colon cancer, 178
  Crohn's cobblestoning, 176–177
  polypoid changes, 177–178
  string sign, 176
  toxic megacolon, 178–179
  ulcerative colitis, 177

Infusion catheters, 283, 284
Inspiratory and expiratory radiographs, 12, 14
Internal intussusception, 183, 187
Interstitial disease
  differential diagnosis, 66
  Kerley lines, 64–65
  peribronchial cuffing, 64–66
  pulmonary interstitium, 63
  reticular and reticulonodular pattern, 65, 67
  secondary pulmonary lobule, 63–64
  subpleural thickening, 65–66
Interstitial edema
  adult respiratory distress syndrome (ARDS), 87
  airspace/alveolar edema, 85–86
  capillary wedge pressure, 85
  COPD, 85–86
  extravascular lung water, 85
Intracranial hemorrhage, 345–346
Intussusception, 162–163
IVC filter placement
  permanent filter, 269
  retrievable filter, 269
  vena cava filter deployment, 271

K
Kaposi's sarcoma, 98–99
Kerley lines, 64–65
Killian's dehiscence, 150
Knee joint effusion, 306, 308, 309

L
Lateral chest
  chest projection
    bilateral pleural effusions, 47
    pleural fluid accumulation, 47
    skin lesion, 45–46
  hemidiaphragms, 47–49
  hilar enlargement, 49
  meshrdical fashion, 45–46
Lesions
  abdominal aortic aneursym, 221, 222
  abscess, 219–220
  colitis, 226–227
  hepatocellular carcinoma, 223, 224
  incidental (*see* Incidental lesions)
  pancreatic mass, 224–226
  pneumoperitoneum, 220–221
  portal venous gas, 224, 225
  renal cell cancer, 222, 223
Linitis plastica, 151
Lipohemarthrosis, 308, 309
Lisfranc injury/fracture, 311
Lordotic projection, 12–13
Lumbar disc herniation, 347–348
Lung ventilation and perfusion
  interpretion, 248
  MAA, 247
  PIOPED criteria, 248, 249
  pulmonary embolus, 247–249
Lymphadenopathy
  abdominal lymph nodes, 189, 190
  computerized tomography (CT) scanning, 190–192
  lymphangiogram, 190
  malignancies, 189
Lymphangiogram, 190
Lymphangitis carcinomatosis, 66

M
Magnetic resonance imaging (MRI)
  advantages and disadvantages, 30
  hydrogen nuclei, 29–30
  neuroradiology and musculoskeletal radiology, 29
  T1-weighted and T2-weighted sequences, 29–30
Mediastinal lymphadenopathy, 97–98
Mediastinum
  lymph nodes, 40–42
  mediastinal divisions, 40–41, 43
  mediastinal masses, 41, 43
Menorrhagia, 126
Microaggregated albumin (MAA), 247
Miscellaneous chest conditions
  asbestos, 101–102
  calcific pericarditis, 95–96
  Kaposi's sarcoma, 98–99
  mediastinal lymphadenopathy, 97–98
  opacified hemithorax, 103
  PCP, 99
  pulmonary embolus, 100–101
  tuberculosis, 96–97
MR enterography, 349–351
MRI. *See* Magnetic resonance imaging (MRI)
Mucosal edema
  barium enema, 172
  prominent transverse colon, 171, 173
  thumbprinting, 171

N
Nasogastric tube, 109–110
Nuclear medicine
  gamma ray detector and camera, 31, 33
  oncologic imaging, 32, 34
  radionuclide, 31
  radiopharmaceutical, 31–32
  technetium bone scan, 31–32, 34

O
Osteoarthritis
  Bouchard's nodes, 318
  Heberden's nodes, 318
  vs. rheumatoid arthritis, 315, 316
Osteoporosis
  calcifications types, 294, 297
  DEXA, 294, 295
Ovarian vein embolization and pelvic congestion syndrome, 132–134

P
Pancreatic lesions, 233–235
Pancreatic mass, 224–226
Parenchymal contusion, 336, 337
Passive atelectasis, 71–72
Patient radiation safety and risk
  CT scanning, 1
  diagnostic/interventional procedure, 1–2
  diagnostic X-ray, 1–2
  interventional fluoroscopy procedure, 4
  nonstochastic (deterministic) effects, 3
  nuclear medicine examination, 1, 3
  radiation dose, 1
  resources, 4–5
  stochastic (probabilistic) effects, 3
Pediatric fracture, 290, 291
Pelvic fracture, 305, 306
Percutaneous nephrostomy placement
  percutaneous drainage, 273
  puncture of kidney
    cope loop, 274, 275
    urological catheters types, 274, 275
Percutaneous transhepatic cholangiogram (PTC), 195, 197
Peribronchial cuffing, 64–66
Pixels and voxels, 23–25
Pneumatosis intestinalis, 144–145
Pneumocystis carinii pneumonia (PCP), 99
Pneumoperitoneum, 143–144, 220–221
Pneumothorax
  deep sulcus sign, 92–93
  definition, 89
  normal and abnormal forces, lung, 89–90
  radiographic appearance, 89–91
  tension, 91–92
Portal venous gas, 224
Positron emission tomography (PET). *See* Fluorine–18 fluorodeoxyglucose
Posterior-anterior (PA) radiograph, 11–12
Postobstructive atelectasis, 70
Preprocedural hysterosalpingogram, 134
Pseudotumor, 58
Pulmonary arteriography
  catheter placement, 267, 268
  IVC filter placement, 269–271
Pulmonary artery hypertension, 77–78
Pulmonary edema
  changes of cephalization, 83–84
  chest radiograph, 83–84
  CHF, 83
  interstitial edema
    adult respiratory distress syndrome (ARDS), 87
    airspace/alveolar edema, 85–86
    capillary wedge pressure, 85
    COPD, 85–86
    extravascular lung water, 85
Pulmonary embolus, 100–101, 247–249
Pulmonary mass lesions
  cavitary lesion, 54–56
  coin lesion, 53–54
  evaluation, 52
  hamartoma, 54–55
  lung masses, 51
  pseudotumor, 58
  pulmonary nodules
    frontal chest radiograph, 56
    metastases, 56–57
    nipple shadows, 53
  round pneumonia, 57–58
Pulmonary nodules
  frontal chest radiograph, 56
  metastases, 56–57
  nipple shadows, 53
Pulmonary vasculature
  pulmonary artery hypertension, 77–78
  pulmonary venous hypertension
    dilated left atrial appendage, 79
    frontal radiograph, 79–80
    obstructive lesion, 80
    pulmonary vascularity, 80–81
  pulmonary vessel distribution, 75–76
  pulmonary vessel identification, 76–77
  shunt vascularity, 78–79

Pulmonary venous hypertension
  dilated left atrial appendage, 79
  frontal radiograph, 79–80
  obstructive lesion, 80
  pulmonary vascularity, 80–81

R

Radiographic densities
  air, 7–8
  bone, 7–8
  fat, 7–8
  soft tissue, 7–8
Radiograph projection
  anteroposterior (AP) radiograph, 11–12
  barium enema, 14–15
  chest rotation, 12–13
  inspiratory and expiratory films, 12, 14
  Lordotic projection, 12–13
  normal kub, 14–15
  posterior-anterior (PA) radiograph, 11–12
Radionucleotide
  bone imaging
    indications for, 241, 242
    lytic *vs.* blastic lesions, 242, 245
    T10 vertebral body, 242, 244
    in young adult, 242, 243
  cardiac imaging
    left ventricular ejection fraction, 251, 252
    red blood cells, 251
    thallium-labeled myocardial perfusion study, 252–253
  GI bleeding, 237–240
Rectocele, 183, 185
Regional enteritis. *See* Crohn's disease (CD)
Renal cell cancer, 222, 223
Renal lesions
  Bosniak criteria, 229–230
  solid renal, 230, 232
  ultrasound, 229, 231
Reticulonodular disease, 65, 67
Rheumatoid arthritis, 316–318
Round pneumonia, 57–58

S

Salter-Harris fracture classification, 291–292
Scottie Dog concept, 304, 305
Screening mammography, 111
Shoulder fracture
  anterior and posterior dislocation, 301, 302
  rotational views, 299, 300
Shunt vascularity, 78–79
Sigmoid diverticuli, 160–161
Silhouette sign, 9–10
Simple fracture, 287, 288
Sphincter dyssynergia, 183, 187
Stroke
  definition, 339
  imaging findings
    cerebral arteries, 340, 341
    CTP, 342, 343
    ischemia, 340
    middle cerebral artery occlusion, 343
    MRI, 341, 342
Subarachnoid hemorrhage, 335–336
Subdural hematoma, 335
Superselective uterine arteriography, 132

T

Technetium 99m methylene diphosphonate (Tc–99m MDP), 31
Tension pneumothorax, 91–92
Testicular torsion, 203, 207
TIPS. *See* Transjugular intrahepatic portosystemic shunt (TIPS)
Tissue ablation techniques, 350–351
Torus fracture, 292
Toxic megacolon, 178–179
Transabdominal ultrasound, 126
Transjugular intrahepatic portosystemic shunt (TIPS)
  30-day mortality, 278
  indications and contraindications, 277
  long-term survival
    childs score, 279, 280
    mortality, 279, 280
  placement, 278–279
Trauma injury
  adrenals, 212, 215
  bowel, 212, 216
  chest, 212, 213
  duodenum, 212, 217
  kidneys, 212, 215
  liver, 212, 214
  pancreas, 212, 216
  spleen, 212, 214
Tuberculosis, 96–97
Tubes and lines
  central venous catheters, 106–108
  endotracheal (ET) tube
    atelectasis, 105–107
    positioning, 105–106
    right main bronchus intubation, 105, 107
  nasogastric tube, 109–110

Tumor, bone
  aggressive lesion, 322, 323
  chondroid matrix, 323, 325
  nonaggressive lesion, 322
  osteoid matrix, 323, 325
  periosteal reaction, 322, 324
Tunneled catheter, 283, 285

U
Ulcerative colitis, 177
Ultrasound
  acoustic enhancement, 19
  "anechoic" cyst, 18
  color and power Doppler imaging, 20
  echogenicity, 17
  gallbladder, 194, 195
  hyperechoic/hypoechoic, 17
  intracranial structures, 21
  inverse square law, 19
  prenatal imaging, 20
  transducer, 17–18
Urinary tract calculi, 141–142
Uterine artery/fibroid embolization, 131–133
Uterine fibroids, 139–140

V
Vascular calcifications
  abdominal aortic aneurysm, 139
  aortic calcification, 139–140
  pelvic phleboliths, 138–139
Venography, 133
Virtual colonoscopy. *See* Barium enema and CT colonography

W
Women's health interventions
  description, 131
  fallopian tube recanalization, 134–135
  ovarian vein embolization and pelvic congestion syndrome (PCS), 132–134
  uterine artery/fibroid embolization, 131–133
Women's ultrasound
  gynecologic and obstetrical condition, 125
  ovaries evaluation
    adnexa, 127
    ascites/peritoneal metastases, 128
    hemorrhagic cyst, 127–128
    "tip of the iceberg" configuration, 128–129
  pregnancy
    fallopian tube patency, 128
    fertilgy, 129–130
    intrauterine, 129
    varicoceles and testicular pathology, 128
  premenstrual evaluation, 126
  uterus and uterine bleeding evaluation, 126–127